

Abha Goyal · Rema Rao
Momin T. Siddiqui *Editors*

Pancreas and Biliary Tract Cytohistology

Essentials in Cytopathology
Series Editor
Momin T. Siddiqui

 Springer

Essentials in Cytopathology

Series Editor

Momin T. Siddiqui
Department of Pathology and
Laboratory Medicine
Weill-Cornell Medicine
New York Presbyterian Hospital
New York, NY
USA

The subspecialty of Cytopathology is 60 years old and has become established as a solid and reliable discipline in medicine. As expected, cytopathology literature has expanded in a remarkably short period of time, from a few textbooks prior to the 1980's to a current library of texts and journals devoted exclusively to cytomorphology that is substantial. Essentials in Cytopathology does not presume to replace any of the distinguished textbooks in Cytopathology. Instead, the series will publish generously illustrated and user-friendly guides for both pathologists and clinicians.

More information about this series at <http://www.springer.com/series/6996>

Abha Goyal • Rema Rao
Momin T. Siddiqui
Editors

Pancreas and Biliary Tract Cytohistology

 Springer

Editors

Abha Goyal
Department of Pathology and
Laboratory Medicine
Weill-Cornell Medicine
New York Presbyterian Hospital
New York, NY
USA

Rema Rao
Department of Pathology and
Laboratory Medicine
Weill-Cornell Medicine
New York Presbyterian Hospital
New York, NY
USA

Momin T. Siddiqui
Department of Pathology and
Laboratory Medicine
Weill-Cornell Medicine
New York Presbyterian Hospital
New York, NY
USA

ISSN 1574-9053

Essentials in Cytopathology

ISBN 978-3-030-22432-5

<https://doi.org/10.1007/978-3-030-22433-2>

ISSN 1574-9061 (electronic)

ISBN 978-3-030-22433-2 (eBook)

© Springer Nature Switzerland AG 2019

This work is subject to copyright. All rights are reserved by the Publisher, whether the whole or part of the material is concerned, specifically the rights of translation, reprinting, reuse of illustrations, recitation, broadcasting, reproduction on microfilms or in any other physical way, and transmission or information storage and retrieval, electronic adaptation, computer software, or by similar or dissimilar methodology now known or hereafter developed.

The use of general descriptive names, registered names, trademarks, service marks, etc. in this publication does not imply, even in the absence of a specific statement, that such names are exempt from the relevant protective laws and regulations and therefore free for general use.

The publisher, the authors, and the editors are safe to assume that the advice and information in this book are believed to be true and accurate at the date of publication. Neither the publisher nor the authors or the editors give a warranty, expressed or implied, with respect to the material contained herein or for any errors or omissions that may have been made. The publisher remains neutral with regard to jurisdictional claims in published maps and institutional affiliations.

This Springer imprint is published by the registered company Springer Nature Switzerland AG

The registered company address is: Gewerbestrasse 11, 6330 Cham, Switzerland

*To my loving parents and
husband, Vineet, for their
constant support and
encouragement*

– Abha Goyal, MD

*To my mother, Kamala
Ramaswamy, for her undying
love and support to me and
living by example*

– Rema Rao, MD

*To my mentors, Drs. Dorothy
Rosenthal and Syed Z. Ali, for
instilling in me a passion for
cytopathology*

– Momin T. Siddiqui, MD

Preface

Cytopathology has evolved over the last 75 years exponentially and is now an established and respected discipline in medicine. Cytopathology and its practitioners provide an accurate diagnosis by assessing fine needle aspiration samples procured by a variety of procedures, including CT image and ultrasound guidance. These samples also provide material for molecular characterization of tumors for targeted therapy. In an era where personalized medicine is the new reality for optimizing diagnosis and treatment of a wide variety of pathologic lesions/tumors, cytopathology continues to be vital, robust, and much in demand. The cytopathology literature continues to evolve, and *Essentials in Cytopathology* has kept pace with these needs by publishing generously illustrated and user-friendly guides for pathologists and clinicians.

In this current text from the *Essentials in Cytopathology*, we focus on all aspects of pancreatic pathology, from key features of benign and malignant lesions to diagnostic pearls for differential diagnosis of encountered entities in pancreatobiliary fine needle aspirations and small biopsies. Most of the authors are faculty members in Weill Cornell Medical College, Department of Pathology and Laboratory Medicine, and the Papanicolaou Cytopathology Laboratory. They bring to this volume the legacy of Dr. George Papanicolaou and the collective experience of a pre-eminent cytopathology service spanning a long time span. All chapters in the current text follow a similar format, a brief introduction and a practical approach to diagnose benign and malignant lesions. The key cytomorphologic features and main

differential diagnoses are also summarized in concise tables, where applicable. Images are also added to complement the text and represent key findings pertaining to the text discussion. An important and current chapter on molecular testing will also be very useful for the readership for their daily practice in this era of targeted therapy.

The editors and authors are indebted to our students and clinical colleagues, who motivate and provide feedback to us to become the best that we possibly can for our patients. We hope that this new addition to the *Essentials in Cytopathology* will be a practical resource for cytotechnologists, cytopathologists, and pathologists who are practicing cytopathology and rendering diagnoses on small biopsy samples on pancreatic lesions.

New York, NY, USA

Momin T. Siddiqui, MD, FIAC

Contents

1	Indications and Techniques of Fine-Needle Aspiration of the Pancreas	1
	Lauren Pioppo and Amy Tyberg	
2	Reporting of Pancreatico-biliary Cytopathology ...	21
	Abha Goyal	
3	Cytology of Normal Pancreas	37
	Ami P. Patel and Rema Rao	
4	Nonneoplastic Solid Mass Lesions of the Pancreas	65
	Simon Sung and Rema Rao	
5	Pancreatic Ductal Adenocarcinoma and Its Variants	95
	Kartik Viswanathan and Rema Rao	
6	Pancreatic Neuroendocrine Tumors and Other Solid Tumors of Pancreas	147
	Jacob Sweeney and Rema Rao	
7	Intraductal Papillary Mucinous Neoplasms	181
	Lorene Yoxtheimer and Abha Goyal	
8	Mucinous Cystic Neoplasms	203
	Lorene Yoxtheimer and Abha Goyal	

9	Other Cystic Lesions of the Pancreas	217
	Abha Goyal	
10	Metastases to the Pancreas	239
	Momin T. Siddiqui	
11	Bile Duct Brush Cytology	259
	Abha Goyal	
12	Ancillary Studies in the Cytologic Diagnosis of Pancreatico-biliary Lesions.	275
	Jonas J. Heymann	
Index.		341

Editors

Abha Goyal, MD Department of Pathology and Laboratory Medicine, Weill-Cornell Medicine, New York Presbyterian Hospital, New York, NY, USA

Momin T. Siddiqui, MD Department of Pathology and Laboratory Medicine, Weill-Cornell Medicine, New York Presbyterian Hospital, New York, NY, USA

Rema Rao, MD Department of Pathology and Laboratory Medicine, Weill-Cornell Medicine, New York Presbyterian Hospital, New York, NY, USA

Contributors

Jonas J. Heymann, MD Department of Pathology and Laboratory Medicine, Weill-Cornell Medicine, New York Presbyterian Hospital, New York, NY, USA

Ami P. Patel, MD Department of Pathology and Laboratory Medicine, Weill-Cornell Medicine, New York Presbyterian Hospital, New York, NY, USA

Lauren Pioppo, MD Rutgers Robert Wood Johnson Medical School and University Hospital, Department of Internal Medicine, New Brunswick, NJ, USA

Simon Sung, MD Columbia University Medical Center-New York Presbyterian, Department of Pathology and Cell Biology, New York, NY, USA

Jacob Sweeney, MD, BA Department of Pathology and Laboratory Medicine, Weill-Cornell Medicine, New York Presbyterian Hospital, New York, NY, USA

Amy Tyberg, MD Rutgers Robert Wood Johnson Medical School and University Hospital, Departments of Internal Medicine, Gastroenterology, and Hepatology, New Brunswick, NJ, USA

Kartik Viswanathan, MD, PhD Department of Pathology and Laboratory Medicine, Weill-Cornell Medicine, New York Presbyterian Hospital, New York, NY, USA

Lorene Yoxtheimer, MD Department of Pathology and Laboratory Medicine, Weill-Cornell Medicine, New York Presbyterian Hospital, New York, NY, USA



Indications and Techniques of Fine-Needle Aspiration of the Pancreas

Lauren Pioppo and Amy Tyberg

Introduction

The prognosis of pancreatic cancer remains poor, despite advances in medical and surgical therapies. Even early-stage tumors have low 5-year survival rates, and this dismal prognosis is thought to be in part from delayed clinical symptoms and accurate diagnosis [1, 2]. Surgery remains the best available therapy, but approximately 80% of patients present with advanced tumors that are not amenable to potentially curative surgical resection [3]. Thus, early diagnosis and intervention may be the only way to prolong survival and improve prognosis [4].

Endoscopic ultrasound (EUS) with fine-needle aspiration (FNA) is currently the standard of care for obtaining a tissue diagnosis in the pancreas. EUS-FNA is a minimally invasive procedure that has been found to be safe, effective, and accurate in pancreatic tissue diagnosis [5]. Multiple considerations must be made in performing a successful EUS-FNA including

L. Pioppo

Rutgers Robert Wood Johnson Medical School and University Hospital,
Department of Internal Medicine, New Brunswick, NJ, USA

A. Tyberg (✉)

Rutgers Robert Wood Johnson Medical School and University Hospital,
Departments of Internal Medicine, Gastroenterology, and Hepatology,
New Brunswick, NJ, USA

e-mail: Amy.tyberg@rutgers.edu

endoscopic technique, needle size and type, lesion location, availability of on-site cytopathology, use of accessories, and use of other imaging techniques such as elastography and contrast-harmonic EUS [6]. Here, we review the indications and major techniques of EUS-FNA.

Diagnostic EUS

EUS is highly sensitive in detecting pancreatic lesions, with multiple studies reporting sensitivity to be 91–100% [7–18]. The two types of echoendoscopes generally used in clinical practice are radial and linear array echoendoscopes [19, 20]. Radial array echoendoscopes generate ultrasound images that are perpendicular to the axis of the endoscope tip, which is not suitable for EUS-guided biopsy sampling. Linear array echoendoscopes produce ultrasound images that are parallel to the long axis of the endoscope and allow FNA to be performed through the instrument under real-time guidance [21]. Linear EUS is generally preferred over radial EUS by endoscopists, even when FNA is not required. This may be due to experience and training, as studies comparing radial and linear EUS in diagnosing pancreatic malignancies have inconsistent results [22–26].

The main objectives of EUS in the management of pancreatic lesions are detection, staging, and obtaining a tissue diagnosis. The pancreatic head, neck, and uncinate process can be viewed from the duodenum and the tail and body of the pancreas from the stomach. The close proximity of the echoendoscope to the pancreas allows for excellent pancreatic visualization [6]. EUS has been shown to be superior to cross-sectional imaging, including conventional and helical computed tomography (CT), in detecting pancreatic tumors [7–18]. An EUS image of a pancreatic adenocarcinoma versus a serous cystadenoma can be seen in Figs. 1.1 and 1.2, respectively. Smaller lesions tend to be more difficult to detect, and EUS remains the most sensitive imaging modality for detecting lesions less than 2 cm [27]. EUS has also consistently

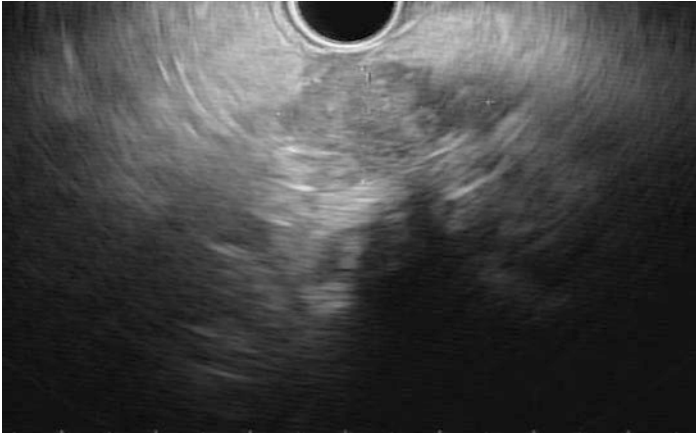


Fig. 1.1 Endoscopic ultrasound image of a pancreatic adenocarcinoma: hypoechoic, heterogenous oval-shaped lesion with irregular borders



Fig. 1.2 Endoscopic ultrasound image of a pancreatic serous cystadenoma: hypoechoic structure with microcystic components

been found to be superior in terms of accuracy to conventional CT for staging and determining tumor extension, but the results are less consistent when comparing EUS to helical CT [7–16, 28–31]. EUS has been demonstrated to be superior to conventional CT in identifying vascular involvement of the tumor, which is important in determining surgical resectability [32]. The reported accuracy of EUS for determining the N-stage of the tumor varies in the literature, ranging from 56 to 87% [7, 33–37].

EUS-FNA

While EUS remains the most sensitive imaging modality for pancreatic lesions, tissue sampling is needed to most accurately distinguish between benign and malignant lesions. The cytopathology and histology obtained from tissue acquired by EUS-FNA can help establish a tissue diagnosis. EUS-FNA has been widely accepted as a safe, effective, and consistent means to diagnose pancreatic cancer [38]. In a large meta-analysis of 41 studies conducted in 1995–2008 with a total of 4766 patients who underwent EUS-FNA, the pooled accuracy was reported to be 86.8% and the specificity 95.8% [39]. The study also found that the accuracy of EUS-FNA was improving with time, which can likely be attributed to more specialized training of endoscopists and the improvement of available instruments [6, 40].

When compared to other modalities, namely, CT-guided percutaneous biopsy and endoscopic retrograde cholangiopancreatography (ERCP), EUS-FNA has been found to be both more sensitive and less invasive [41, 42]. EUS-FNA has also been shown to be more sensitive for detecting and sampling malignant ascites than CT-guided biopsies and has been established as a safe and effective salvage maneuver in cases of a nondiagnostic ERCP brush cytology or CT-guided biopsy [43, 44].

EUS-FNA is also used for the sampling of pancreatic cysts, particularly those with high-risk features seen on CT or MRI. Concerning features include cyst size larger than 2 cm, main pancreatic duct diameter larger than 5 mm, and presence of a mural nodule. The risk of mortality from a potentially malig-



Fig. 1.3 Endoscopic ultrasound image of a pancreatic cyst being sampled by fine-needle aspiration (FNA): anechoic, round, homogenous structure with a hyperechoic FNA needle in the center

nant cyst should also be considered. The Charlson comorbidity index can be used to help determine which patients are reasonable candidates for EUS-FNA of a pancreatic cyst versus those patients who have a high risk of death from other medical comorbidities [45, 46]. EUS can be performed to determine if the cyst contains a solid component, and cyst content can be obtained by FNA [47] (Fig. 1.3). Cyst fluid analysis may include cytology, tumor markers, mucin, biochemical tests, and molecular analysis [48]. However, low cellular content of aspirates from pancreatic cysts limits the sensitivity of cytology for malignancy [49]. As discussed later in the chapter, use of microforceps biopsy may help increase cellular yield.

EUS-FNA Techniques

When performing EUS-FNA, many considerations must be made for successful sampling. These include the position of the echoendoscope during the procedure and the number of passes needed

to procure a diagnostic sample and minimize complications. The endoscopist also must consider the choice of needle and whether to use suction technique and/or the stylet with pull-back technique. Finally, tissue yield may also be affected by the availability of on-site cytopathology to provide real-time feedback on the quality of the sample.

Position and Number of Passes

Positioning of the echoendoscope is critical when performing FNA to allow for easy passage of the needle into the target lesion. The transesophageal and transgastric position of the echoendoscope is preferred over the transduodenal position to allow the echoendoscope to be in a stable position with a straight tip. This position facilitates passage of the FNA needle. Needle passage is more difficult when the tip of the echoendoscope is flexed, as when targeting the uncinate process or pancreatic neck from the duodenal bulb. Methods of troubleshooting this issue include using a smaller gauge needle or maneuvering the echoendoscope into the long position [50].

It is generally recommended that the endoscopist samples multiple sections of a pancreatic lesion rather than a single section to improve diagnostic yield. Neoplastic lesions tend to be heterogeneous; thus sampling multiple areas, especially the periphery, improves cellular and diagnostic yield [50]. A fanning technique in which multiple areas of the lesion are sampled by repositioning the needle angle using the dials and elevator intermittently has also been described. This method has been shown to increase diagnostic yield by almost 30% and also decreases the amount of blood and artifact from previous tract sites [50–52].

Currently, there is no consensus regarding the optimal number of passes or sampling techniques for EUS-FNA. The ideal number has been estimated by various studies to be between 3 and 7, and a recent study suggests that sensitivity was highest after four passes and did not increase significantly beyond that [53–56]. When deciding the number of passes to take, the endoscopist must weigh the benefit of higher diagnostic yield against the increased

risk of cellular injury and complications with each sampling. This is greatly simplified by the availability of on-site cytopathology to provide real-time feedback on FNA cellular yield. However, deciding the optimal and safest number of passes remains a difficult decision in centers without the convenience of on-site cytopathology and relies heavily on the knowledge and expertise of the endoscopist.

Needle Choice

Generally, the choice of needle to use in EUS-FNA is dependent on the performing endoscopist's clinical judgment. The endoscopist must consider which needle will provide the highest cellular yield, as well as the lowest chance of sample contamination and procedure complications. The flexibility of the needle relative to the location of the targeted pancreatic lesion must also be considered. When the tip of the echoendoscope is flexed, as when sampling the uncinate process or pancreatic neck from the duodenal bulb, a more pliable needle may be necessary [6].

There are three available gauges of needles available for FNA: 19 G, 22 G, and 25 G. Multiple randomized controlled trials showed no significant difference in diagnostic accuracy when using 22 G and 25 G needles [53–56], and a recent meta-analysis of seven randomized controlled trials revealed non-superiority in terms of sensitivity of 25 G over 22 G needles and no significant difference in specificity [56]. However, three randomized controlled trials found that the 25 G needle was superior for sampling lesions of the pancreatic head and uncinate process [53, 54, 57]. There are fewer studies comparing the 19 G needle, but one series reported higher diagnostic accuracy and improved sample quality using the 19 G needle as compared to the 22 G or 25 G. However, this study also found an increase in technical failure of the 19 G needle when sampling the pancreatic head or uncinate process, suggesting that the 19 G needle has lower efficacy in sampling pancreatic head lesions [58]. Needle choice remains heavily dependent on the experience, familiarity, and preference of the performing endoscopist.

Histology and Fine-Needle Biopsy

Tissue sampling by FNA does have some limitations. As stated earlier, there is no clear guideline regarding the optimal number of passes to take when sampling a lesion especially when on-site cytopathology is not available. There is also an increased chance of obtaining an inadequate sample when there is significant pancreatic fibrosis and tissue distortion, which is seen in chronic pancreatitis [59] (Fig. 1.4). FNA is less helpful in diagnosing certain conditions including lymphoma, stromal tumors, and autoimmune pancreatitis because the cytology obtained does not maintain the native tissue architecture. These special circumstances warrant another technique, namely, fine-needle biopsy (FNB). FNB is characterized by a core trap, which reduces the number of passes, and thus likely complications, needed to establish a tissue diagnosis. Studies report inconsistent results when comparing diagnostic yield of EUS-FNB to FNA, but overall appear to be in favor of EUS-FNB [60–65]. A recent meta-analysis of 11 randomized controlled trials reported EUS-FNB yielded better specimen adequacy, higher diagnostic accuracy, and fewer number of



Fig. 1.4 Endoscopic ultrasound image of chronic pancreatitis: hyperechoic stranding and lobularity with calcifications

needle passes [66]. However, earlier studies found that the two methods were comparable in terms of accuracy [65, 67–69]. It has also been suggested that EUS-FNB should be used when there is no available on-site cytopathology [70].

There are many EUS-compatible core biopsy needles that are able to obtain a solid core of tissue with preserved architecture [6]. Similar to FNA needles, these needles are available in three gauges: 19 G, 22 G, and 25 G. Standard FNA needles may also be used for FNB, but needles with more flexible tips have also been developed for FNB. Among these needles are the reverse bevel needle, Procore™, fork-tip needle, SharkCore™, and Franseen crown-tip needle with three cutting edges, Acquire® [71, 72]. A recent meta-analysis revealed no significant difference between the Procore™ 22 G FNB needle and standard 22 G FNA needles [73]. Other studies have found that the fork-tip needle had a higher diagnostic sensitivity than the reverse bevel needle, but another study demonstrated no significant difference in diagnostic yield between the two needles [74, 75]. No significant difference has been found between the SharkCore™ 22 G and 25 G needles, and these needles have been found to have an excellent pathologic diagnostic yield of 86% for pancreatic lesions [76]. Most recently, the Acquire® Franseen needle has been found to provide a histologically superior sample with fewer passes as compared to standard FNA needles [77]. However, other studies have demonstrated that the diagnostic accuracy was significantly improved when using a fork-tip needle compared to a Franseen needle, while another study found no significant difference in histologic tissue yield between the two needles [71, 78].

As discussed earlier, FNA of pancreatic cysts tends to be limited by scant cellularity of the sample [49]. Recently, a microforceps biopsy device has been designed to sample cysts that can be accessed with a 19 G EUS-FNA needle. An image of a microforceps biopsy is provided in Fig. 1.5. A recent small study of 42 patients reported a 90% cyst tissue acquisition yield with microforceps biopsy and found that microforceps biopsy was superior to cytology for providing a specific cyst diagnosis. Microforceps biopsy was comparable to EUS-FNA in differentiating between mucinous/non-mucinous cysts and diagnosing high-risk cysts, however



Fig. 1.5 Endoscopic ultrasound image of a microforceps biopsy

[79]. Mittal et al. reported a 100% technical success rate of microforceps biopsy of a pancreatic cyst in 27 patients, with 88.9% of samples yielding a pathology diagnosis [80].

Suction

Tissue can be drawn into the needle using different techniques, specifically suction on the FNA needle system versus the pull-back technique where the stylet is slowly pulled back as the needle is advanced. The use of suction on the FNA needle system was initially standard of care because it seemed logical that suction would increase cellular yield. However, while suction has been found to increase cellular yield in some studies, it has also been found to increase bloodiness, thus decreasing the overall quality of the sample [54, 81, 82]. There is no consensus regarding the use of suction during EUS-FNA, but it is generally recommended to avoid use of suction when sampling softer lesions that may contain blood and necrotic tissue. Suction may be useful in cases where low cellular yield is of particular concern, as when sampling a lesion in chronic pancreatitis [6].

Stylet

Every EUS-FNA system includes a rigid metal wire that runs through the length of the FNA needle called a stylet. The stylet is preloaded to the tip of the needle and is designed to prevent tissue plugs [50]. Three well-designed randomized controlled studies have shown that there is no significant increase in cellular yield when using the stylet, but there is a significant increase in bloodiness of the samples [83–86]. Two other randomized controlled studies found no difference between EUS-FNA with or without the use of the stylet but also found no significant difference in cellularity, contamination, bloodiness, and diagnostic accuracy [87, 88]. Some endoscopists also generally avoid using the stylet because it can increase the chance for needle-stick injuries. Thus, the use of the stylet feature is at the discretion of the endoscopist.

On-Site Cytopathology

On-site cytopathology has been shown to increase the diagnostic yield of EUS-FNA and decrease the number of unsatisfactory samples in multiple studies [87–90]. However, this is not a luxury available at every endoscopy center. Without on-site cytopathology, an average of 20% of EUS-FNA samples may be nondiagnostic [91]. The preparation of slides by a trained cytotechnologist rather than by an endoscopy nurse or technician has also been shown to increase diagnostic yield by 22% [92]. While on-site cytopathology comes with an increased cost for institutions, real-time feedback on cellular yield decreases the number of needles used and complication rates, which translates into cost savings via lower equipment costs, shorter procedure times, and fewer repeat procedures [91].

Complementary Techniques

The overall poor prognosis associated with delayed diagnosis of pancreatic malignancy has led to the development of complementary imaging modalities to improve EUS-FNA. Elastography

measures tissue stiffness and can help differentiate benign from malignant lesions. This is because malignancy tends to increase inflammation and fibrosis [93]. This technique can also allow endoscopists to target specific areas with the highest levels of inflammation. Hue histogram analysis of elastography images has been shown to have accuracy rates of up to 89% in differentiating benign from malignant lesions and lymph nodes [92, 94]. Another complementary imaging modality used in EUS-FNA is contrast-harmonic echo (CHE), which enhances vascular imaging by the injection of intravenous contrast agents that contain gas-filled microbubbles into peripheral veins. Better visualization of the microvasculature of a pancreatic lesion aids in the diagnosis of malignant lesions [6].

Standard confocal laser endomicroscopy (CLE) is performed by illuminating the targeted tissue and allows the real-time visualization of cellular and subcellular structures with up to 1000 times magnification and providing what is referred to as an optical biopsy [95]. Contrast is then administered intravenously or topically to accentuate the cellular, subcellular, and vasculature elements. Needle-CLE is another version of CLE and can be performed during EUS, which allows real-time histological diagnosis and decreases inconclusive results [96].

Summary

EUS-FNA is a noninvasive and accurate technique to sample a pancreatic lesion. It has been shown to be more sensitive than other available techniques and has the advantage of imaging and sampling the lesion simultaneously. A successful EUS-FNA requires a skilled endoscopist and multiple considerations, including position of the echoendoscope and target lesion, number of passes to take, and needle choice. Availability of on-site cytopathology provides real-time feedback on the cellular yield and overall reduces procedure time, cost, and complications. While FNA is not ideal in cases of chronic fibrosis of the pancreas, such as in chronic pancreatitis, other options are available including fine-needle biopsy, which can also be performed during EUS. Use of complementary

imaging modalities such as elastography, contrast-harmonic echo, and needle-confocal laser endomicroscopy should be considered to increase diagnostic yield. EUS-FNA remains the standard of care for sampling pancreatic tissue, and sensitivity and accuracy can be expected to improve over time with the improvement of instruments and specialized training of advanced endoscopists.

References

1. Jemal A, Siegel R, Ward E, Hao Y, Xu J, Thun MJ. Cancer statistics. *CA Cancer J Clin.* 2009;59:225–49.
2. Helmstaedter L, Riemann JF. Pancreatic cancer--EUS and early diagnosis. *Langenbeck's Arch Surg.* 2008;393:923–7.
3. Hidalgo M. Pancreatic cancer. *N Engl J Med.* 2010;362:1605–17.
4. Gansauge S, Gansauge F, Beger HG. Molecular oncology in pancreatic cancer. *J Mol Med.* 1996;74:313–20.
5. Vilmann P, Jacobsen GK, Henriksen FW, Hancke S. Endoscopic ultrasonography with guided fine needle aspiration biopsy in pancreatic disease. *Gastrointest Endosc.* 1992;38:172–3.
6. Kedia P, Gaidhane M, Kahaleh M. Technical advances in endoscopic ultrasound (EUS)-guided tissue acquisition for pancreatic Cancers: how can we get the best results with EUS-guided fine needle aspiration? *Clin Endosc.* 2013;46:552–62.
7. Rösch T, Braig C, Gain T, Feuerbach S, Siewert JR, Schusdziarra V, et al. Staging of pancreatic and ampullary carcinoma by endoscopic ultrasonography. Comparison with conventional sonography, computed tomography, and angiography. *Gastroenterology.* 1992;102:188–99.
8. Palazzo L, Roseau G, Gayet B, Vilgrain V, Belghiti J, Fékété F, et al. Endoscopic ultrasonography in the diagnosis and staging of pancreatic adenocarcinoma. Results of a prospective study with comparison to ultrasonography and CT scan. *Endoscopy.* 1993;25:143–50.
9. Müller MF, Meyenberger C, Bertschinger P, Schaer R, Marincek B. Pancreatic tumors: evaluation with endoscopic US, CT, and MR imaging. *Radiology.* 1994;190:745–51.
10. Legmann P, Vignaux O, Dousset B, Baraza AJ, Palazzo L, Dumontier I, et al. Pancreatic tumors: comparison of dual-phase helical CT and endoscopic sonography. *AJR Am J Roentgenol.* 1998;170:1315–22.
11. Gress FG, Hawes RH, Savides TJ, Ikenberry SO, Cummings O, Kopecky K, et al. Role of EUS in the preoperative staging of pancreatic cancer: a large single-center experience. *Gastrointest Endosc.* 1999;50:786–91.
12. Marty O, Aubertin JM, Bouillot JL, Hernigou A, Bloch F, Petite JP. Prospective comparison of ultrasound endoscopy and computed

- tomography in the assessment of locoregional invasiveness of malignant ampullar and pancreatic tumors verified surgically. *Gastroenterol Clin Biol.* 1995;19:197–203.
13. Melzer E, Avidan B, Heyman Z, Coret A, Bar-Meir S. Preoperative assessment of blood vessel involvement in patients with pancreatic cancer. *Isr J Med Sci.* 1996;32:1086–8.
 14. Sugiyama M, Hagi H, Atomi Y, Saito M. Diagnosis of portal venous invasion by pancreatobiliary carcinoma: value of endoscopic ultrasonography. *Abdom Imaging.* 1997;22:434–8.
 15. Rivadeneira DE, Pochapin M, Grobmyer SR, Lieberman MD, Christos PJ, Jacobson I, et al. Comparison of linear array endoscopic ultrasound and helical computed tomography for the staging of periampullary malignancies. *Ann Surg Oncol.* 2003;10:890–7.
 16. DeWitt J, Devereaux B, Chriswell M, McGreevy K, Howard T, Imperiale TF, et al. Comparison of endoscopic ultrasonography and multidetector computed tomography for detecting and staging pancreatic cancer. *Ann Intern Med.* 2004;141:753–63.
 17. Mertz HR, Sechopoulos P, Delbeke D, Leach SD. EUS, PET, and CT scanning for evaluation of pancreatic adenocarcinoma. *Gastrointest Endosc.* 2000;52:367–71.
 18. Agarwal B, Abu-Hamda E, Molke KL, Correa AM, Ho L. Endoscopic ultrasound-guided fine needle aspiration and multidetector spiral CT in the diagnosis of pancreatic cancer. *Am J Gastroenterol.* 2004;99:844–50.
 19. Byrne MF, Jowell PS. Gastrointestinal imaging: endoscopic ultrasound. *Gastroenterology.* 2002;122:1631–48.
 20. ASGE TECHNOLOGY COMMITTEE, Tierney WM, Adler DG, Chand B, Conway JD, Croffie JMB, et al. Echoendoscopes. *Gastrointest Endosc.* 2007;66:435–42.
 21. Shin EJ, Topazian M, Goggins MG, Syngal S, Saltzman JR, Lee JH, et al. Linear-array EUS improves detection of pancreatic lesions in high-risk individuals: a randomized tandem study. *Gastrointest Endosc.* 2015;82:812–8.
 22. Gress F, Savides T, Cummings O, Sherman S, Lehman G, Zaidi S, et al. Radial scanning and linear array endosonography for staging pancreatic cancer: a prospective randomized comparison. *Gastrointest Endosc.* 1997;45:138–42.
 23. Jamil LH, Gill KRS, Gross S, Crook J, Raimondo M, Woodward T, et al. Radial versus linear EUS in evaluation of suspected pancreatic cancer: is it sufficient to use linear eus alone? *Gastrointest Endosc.* 2009;69:S266.
 24. Matthes K, Bounds BC, Collier K, Gutierrez A, Brugge WR. EUS staging of upper GI malignancies: results of a prospective randomized trial. *Gastrointest Endosc.* 2006;64:496–502.
 25. Siemsen M, Svendsen LB, Knigge U, Vilmann P, Jensen F, Rasch L, et al. A prospective randomized comparison of curved array and radial echoen-

- doscopy in patients with esophageal cancer. *Gastrointest Endosc.* 2003;58:671–6.
26. Rösch T. Endoscopic ultrasonography in pancreatic cancer. *Endoscopy.* 1994;26:806–7.
 27. Shrikhande SV, Barreto SG, Goel M, Arya S. Multimodality imaging of pancreatic ductal adenocarcinoma: a review of the literature. *HPB (Oxford).* 2012;14:658–68.
 28. Mukai H, Nakajima M, Yasuda K, Cho E, Mizuma Y, Hayakumo T, et al. Preoperative diagnosis and staging of pancreatic cancer by endoscopic ultrasonography (EUS)--a comparative study with other diagnostic tools. *Nihon Shokakibyō Gakkai Zasshi.* 1991;88:2132–42.
 29. Midwinter MJ, Beveridge CJ, Wilsdon JB, Bennett MK, Baudouin CJ, Charnley RM. Correlation between spiral computed tomography, endoscopic ultrasonography and findings at operation in pancreatic and ampullary tumours. *Br J Surg.* 1999;86:189–93.
 30. Soriano A, Castells A, Ayuso C, Ayuso JR, de Caralt MT, Ginès MA, et al. Preoperative staging and tumor resectability assessment of pancreatic cancer: prospective study comparing endoscopic ultrasonography, helical computed tomography, magnetic resonance imaging, and angiography. *Am J Gastroenterol.* 2004;99:492–501.
 31. Ramsay D, Marshall M, Song S, Zimmerman M, Edmunds S, Yusoff I, et al. Identification and staging of pancreatic tumours using computed tomography, endoscopic ultrasound and mangafodipir trisodium-enhanced magnetic resonance imaging. *Australas Radiol.* 2004;48:154–61.
 32. Yang R, Lu M, Qian X, Chen J, Li L, Wang J, et al. Diagnostic accuracy of EUS and CT of vascular invasion in pancreatic cancer: a systematic review. *J Cancer Res Clin Oncol.* 2014;140:2077–86.
 33. Nakaizumi A, Uehara H, Iishi H, Tatsuta M, Kitamura T, Kuroda C, et al. Endoscopic ultrasonography in diagnosis and staging of pancreatic cancer. *Dig Dis Sci.* 1995;40:696–700.
 34. Kulig J, Popiela T, Zajac A, Kłęk S, Kołodziejczyk P. The value of imaging techniques in the staging of pancreatic cancer. *Surg Endosc.* 2005;19:361–5.
 35. Buscail L, Pagès P, Berthélemy P, Fourtanier G, Frexinos J, Escourrou J. Role of EUS in the management of pancreatic and ampullary carcinoma: a prospective study assessing resectability and prognosis. *Gastrointest Endosc.* 1999;50:34–40.
 36. Ahmad NA, Lewis JD, Ginsberg GG, Rosato EF, Morris JB, Kochman ML. EUS in preoperative staging of pancreatic cancer. *Gastrointest Endosc.* 2000;52:463–8.
 37. Akahoshi K, Chijiwa Y, Nakano I, Nawata H, Ogawa Y, Tanaka M, et al. Diagnosis and staging of pancreatic cancer by endoscopic ultrasound. *Br J Radiol.* 1998;71:492–6.

38. Hasan MK, Hawes RH. EUS-guided FNA of solid pancreas tumors. *Gastrointest Endosc Clin N Am.* 2012;22:155–67. vii.
39. Puli SR, Bechtold ML, Buxbaum JL, Eloubeidi MA. How good is endoscopic ultrasound-guided fine-needle aspiration in diagnosing the correct etiology for a solid pancreatic mass?: a meta-analysis and systematic review. *Pancreas.* 2013;42:20–6.
40. Chen J, Yang R, Lu Y, Xia Y, Zhou H. Diagnostic accuracy of endoscopic ultrasound-guided fine-needle aspiration for solid pancreatic lesion: a systematic review. *J Cancer Res Clin Oncol.* 2012;138:1433–41.
41. Horwhat JD, Paulson EK, McGrath K, Branch MS, Baillie J, Tyler D, et al. A randomized comparison of EUS-guided FNA versus CT or US-guided FNA for the evaluation of pancreatic mass lesions. *Gastrointest Endosc.* 2006;63:966–75.
42. Athanassiadou P, Grapsa D. Value of endoscopic retrograde cholangiopancreatography-guided brushings in preoperative assessment of pancreaticobiliary strictures: what's new? *Acta Cytol.* 2008;52:24–34.
43. Harewood GC, Wiersema MJ. Endosonography-guided fine needle aspiration biopsy in the evaluation of pancreatic masses. *Am J Gastroenterol.* 2002;97:1386–91.
44. DeWitt J, LeBlanc J, McHenry L, McGreevy K, Sherman S. Endoscopic ultrasound-guided fine-needle aspiration of ascites. *Clin Gastroenterol Hepatol.* 2007;5:609–15.
45. Sahara K, Ferrone CR, Brugge WR, Morales-Oyarvide V, Warshaw AL, Lillemoe KD, et al. Effects of comorbidities on outcomes of patients with Intraductal papillary mucinous neoplasms. *Clin Gastroenterol Hepatol.* 2015;13:1816–23.
46. Charlson M, Szatrowski TP, Peterson J, Gold J. Validation of a combined comorbidity index. *J Clin Epidemiol.* 1994;47:1245–51.
47. Barkin JA, Barkin JS. Pancreatic cysts: controversies, advances, diagnoses, and therapies. *Pancreas.* 2017;46:735–41.
48. Yoon WJ, Brugge WR. Pancreatic cystic neoplasms: diagnosis and management. *Gastroenterol Clin N Am.* 2012;41:103–18.
49. Khalid A, Brugge W. ACG practice guidelines for the diagnosis and management of neoplastic pancreatic cysts. *Am J Gastroenterol.* 2007;102:2339–49.
50. Varadarajulu S, Fockens P, Hawes RH. Best practices in endoscopic ultrasound-guided fine-needle aspiration. *Clin Gastroenterol Hepatol.* 2012;10:697–703.
51. Bang JY, Magee SH, Ramesh J, Trevino JM, Varadarajulu S. Randomized trial comparing fanning with standard technique for endoscopic ultrasound-guided fine-needle aspiration of solid pancreatic mass lesions. *Endoscopy.* 2013;45:445–50.
52. Lee JM, Lee HS, Hyun JJ, Lee JM, Yoo IK, Kim SH, et al. Slow-pull using a fanning technique is more useful than the standard suction technique in EUS-guided fine needle aspiration in pancreatic masses. *Gut Liver.* 2018;12:360–6.

53. Siddiqui UD, Rossi F, Rosenthal LS, Padda MS, Murali-Dharan V, Aslanian HR. EUS-guided FNA of solid pancreatic masses: a prospective, randomized trial comparing 22-gauge and 25-gauge needles. *Gastrointest Endosc.* 2009;70:1093–7.
54. Camellini L, Carlinfante G, Azzolini F, Iori V, Cavina M, Sereni G, et al. A randomized clinical trial comparing 22G and 25G needles in endoscopic ultrasound-guided fine-needle aspiration of solid lesions. *Endoscopy.* 2011;43:709–15.
55. Fabbri C, Polifemo AM, Luigiano C, Cennamo V, Baccharini P, Collina G, et al. Endoscopic ultrasound-guided fine needle aspiration with 22- and 25-gauge needles in solid pancreatic masses: a prospective comparative study with randomisation of needle sequence. *Dig Liver Dis.* 2011;43:647–52.
56. Facciorusso A, Stasi E, Di Maso M, Serviddio G, Ali Hussein MS, Muscatiello N. Endoscopic ultrasound-guided fine needle aspiration of pancreatic lesions with 22 versus 25 gauge needles: a meta-analysis. *United European Gastroenterol J.* 2017;5:846–53.
57. Sakamoto H, Kitano M, Komaki T, Noda K, Chikugo T, Dote K, et al. Prospective comparative study of the EUS guided 25-gauge FNA needle with the 19-gauge Trucut needle and 22-gauge FNA needle in patients with solid pancreatic masses. *J Gastroenterol Hepatol.* 2009;24:384–90.
58. Song TJ, Kim JH, Lee SS, Eum JB, Moon SH, Park DH, et al. The prospective randomized, controlled trial of endoscopic ultrasound-guided fine-needle aspiration using 22G and 19G aspiration needles for solid pancreatic or peripancreatic masses. *Am J Gastroenterol.* 2010;105:1739–45.
59. Aithal GP, Anagnostopoulos GK, Tam W, Dean J, Zaitoun A, Kocjan G, et al. EUS-guided tissue sampling: comparison of “dual sampling” (Trucut biopsy plus FNA) with “sequential sampling” (Trucut biopsy and then FNA as required). *Endoscopy.* 2007;39:725–30.
60. Iglesias-Garcia J, Poley J-W, Larghi A, Giovannini M, Petrone MC, Abdulkader I, et al. Feasibility and yield of a new EUS histology needle: results from a multicenter, pooled, cohort study. *Gastrointest Endosc.* 2011;73:1189–96.
61. van Riet PA, Cahen DL, Poley J-W, Bruno MJ. Mapping international practice patterns in EUS-guided tissue sampling: outcome of a global survey. *Endosc Int Open.* 2016;4:E360–70.
62. Aadam AA, Wani S, Amick A, Shah JN, Bhat YM, Hamerski CM, et al. A randomized controlled cross-over trial and cost analysis comparing endoscopic ultrasound fine needle aspiration and fine needle biopsy. *Endosc Int Open.* 2016;4:E497–505.
63. Kamata K, Kitano M, Yasukawa S, Kudo M, Chiba Y, Ogura T, et al. Histologic diagnosis of pancreatic masses using 25-gauge endoscopic ultrasound needles with and without a core trap: a multicenter randomized trial. *Endoscopy.* 2016;48:632–8.

64. Choi HJ, Moon JH, Kim HK, Lee YN, Kim DC, Lee TH, et al. Mo1488 comparison of EUS-fine needle biopsy with EUS-fine needle aspiration as a historical control for diagnosis of pancreatic solid masses. *Gastrointest Endosc.* 2013;77:AB401.
65. Alatawi A, Beuvon F, Grabar S, Leblanc S, Chaussade S, Terris B, et al. Comparison of 22G reverse-beveled versus standard needle for endoscopic ultrasound-guided sampling of solid pancreatic lesions. *United European Gastroenterol J.* 2015;3:343–52.
66. Li H, Li W, Zhou Q-Y, Fan B. Fine needle biopsy is superior to fine needle aspiration in endoscopic ultrasound guided sampling of pancreatic masses: a meta-analysis of randomized controlled trials. *Medicine (Baltimore).* 2018;97:e0207.
67. Wang J, Zhao S, Chen Y, Jia R, Zhang X. Endoscopic ultrasound guided fine needle aspiration versus endoscopic ultrasound guided fine needle biopsy in sampling pancreatic masses: a meta-analysis. *Medicine (Baltimore).* 2017;96:e7452.
68. Witt BL, Adler DG, Hilden K, Layfield LJ. A comparative needle study: EUS-FNA procedures using the HD ProCore™ and EchoTip® 22-gauge needle types. *Diagn Cytopathol.* 2013;41:1069–74.
69. Nagula S, Pourmand K, Aslanian H, Bucobo JC, Gonda TA, Gonzalez S, et al. Comparison of endoscopic ultrasound-fine-needle aspiration and endoscopic ultrasound-fine-needle biopsy for solid lesions in a multicenter, randomized trial. *Clin Gastroenterol Hepatol.* 2018;16:1307–1313.e1.
70. Varadarajulu S, Hawes RH. The changing paradigm in EUS-guided tissue acquisition. *Gastrointest Endosc Clin N Am.* 2014;24:1–7.
71. Bang JY, Hebert-Magee S, Navaneethan U, Hasan MK, Hawes R, Varadarajulu S. Randomized trial comparing the Franseen and fork-tip needles for EUS-guided fine-needle biopsy sampling of solid pancreatic mass lesions. *Gastrointest Endosc.* 2018;87:1432–8.
72. Attili F, Rimbaş M, Fantin A, Fabbri C, Carrara S, Di Maurizio L, et al. Performance of a new histology needle for EUS-guided fine needle biopsy: a retrospective multicenter study. *Dig Liver Dis.* 2018;50:469–74.
73. Bang JY, Hawes R, Varadarajulu S. A meta-analysis comparing ProCore and standard fine-needle aspiration needles for endoscopic ultrasound-guided tissue acquisition. *Endoscopy.* 2016;48:339–49.
74. Abdelfatah MM, Hamed A, Koutlas NJ, Aly FZ. The diagnostic and cellularity yield of reverse bevel versus fork-tip fine needle biopsy. *Diagn Cytopathol.* 2018;46:649. <https://doi.org/10.1002/dc.23966>.
75. Nayar MK, Paranandi B, Dawwas MF, Leeds JS, Darne A, Haugk B, et al. Comparison of the diagnostic performance of 2 core biopsy needles for EUS-guided tissue acquisition from solid pancreatic lesions. *Gastrointest Endosc.* 2017;85:1017–24.
76. DiMaio CJ, Kolb JM, Benias PC, Shah H, Shah S, Haluszka O, et al. Initial experience with a novel EUS-guided core biopsy needle (SharkCore): results of a large North American multicenter study. *Endosc Int Open.* 2016;4:E974–9.

77. El Hajj WH II, Reuss S, Randolph M, Harris A, Gromski MA, et al. Prospective assessment of the performance of a new fine needle biopsy device for EUS-guided sampling of solid lesions. *Clin Endosc.* 2018;51:576–83.
78. Abdelfatah MM, Grimm IS, Gangarosa LM, Baron TH. Cohort study comparing the diagnostic yields of 2 different EUS fine-needle biopsy needles. *Gastrointest Endosc.* 2018;87:495–500.
79. Basar O, Yuksel O, Yang DJ, Samarasena J, Forcione D, DiMaio CJ, et al. Feasibility and safety of microforceps biopsy in the diagnosis of pancreatic cysts. *Gastrointest Endosc.* 2018;88:79–86.
80. Mittal C, Obuch JC, Hammad H, Edmundowicz SA, Wani S, Shah RJ, et al. Technical feasibility, diagnostic yield, and safety of microforceps biopsies during EUS evaluation of pancreatic cystic lesions (with video). *Gastrointest Endosc.* 2018;87:1263–9.
81. LeBlanc JK, Ciaccia D, Al-Assi MT, McGrath K, Imperiale T, Tao L-C, et al. Optimal number of EUS-guided fine needle passes needed to obtain a correct diagnosis. *Gastrointest Endosc.* 2004;59:475–81.
82. Ge PS, Wani S, Watson RR, Sedarat A, Kim S, Marshall C, et al. Per-pass performance characteristics of endoscopic ultrasound-guided fine-needle aspiration of malignant solid pancreatic masses in a large multicenter cohort. *Pancreas.* 2018;47:296–301.
83. Kundu S, Conway J, Evans JA, Perkins LA, Geisinger K, Mishra G. A prospective, blinded, randomized trial assessing the yield of endoscopic ultrasound guided fine needle sampling (EUS-FNS) of solid lesions with suction versus no suction. *Gastrointest Endosc.* 2009;69:AB323–4.
84. Bang JY, Navaneethan U, Hasan MK, Hawes R, Varadarajulu S. Endoscopic ultrasound-guided specimen collection and evaluation techniques affect diagnostic accuracy. *Clin Gastroenterol Hepatol.* 2018;16:1820–1828.e4.
85. Sahai AV, Paquin SC, Gariépy G. A prospective comparison of endoscopic ultrasound-guided fine needle aspiration results obtained in the same lesion, with and without the needle stylet. *Endoscopy.* 2010;42:900–3.
86. Wani S, Early D, Kunkel J, Leathersich A, Hovis CE, Hollander TG, et al. Diagnostic yield of malignancy during EUS-guided FNA of solid lesions with and without a stylet: a prospective, single blind, randomized, controlled trial. *Gastrointest Endosc.* 2012;76:328–35.
87. Abe Y, Kawakami H, Oba K, Hayashi T, Yasuda I, Mukai T, et al. Effect of a stylet on a histological specimen in EUS-guided fine-needle tissue acquisition by using 22-gauge needles: a multicenter, prospective, randomized, controlled trial. *Gastrointest Endosc.* 2015;82:837–844.e1.
88. Rastogi A, Wani S, Gupta N, Singh V, Gaddam S, Reddymasu S, et al. A prospective, single-blind, randomized, controlled trial of EUS-guided FNA with and without a stylet. *Gastrointest Endosc.* 2011;74:58–64.
89. Wani S, Gupta N, Gaddam S, Singh V, Uluarac O, Romanas M, et al. A comparative study of endoscopic ultrasound guided fine needle aspiration with and without a stylet. *Dig Dis Sci.* 2011;56:2409–14.

90. Klapman JB, Logrono R, Dye CE, Waxman I. Clinical impact of on-site cytopathology interpretation on endoscopic ultrasound-guided fine needle aspiration. *Am J Gastroenterol.* 2003;98:1289–94.
91. Alsohaibani F, Girgis S, Sandha GS. Does onsite cytotechnology evaluation improve the accuracy of endoscopic ultrasound-guided fine-needle aspiration biopsy? *Can J Gastroenterol.* 2009;23:26–30.
92. Iglesias-Garcia J, Dominguez-Munoz JE, Abdulkader I, Larino-Noia J, Eugenyeva E, Lozano-Leon A, et al. Influence of on-site cytopathology evaluation on the diagnostic accuracy of endoscopic ultrasound-guided fine needle aspiration (EUS-FNA) of solid pancreatic masses. *Am J Gastroenterol.* 2011;106:1705–10.
93. Nasuti JF, Gupta PK, Baloch ZW. Diagnostic value and cost-effectiveness of on-site evaluation of fine-needle aspiration specimens: review of 5,688 cases. *Diagn Cytopathol.* 2002;27:1–4.
94. Mohanty SK, Pradhan D, Sharma S, Sharma A, Patnaik N, Feuerman M, et al. Endoscopic ultrasound guided fine-needle aspiration: what variables influence diagnostic yield? *Diagn Cytopathol.* 2018;46:293–8.
95. Giovannini M, Thomas B, Erwan B, Christian P, Fabrice C, Benjamin E, et al. Endoscopic ultrasound elastography for evaluation of lymph nodes and pancreatic masses: a multicenter study. *World J Gastroenterol.* 2009;15:1587–93.
96. Săftoiu A, Vilmann P, Ciurea T, Popescu GL, Lordache A, Hassan H, et al. Dynamic analysis of EUS used for the differentiation of benign and malignant lymph nodes. *Gastrointest Endosc.* 2007;66:291–300.



Reporting of Pancreatico-biliary Cytopathology

Abha Goyal

After the widespread adoption of standardized reporting and nomenclature for cervical cytology and thyroid cytology, in recent years, increasing efforts have been made to develop such unified diagnostic terminologies for cytology of other body sites as well. There are several advantages for such standardized reports, the foremost being the impact on patient management. The specific diagnostic categories attempt to correlate with the biologic behavior of different lesions and imply a certain risk of associated neoplasia/malignancy. Therefore, the use of such nomenclature provides more meaningful information to the clinician who can plan the management for the patient more effectively. The reporting systems also enable better extraction of information from laboratory information systems for research and quality assurance purposes.

Considering the importance of cytology in the diagnosis of pancreatic lesions and biliary strictures, the Papanicolaou Society of Cytopathology (Pap Society) recently proposed guidelines regarding various aspects of pancreatico-biliary cytology including the indications, techniques, terminology and nomenclature, ancillary studies, and postprocedure management.

A. Goyal (✉)

Department of Pathology and Laboratory Medicine, Weill-Cornell Medicine, New York Presbyterian Hospital, New York, NY, USA
e-mail: abg9017@med.cornell.edu

These guidelines were developed by a multidisciplinary group of experts following review of literature and discussion through an interactive Web-based forum and presentation at national and international meetings.

The Pap Society reporting scheme includes six categories:

- I. Nondiagnostic
- II. Negative (for malignancy)
- III. Atypical
- IV. Neoplastic
 - Neoplastic: Benign
 - Neoplastic: Other
- V. Suspicious for malignancy
- VI. Positive (malignant)

These guidelines emphasize a multidisciplinary approach, i.e., incorporating the clinical presentation, the imaging and ultrasound findings, results of cyst fluid biochemistry, and molecular analysis in formulating a cytologic diagnosis [1, 2]. This chapter will discuss the Pap Society nomenclature for pancreatico-biliary cytology and its practical application in daily practice.

Diagnostic Categories

Nondiagnostic

This diagnosis implies that no diagnostic or useful information can be obtained from the sample. Usually, nondiagnostic specimens result from technical and/or sampling issues. For example, the sampling of benign pancreatic tissue in the presence of a distinct pancreatic mass on imaging is nondiagnostic. An acellular aspirate of a cystic lesion without ancillary evidence of mucinous etiology will also be considered nondiagnostic. The presence of only gastric or duodenal contaminant epithelium in the aspirate of a pancreatic lesion will be placed in this category as well. Any cellular atypia in the aspirate will preclude the categorization of the sample as nondiagnostic.

Sample reports:

1. Nondiagnostic aspirate sample
 - Blood with gastrointestinal contaminant only.
2. Nondiagnostic aspirate sample
 - Benign pancreatic acinar and ductal epithelium (see note).
 - Note: In the presence of the pancreatic mass identified on imaging, the cytologic findings are considered nondiagnostic.
3. Nondiagnostic aspirate sample
 - Marked air-drying artifact precludes cytologic evaluation.

Negative

The negative category indicates that no malignancy or neoplasm or cellular atypia is identified in an adequately cellular sample obtained for evaluation of a lesion identified on imaging. The negative diagnosis on cytology, many a times, tends to be descriptive. For instance, there is often insufficient material for architectural and immunohistochemical evaluation for a diagnosis of autoimmune pancreatitis on cytology. However, an increased number of stromal fragments with chronic inflammatory cells can suggest this diagnosis on cytology. Similarly, a diagnosis of pseudocyst requires a low CEA level and a high amylase level. A cytologic diagnosis of pseudocyst may be suggested in the presence of histiocytes, inflammatory cells, and yellow amorphous pigment.

Pancreatic cyst aspirates with nonspecific cyst contents (i.e., histiocytes and debris) and without identifiable thick mucin and neoplastic epithelium and any ancillary testing can be problematic to diagnose. In our practice, we categorize these cases as “negative” with a note emphasizing the absence of high-grade epithelial atypia in the sample. The negative predictive value of cytology is reportedly 99% in the absence of “high-risk” stigmata and “worrisome” features (as defined by the 2012 international consensus guidelines for the management of pancreatic mucinous neoplasms) [3, 4]. This “negative” interpretation on cytology in

the context of the clinical and imaging findings aids the clinicians in conservative management and follow-up of the cyst.

It is important to note that bile duct brushings are known for their limited sensitivity (20–60% as per different studies) and a high false-negative rate [5–9]. This is more often due to sampling difficulties but could also be associated with interpretative challenges in the setting of well-differentiated adenocarcinomas and confounding factors such as primary sclerosing cholangitis and indwelling stents [8, 9].

Sample reports:

1. Negative for malignant cells
 - Cellular stromal fragments with chronic inflammatory cells (see note).
 - Note: The cytologic findings are suggestive of autoimmune pancreatitis. Clinical and radiologic correlation is recommended.
2. Negative for malignant cells
 - Cyst contents with inflammatory cells and yellow amorphous pigment (see note).
 - Note: The cytologic findings are suggestive of a pseudocyst. Correlation with clinical and imaging findings and results of cyst fluid analysis is recommended.
 - If available, cyst fluid biochemistry results including CEA and amylase levels can also be mentioned in the report.
3. Negative for malignant cells
 - Cyst contents with scant thick mucin (see note).
 - Note: No high-grade epithelial atypia is identified. The cytologic findings are suggestive but not diagnostic of a neoplastic mucinous cyst. Correlation with clinical and imaging findings and results of cyst fluid analysis is recommended.
4. Negative for malignant cells
 - Nonspecific cyst contents (see note).
 - Note: No diagnostic thick mucin or high-grade epithelial atypia is identified. Correlation with clinical and imaging findings and results of cyst fluid analysis is recommended.

Atypical

This category denotes that the cytologic findings are beyond the normal or reactive spectrum but are insufficient for the diagnosis of neoplasm or of suspicious for high-grade malignancy. Atypical category is often utilized in cases of limited cellularity or when the distinction between reactive atypia and malignancy cannot be made with certainty (Figs. 2.1, 2.2, and 2.3). It can also include changes of low-grade dysplasia in bile duct brushings.

Virk and colleagues reported that “atypical” cytology diagnoses of solid pancreatic mass lesions were associated with a 33–67% malignant rate. They found that the implementation of departmental consensus review can help lower the rate of

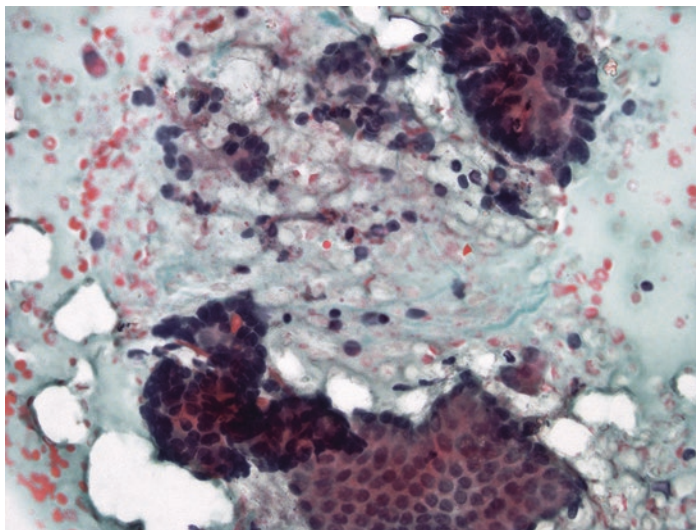


Fig. 2.1 Few crowded groups of epithelial cells in a background of gastrointestinal contamination and air-drying artifact. These findings are not qualitatively or quantitatively sufficient for either “suspicious for malignancy” or for “positive/malignant.” Such findings should be placed in the “atypical” category

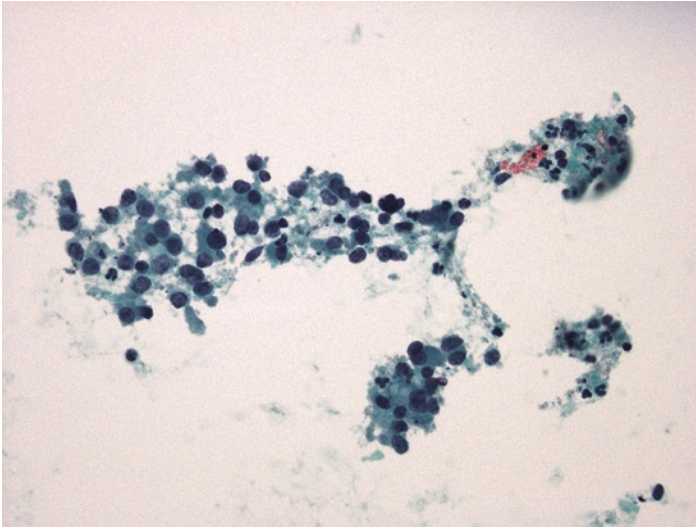


Fig. 2.2 Paucicellular pancreatic fine needle aspiration (FNA) specimen composed of polygonal cells with eccentrically located nuclei and coarse chromatin. Although the findings raise concern for the possibility of a pancreatic neuroendocrine tumor (PanNET), they are not diagnostic. Hence, these findings should be categorized as “atypical”

indeterminate diagnoses [10]. Similarly, in a meta-analysis of 23 studies, Abdelgawwad et al. reported that the frequency of atypical diagnoses for solid pancreatic masses ranged from 1 to 14% with an associated malignancy rate of 25–100% [11]. Likewise, bile duct brushings with atypical diagnoses are also associated with a high rate of malignancy (47–62%) [12, 13]. Considering the high rate of malignant outcome of this category, follow-up evaluation is warranted for these patients.

Sample reports:

1. Limited cellularity sample

- Atypical glandular epithelium (see note).
- Note: The cytologic findings are not diagnostic of malignancy.

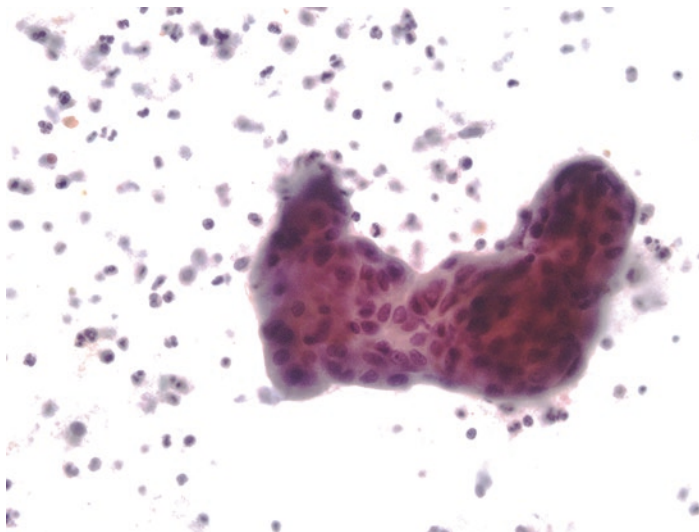


Fig. 2.3 Atypical glandular cells in a background of acute inflammatory cells in a pancreatic FNA. The cells are mildly disorganized with fine chromatin, mild degree of anisonucleosis, and a low nuclear-cytoplasmic ratio. These findings are consistent with reactive atypia of ductal cells and may be placed in the “atypical” category

2. Atypical ductal epithelium (see note)
 - Note: The evaluation of the sample is limited by scant cellularity and air-drying artifact.
3. Atypical findings (see note)
 - Note: The aspirate reveals a limited number of monomorphic polygonal cells with coarse chromatin. There is insufficient material for ancillary studies. Additional sampling may be helpful for further characterization.
4. Atypical bile duct epithelium

Neoplastic

The category “neoplastic” is further subdivided into “neoplastic: benign” and “neoplastic: other.”

Neoplastic: Benign

This category includes the neoplastic entities that are benign. The sample needs to be adequately cellular and representative for this diagnosis. For practical purposes, this category mainly comprises of serous cystadenoma of the pancreas. However, the cytologic samples are often limited in serous cystadenomas. Usually, the cytologic interpretation is descriptive or nondiagnostic due to lack of sufficient cellularity. Correlation with the clinical, imaging, and cyst fluid analysis findings (if available) is often helpful in this regard. Serous cystadenomas tend to be associated with very low CEA (<5 ng/ml) and amylase levels with rare exceptions [14].

Other rare benign neoplasms of the pancreas such as cystic teratoma and schwannoma will also be included in this category .

Sample reports:

1. Neoplastic: Benign

- Limited cellularity sample composed of cytologically bland non-mucinous epithelium in a background of hemosiderin-laden macrophages (see note).
- Note: In the context of appropriate clinical and imaging findings, the cytology findings are consistent with serous cystadenoma.
- If available, results of cyst fluid analysis can be mentioned in the report as well.

Neoplastic: Other

This category encompasses premalignant neoplasms, i.e., intraductal papillary mucinous neoplasms (IPMNs) and mucinous cystic neoplasms (MCNs) and neoplasms with low-grade malignant behavior (well-differentiated pancreatic neuroendocrine tumors and solid pseudopapillary neoplasms). Due to the remarkable difference in biologic behavior and potential for conservative management for at least some of the aforementioned entities, a need was felt to separate them into a category distinct from high-grade malignancies. These neoplasms cannot be placed into the benign category either due to their potential for malignant behavior.

Grading of dysplasia for IPMNs and MCNs is problematic in cytology samples. The Pap Society guidelines recommend a

two-tiered approach for grading dysplasia in neoplastic mucinous cysts—low-grade atypia (that usually correlates with low-grade dysplasia and intermediate-grade dysplasia on histology) and high-grade atypia (that is usually associated with high-grade dysplasia or invasive carcinoma on follow-up). Intermediate-grade dysplasia may be more difficult to accurately grade on cytology. The Pap Society recommends intermediate-grade dysplasia to be classified as low-grade atypia on cytology [1, 2]. Grouping intermediate-grade dysplasia in the low-grade rather than the high-grade category produces a much better negative predictive value for the presence of a high-grade cyst (78% vs. 33%, respectively) [15].

Sample reports:

1. Neoplastic: Other
 - Abundant thick mucin present, consistent with a neoplastic mucinous cyst (see note).
 - No high-grade epithelial atypia is identified.
 - Note: Correlation with clinical and imaging findings and results of cyst fluid analysis is recommended.
 - If available, results of cyst fluid analysis, especially the CEA level, can be incorporated in the report.
2. Neoplastic: Other
 - Consistent with a neoplastic mucinous cyst (see note).
 - No high-grade epithelial atypia is identified.
 - Note: No diagnostic thick mucin is identified in the cytology sample. However, the presence of a cyst fluid CEA level of 856 ng/ml supports the above diagnosis. Correlation with clinical and imaging findings is recommended.
3. Neoplastic: Other
 - High-grade epithelial atypia identified in a background of cyst contents (see note).
 - Note: The presence of a cyst fluid CEA level of 1105 ng/ml and a *KRAS* point mutation in the sample support the above diagnosis. The high-grade epithelial atypia is consistent with high-grade dysplasia; however, an invasive carcinoma cannot be excluded. Correlation with clinical and imaging findings is recommended.

4. Neoplastic: Other

- Pancreatic neuroendocrine tumor (see note).
- Note: On immunohistochemistry, the tumor cells are diffusely positive for cytokeratin AE1/3, synaptophysin, and chromogranin, supporting the above diagnosis. On the limited cell block material, a Ki-67 proliferation index is approximately 1%, suggestive of a low-grade tumor.

5. Neoplastic: Other

- Solid pseudopapillary neoplasm (see note).
- Note: On immunohistochemistry, the neoplastic cells reveal nuclear positivity with beta-catenin. They are positive for progesterone receptor and negative for E-cadherin, synaptophysin, and chromogranin. These results support the above diagnosis.

Suspicious for Malignancy

This category indicates that the cytologic sample is qualitatively or quantitatively insufficient for the diagnosis of a high-grade malignancy, most commonly, pancreatic ductal adenocarcinoma (PDA). This diagnosis may result from scant cellularity of the aspirate, difficulty in diagnosing well-differentiated adenocarcinomas, difficulty in distinguishing reactive ductal atypia from malignancy, and conservative interpretation of malignancies. Indeterminate diagnoses are usually attributable to three types of factors: technical, lesion-related, and pathologist-related. The technical factors would be how accessible the lesion is, the expertise of the endosonographer, and the availability of rapid on-site evaluation (ROSE) that can influence the amount and triage of diagnostic material and the quality of cytologic preparations. Lesion-related variables include the presence of extensive desmoplasia, necrosis, and cystic change that may result in scant cellularity of the aspirate. Pathologist-related factors include the pathologists' experience and expertise in the interpretation of pancreatobiliary cytology. Departmental consensus review may be helpful in the decreasing the rate of indeterminate diagnoses [10].

Sample reports:

1. Suspicious for malignancy
 - Suspicious for adenocarcinoma.
2. Suspicious for malignancy
 - Mucinous cyst with high-grade epithelial atypia in a background of coagulative necrosis, suspicious for adenocarcinoma.

Positive/Malignant

This category comprises of high-grade malignancies including PDA and its variants, high-grade neuroendocrine carcinomas (small cell carcinomas and large cell neuroendocrine carcinomas), acinar cell carcinomas, and pancreatoblastomas. It also includes lymphomas, sarcomas and metastases involving the pancreas. Adenocarcinomas in a bile duct brushing specimen are also included in this category.

The specificity of a “positive” diagnosis for pancreatobiliary cytology is high, >95% in many studies [16–18].

Sample reports:

1. Positive for malignant cells
 - Adenocarcinoma.
2. Positive for malignant cells
 - Consistent with metastatic clear cell renal cell carcinoma (see note).
 - Note: The patient’s history of clear cell renal cell carcinoma is noted. On immunohistochemistry, the tumor cells are positive for PAX-8 and CD10, while being negative for CK7, CK20, synaptophysin, and chromogranin, supporting the above diagnosis.
3. Positive for malignant cells
 - Involvement by large B-cell lymphoma (see note).
 - Note: The aspirate is composed of large atypical lymphoid cells which on immunohistochemistry are positive for CD20, PAX-5, CD10, and BCL-6 and negative for AE1/3,

CD3, CD5, and MUM-1, supporting the above diagnosis. See also results of concurrent flow cytometric analysis and core biopsy for additional information.

Risk of Malignancy

Layfield et al. categorized 317 EUS-FNA cases as per the Pap Society guidelines and based on the surgical or clinical follow-up calculated the associated risk of malignancy. They reported the malignancy risk for the benign (negative), atypical, suspicious, malignant, neoplasm, and nondiagnostic categories of the Pap Society as 12.6%, 73.9%, 81.8%, 97.2%, 14.2%, and 21.4%, respectively. Thus, they showed that the risk of malignancy increases from the benign to the malignant categories. Aspirates designated benign have the lowest risk of malignancy (13%) and aspirates designated malignant, the highest (97%) [19].

Smith et al. analyzed a cohort of 127 cases of pancreatic neoplastic mucinous cysts and categorized them as per the Pap Society guidelines. Their results were similar with an increasing risk of malignancy associated with the different categories: 0% for a negative diagnosis, 13% for a neoplastic diagnosis, 63.6% for an atypical diagnosis, 80% for a suspicious diagnosis, and 100% for a positive diagnosis. The nondiagnostic category was associated with a 17.4% risk of malignancy [20].

These findings verify that the categorization proposed by the Pap Society provides valuable information regarding risk stratification of pancreatico-biliary lesions for patient management.

Impact of Pap Society Guidelines

The main impact of Pap Society guidelines has reportedly been on specimens that were previously classified as atypical or suspicious. These lesions mainly comprise of premalignant mucinous neoplasms. In a retrospective review of 155 EUS-FNA samples, Saieg et al. reported that all of their previously classified “atypi-

cal” samples and half of the “suspicious” ones were re-categorized as “neoplastic: other.” According to their old classification, specimens that showed mucinous epithelium that lacked high-grade features were considered atypical; and mucinous neoplasms with at least high-grade features were considered suspicious for malignancy. According to the new terminology, they were all classified as “neoplastic: other” [21].

Similarly, McKinley and Newman reclassified previously reported 232 pancreatico-biliary cytology specimens as per these guidelines. Twenty-five cases (11%) were recategorized in their study, the majority being premalignant and low-grade neoplasms that were reclassified as “neoplastic: other” or “atypical.” Challenges in utilization of the scheme included the amount and the quality of the available clinical and imaging information [22].

We have incorporated the Pap Society recommendations in the reporting of pancreatico-biliary cytology specimens in our practice. The cases are also discussed at multidisciplinary conferences whereby all the clinical, imaging, and pathologic findings and results of ancillary testing are integrated to develop management options for the patient.

References

1. Pitman MB, Centeno BA, Ali SZ, Genevay M, Stelow E, Mino-Kenudson M, et al. Standardized terminology and nomenclature for pancreatobiliary cytology: the Papanicolaou Society of Cytopathology guidelines. *Diagn Cytopathol.* 2014;42:338–50. <https://doi.org/10.1002/dc.23092>.
2. Pitman MB, Layfield LJ. Guidelines for pancreaticobiliary cytology from the Papanicolaou Society of Cytopathology: a review. *Cancer Cytopathol.* 2014;122:399–411. <https://doi.org/10.1002/cncy.21427>.
3. Wu RI, Yoon WJ, Brugge WR, Mino-Kenudson M, Pitman MB. Endoscopic ultrasound-guided fine needle aspiration (EUS-FNA) contributes to a triple-negative test in preoperative screening of pancreatic cysts. *Cancer Cytopathol.* 2014;122:412–9. <https://doi.org/10.1002/cncy.21385>.
4. Tanaka M, Fernández-del Castillo C, Adsay V, Chari S, Falconi M, Jang JY, et al. International consensus guidelines 2012 for the management of IPMN and MCN of the pancreas. *Pancreatol.* 2012;12:183–97. <https://doi.org/10.1016/j.pan.2012.04.004>.

5. Barr Fritcher EG, Caudill JL, Blue JE, Djuric K, Feipel L, Maritim BK, et al. Identification of malignant cytologic criteria in pancreatobiliary brushings with corresponding positive fluorescence in situ hybridization results. *Am J Clin Pathol.* 2011;136:442–9. <https://doi.org/10.1309/AJCPDULIOEOTUZ5H>.
6. Volmar KE, Vollmer RT, Routbort MJ, Creager AJ. Pancreatic and bile duct brushing cytology in 1000 cases: review of findings and comparison of preparation methods. *Cancer.* 2006;108:231–8.
7. Stewart CJ, Mills PR, Carter R, O'Donohue J, Fullarton G, Imrie CW, et al. Brush cytology in the assessment of pancreatobiliary strictures: a review of 406 cases. *J Clin Pathol.* 2001;54:449–55.
8. Kocjan G, Smith AN. Bile duct brushings cytology: potential pitfalls in diagnosis. *Diagn Cytopathol.* 1997;16:358–63.
9. Logrono R, Kurtycz DF, Molina CP, Trivedi VA, Wong JY, Block KP. Analysis of false-negative diagnoses on endoscopic brush cytology of biliary and pancreatic duct strictures: the experience at 2 university hospitals. *Arch Pathol Lab Med.* 2000;124:387–92.
10. Virk RK, Gamez R, Mehrotra S, Atieh M, Barkan GA, Wojcik EM, et al. Variation of cytopathologists' use of the indeterminate diagnostic categories "atypical" and "suspicious for malignancy" in the cytologic diagnosis of solid pancreatic lesions on endoscopic ultrasound-guided fine-needle aspirates. *Diagn Cytopathol.* 2017;45:3–13. <https://doi.org/10.1002/dc.23565>.
11. Abdelgawwad MS, Alston E, Eltoun IA. The frequency and cancer risk associated with the atypical cytologic diagnostic category in endoscopic ultrasound-guided fine-needle aspiration specimens of solid pancreatic lesions: a meta-analysis and argument for a Bethesda system for reporting cytopathology of the pancreas. *Cancer Cytopathol.* 2013;121:620–8. <https://doi.org/10.1002/cncy.21337>.
12. Choi WT, Swanson PE, Grieco VS, Wang D, Westerhoff M. The outcomes of "atypical" and "suspicious" bile duct brushings in the identification of pancreatobiliary tumors: follow-up analysis of surgical resection specimens. *Diagn Cytopathol.* 2015;43:885–91. <https://doi.org/10.1002/dc.23323>.
13. Chadwick BE, Layfield LJ, Witt BL, Schmidt RL, Cox RN, Adler DG. Significance of atypia in pancreatic and bile duct brushings: follow-up analysis of the categories atypical and suspicious for malignancy. *Diagn Cytopathol.* 2014;42:285–91. <https://doi.org/10.1002/dc.23035>.
14. Belsley NA, Pitman MB, Lauwers GY, Brugge WR, Deshpande V. Serous cystadenoma of the pancreas: limitations and pitfalls of endoscopic ultrasound-guided fine-needle aspiration biopsy. *Cancer.* 2008;114(2):102–10. <https://doi.org/10.1002/cncr.23346>.
15. Pitman MB, Centeno BA, Genevay M, Fonseca R, Mino-Kenudson M. Grading epithelial atypia in endoscopic ultrasound-guided fine-needle aspiration of intraductal papillary mucinous neoplasms: an international

- interobserver concordance study. *Cancer Cytopathol.* 2013;121:729–36. <https://doi.org/10.1002/cncy.21334>.
16. Bhutani MS, Hawes RH, Baron PL, Sanders-Cliette A, van Velse A, Osborne JF, et al. Endoscopic ultrasound guided fine needle aspiration of malignant pancreatic lesions. *Endoscopy.* 1997;29:854–8.
 17. Layfield LJ, Wax TD, Lee JG, Cotton PB. Accuracy and morphologic aspects of pancreatic and biliary duct brushings. *Acta Cytol.* 1995;39(1):11–8.
 18. Eloubeidi MA, Chen VK, Eltoun IA, Jhala D, Chhieng DC, Jhala N, et al. Endoscopic ultrasound-guided fine needle aspiration biopsy of patients with suspected pancreatic cancer: diagnostic accuracy and acute and 30-day complications. *Am J Gastroenterol.* 2003;98:2663–8.
 19. Layfield LJ, Dodd L, Factor R, Schmidt RL. Malignancy risk associated with diagnostic categories defined by the Papanicolaou Society of Cytopathology pancreaticobiliary guidelines. *Cancer Cytopathol.* 2014;122:420–7. <https://doi.org/10.1002/cncy.21386>.
 20. Smith AL, Abdul-Karim FW, Goyal A. Cytologic categorization of pancreatic neoplastic mucinous cysts with an assessment of the risk of malignancy: a retrospective study based on the Papanicolaou Society of Cytopathology guidelines. *Cancer Cytopathol.* 2016;124:285–93. <https://doi.org/10.1002/cncy.21657>.
 21. Saieg MA, Munson V, Colletti S, Nassar A. The impact of the new proposed Papanicolaou Society of Cytopathology terminology for pancreaticobiliary cytology in endoscopic US-FNA: a single-institutional experience. *Cancer Cytopathol.* 2015;123(8):488–94. <https://doi.org/10.1002/cncy.21559>.
 22. McKinley M, Newman M. Observations on the application of the Papanicolaou Society of Cytopathology standardised terminology and nomenclature for pancreaticobiliary cytology. *Pathology.* 2016;48:353–6. <https://doi.org/10.1016/j.pathol.2016.03.004>.



Cytology of Normal Pancreas

3

Ami P. Patel and Rema Rao

Introduction and Approach to Pancreaticobiliary Fine-Needle Aspiration

The evaluation of pancreatic lesions begins with a thorough clinical history along with imaging studies, preferably computed tomography (CT), magnetic resonance imaging (MRI), or magnetic resonance cholangiopancreatography (MRCP) [1–3]. The location of the lesion as well as the presence of solid, cystic, multicystic, or mixed elements should be noted. Pancreatic tissue procurement most commonly occurs with fine-needle aspiration through endoscopic ultrasound guidance (EUS). Other guidance techniques include direct visualization during laparotomy, computed tomography (CT), transabdominal ultrasound (TUS), or intraoperative ultrasound (IUS) [4]. Endoscopic retrograde cholangiopancreatography (ERCP) is more common in the setting of biliary strictures wherein cytologic sampling of ductal epithelium is restricted to exfoliative cells in bile and/or brush samples.

A. P. Patel · R. Rao (✉)

Department of Pathology and Laboratory Medicine, Weill-Cornell Medicine, New York Presbyterian Hospital, New York, NY, USA
e-mail: rer9052@med.cornell.edu

© Springer Nature Switzerland AG 2019

A. Goyal et al. (eds.), *Pancreas and Biliary Tract Cytohistology*,
Essentials in Cytopathology 28,
https://doi.org/10.1007/978-3-030-22433-2_3

37

Although there has been tremendous progress in the technique of sample procurement, ERCP still shows relatively low sensitivity of ~ 60–65%, low negative predictive value, and excellent specificity of ~ 98–100% [1, 5–8].

Endoscopic ultrasound-guided fine-needle aspiration (EUS-FNA) is increasingly being recognized as a minimally invasive, safe, accurate, and cost-effective method [9, 10]. Through multiple systematic reviews, it has been shown to have a pooled sensitivity and specificity approaching 95% with complication rates ranging from 0 to 5% [1, 11–14]. In addition, EUS-FNA has shown to have greater accuracy for small lesions (<3 cm) as compared to CT and shown to have less risk for peritoneal seeding compared to percutaneous core needle biopsy [15–17].

One cannot delve into the complexities of the neoplastic pancreas without a complete and vital discussion on benign pancreatic cytology. An awareness of the approach for pancreatic fine-needle aspiration and regional anatomy is also important to avoid common (and potentially catastrophic) pitfalls and to ensure an accurate and timely diagnosis.

Anatomy and Embryology of Pancreas

The pancreas is an exocrine-endocrine gland and is located transversely in the retroperitoneum, lying obliquely across and behind the stomach, extending transversely toward the spleen. The gland is divided into three parts: the head, body, and tail. The pancreatic head is surrounded by the second portion of the duodenum, and the tail extends to the hilum of the spleen.

The pancreas buds from the endodermal epithelium of the foregut (i.e., duodenum) at approximately the third week of gestation. The dorsal bud and the smaller ventral bud, from which the pancreas arises, first appear around the fourth week of gestation. With rotation of the duodenum, fusion of the two buds creates the head of the pancreas. The remaining portion of the dorsal bud becomes the tapering body and tail. The main pancreatic duct (i.e., duct of Wirsung) is formed by the fusion of the ventral duct and the distal portion of the dorsal duct, which occurs at the 6th–7th week of gestation (Fig. 3.1). In approximately 40% of people, the

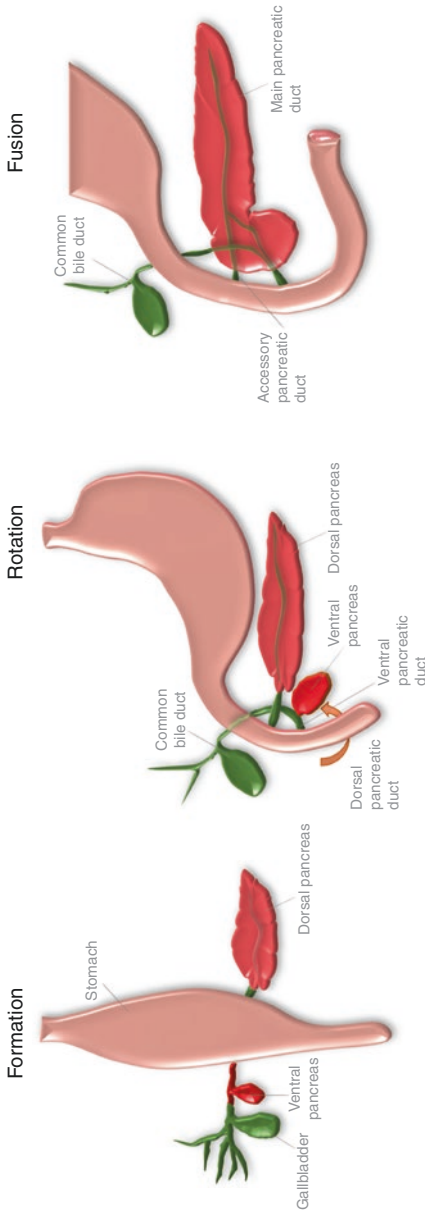


Fig. 3.1 The dorsal pancreatic bud and the smaller ventral pancreatic bud first appear around the fourth week of gestation (formation). With rotation of the duodenum, fusion of the two buds creates the head of the pancreas (rotation). The remaining portion of the dorsal bud becomes the tapering body and tail (Image illustration: Ms. Lauren Soong, BA)

proximal portion of the dorsal duct persists as the accessory duct of Santorini [18, 19].

The exocrine pancreas comprises 80–85% of the gland and consists of acini, ducts, and the corresponding blood vessels. The acinar cells secrete digestive enzymes that drain into ductules (intralobular ducts), which then communicate with interlobular ducts that join to form the main pancreatic duct. This duct drains into the duodenum via the major duodenal papilla (ampulla of Vater).

The endocrine pancreas comprises approximately 2% of the gland and consists of more than one million islets of Langerhans scattered throughout the pancreas. The islets secrete hormones such as insulin, glucagon, and somatostatin, which are drained by a network of capillaries intimately associated with the islets and are thereby delivered into the bloodstream.

Cytology of Normal Pancreas

Benign Ductal Cells

The pancreas is primarily composed of exocrine ductal and acinar cells. Aspirates display mainly acinar cells with few ductal cells, in contrast to pancreatic and bile duct brushings which consist mostly of ductal cells [20]. Occasionally, ductal cells form thick, multilayered sheets, with artifactual crowding of nuclei. In these cases, examination of the edges of the thick clusters may allow for closer evaluation of the nuclei, which should fail to show nuclear abnormalities characteristic of carcinoma [21].

Important Cytologic Features

The cytologic features of benign ductal cells include the following (Figs. 3.2a and 3.3):

- Cohesive sheets of uniform cells in a “honeycomb” arrangement with little or no nuclear overlap or crowding.
- Ductal cells range from low cuboidal to tall columnar as the ducts get larger.

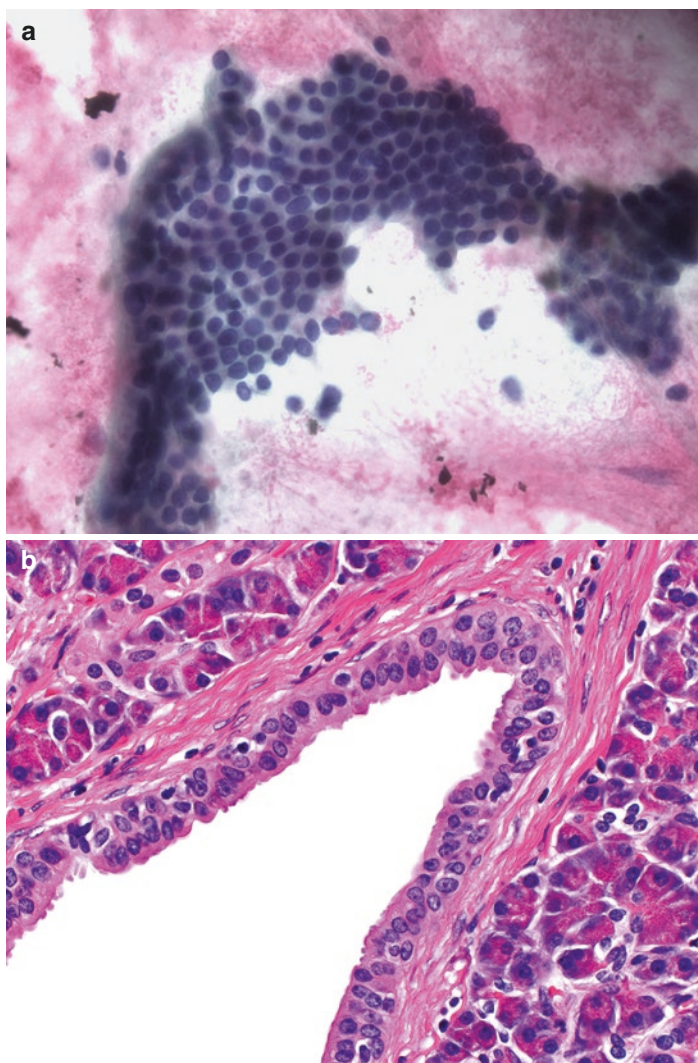


Fig. 3.2 (a) A cohesive group of benign ductal cells with uniform cells in a “honeycomb” arrangement with little or no nuclear overlap or crowding. (b) The histologic counterpart of an interlobular duct lined by cuboidal-type epithelial cells with small nuclei (same size as the adjoining acinar cells), bland chromatin, and small inconspicuous nucleoli. [(a) Pap stain CS 40 \times , (b) H&E stain]



Fig. 3.3 A TP slide showing a cohesive group of benign ductal cells with “honeycomb” arrangement with little to no overlap and bland nuclei (Pap stain TP, 60×)

- The edge of the clusters derived from large ducts may show cells with columnar configuration, parallel to each other, with basally placed nuclei.
- Well-demarcated cytoplasmic borders.
- Cytoplasm is transparent in fixed smears stained with Papanicolaou stain, accounting for the honeycomb pattern of the flat clusters.
- Nuclei are round or ovoid, equally spaced, without nuclear contour abnormalities.
- Chromatin is finely granular and uniformly distributed.
- Tiny nucleoli may be visible.

Histologic Correlation

The histologic features of benign ductal cells include the following (Fig. 3.2b):

- The smallest intralobular ducts are lined by flattened to cuboidal epithelium.
- Interlobular ducts, both small and large, are lined by columnar epithelium.

Differential Diagnosis and Pitfalls

A well-differentiated pancreatic adenocarcinoma is in the differential diagnosis (Fig. 3.4a, b) and exhibits the features found in Table 3.1.

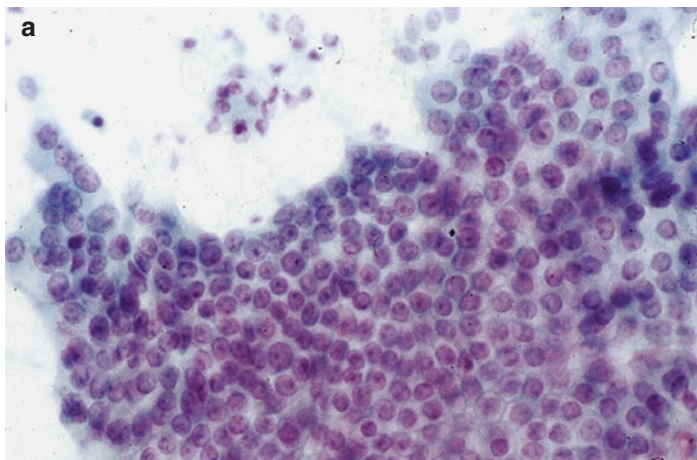


Fig. 3.4 (a). A disorderly ductal group with crowding, high N:C ratio, irregular nuclear membranes, and visible nucleoli. (b) The corresponding histology on this case was a well-differentiated adenocarcinoma. [(a) Ultrafast Pap stain CS, 20 \times , (b) H&E stain] (Image courtesy of Dr. Grace Yang, MD)

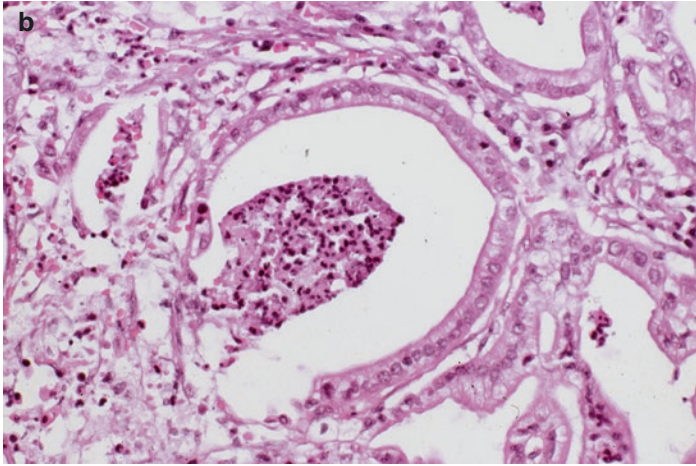


Fig. 3.4 (continued)

Table 3.1 Differential diagnosis and pitfalls of benign ductal cells

Ductal adenocarcinoma, well differentiated	Cellular aspirate Crowded architecture Higher nuclear to cytoplasmic (N:C) ratio Irregular nuclear membranes Anisonucleosis to the extent of at least 1:4
--	---

Benign Acinar Cells

Benign pancreatic acini typically form prominent organoid configurations with retention of the normal acinar architecture. Acinar cells are notable for their granular cytoplasm owing to the presence of zymogen granules that contain enzymes such as trypsin, lipase, and chymotrypsin [4, 22]. However, degranulation of the cytoplasm can occur resulting in a clear or vacuolated appearance [21]. Acinar cell carcinoma may be a diagnostic consideration when acinar tissue is abundant and has an altered

architecture [4, 20]. However, a diagnosis of any neoplasm should not be considered when a mass lesion has not been identified on imaging studies.

Important Cytologic Features

The cytologic features of benign acinar cells include the following (Fig. 3.5a–d):

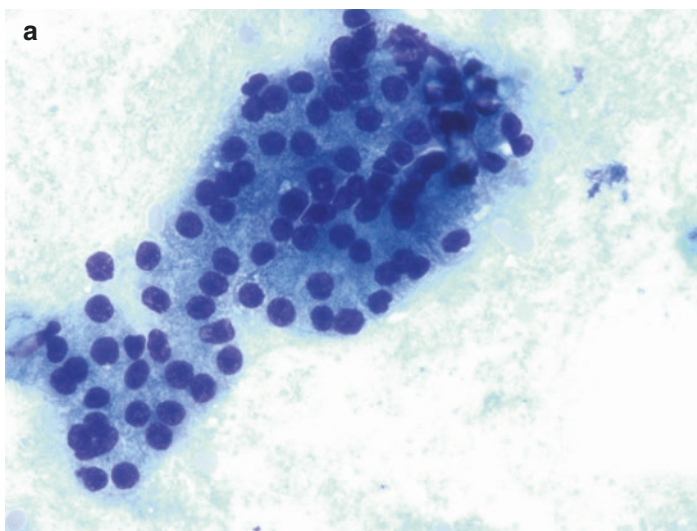


Fig. 3.5 (a) Low-power image of acinar cells in a tightly knit cluster with a lobular “grapelike” configuration. The center of the cluster is dark; the acinar cells are better appreciated in the periphery of these clusters. (b) Similar tight cluster of acinar cells in an alcohol-fixed preparation showing bland nuclei. The nuclear size is small and comparable to that of the adjacent red blood cells. The nucleoli are very small to inconspicuous in benign acinar cells (c). A higher magnification of the acinar cells on ultrafast Pap stain with similar cytology such as basal nuclei, small inconspicuous nucleoli, and apical vacuolated to granular blue-green cytoplasm (Image courtesy of Dr. Grace Yang). (d) A higher magnification of the acinar cells with purple granules (Image courtesy of Dr. Grace Yang). (e) The histology of benign acini showing pyramidal cells with basally oriented nuclei and apical pink cytoplasm. [(a) Diff-Quik stain CS 10 \times , (b) Pap stain CS 10 \times , (c) ultrafast Pap stain CS 100 \times , (d) Diff-Quik stain CS 100 \times , (e) H&E stain]

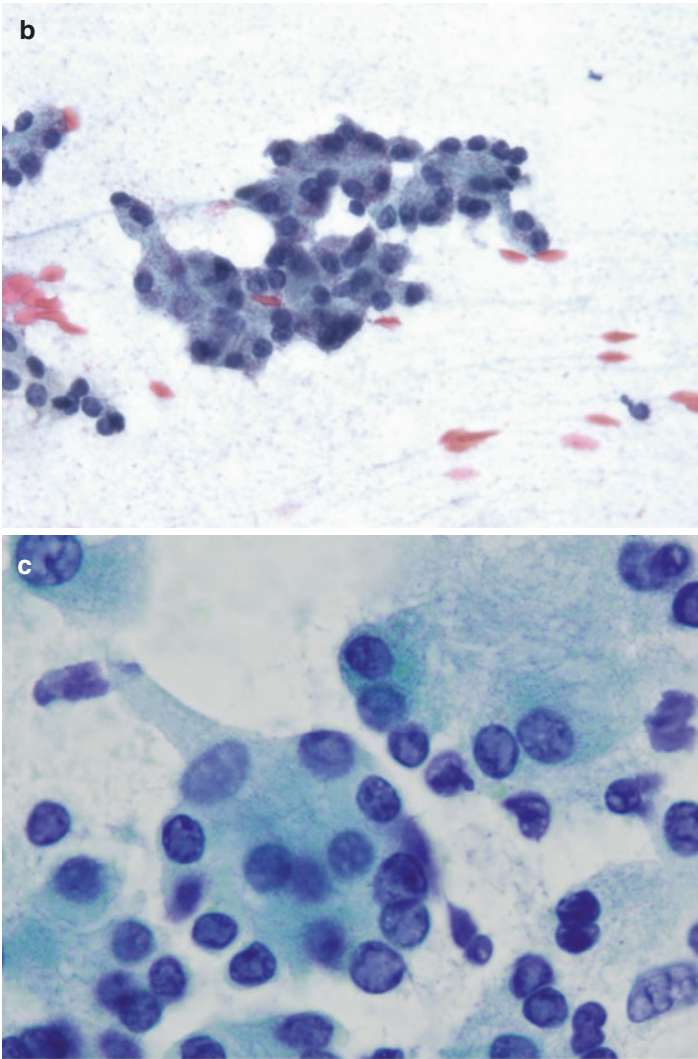


Fig. 3.5 (continued)

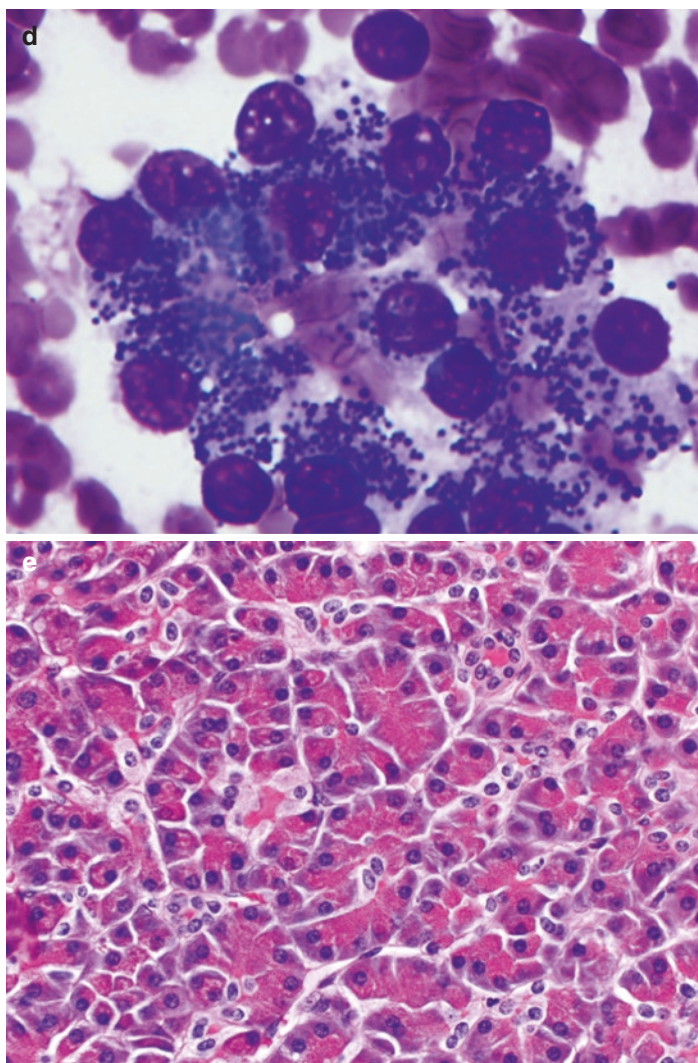


Fig. 3.5 (continued)

- Small, tightly knit clusters with a lobular arrangement around loose vascular connective tissue, like “grapes on a vine.”
- Cells are pyramidal in shape and arranged around a central lumen—resembling a rosette, with the nuclei aligned at the periphery of the cells.
- Cells have abundant, granular cytoplasm (in air-dried or well-fixed cells), which appears blue-green (on Papanicolaou stain) or purple (on Diff-Quik stain).
- Degranulation of the cytoplasm can also occur resulting in a clear or vacuolated appearance (on Diff-Quik stain).
- Nuclei are uniform, small, and round, approximately the size of a RBC, with a smooth membrane and basally located.
- Chromatin is moderately granular and evenly distributed, with inconspicuous nucleoli.

Histologic Correlation

The histologic features of benign acinar cells include the following (Fig. 3.5e):

- Acini are lined by pyramidal cells that surround a central lumen.
- Acinar cells have basally located round nuclei.
- Pink-purple cytoplasm containing a variable number of zymogen granules.

Differential Diagnosis and Pitfalls

Acinar cell carcinoma is in the differential diagnosis (Fig. 3.6a, b) and exhibits the features found in Table 3.2.

Islet Cells

Islets of Langerhans are scattered throughout the gland with most located in the tail of the pancreas. In general, islet cells are infrequently detected in aspirates. However, they are more likely to be detected in pancreatic atrophy or chronic pancreatitis with islet cell hyperplasia [4, 23]. Islet cells form loose, spherical, or oval aggregates of cells with scant, wispy cytoplasm. The cell bor-

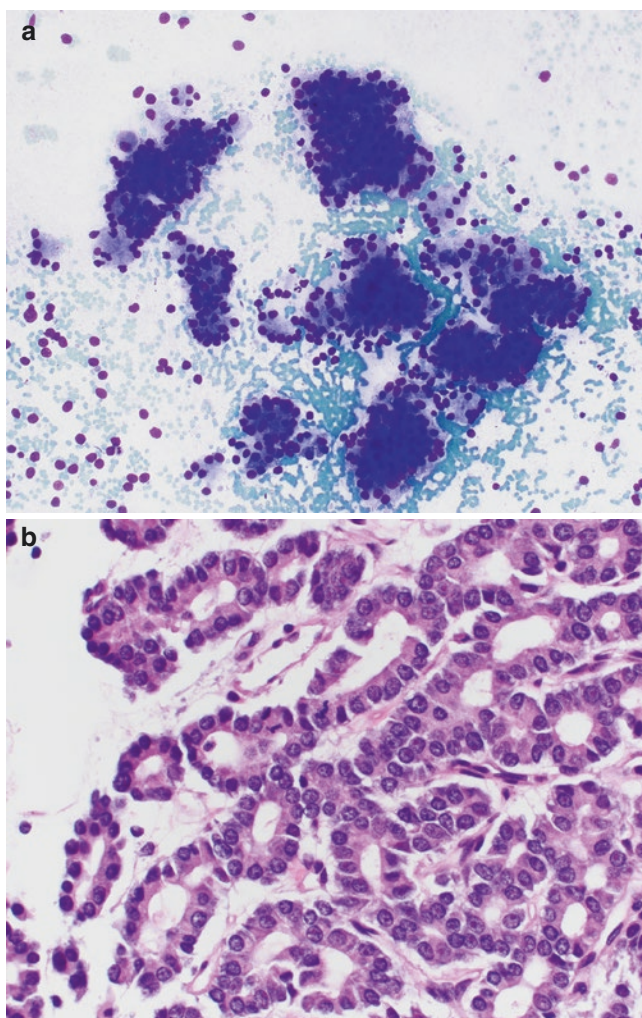


Fig. 3.6 (a). Disorderly and loosely cohesive clusters of large and small acini with granular cytoplasm with prominent vacuoles, round basally placed nuclei with high N:C ratio and purplish granules, nuclear atypia, and abundant bare (naked) nuclei in the background. (b) The corresponding histology with proliferation of cells in a prominent acinar architecture and nuclear atypia such as high N:C ratio and very prominent nucleoli. [(a) Diff-Quik stain CS 40 \times , (b) H&E stain]

Table 3.2 Differential diagnosis and pitfalls of benign acinar cells

Acinar cell carcinoma	Cellular aspirates Disorderly and loosely cohesive clusters of large and small acini with granular cytoplasm with prominent vacuoles, round basally placed nuclei, purplish granules, and nuclear atypia Abundant bare (naked) nuclei in the background Enlarged nuclei, high N:C ratio, and single large central nucleolus Solid or acinar architecture No desmoplastic reaction
-----------------------	--

ders are indistinct. The nuclei are regular and round. The nuclear chromatin may show “salt and pepper” granularity and a visible nucleolus. Overinterpretation of hyperplastic pancreatic islet cells as a pancreatic neuroendocrine tumor could be potentially problematic [4, 24, 25].

Important Cytologic Features

The cytologic features of benign islet cells include the following (Fig. 3.7a, b):

- Few in quantity.
- Form loose, spherical, or oval aggregates of cells.
- Scant, wispy cytoplasm.
- Indistinct cell borders.
- Nuclei are regular and round.
- “Salt and pepper” nuclear chromatin.
- Visible small nucleolus.

Histologic Correlation

The histologic features of benign islets include the following (Fig. 3.7c):

- Islets are composed of small polyhedral cells arranged in nests, separated by capillaries, and are seen on H&E as a collection of small clear cells.

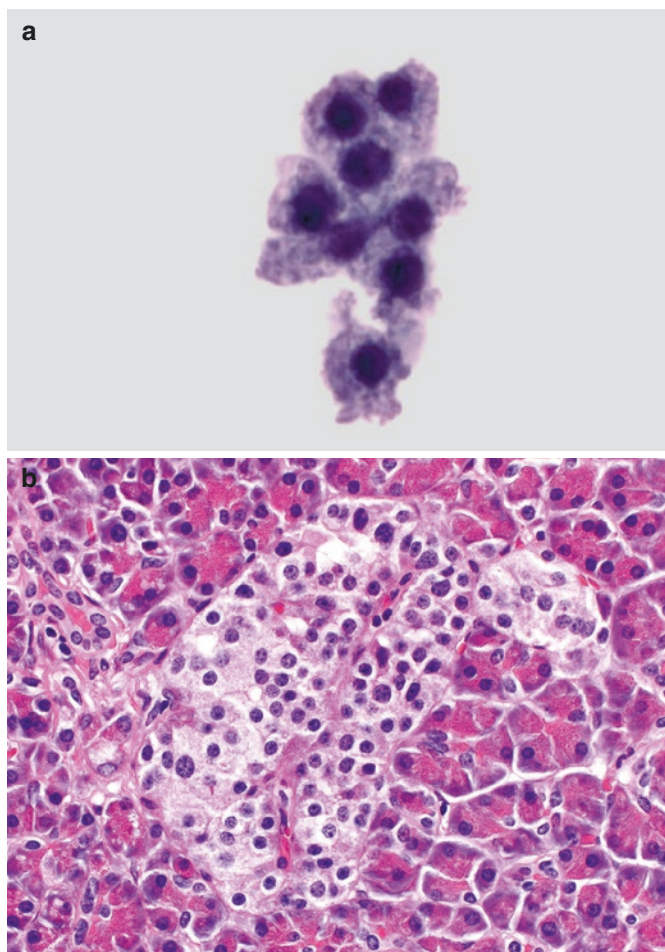


Fig. 3.7 (a). Islets are rarely detected in aspirates and are mostly seen in the aspirates of chronic pancreatitis as a result of islet cell hyperplasia. Typically they form loose, spherical, or oval aggregates of cells with scant, wispy cytoplasm. The cell borders are indistinct. The nuclei are regular and round and may show salt and pepper granularity with a visible nucleolus. (b). The histology of the islets, which are small polyhedral cells, arranged in nests, with round and regular nuclei, and salt and pepper “neuroendocrine” chromatin. [(a) Pap stain TP 60 \times , (b) H&E stain]

Differential Diagnosis and Pitfalls

Pancreatic neuroendocrine tumors are in the differential diagnosis (Fig. 3.8a–c) and exhibit the features listed in Table 3.3.

Contamination

A major diagnostic concern in pancreatic cytopathology is the overinterpretation of benign tissue contaminants [7, 20, 26, 27]. During EUS-FNA sampling, the needle may traverse either the gastric, duodenal, or normal pancreatic parenchyma. In addition,

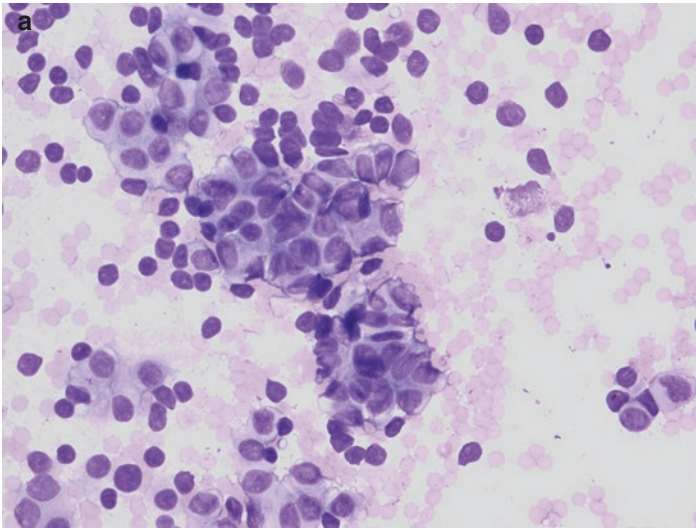


Fig. 3.8 (a, b). A dyshesive population of cells predominantly in small clusters/pseudorosettes and single cells with a plasmacytoid appearance and moderate to abundant granular cytoplasm. The nuclei are monotonous and round with a “salt and pepper” type nuclear chromatin. (c). Corresponding histology with relatively uniform epithelial cells arranged in nests and trabeculae separated by a fibrovascular stroma. [(a) Diff-Quik stain CS 40 \times , (b) Pap stain CS 20 \times , (c) H&E stain]

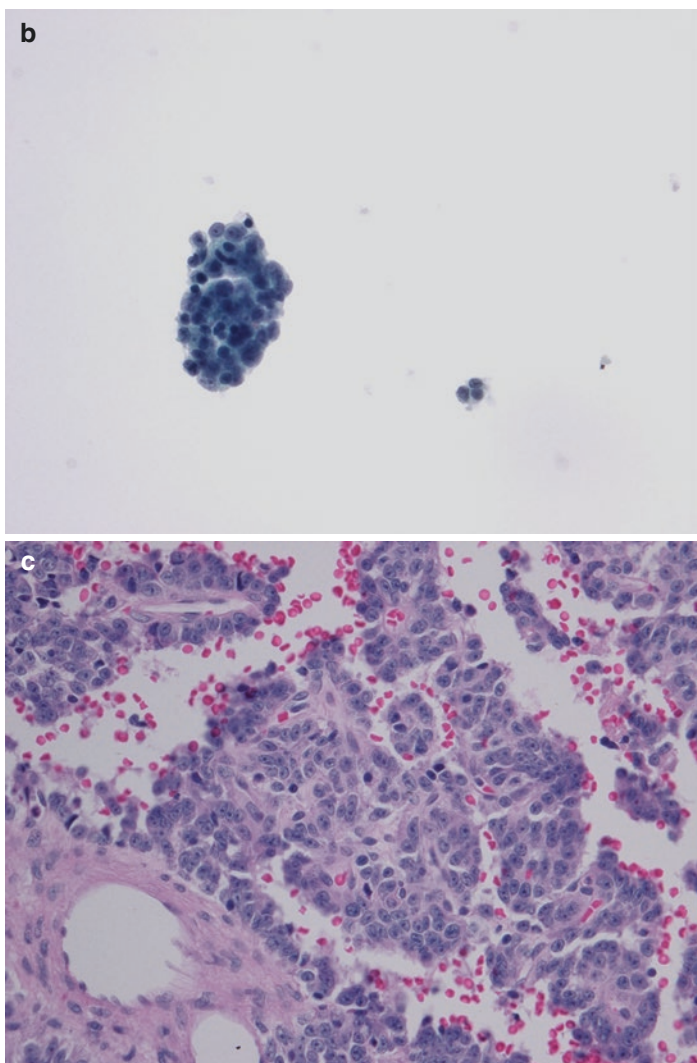


Fig. 3.8 (continued)

Table 3.3 Differential diagnosis and pitfalls of benign islets

Pancreatic Neuroendocrine tumor	Very cellular aspirate Dyshesive population of cells mainly in sheets, small groups, and single plasmacytoid cells Monotonous nuclear features, “salt and pepper” nuclear chromatin Moderate to abundant cytoplasm, typically granular, but may be vacuolated or oncocytic Prominent vascularity can be seen
------------------------------------	---

during the CT-guided approach, it is not unusual for the needle to carry contaminant mesothelial, colonic, renal, hepatic, splenic, or gastric tissue. Benign gastric and duodenal epithelium may be misinterpreted as well-differentiated ductal adenocarcinoma of the pancreas (Fig. 3.4a, b) [26]. A particularly difficult distinction is between benign gastric and duodenal elements and the lining epithelium of neoplastic mucinous cysts such as intra-ductal papillary mucinous neoplasms (IPMNs). Distinguishing low-grade neoplastic mucinous epithelium of the gastric foveolar type with gastric foveolar-type cells from contamination is essentially impossible [4, 20]. The presence of thick neoplastic colloid-type mucin, which can be distinguished from contaminating gastrointestinal mucin, is a helpful feature to differentiate these benign entities from neoplasms and to avoid this potential pitfall (Fig. 3.9a) [7, 28–30].

Important Cytologic Features

Benign Duodenal Epithelium

The cytologic features of benign duodenal epithelium include the following (Fig. 3.10a, b):

- Honeycomb, flat, cohesive sheets of cells in a clean background.
- Non-mucinous, non-vacuolated epithelial cells with brush border.

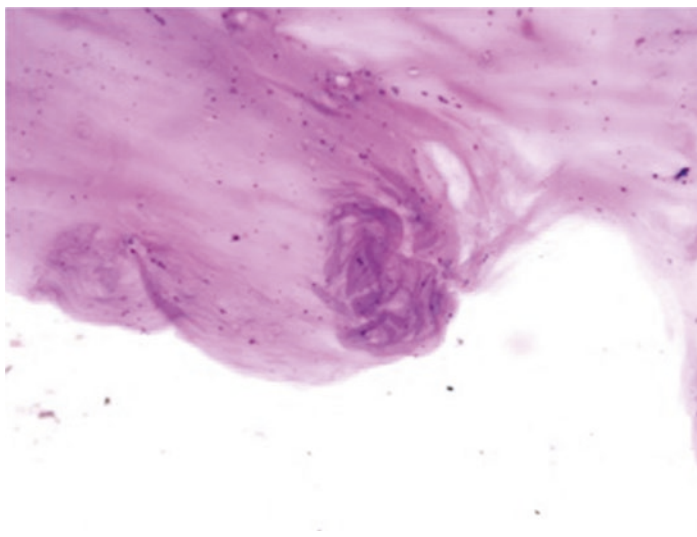


Fig. 3.9 Thick, extracellular, neoplastic mucin, with a well-defined edge, on an air-dried smear (Diff-Quik stain CS, 40 \times)

- Goblet cells—on alcohol-fixed preparations, they have a fried egg appearance due to a clear halo surrounding the centrally placed nucleus.
- Intraepithelial lymphocytes may be present.

Benign Gastric Epithelium

The cytologic features of benign gastric epithelium include the following (Fig. 3.11a, b):

- Small strip or sheet of honeycombed vacuolated cells in a clean background
- Mucinous cytoplasm forming an apical cup
- Naked nuclei with grooves, floating in thin contaminant mucin
- Lacks brush border or goblet cells

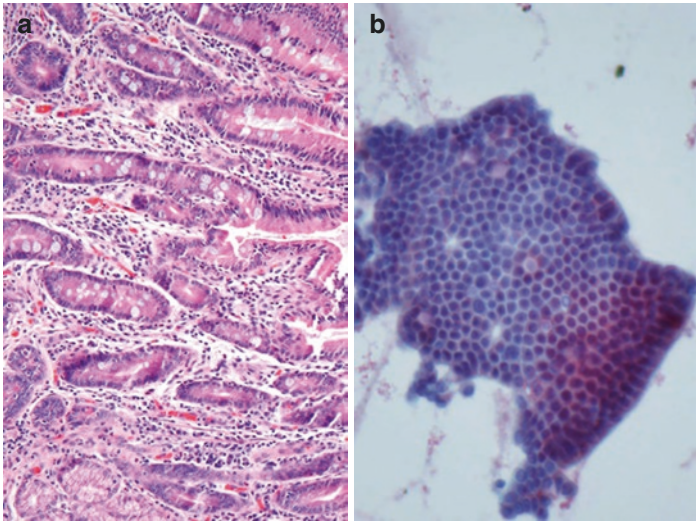


Fig. 3.10 (a) Histology of intestinal mucosa arranged in villi and crypts comprised of columnar absorptive cells and interspersed goblet cells. (b) A cohesive sheet of benign duodenal cells arranged in a “honeycomb” configuration with a brush border. The background is clean. Centrally placed goblet cell nuclei are also identified surrounded by a clear halo. [(a) H&E stain, (b) Pap stain TP, 20 \times]

Benign Mesothelial Cells

The cytologic features of benign mesothelial cells include the following (Fig. 3.12):

- Honeycombed flat sheet of cells
- Characteristic intercellular windows
- Grooved bland nuclei with even chromatin

Benign Hepatocytes

The cytologic features of benign hepatocytes include the following (Fig. 3.13a–c):

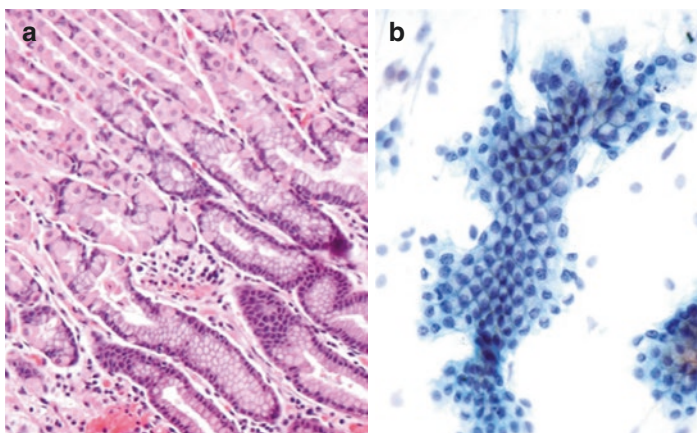


Fig. 3.11 (a) Histology of benign gastric mucosa with foveolar epithelium and underlying oxyntic glands. (b) A sheet of vacuolated cells in a “honey-comb” configuration lacking a brush border or goblet cells. The background is clean. The cells have mucinous cytoplasm which forms an apical cup. Naked nuclei are also seen in the periphery. [(a) H&E stain, (b) Pap stain TP, 20×]

- Polygonal cells
- Abundant, well-defined granular cytoplasm
- Round to oval nuclei and prominent nucleoli
- +/- cytoplasmic pigment and bile

Differential Diagnosis and Pitfalls

The differential diagnosis and pitfalls of contamination are outlined in Table 3.4.

Approach to Pancreatic EUS-FNA Cytology

The diagnostic evaluation of pancreatic lesions involves a multidisciplinary approach that includes findings from clinical history,

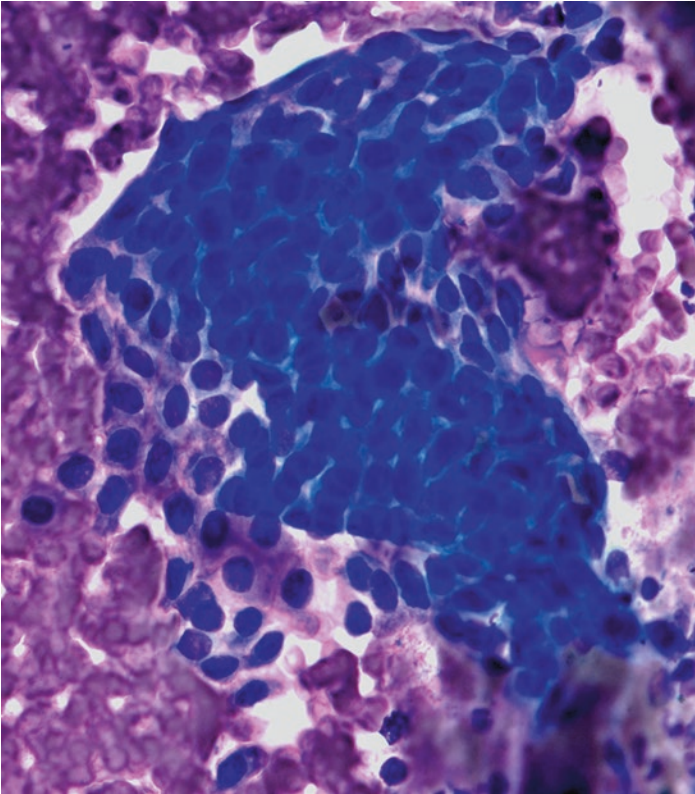


Fig. 3.12 A flat sheet of mesothelial cells with “honeycomb” arrangement and characteristic intercellular windows. [(a) Diff-Quik stain CS, 40×]

imaging, and ancillary tests (such as cyst fluid analysis and molecular testing) in combination with the cytohistology (Fig. 3.14). The recent advances in sampling techniques have added tremendous value in making an accurate diagnosis. The EUS next-generation biopsy needles such as the Moray™ microforceps (US Endoscopy, Mentor, OH) and the SharkCore™ (Medtronic, Inc., Minneapolis, MN) core biopsy needles allow for better sampling of cyst wall and solid lesions, respectively.

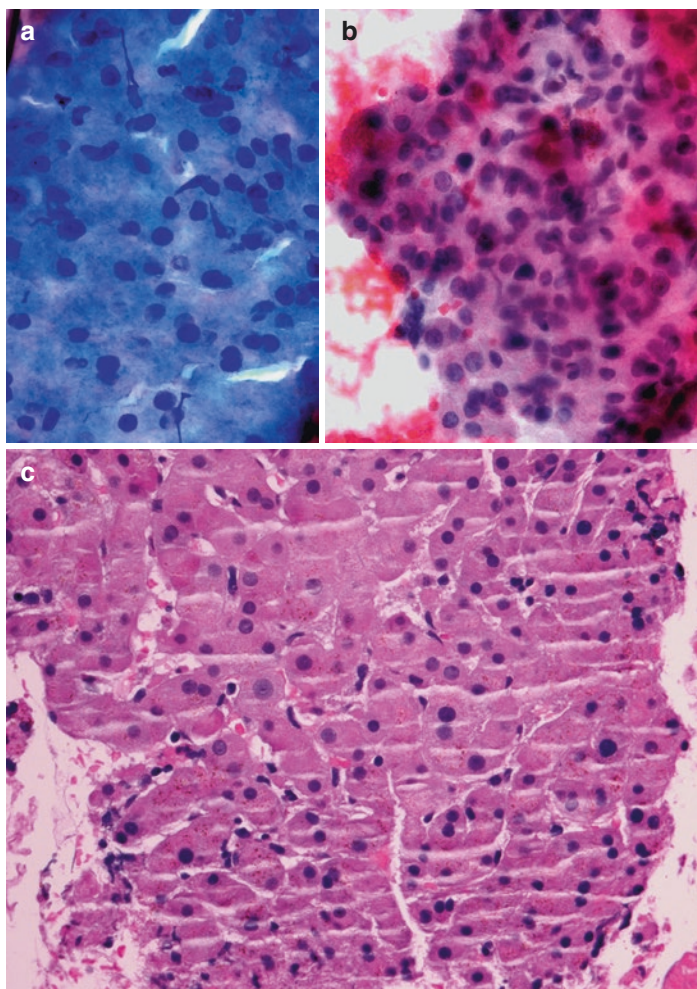


Fig. 3.13 (a, b) A cluster of polygonal cells with abundant granular cytoplasm. The nuclei are centrally placed and round with prominent nucleoli. (c) Histology of hepatocytes arranged in cords separated by sinusoids. The hepatocytes are polygonal cells with centrally located round nuclei, with nucleoli, and pigmented granular cytoplasm. [(a) Diff-Quik stain CS, 60 \times , (b) Pap stain CS, 40 \times , (c) H&E stain]

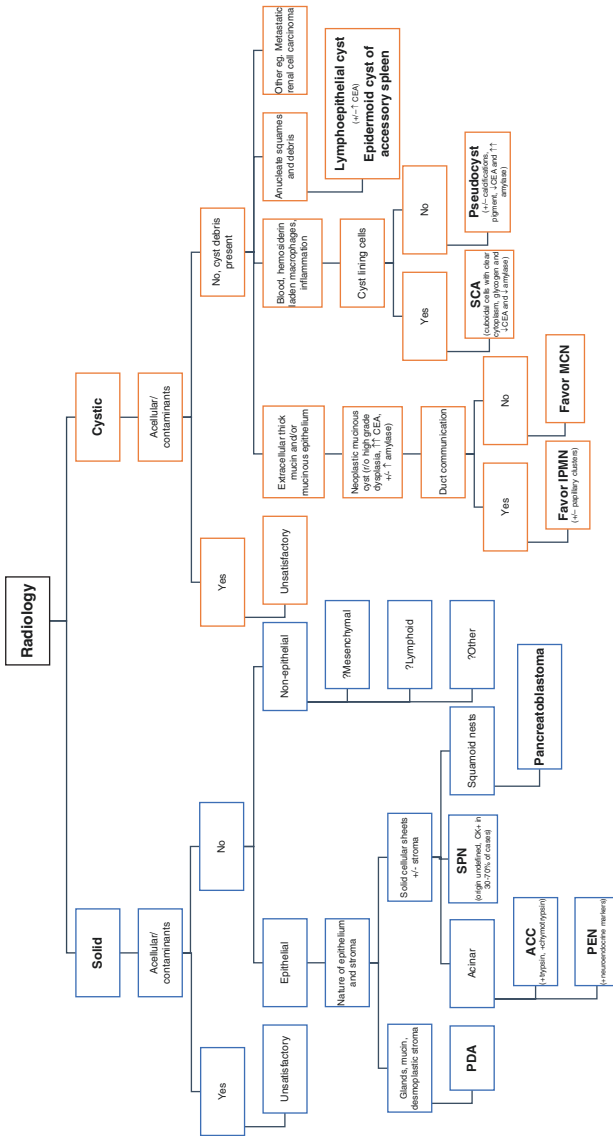


Fig. 3.14 An algorithmic approach in the EUS-FNA cytology of pancreatic neoplasms (PDA pancreatic ductal adenocarcinoma, IPMN intraductal papillary mucinous neoplasm, PEN pancreatic endocrine neoplasm, SCA serous cystadenoma, ACC acinar cell carcinoma, SPN solid pseudopapillary neoplasm, r/o rule out, CEA carcinoembryonic antigen, CK cytokeratin)

Table 3.4 Differential diagnosis and pitfalls of gastrointestinal contamination

Well-differentiated ductal adenocarcinoma	Small groups and sheets of glandular cells with crowded architecture (“drunken” honeycomb) High nuclear/cytoplasmic (N:C) ratio Irregular nuclear membranes Anisonucleosis to the degree of at least 1:4
Intraductal papillary mucinous neoplasm (IPMN)	Cystic dilation of main pancreatic ducts and/or side branches with or without a solid component Thick, viscid, colloid-like neoplastic mucin Low-grade dysplasia may be impossible to separate from benign gastric or duodenal epithelium High-grade dysplasia—cells with increased N:C ratio and significant chromatin abnormalities

References

1. Collins JA, Ali SZ, VandenBussche CJ. Pancreatic cytopathology. *Surg Pathol Clin.* 2016;9(4):661–76.
2. Edge SB, Compton CC. The American joint committee on Cancer: the 7th edition of the AJCC cancer staging manual and the future of TNM. *Ann Surg Oncol.* 2010;17(6):1471–4.
3. Coley SC, Strickland NH, Walker JD, Williamson RC. Spiral CT and the pre-operative assessment of pancreatic adenocarcinoma. *Clin Radiol.* 1997;52(1):24–30.
4. Centeno BA. Pancreatic cytopathology: practical points to avoid common pitfalls. United States and Canadian Academy of Pathology. 2011.
5. Kurzawinski TR, Deery A, Dooley JS, Dick R, Hobbs KE, Davidson BR. A prospective study of biliary cytology in 100 patients with bile duct strictures. *Hepatology.* 1993;18(6):1399–403.
6. Fogel EL, Sherman S. How to improve the accuracy of diagnosis of malignant biliary strictures. *Endoscopy.* 1999;31(9):758–60.

7. Hoda RS, Pitman MB. Pancreatic cytology. *Surg Pathol Clin.* 2018;11(3):563–88.
8. Avadhani V, Hacıhasanoglu E, Memis B, Pehlivanoglu B, Hanley KZ, Krishnamurti U, et al. Cytologic predictors of malignancy in bile duct brushings: a multi-reviewer analysis of 60 cases. *Mod Pathol.* 2017;30(9):1273–86.
9. Conrad R, Castelino-Prabhu S, Cobb C, Raza A. Cytopathology of the pancreatobiliary tract—the agony, and sometimes, the ease of it. *J Gastrointest Oncol.* 2013;4(2):210–9.
10. Bellizzi AM, Stelow EB. Pancreatic cytopathology: a practical approach and review. *Arch Pathol Lab Med.* 2009;133(3):388–404.
11. Puli SR, Bechtold ML, Buxbaum JL, Eloubeidi MA. How good is endoscopic ultrasound-guided fine-needle aspiration in diagnosing the correct etiology for a solid pancreatic mass?: a meta-analysis and systematic review. *Pancreas.* 2013;42(1):20–6.
12. Chen J, Yang R, Lu Y, Xia Y, Zhou H. Diagnostic accuracy of endoscopic ultrasound-guided fine-needle aspiration for solid pancreatic lesion: a systematic review. *J Cancer Res Clin Oncol.* 2012;138(9):1433–41.
13. Horwhat JD, Paulson EK, McGrath K, Branch MS, Baillie J, Tyler D, et al. A randomized comparison of EUS-guided FNA versus CT or US-guided FNA for the evaluation of pancreatic mass lesions. *Gastrointest Endosc.* 2006;63(7):966–75.
14. Affolter KE, Schmidt RL, Matynia AP, Adler DG, Factor RE. Needle size has only a limited effect on outcomes in EUS-guided fine needle aspiration: a systematic review and meta-analysis. *Dig Dis Sci.* 2013;58(4):1026–34.
15. Volmar KE, Vollmer RT, Jowell PS, Nelson RC, Xie HB. Pancreatic FNA in 1000 cases: a comparison of imaging modalities. *Gastrointest Endosc.* 2005;61(7):854–61.
16. Micames C, Jowell PS, White R, Paulson E, Nelson R, Morse M, et al. Lower frequency of peritoneal carcinomatosis in patients with pancreatic cancer diagnosed by EUS-guided FNA vs. percutaneous FNA. *Gastrointest Endosc.* 2003;58(5):690–5.
17. Chong A, Venugopal K, Segarajasingam D, Lisewski D. Tumor seeding after EUS-guided FNA of pancreatic tail neoplasia. *Gastrointest Endosc.* 2011;74(4):933–5.
18. Krasinskas AM. Developmental disorders of the gallbladder, extrahepatic biliary tract, and pancreas. In: Odze RD, Goldblum JR, editors. *Surgical pathology of the GI tract, liver, biliary tract and pancreas*: Saunders; 2015. p. 980–94.
19. Kozu T, Suda K, Toki F. Pancreatic development and anatomical variation. *Gastrointest Endosc Clin N Am.* 1995;5(1):1–30.
20. Pitman MB. Pancreas and biliary tree. In: *Cytology: diagnostic principles and clinical correlates*: Saunders; 2014. p. 399–421.
21. Zaman MB. The pancreas. In: Koss LG, editor. *Diagnostic cytology and its histopathologic bases*, 2. 5th ed: Lippincott Williams & Wilkins; 2006. p. 1428–56.

22. Stelow EB, Bardales RH, Shami VM, Woon C, Presley A, Mallery S, et al. Cytology of pancreatic acinar cell carcinoma. *Diagn Cytopathol.* 2006;34(5):367–72.
23. Centeno B. Diagnostic cytology of the biliary tract and Pancreas. In: Odze RD, Goldblum JR, editors. *Surgical pathology of the GI tract, liver, biliary tract and pancreas.* 4th ed: Saunders; 2015. p. 950–79.
24. Collins BT, Cramer HM. Fine-needle aspiration cytology of islet cell tumors. *Diagn Cytopathol.* 1996;15(1):37–45.
25. Nguyen GK, Rayani NA. Hyperplastic and neoplastic endocrine cells of the pancreas in aspiration biopsy. *Diagn Cytopathol.* 1986;2(3):204–11.
26. Layfield LJ, Jarboe EA. Cytopathology of the pancreas: neoplastic and nonneoplastic entities. *Ann Diagn Pathol.* 2010;14(2):140–51.
27. Stelow EB, Bardales RH, Stanley MW. Pitfalls in endoscopic ultrasound-guided fine-needle aspiration and how to avoid them. *Adv Anat Pathol.* 2005;12(2):62–73.
28. Nagle JA, Wilbur DC, Pitman MB. Cytomorphology of gastric and duodenal epithelium and reactivity to B72.3: a baseline for comparison to pancreatic lesions aspirated by EUS-FNAB. *Diagn Cytopathol.* 2005;33(6):381–6.
29. Stelow EB, Stanley MW, Bardales RH, Mallery S, Lai R, Linzie BM, et al. Intraductal papillary-mucinous neoplasm of the pancreas. The findings and limitations of cytologic samples obtained by endoscopic ultrasound-guided fine-needle aspiration. *Am J Clin Pathol.* 2003;120(3):398–404.
30. Emerson RE, Randolph ML, Cramer HM. Endoscopic ultrasound-guided fine-needle aspiration cytology diagnosis of intraductal papillary mucinous neoplasm of the pancreas is highly predictive of pancreatic neoplasia. *Diagn Cytopathol.* 2006;34(7):457–62.



Nonneoplastic Solid Mass Lesions of the Pancreas

Simon Sung and Rema Rao

Introduction

Lesions that mimic solid pancreatic neoplasms are often incidentally detected during clinical workup. While imaging techniques have improved, it is difficult to diagnose pancreatic neoplasms with radiologic imaging alone, and clinical presentations can also be misleading. Approximately 5% to 10% of pancreatectomies performed with clinical and radiologic suspicion of malignancy prove to be nonneoplastic lesions [1, 2]. Nonneoplastic lesions that usually appear as a solid mass on imaging include chronic pancreatitis (CP), heterotopic spleen, sarcoidosis, and rare infectious diseases among others [3, 4]. Correlation between clinical, radiologic, and cytomorphologic features can help in the diagnosis.

S. Sung

Columbia University Medical Center-New York Presbyterian,
Department of Pathology and Cell Biology, New York, NY, USA

R. Rao (✉)

Department of Pathology and Laboratory Medicine, Weill-Cornell
Medicine, New York Presbyterian Hospital, New York, NY, USA
e-mail: rer9052@med.cornell.edu

Chronic Pancreatitis

Background

A vast majority of nonneoplastic solid mass lesions in the pancreas are due to chronic pancreatitis (CP). The causes of pancreatitis include alcohol, autoimmune, ductal obstruction, paraduodenal (“groove”) pancreatitis, hypercalcemia, hyperlipidemia, eosinophilia (parasitic infections, allergies, or paraneoplastic syndromes), hereditary (cystic fibrosis) causes, trauma (radiation, procedure), or drug related [5, 6]. Pancreatitis can occur at any age, including in children, with genetic predispositions. The most common cause of pancreatitis in adults includes alcoholic pancreatitis [7]. Clinically, patients initially present with epigastric pain and steatorrhea due to fat malabsorption [8]. Progressively, there is destruction of pancreatic tissue and loss of function, leading to diabetes mellitus and other pancreatic enzyme insufficiencies. In advanced disease, more worrisome signs develop that include splenic/portal vein thrombosis, jaundice, weight loss, and ascites. Significant laboratory findings include elevated serum amylase and lipase levels [5–8].

The symptoms of CP can be intermittent and have a prolonged course unless managed appropriately. Treatment includes removing the offending agent, dietary management, pancreatic enzyme replacement, and surgical resection in severe cases [9]. Long-standing CP has increased risk of development of pancreatic cancer. When a mass-like lesion is seen on imaging, EUS-FNA is often performed to rule out malignancy and to avoid unnecessary surgery.

Imaging and Gross Findings

Radiology can be of immense help in diagnosing CP and also help identify the cause in some cases such as in cases of obstructing pancreatic stones. Endoscopic retrograde cholangiopancreatography (ERCP) can detect subtle changes in the main pancreatic duct

and its side branches, which can be helpful in recognizing early stages of CP. Conventional computed tomography (CT) scan can identify changes in pancreas size, echogenicity, contour, ductal dilatation, and pancreatic calcifications and characterize CP to a certain degree [5, 8]. However, in late stages of CP, presence of extensive fibrosis can mimic adenocarcinoma on CT scan [5].

Grossly, CP may involve the pancreas in a focal, segmental, or diffuse manner. The involved pancreas appears firm, indurated, and fibrotic with ductal distortion including upstream ductal dilation, cystic change, and occasional calculi. With progression, the gland tends to become more fibrotic (“rock hard”) and can undergo atrophy.

Key Cytomorphologic Features

CP can produce a wide spectrum of cytomorphologic changes depending on the stage [10]. Usually, the exocrine glands are lost and replaced by dense fibrous tissue and inflammatory cells, leading to a hypocellular sample on fine-needle aspiration (FNA). The background material may show mixed inflammatory and calcific debris [11]. A spectrum of benign ductal cells and acini may be seen, albeit scant. The ductal groups can show mild reactive atypia, but there is a lack of anisonucleosis (nuclear size variation of 1:4), and the N/C ratio and architecture are maintained [10]. The key cytologic features of CP are listed below and include the following (Figs. 4.1, 4.2, 4.3, 4.4, and 4.5):

- Low cellularity.
- Flat cohesive ductal sheets with slight crowding.
- Low N/C ratio.
- Slightly enlarged nuclei with little variation in size (less than 4 times).
- Round smooth nuclear membranes.
- Prominent nucleoli.
- Background shows stromal cells and inflammatory cells with lymphoid predominance and calcific debris if present.

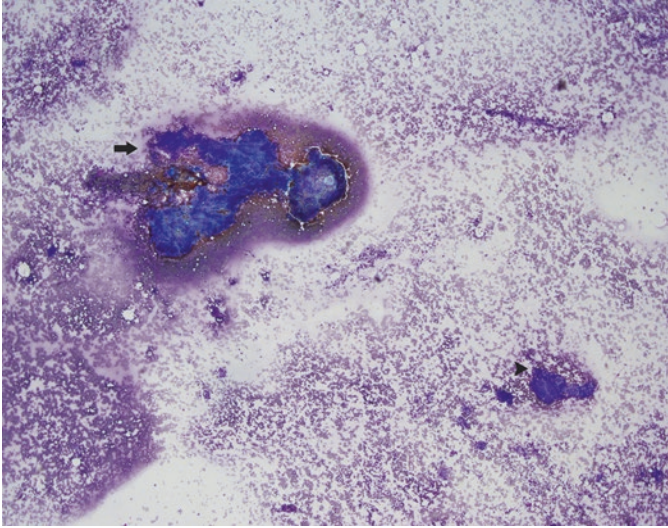


Fig. 4.1 Low-power view of Diff-Quik stained smear of chronic pancreatitis shows low cellular sample with stromal fragments (arrow) and scant ductal epithelial clusters (arrowhead)

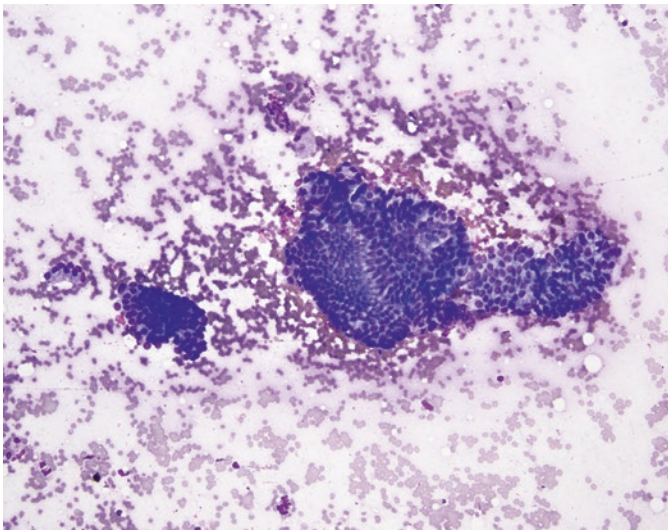


Fig. 4.2 High-power magnification of Diff-Quik stained smear shows columnar cells in a flat cohesive sheet. These cells appear benign without atypia

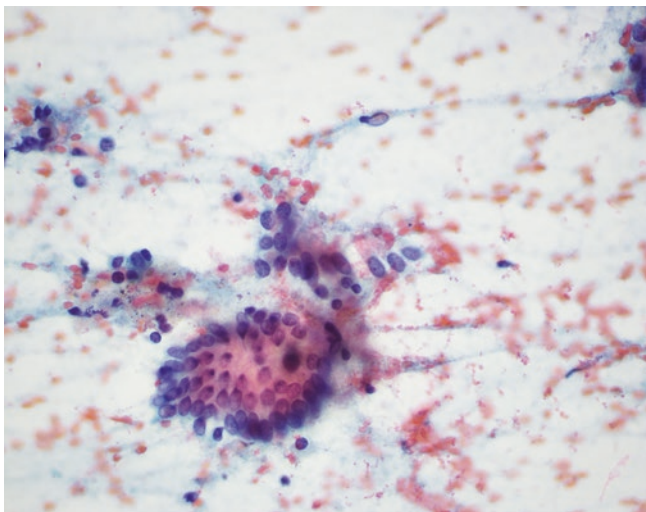


Fig. 4.3 Pap-stained smear slide demonstrates bland columnar cells with occasional nucleoli. The nuclei appear slightly enlarged, but the N/C ratio is low with a smooth nuclear membrane contour

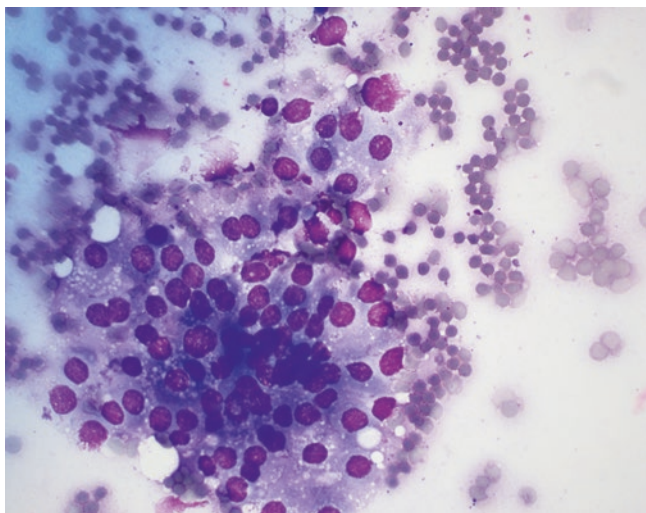


Fig. 4.4 Reactive pancreatic ductal cells can show mild nuclear atypia with slight crowding and overlapping nuclei forming 3-D structures. Mild anisonucleosis can be appreciated. However, the changes are not enough to warrant atypical or suspicious diagnosis

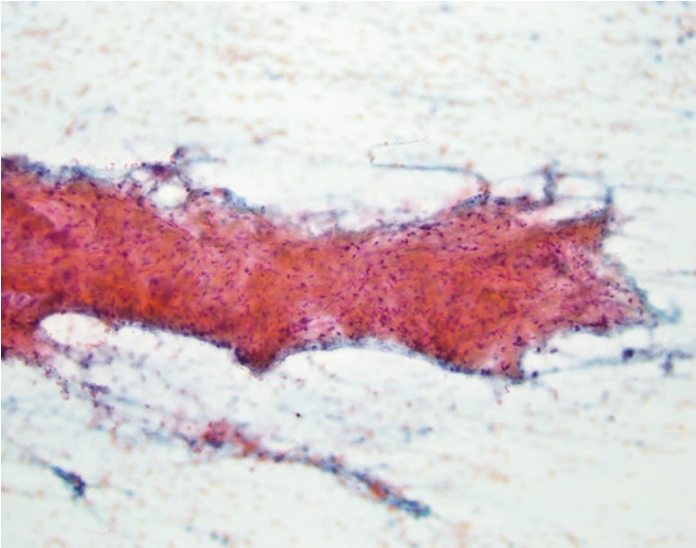


Fig. 4.5 Higher magnification of Pap-stained smear slide shows stromal fragments with few inflammatory cells. Prominent fibroinflammatory fragments without significant ductal epithelium indicate significant atrophy of pancreas. A careful attention must be paid to any associated ductal cells to rule out desmoplastic stroma in adenocarcinoma

Key Histologic Features

Histologically, CP demonstrates fibrotic pancreas with loss of acinar cells and presence of atrophic ductal cells [12]. The dense fibrous stroma and lymphocytic infiltrate may mimic desmoplasia; however, the lobular architecture of the pancreatic parenchyma is preserved. The pattern of fibroinflammatory process can be diffuse. The key histologic features of CP are listed below (Figs. 4.6 and 4.7):

- Atrophy and obliteration of pancreatic acini and ducts with preserved lobular architecture
- Preserved islet cells or focal islet cell hyperplasia
- Fibrosis and duct dilatation due to fibrosis

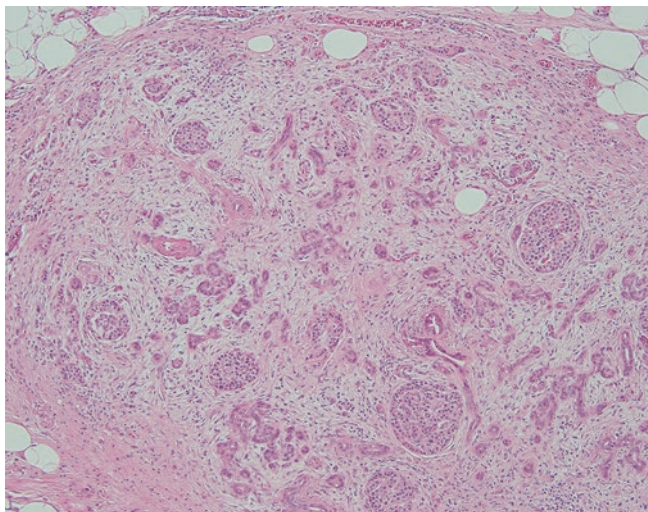


Fig. 4.6 Surgical resection of chronic pancreatitis shows loss of exocrine glands and marked fibrosis with chronic inflammation. The lobular architecture is preserved. The residual islet cells of Langerhans and ductules are seen. These changes can be diffuse in chronic pancreatitis, compared to autoimmune pancreatitis, which shows periductal fibrosis

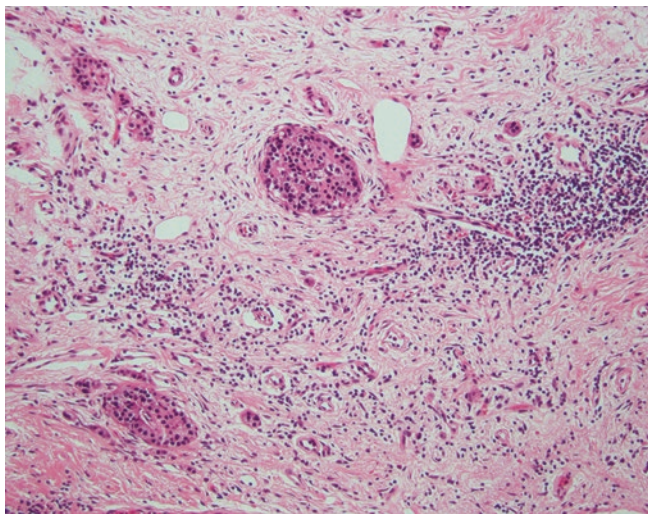


Fig. 4.7 Photomicrograph of higher magnification of surgical resection of chronic pancreatitis shows residual islet cells and lymphocytic predominant inflammation

- Lymphocytic predominant inflammation
- Squamous, mucinous, and pyloric gland metaplasia

Differential Diagnosis

The main differential diagnosis in cytology includes adenocarcinoma and acini prominent neoplasms such as neuroendocrine neoplasms, acinar cell carcinoma, and pancreatoblastoma. CP in particular can mimic a well-differentiated ductal adenocarcinoma both on imaging and cytology. Adenocarcinoma commonly shows a disorganized honeycomb appearance with anisonucleosis (nuclear size variation greater than 4 times), marked nuclear membrane irregularity, and clumpy chromatin pattern (Table 4.1). Retained nuclear expression of SMAD4 (lost in up to 50% of ductal carcinomas) can be helpful.

Autoimmune Pancreatitis

Background

Autoimmune pancreatitis (AIP) is an important subtype of CP marked by lymphoplasmacytic inflammation. AIP is being increasingly recognized and the prevalence has been reported from 5 to 26% of CP [12–16]. It commonly forms a mass-like focus or “pseu-

Table 4.1 Chronic pancreatitis versus adenocarcinoma

	CP	Adenocarcinoma
Nuclear enlargement	Present	Present
Prominent nucleoli	Present	Present
Mitosis	Present	Present
Anisonucleosis	<4×	>4×
Chromatin pattern	Even distribution	Clumpy chromatin, paranucleolar clearing
Amylase, lipase	Elevated	Normal
SMAD4 nuclear expression	Retained	Lost in up to 50% cases
Nuclear membrane contour	Slightly irregular	Markedly irregular

dotumors” formed by marked scarring. AIP shows duct-centric inflammation that often causes duct destruction and obstruction leading to jaundice. There are two types of AIP. Type 1 AIP is the classic lymphoplasmacytic sclerosing pancreatitis with elevated serum IgG4 and increased IgG4-positive plasma cells on histology. The pancreas here may be involved as part of a systemic IgG4-related disease with other co-manifestations. Type II, or idiopathic CP, tends to show no systemic involvement and therefore may not show elevated IgG4 and typically affects younger patients. The elevated serum IgG4 or immunohistochemical stain showing increased IgG4/IgG ratio can help distinguish AIP from adenocarcinoma. Patients may also have elevated antinuclear antibody (ANA). AIP is believed to be a systemic manifestation of a fibroinflammatory disease process with coexisting autoimmune diseases, such as diabetes mellitus, ulcerative colitis, inflammatory bowel disease, Sjogren disease, and systemic lupus erythematosus. Therefore, it is imperative to obtain all available clinical information when analyzing a solid mass-like lesion with lymphoplasmacytic inflammation. Steroid therapy is highly effective, but occasionally surgical approach is considered when clinical, imaging, and cytologic distinction from adenocarcinoma appears challenging.

The international consensus diagnostic criteria (ICDC) for AIP recommend surgical core biopsy for a histologic diagnosis of AIP [17]. The use of FNA for diagnosing AIP has been implicated in a few studies with conflicting results [18–21]. However, EUS-FNA is commonly used to rule out carcinoma and still remains an important tool in the evaluation of AIP. While EUS-FNA may not be a sensitive diagnostic tool for AIP, it can be a helpful diagnostic approach to rule out carcinoma. While some cytomorphologic features can overlap, there are helpful clues to distinguish AIP from adenocarcinoma on cytology.

Imaging and Gross Findings

Conventional CT can be used to assess the pattern of involvement, diffuse, focal, and multifocal. Unlike other types of CP, calcification is rare, and the ducts may be non-dilated or diffusely narrow. On ERCP, AIP shows focal, segmental, or diffuse narrowing of the main pancreatic duct and non-visualization of side branches.

When a mass-like focus is present, it can cause upstream dilatation, mimicking carcinoma.

Gross examination of the resected specimen will show focal, multifocal, or diffuse involvement of AIP. The focal type commonly involves the head of pancreas and shows white firm fibrotic lesion, mimicking carcinoma. The main pancreatic duct shows narrowing, in contrast to other types of CP.

Key Cytomorphologic Features

In the focal type of AIP presenting as a mass, FNA is often performed to rule out carcinoma. The cytomorphologic features are similar to CP of other etiologies. The aspirate is hypocellular with few ductal cells (Fig. 4.8). The pancreatic acinar cells are readily aspirated providing an acinar-rich aspirate in a few cases.

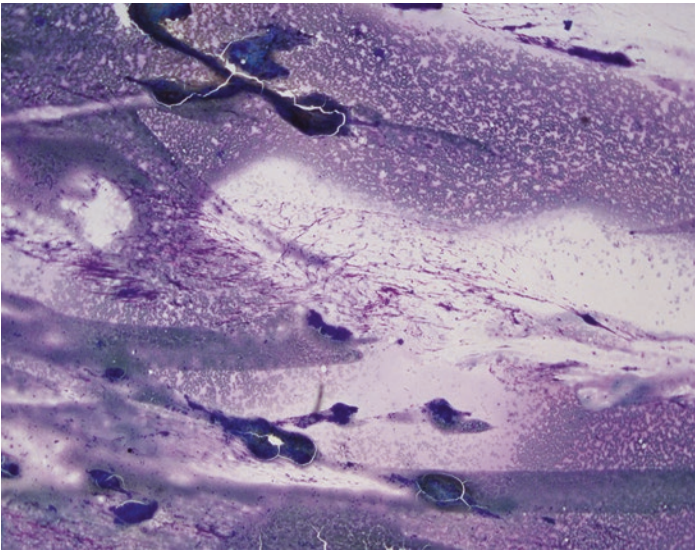


Fig. 4.8 Low-power image of Diff-Quik stained FNA smear slide shows lack of epithelial cells. Fibroinflammatory fragments are identified with few lymphoid cells with crush artifact in the background. Fibroinflammatory fragments with plasmacytoid cells may raise suspicion for autoimmune pancreatitis; however, plasma cells may be scant on smear samples

The most helpful clue might be the increased IgG4-positive plasma cells; however, these may be scant or absent. The ductal epithelium can show marked reactive atypia, warranting a careful examination (Figs. 4.9, 4.10, 4.11, and 4.12). The ductal cells with atypia can show overlap and appear as three-dimensional aggregates with crowding, lack of polarity, and increased N/C ratio. Fibroblastic stromal cells may be scant, as these are difficult to aspirate. Lymphocytes are noted in the background and embedded within the stromal fragments (cellular stromal fragments) (Figs. 4.13 and 4.14). The key cytomorphologic features are listed below:

- Low cellularity
 - Ductal cells may show cytologic atypia
 - Nuclear crowding
 - Loss of polarity

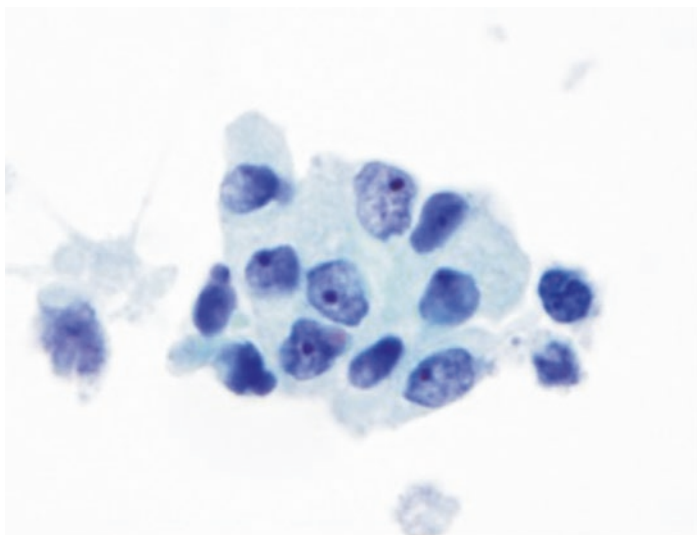


Fig. 4.9 Photomicrograph of high-power image of ThinPrep image of AIP, demonstrating marked nuclear atypia with irregular nuclear membrane contour, hyperchromatic chromatin pattern, and prominent nucleoli. These features mimic adenocarcinoma, warranting a careful examination of the entire sample and review of clinical history

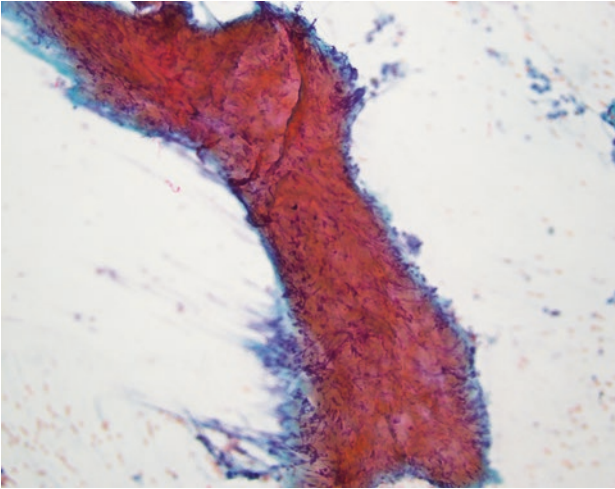


Fig. 4.10 High-power image of Pap-stained smear demonstrates fibroinflammatory clusters without associated epithelial cells. These fragments can also be seen in chronic pancreatitis and in invasive carcinomas. Careful documentation of clinical history and ancillary studies are warranted if AIP is suspected

- Increased N/C ratio
- Irregular nuclear contour
- Fibroinflammatory stromal cells
- Lymphoplasmacytic inflammation may be present
 - Increased IgG4/IgG positive cells

Key Histologic Features

Histologic features are different for the two types of AIP. In general, AIP demonstrates dense, periductal, lymphoplasmacytic inflammation, with storiform fibrosis (Fig. 4.15). AIP type I is accompanied by numerous IgG4-positive plasma cells (more than 10/HPF), phlebitis, and lymphoid aggregates (Fig. 4.16). Type II is defined by granulocytic epithelial lesions consisting of neutrophilic destruction of the ductal epithelium [17].

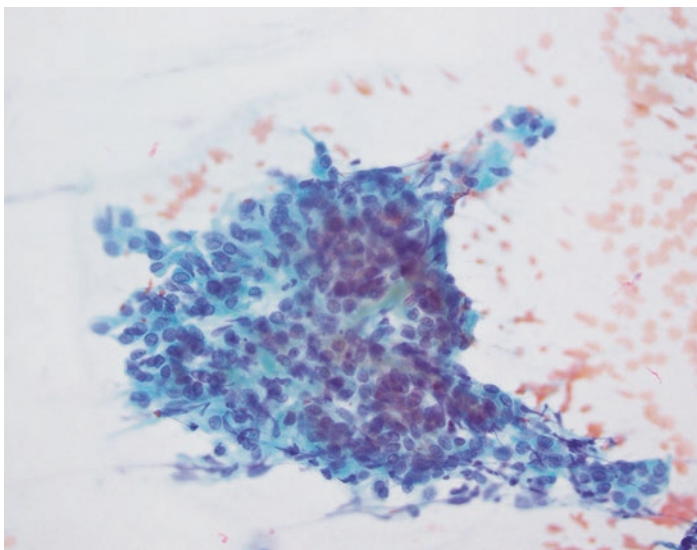


Fig. 4.11 AIP can have increased cytomorphologic atypia. The image of Pap-stained smear slide shows disorganized glandular cells with nuclear crowding and loss of polarity. These features can lead to atypical diagnosis and rarely adenocarcinoma on FNA biopsy samples. Again, clinical history and ancillary studies are crucial

- Periductal chronic inflammation and storiform fibrosis
 - IgG4-positive plasma cells (>10/HPF) in Type I AIP
- Obliterative phlebitis
- Granulocytic epithelial lesion (type II)

Differential Diagnosis

The main differential diagnosis to consider when considering AIP is adenocarcinoma. A careful review of the FNA sample along with pertinent clinical and imaging findings is warranted when AIP is suspected. Many cases of AIP are diagnosed as atypia and rarely as a malignant neoplasm on FNA. Cytomorphologic features of AIP and well-differentiated adenocarcinoma can overlap. When cytomor-

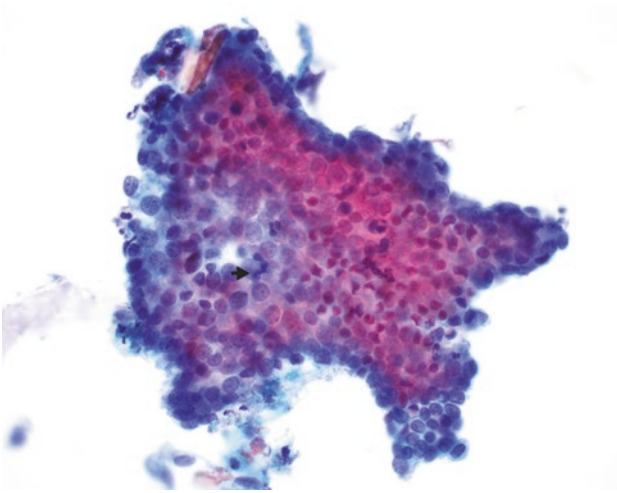


Fig. 4.12 A ThinPrep slide can show similar findings. Again seen, are overlapping crowded glandular cells with low N/C ratio. Occasional mitotic figures (arrow) can be seen

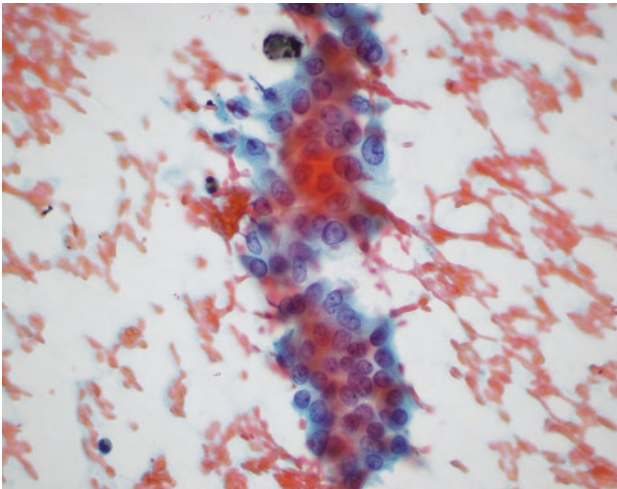


Fig. 4.13 High-power magnification of the atypical ductal cells in AIP demonstrates worrisome nuclear atypia, including macronucleoli, marked nuclear membrane irregularities, and moderate anisonucleosis in a cohesive cluster. No single malignant cells were seen, which can be a helpful clue

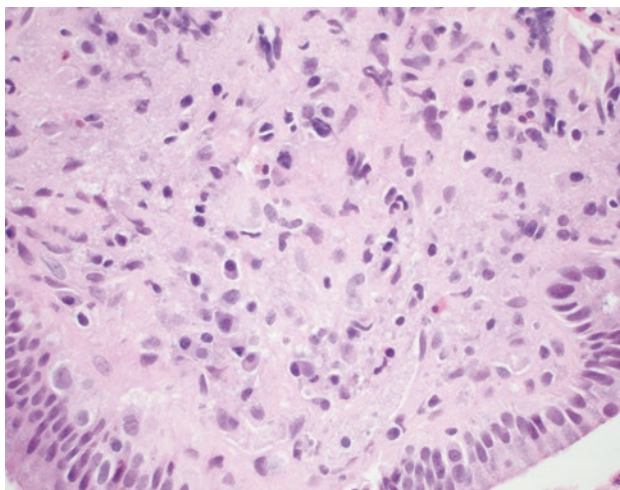


Fig. 4.14 Cell block preparation may be helpful to identify fibroinflammatory fragments with lymphoplasmacytic inflammation. Few plasma cells are seen in this cell block section, in which IgG4 and IgG immunohistochemical stains can be performed. Note that type II AIP does not have increased IgG4 expression

phologic features cannot distinguish a neoplasm from AIP, further exploration into clinical history is warranted (Table 4.2). Another differential diagnosis to consider is inflammatory myofibroblastic tumor especially when there is a prominent “cellular” stromal component. Immunohistochemical stain with ALK and IgG4 can be helpful in distinguishing these two lesions in addition to the presence of benign pancreatic elements intermixed with inflammation in AIP.

Potential pitfalls in cytologic diagnosis can be related to the significant centroacinar component that can be seen in these aspirates. The presence of a prominent acinar component to these smears raises a differential diagnoses that include acinar cell carcinoma, neuroendocrine tumors (NET), and solid pseudopapillary neoplasms. The lack of significant nuclear atypia and bare nuclei in these aspirates should help rule out an acinar cell carcinoma. NET shows plasmacytoid, oval, spindled, or rarely clear cells with neuroendocrine chromatin that is lacking in AIP.

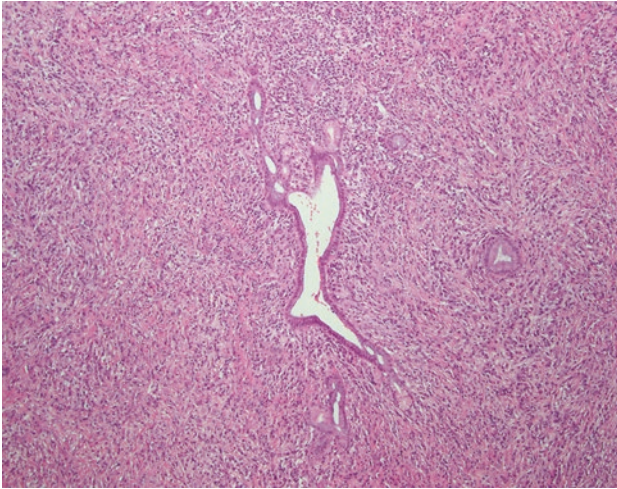


Fig. 4.15 Surgical resection of AIP shows dense fibroinflammatory process centered around the pancreatic duct. Alcohol-related or other chronic pancreatitis can show markedly diffuse fibroinflammatory process, but periductal inflammation is rare. Inflammatory myofibroblastic tumor may be considered in the differential. Ancillary studies with ALK1 and IgG4 immunohistochemical stains can help distinguish these lesions

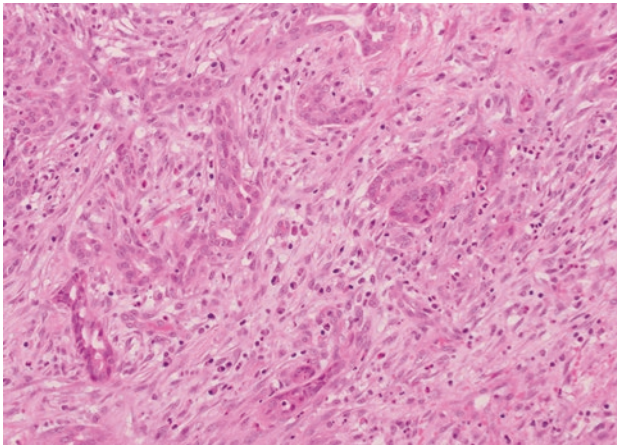


Fig. 4.16 High-power view of AIP shows compressed ductal epithelium, but does not appear infiltrative. Abundant plasma cells are appreciated. Increased IgG4/IgG ratio or increased serum level of IgG4 can help diagnose AIP

Table 4.2 AIP versus adenocarcinoma, key features

	AIP	Adenocarcinoma
Nuclear atypia	Mild to moderate	Marked
Cell crowding/3-D clusters	Present	Present
Single cells	Likely GI contamination	Single tumor cells
IgG4/IgG positive cells	May be elevated	Not elevated
Serum IgG4	May be elevated	Not elevated
Serum ANA	May be elevated	Not elevated

Paraduodenal Groove Pancreatitis

Background

Paraduodenal (groove) pancreatitis (GP) is another subtype of CP that can present as an ill-defined suspicious mass. As the name suggests, it affects the pancreaticoduodenal groove, the space between the duodenum, pancreatic head, and the distal common bile duct (CBD). It is believed to result from a focal CP that affects the minor papilla of the duodenum [22]. Commonly affected patients are middle-aged men with significant alcohol abuse [23]. GP predominantly involves the duodenal wall causing dilated ducts, inspissated secretions, and pseudocystic changes with dense stromal fibrosis that can “spillover” into the pancreatic parenchyma [22]. These lesions can clinically and radiologically mimic carcinoma. Surgical resection is sometimes performed when carcinoma cannot be excluded by imaging and EUS-FNA. Otherwise, patients are treated conservatively and show excellent prognosis.

Imaging and Gross Findings

CT imaging findings can vary from ill-defined fat stranding and inflammatory changes to a frank mass-like lesion, raising the suspicion for a neoplasm. Calcifications, small cysts, and focally thickened duodenal wall can be features suggestive of GP on CT imaging [23, 24]. Fibroinflammatory involvement of the pancreas can be seen on CT and MRI imaging [23, 25]. Grossly the pancreas may show fibrotic pancreatic parenchyma and small cysts, mirroring radiologic findings (Fig. 4.17).

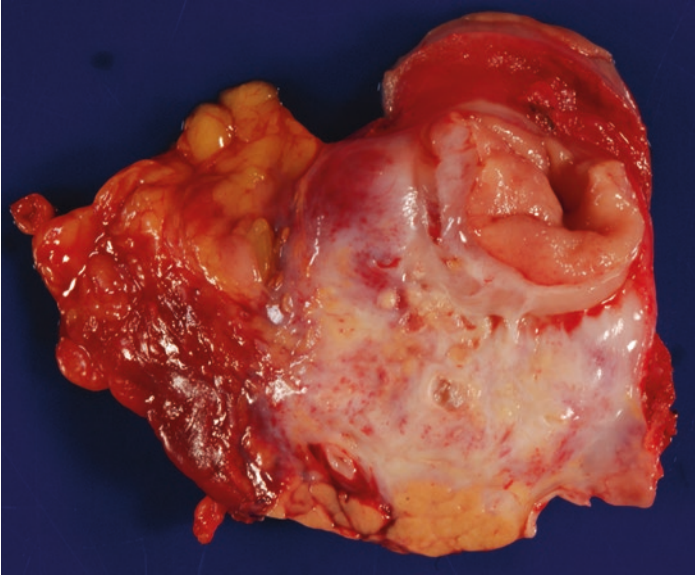


Fig. 4.17 Gross image of GP showing ill-defined white fibrotic area surrounding the pancreaticoduodenal area (Photograph credit: Dr. Meredith Pittman, New York-Presbyterian-Weill Cornell Medicine)

Key Cytomorphologic Features

The key cytomorphologic features include the following [26]:

- Foamy cells
- Spindled cells with plump epithelioid nuclei and prominent nucleoli
- Granular proteinaceous debris
- Brunner's gland hyperplasia
- Fibroblastic stromal fragments
- Occasional multinucleate giant cells

Key Histologic Features

The key histologic features include the following [22]:

- Thickened duodenal wall and minor ampulla:
 - Marked fibrosis involving adjacent pancreas
- Dilated pancreatic duct with inspissated secretions
- Brunner's gland hyperplasia
- Paraduodenal cysts

Intrapancreatic Accessory Spleen

Background

Intrapancreatic accessory spleen (IPAS) is a congenital abnormality that can be found in the tail of pancreas [27]. It is thought to result from the failure of fusion of multiple splenic anlagen during embryonic development [27]. Accessory spleen (AS) can also be found in the splenic hilum, omentum, and the splenic ligament [28]. The prevalence of AS is reported to be from 10% to 20% and IPAS is thought to be less common [27, 29, 30]. It is a benign entity, which does not require any treatment. However, it can be mistaken for a neoplasm. Thus, an accurate diagnosis is crucial to avoid unnecessary surgery.

Imaging and Gross Findings

Ultrasound, CT, and MRI imaging findings show hypervascular solid nodules with homogeneous density equal to spleen, commonly located in the pancreatic tail, which can be indistinguishable from a nonfunctioning pancreatic neuroendocrine tumor [28, 31, 32]. Gross examination will reveal a well-circumscribed lesion with white pulp and red pulp, resembling spleen.

Key Cytologic Features

The key cytomorphic features include the following (Figs. 4.18, 4.19, and 4.20):

- Polymorphous population of lymphocytes
- Mixed inflammatory cells, including eosinophils, macrophages, plasmacytoid cells, and neutrophils
- Endothelial cells (splenic sinusoidal cells)
 - CD8-positive endothelial cells
- Numerous platelet aggregates
- Hemosiderin-laden macrophages
- No tingible body macrophages

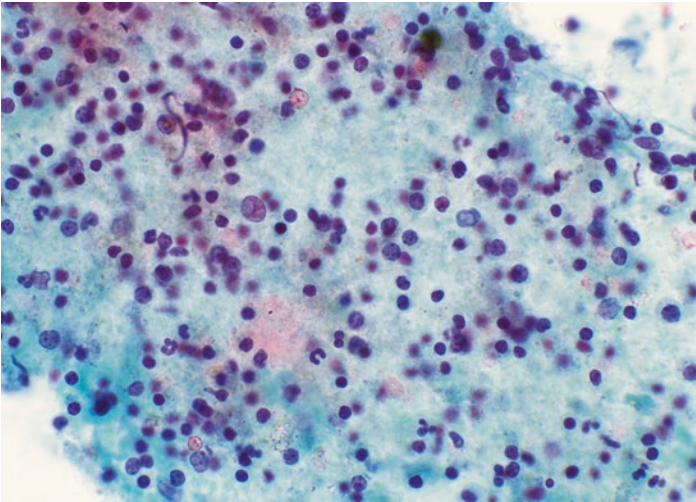


Fig. 4.18 ThinPrep slide of intrapancreatic spleen shows polymorphous population of lymphocytes with some neutrophils and background of granular proteinaceous debris and hemosiderin pigments. The background debris may represent platelet aggregates

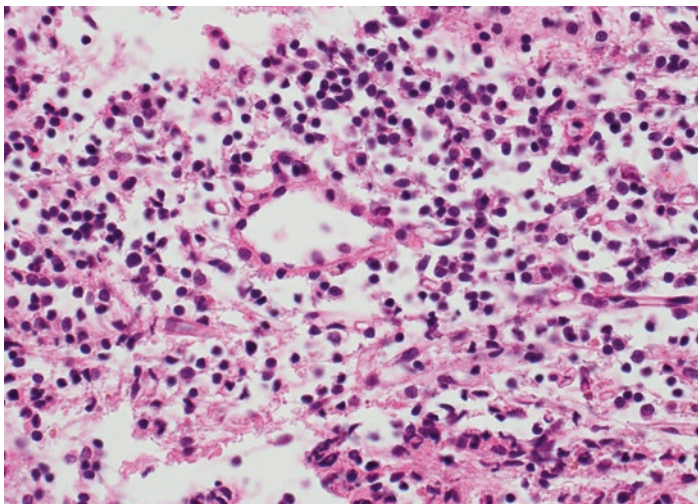


Fig. 4.19 Cell block preparation shows a vascular space lined with endothelial-type cells on a background of a polymorphous population of lymphocytes

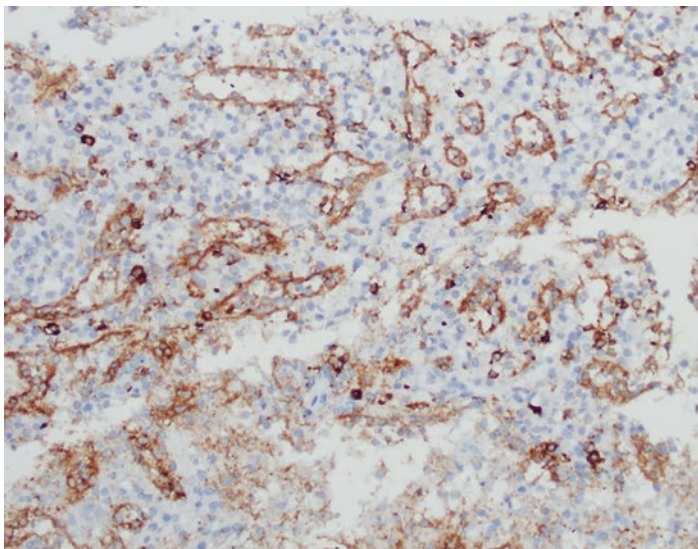


Fig. 4.20 The sinusoidal endothelial cells express CD8, showing positive cytoplasmic stain

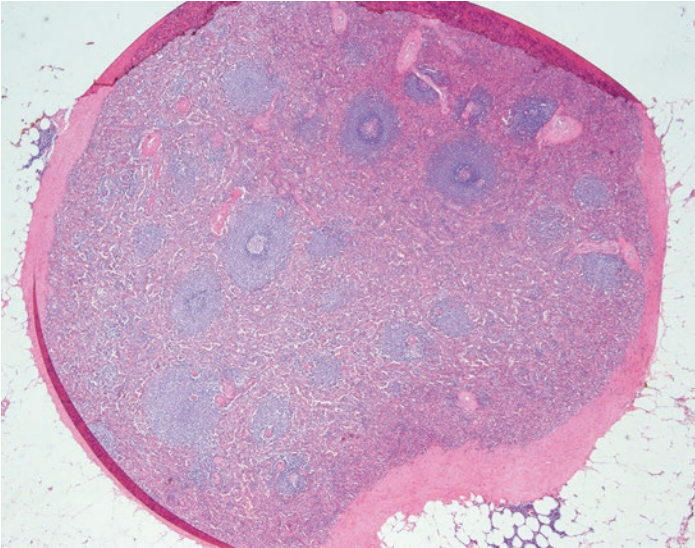


Fig. 4.21 Micrograph of peripancreatic spleen resembles normal spleen with white pulp and red pulp. On radiologic imaging, these well-circumscribed lesions in the tail of pancreas can raise suspicion for a pancreatic neuroendocrine neoplasm. FNA biopsy can help avoid unnecessary surgeries

Histologic Features

The key histologic features include the following (Fig. 4.21):

- Resembles normal spleen
 - Varying portion of red and white pulp with sinuses lined by littoral cells

Differential Diagnosis

On imaging, as mentioned above, IPAS can mimic PNET due to its location and similar radiologic appearance. FNA samples can rule out PNET based on cytomorphology and immunohistochemical stains if necessary. The other main differential to consider is a reactive lymph node. A reactive lymph node (discussed below in detail) does not have sinusoidal endothelial cells and

has tingible-body macrophages. Both are benign lesions; however, lymphoma must be considered and rule out. When abundant lymphoid component is seen on an FNA, submitting a fresh sample in RPMI for flow cytometry is recommended to rule out lymphoma.

Intrapancreatic Reactive Lymph Node

Intrapancreatic reactive lymph nodes can present as solid pancreatic lesions on CT imaging [33]. Infections, drugs, and other systemic inflammatory conditions can cause lymphadenopathy, prompting an EUS-FNA to rule out malignancy. Polymorphous population of lymphocytes with tingible body macrophages and lymphoglandular bodies can be reassuring features of this benign lesion; however, a lymphoma must be rule out if clinically suspicious. In such cases, a dedicated pass in RPMI is warranted for flow cytometry analysis.

Key Cytomorphologic Features

The key cytologic features include the following (Fig. 4.22).

- Polymorphous population of lymphocytes
- Tingible body macrophages
- Lymphoglandular bodies

Sarcoidosis

Background

Sarcoidosis is a systemic, chronic, inflammatory process that can affect any organ [34]. It manifests as noncaseating granulomas that is readily recognizable in surgical histology and cytopathology samples. Clinically, patients can present with fever, weight loss, anorexia, and fatigue. Radiologically, high-resolution CT can detect lymphadenopathy and micronodules along perilymphatic

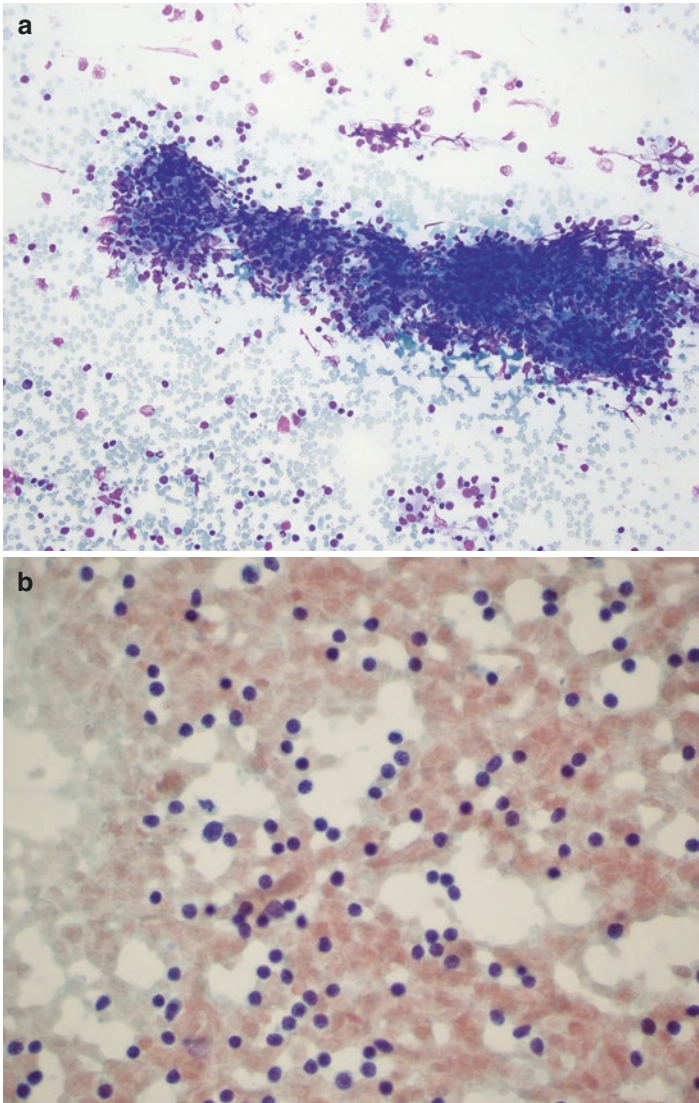


Fig. 4.22 (a, b) FNA of an intrapancreatic lymph node demonstrating a polymorphous population of lymphocytes. If lymphoma is suspected, sending additional biopsy for flow cytometry is warranted

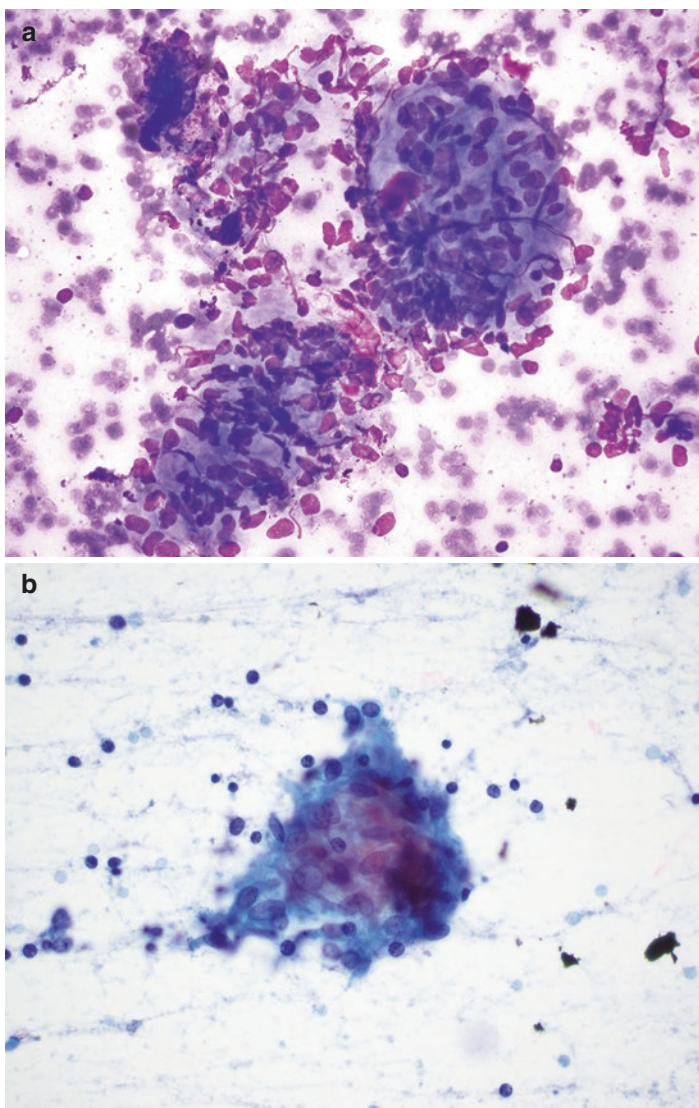


Fig. 4.23 (a, b) The micrograph of Diff-Quik and Pap-stained smear slide shows aggregates of epithelioid histiocytes. The histiocytes show elongated and often “kidney bean” shaped nuclei. Sarcoidosis is a systemic disease, and infectious etiology must be ruled out when granulomas are identified on FNA biopsy samples

distribution; however, atypical manifestation can demonstrate a mass-like lesion [35]. Pancreatic involvement of sarcoidosis is rare with only few cases reported in the literature [36–44]. However, it can present as a mass-like lesion, causing ductal obstruction and jaundice, masquerading as an adenocarcinoma [3, 37, 42, 43]. Corticosteroids can be effective; thus, it is an important differential diagnosis to consider in order to avoid unnecessary surgery.

Key Cytologic Features

The key cytologic features include the following (Fig. 4.23):

- Epithelioid histiocytic aggregates
- No necrosis (rare necrosis may be seen)
- Multinucleate giant cells

Histologic Features

- Well-formed noncaseating granulomas
- No microorganisms

References

1. Adsay NV, Basturk O, Klimstra DS, Kloppel G. Pancreatic pseudotumors: non-neoplastic solid lesions of the pancreas that clinically mimic pancreas cancer. *Semin Diagn Pathol.* 2004;21(4):260–7.
2. Wick MR, Tazelaar HD. Pseudoneoplastic lesions: general considerations. *Arch Pathol Lab Med.* 2010;134(3):351–61.
3. Okun SD, Lewin DN. Non-neoplastic pancreatic lesions that may mimic malignancy. *Semin Diagn Pathol.* 2016;33(1):31–42.
4. Frampas E, Morla O, Regenet N, Eugene T, Dupas B, Meurette G. A solid pancreatic mass: tumour or inflammation? *Diagn Interv Imaging.* 2013;94(7–8):741–55.
5. Anaizi A, Hart PA, Conwell DL. Diagnosing chronic pancreatitis. *Dig Dis Sci.* 2017;62(7):1713–20.
6. Kleeff J, Whitcomb DC, Shimosegawa T, Esposito I, Lerch MM, Gress T, et al. Chronic pancreatitis. *Nat Rev Dis Primers.* 2017;3:17060.

7. Uc A, Fishman DS. Pancreatic disorders. *Pediatr Clin N Am*. 2017;64(3):685–706.
8. Tirkes T. Chronic pancreatitis: what the clinician wants to know from MR imaging. *Magn Reson Imaging Clin N Am*. 2018;26(3):451–61.
9. Patel V, Willingham F. The management of chronic pancreatitis. *Med Clin North Am*. 2019;103(1):153–62.
10. Stelow EB, Bardales RH, Lai R, Mallery S, Linzie BM, Crary GS, et al. The cytological spectrum of chronic pancreatitis. *Diagn Cytopathol*. 2005;32(2):65–9.
11. Samad A, Attam R, Pambuccian SE. Calcifications in an endoscopic ultrasound-guided fine-needle aspirate of chronic pancreatitis. *Diagn Cytopathol*. 2013;41(12):1081–5.
12. Notohara K, Burgart LJ, Yadav D, Chari S, Smyrk TC. Idiopathic chronic pancreatitis with periductal lymphoplasmacytic infiltration: clinicopathologic features of 35 cases. *Am J Surg Pathol*. 2003;27(8):1119–27.
13. Hardacre JM, Iacobuzio-Donahue CA, Sohn TA, Abraham SC, Yeo CJ, Lillemoe KD, et al. Results of pancreaticoduodenectomy for lymphoplasmacytic sclerosing pancreatitis. *Ann Surg*. 2003;237(6):853–8; discussion 8–9.
14. Nishimori I, Tamakoshi A, Otsuki M. Research Committee on Intractable Diseases of the Pancreas MoHL, Welfare of J. Prevalence of autoimmune pancreatitis in Japan from a nationwide survey in 2002. *J Gastroenterol*. 2007;42(Suppl 18):6–8.
15. Weber SM, Cubukcu-Dimopulo O, Palesty JA, Suriawinata A, Klimstra D, Brennan MF, et al. Lymphoplasmacytic sclerosing pancreatitis: inflammatory mimic of pancreatic carcinoma. *J Gastrointest Surg*. 2003;7(1):129–37; discussion 37–9.
16. Zamboni G, Luttes J, Capelli P, Frulloni L, Cavallini G, Pederzoli P, et al. Histopathological features of diagnostic and clinical relevance in autoimmune pancreatitis: a study on 53 resection specimens and 9 biopsy specimens. *Virchows Arch*. 2004;445(6):552–63.
17. Shimosegawa T, Chari ST, Frulloni L, Kamisawa T, Kawa S, Mino-Kenudson M, et al. International consensus diagnostic criteria for autoimmune pancreatitis: guidelines of the International Association of Pancreatology. *Pancreas*. 2011;40(3):352–8.
18. Adler JM, Gardner TB. Fine-needle aspiration for autoimmune pancreatitis-not ready for prime time. *Gastrointest Endosc*. 2016;84(2):249–51.
19. Ishikawa T, Itoh A, Kawashima H, Ohno E, Matsubara H, Itoh Y, et al. Endoscopic ultrasound-guided fine needle aspiration in the differentiation of type 1 and type 2 autoimmune pancreatitis. *World J Gastroenterol*. 2012;18(29):3883–8.
20. Kanno A, Ishida K, Hamada S, Fujishima F, Unno J, Kume K, et al. Diagnosis of autoimmune pancreatitis by EUS-FNA by using a 22-gauge needle based on the International Consensus Diagnostic Criteria. *Gastrointest Endosc*. 2012;76(3):594–602.

21. Majumder S, Chari ST. EUS-guided FNA for diagnosing autoimmune pancreatitis: Does it enhance existing consensus criteria? *Gastrointest Endosc.* 2016;84(5):805–7.
22. Adsay NV, Zamboni G. Paraduodenal pancreatitis: a clinicopathologically distinct entity unifying “cystic dystrophy of heterotopic pancreas”, “para-duodenal wall cyst”, and “groove pancreatitis”. *Semin Diagn Pathol.* 2004;21(4):247–54.
23. Raman SP, Salaria SN, Hruban RH, Fishman EK. Groove pancreatitis: spectrum of imaging findings and radiology-pathology correlation. *AJR Am J Roentgenol.* 2013;201(1):W29–39.
24. Shin LK, Jeffrey RB, Pai RK, Raman SP, Fishman EK, Olcott EW. Multidetector CT imaging of the pancreatic groove: differentiating carcinomas from paraduodenal pancreatitis. *Clin Imaging.* 2016;40(6):1246–52.
25. Mittal PK, Harri P, Nandwana S, Moreno CC, Muraki T, Adsay V, et al. Paraduodenal pancreatitis: benign and malignant mimics at MRI. *Abdom Radiol (NY).* 2017;42(11):2652–74.
26. Brosens LA, Leguit RJ, Vleggaar FP, Veldhuis WB, van Leeuwen MS, Offerhaus GJ. EUS-guided FNA cytology diagnosis of paraduodenal pancreatitis (groove pancreatitis) with numerous giant cells: conservative management allowed by cytological and radiological correlation. *Cytopathology.* 2015;26(2):122–5.
27. Li BQ, Xu XQ, Guo JC. Intrapancreatic accessory spleen: a diagnostic dilemma. *HPB (Oxford).* 2018;20(11):1004–11.
28. Kim SH, Lee JM, Han JK, Lee JY, Kim KW, Cho KC, et al. Intrapancreatic accessory spleen: findings on MR Imaging, CT, US and scintigraphy, and the pathologic analysis. *Korean J Radiol.* 2008;9(2):162–74.
29. Movitz D. Accessory spleens and experimental splenosis. *Principles of growth.* *Chic Med Sch Q.* 1967;26(4):183–7.
30. Dodds WJ, Taylor AJ, Erickson SJ, Stewart ET, Lawson TL. Radiologic imaging of splenic anomalies. *AJR Am J Roentgenol.* 1990;155(4):805–10.
31. Ding Q, Ren Z, Wang J, Ma X, Zhang J, Sun G, et al. Intrapancreatic accessory spleen: evaluation with CT and MRI. *Exp Ther Med.* 2018;16(4):3623–31.
32. Bhutiani N, Egger ME, Doughtie CA, Burkardt ES, Scoggins CR, Martin RC 2nd, et al. Intrapancreatic accessory spleen (IPAS): a single-institution experience and review of the literature. *Am J Surg.* 2017;213(4):816–20.
33. Tummala Md P, Rao Md S, Agarwal Md B. Differential diagnosis of focal non-cystic pancreatic lesions with and without proximal dilation of pancreatic duct noted on CT scan. *Clin Transl Gastroenterol.* 2013;4:e42.
34. Prasse A. The diagnosis, differential diagnosis, and treatment of sarcoidosis. *Dtsch Arztebl Int.* 2016;113(33–34):565–74.
35. Low G, Panu A, Millo N, Leen E. Multimodality imaging of neoplastic and nonneoplastic solid lesions of the pancreas. *Radiographics.* 2011;31(4):993–1015.

36. Seki K, Sakatani M, Tachibana T. Extrapulmonary lesions of sarcoidosis. *Nihon Kyobu Shikkan Gakkai Zasshi*. 1990;28(1):74–9.
37. Soyer P, Gottlieb L, Bluemke DA, Fishman E. Sarcoidosis of the pancreas mimicking pancreatic cancer: CT features. *Eur J Radiol*. 1994;19(1):32–3.
38. Bonhomme A, Dhadamus A, De Bie P, Van Hoe L, Baert AL. Pancreatic involvement in systemic sarcoidosis: CT findings. *J Belg Radiol* 1997;80(3):116–117.
39. Shukla M, Hassan MF, Toor V, Kaur J, Solomon C, Cohen H. Symptomatic pancreatic sarcoidosis. Case report and review of literature. *JOP*. 2007;8(6):770–4.
40. Wijkstrom M, Bechara RI, Sarmiento JM. A rare nonmalignant mass of the pancreas: case report and review of pancreatic sarcoidosis. *Am Surg*. 2010;76(1):79–84.
41. Delgado-Bolton RC, Arias Navalon JA, Rodriguez Alfonso B, Delgado-Bolton AN, Perez-Castejon MJ, Sanchez-Escribano R, et al. Pancreatic involvement detected with (18)F-FDG PET/CT in disseminated sarcoidosis. *Rev Esp Med Nucl*. 2011;30(1):29–32.
42. Zhang LN, Xue QL, Wang JX. Mimicking pancreatic malignancy: a systemic sarcoidosis. *Ann Saudi Med*. 2014;34(1):70–4.
43. Mony S, Patil PD, English R, Das A, Culver DA, Panchabhai TS. A rare presentation of sarcoidosis as a pancreatic head mass. *Case Rep Pulmonol*. 2017;2017:7037162.
44. Matsuura S, Mochizuka Y, Oishi K, Miyashita K, Naoi H, Mochizuki E, et al. Sarcoidosis with pancreatic mass, endobronchial nodules, and military opacities in the lung. *Intern Med*. 2017;56(22):3083–7.



Pancreatic Ductal Adenocarcinoma and Its Variants

Kartik Viswanathan and Rema Rao

Introduction and Clinical Presentation

Pancreatic cancer represents the fourth most common cancer in the United States, and every year, approximately 44,000 patients are diagnosed with the disease. Within the population, pancreatic cancer accounts for 37,400 deaths per year. Over the next decade, pancreatic cancer is projected to be the second leading cause of deaths from cancer [1]. Pancreatic ductal adenocarcinoma (PDCA) and the associated variants predominantly occur in older patients in their sixth or seventh decade of life. There is equal prevalence in both sexes, although there is a trend towards increased incidence in African Americans compared to Caucasians. The development of pancreatic cancer is a complex multifactorial process that takes into account both genetic and environmental risk factors. Environmental risk factors that contribute to the development on PDCA include cigarette smoking (almost 25–30% of the cases),

K. Viswanathan · R. Rao (✉)

Department of Pathology and Laboratory Medicine, Weill-Cornell Medicine, New York Presbyterian Hospital, New York, NY, USA
e-mail: rer9052@med.cornell.edu

© Springer Nature Switzerland AG 2019

A. Goyal et al. (eds.), *Pancreas and Biliary Tract Cytohistology*,
Essentials in Cytopathology 28,
https://doi.org/10.1007/978-3-030-22433-2_5

significant alcohol consumption (>4 drinks per day), chronic pancreatitis, long-standing diabetes mellitus (type 2), and exposure to hydrocarbons [1–3]. While most cases of pancreatic cancer are sporadic, a small proportion occur secondary to underlying hereditary causes. Familial syndromes include hereditary nonpolyposis colorectal cancer, familial adenomatous polyposis, BRCA2 alterations, familial atypical multiple mole melanoma (or FAMMM), hereditary pancreatitis, and Peutz-Jeghers syndrome. Patients with multiple first-degree relatives with pancreatitis are in a high-risk category for developing pancreatic cancer and account for at least 10% of the cases of reported pancreatic cancer [4].

Although the symptomatology can vary depending on the location of the tumor, most are nonspecific [1, 4–6]. Abdominal pain, anorexia, nausea, vomiting, and weakness have been reported in both instances. Other nonspecific symptoms include depression, dyspepsia, and early satiety. A new sudden-onset unexplained diabetes mellitus in an elderly thin patient that is challenging to control has been reported to be a possible indication of pancreatic cancer. When the tumor is localized to the head, there is an increased likelihood of bile duct obstruction leading to jaundice, dark urine, and acholic stools due to decreased bile entry into the intestinal tract.

Patients can also have varied findings on physical examination at the time of presentation [1]. If the pancreatic cancer is at an early stage, then the patient is likely to show very few if any physical signs. Conversely, on the other extreme, patients presenting with late-stage pancreatic cancer could show jaundice, abdominal tenderness, cachexia, and a non-tender palpable gallbladder due to obstruction of the common bile duct. The latter physical sign, also known as the Courvoisier sign, has a high specificity of up to 90% but a low sensitivity of up to 55%. Other notable physical findings that may occur in patients with pancreatic cancer include migratory superficial thrombophlebitis due to a hypercoagulable state (Trousseau sign), left supraclavicular lymphadenopathy (Virchow sign), and nodular subcutaneous fat necrosis (pancreatic panniculitis). Given the nonspecific findings, at the time of presentation, in addition to malignancy, the differential is vast and includes duodenal or gastric ulcers, lymphoma, aneurysm, chole-

dochal cysts, choledocholithiasis, gastritis, and pancreatitis among others. Laboratory testing is useful for providing supporting evidence, including demonstrating elevated conjugated bilirubin and urobilinogen depending on the extent of biliary tract obstruction, altered blood glucose levels, and elevated serum pancreatic enzyme levels secondary to obstructive pancreatitis and exocrine damage. However, to date, there are no sensitive or specific biomarkers for pancreatic cancers, and thus, screening protocols for pancreatic cancer do not exist. Thus, additional workup including radiologic imaging is imperative to rule out an underlying malignancy.

The prognosis of PDCA is extremely poor [1–3]. Given that most patients present with symptoms associated with late-stage disease (approximately 53% present with stage IV disease), the median survival time is less than a year and the survival rate ranges from <5% to 10%. Patients presenting with stage 0 pancreatic cancer have the highest 5-year survival at 21% that steadily declines with progressive stages down to 1.9%. The use of imaging is crucial in this setting to assess resectability, and approximately 20% of the cases will be managed surgically using a Whipple procedure if it involves the head of the pancreas or distal pancreatectomy with or without splenectomy if it involves the body or tail of the pancreas. In settings where PDCA cannot be resected (approximately 80% of the cases) due to involvement of critical structures (such as encasement of the celiac trunk, portal tract occlusion, or involvement of large mesenteric vessels) or extensive metastases, chemotherapy is the mainstay treatment with or without the addition of radiation therapy.

PDCA has several unique histologic variants, most of which share a similar dismal prognosis (Table 5.1). The only variant that serves as an exception is colloid carcinoma. Patients with colloid carcinoma have almost fivefold higher probability of survival in 5 years compared to the conventional PDCA (57% for colloid carcinoma and 12% for conventional PDCA) [3, 7, 8]. On the other hand, most of the other variants behave either similarly or are more aggressive compared to the conventional type PDCA and are further discussed later in the chapter.

Table 5.1 Summary of cytologic and histologic features of pancreatic ductal adenocarcinoma and its variants along with ancillary immunohistochemistry and molecular studies

Morphologic pattern of pancreatic ductal adenocarcinoma	Cytologic features	Histologic features	Immunohistochemistry	Molecular alterations
Conventional type	Malignant glandular component	Malignant glandular component in a desmoplastic stroma	Positive, CK7, CK8, CK18, CK19, CAM5.2, CKAE1/3, MUC1, MUC3, MUC4, MUC5AC, CEA, CA19.9, CA125; variable, CK17, CK20	KRAS, p53, p16, SMAD4/DPC4
Undifferentiated (anaplastic carcinoma)	Pleomorphic single cells, spindle or sarcomatoid single cells, bizarre multinucleated cells, cannibalism	Pleomorphic single cells, sarcomatoid cells, bizarre multinucleated cells, lack desmoplastic stroma	Positive: CK7, CK8, CK18, CK19, CAM5.2, CKAE1/3, vimentin; variable, CEA, MUC1, CA19.9	KRAS, p53, p16, SMAD4/DPC4 in carcinomatous component
Undifferentiated carcinoma with osteoclast-like giant cells	Osteoclast-type giant cells, bizarre multinucleated cells, pleomorphic single cells	Osteoclast-type giant cells, pleomorphic single cells, bizarre multinucleated cells, lack desmoplastic stroma	Positive, vimentin in carcinoma component, CD68, CD45, and vimentin in giant cell component; variable, CAM5.2, CK7, CKAE1/3, CEA, EMA	KRAS, p53 (50%)

Adenosquamous carcinoma	Admixture of malignant squamous cells and glandular cells	Malignant glandular component, at least 30% is malignant squamous component, admixed or separate	Positive: CK5/6, p63, p40 in squamous component, CK7, CK8, CK18, CK19, CAM5.2, CKAE1/3, MUC1, MUC3, MUC4, MUC5 AC, CEA, CA19.9, CA125 in glandular component	KRAS, p53, p16, SMAD4/DPC4 in carcinomatous component, loss of E-cadherin
Colloid (mucinous noncystic) carcinoma	Abundant thick mucin and malignant glandular component	Small clusters or single cells in mucin lakes, 80% mucin, signet ring cells may be present	Positive, mucicarmine, CK, CEA, CA19.9, MUC2, CDX2; negative, MUC1, MUC5	KRAS, p53, MSS, intact SMAD4/DPC4
Signet ring cell carcinoma	Signet ring morphology	Signet ring cells in a mucinous background	Positive, mucin, CKAE1/3, CAM5.2, CK7, CK19, MUC1, MUC 5 AC, CEA, EMA; negative for MUC2 and CDX2	Not available
Mixed ductal-endocrine carcinoma	Two populations: endocrine—monomorphic cells, granular cytoplasm, round nuclei, salt-and-pepper chromatin. Exocrine—component similar to other ductal variants	Cellular, two nodular populations: exocrine and at least 33–50% of tumor being endocrine	Endocrine component: positive for synaptophysin and chromogranin, loss of Rb or mutant p53 in poorly differentiated endocrine tumors. Exocrine: similar to the conventional type ductal carcinoma	KRAS, p53, p16, SMAD4/DPC4 for exocrine component; MEN1, DAXX, ATRX for the endocrine component

(continued)

Table 5.1 (continued)

Morphologic pattern of pancreatic ductal adenocarcinoma	Cytologic features	Histologic features	Immunohistochemistry	Molecular alterations
Medullary carcinoma	Cytologic fragments, eosinophilic cytoplasm, and nuclei with prominent nucleoli and smooth nuclear membrane contours. Background lymphocytes, plasma cells, and necrosis	Syncytial sheets with abundant cytoplasm with pushing borders, marked nuclear pleomorphism, and intra-tumoral lymphocytes	Positive, CK7, pan-CK; negative, lipase, CK20, CEA, chromogranin, S100, CEA, and CD45. Mucicarmine may highlight focal to diffuse mucin in tumors. Lymphoepithelial variant: positive for EBV on in situ hybridization	Wild-type KRAS, microsatellite instability
Hepatoid variant of pancreatic ductal adenocarcinoma	Epithelioid, abundant cytoplasm, nuclear atypia with possible transgressing vessels	Solid, nests, or trabeculae of polygonal cells with abundant cytoplasm, distinct cell borders, and prominent nucleoli. Bile may be present	Positive for HepPar1, alpha-fetoprotein, and alpha-1 antitrypsin. Polyclonal CEA and CD10 show canalicular pattern	No consistent pathogenic mutation yet identified

Radiographic Features and Fine Needle Aspiration

The diagnosis of pancreatic ductal adenocarcinoma relies on multiple diagnostic techniques, in particular radiologic imaging in conjunction with EUS-fine needle aspiration [6, 9]. Several non-invasive imaging modalities, including computed tomography (CT), magnetic resonance imaging (MRI), magnetic resonance cholangiopancreatography (MRCP), and endoscopic ultrasound (EUS), could be used to characterize pancreatic masses in a non-invasive manner (Fig. 5.1a–c) [9–14]. Imaging is valuable in not only identifying the lesion but can also help determine staging and resectability of the tumor.

Conventional abdominal ultrasound can help identify pancreatic masses with a sensitivity of 50–70%; the technique is hampered by body habitus, bowel gas, and patient discomfort [10, 12]. For this

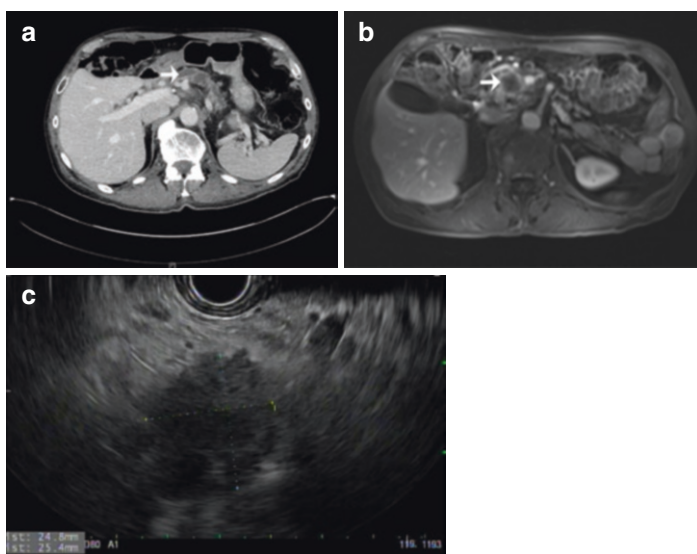


Fig. 5.1 Radiologic appearance of a pancreatic ductal adenocarcinoma on (a) CT, (b) MRI, and (c) EUS. All three modalities shown here highlight an ill-defined centrally hypoechoic mass within the head of the pancreas

reason, computed tomography (CT) with intravenous contrast is the first imaging modality used in the initial evaluation of a suspected pancreatic malignancy. CT with contrast is quite sensitive (up to 92%) in identifying PDAC. PDACs on CT imaging typically present as an area of hypoattenuation or isoattenuation, which is due to the hypovascular nature of PDACs in comparison to the surrounding highly vascular pancreatic parenchyma (Fig. 5.1a). Other imaging signs that may assist in the diagnosis include the presence of distal atrophic parenchyma, mass effect on the surrounding pancreas, the interrupted duct sign—the abrupt cut off of the pancreatic duct PD dilation—and the double duct sign with extrahepatic biliary and PD dilation [10, 12].

MRI and MRCP can both be useful in circumstances where the CT findings are equivocal [10, 12–14]. These alternatives are also useful in settings where the use of contrast is contraindicated, especially in patients with renal failure. As described previously, given that PDACs are hypovascular relative to the adjacent parenchyma, tumors are hypointense on gadolinium-enhanced T1-weighted images (Fig. 5.1b). MRI is also useful in delineating features of cystic lesions within the pancreas. However, chronic pancreatitis, the key benign entity on the differential diagnosis, shows similar MRI findings with low signal on T1-weighted imaging. In these cases, MRCP is helpful in visualizing the anatomy of both the pancreatic duct and the biliary tree. The presence of a non-obstructed pancreatic duct, also known as the duct-penetrating sign, can be of significant value in distinguishing cases of PDAC from chronic pancreatitis.

Positron emission tomography (PET) imaging relies on the concept that tumor cells demonstrate the Warburg effect with a shift toward glycolysis and increased uptake of 18-fluorodeoxyglucose (FDG) tracer. The sensitivity and specificity of PET/CT are comparable to CT and MR imaging and are therefore not considered first-line in the workup of a pancreatic mass. However, PET imaging can be a useful adjunct to CT and MR imaging, especially in identifying metastatic disease that can alter downstream management. An important pitfall is chronic pancreatitis that can also show significant FDG uptake [10, 12].

While imaging characteristics of most variants resemble that of the conventional type PDCA, unique differences have been reported. In contrast to conventional type PDCA which shows delayed enhancement due to the desmoplastic stroma (Fig. 5.2a), colloid carcinomas appear lobulated with ill-defined margins and are markedly T2-hyperintense on MR imaging due to abundant extracellular mucin (Fig. 5.2b). With dynamic pancreatic imaging, colloid carcinomas show gradual peripheral and internal mesh-like enhancement of the stroma without significant enhancement from the pools of mucin [14]. Undifferentiated carcinoma with osteoclast-like giant cells (UOGC) can have varying findings on both CT and MR imaging depending on the degree of necrosis and hemorrhage and thus range from homogeneous to inhomogeneous enhancement (Fig. 5.2c) [13]. Scant reports on CT and MR

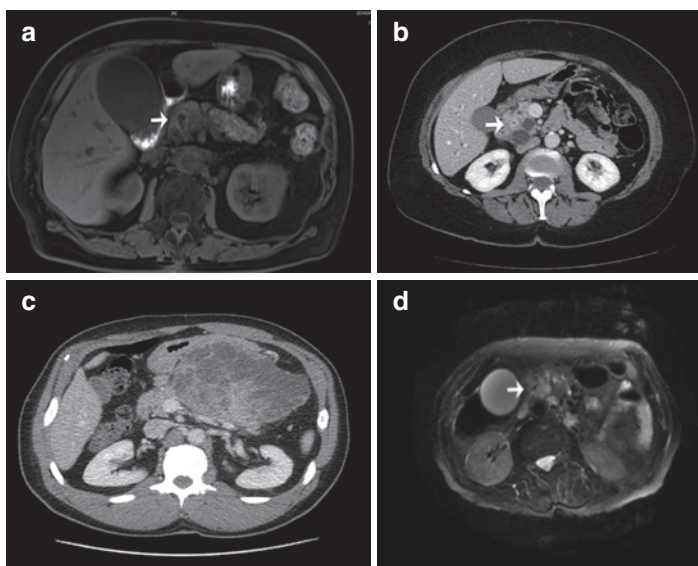


Fig. 5.2 Radiology of select pancreatic ductal adenocarcinoma variants. (a) Conventional type with ill-defined margins and hypointensity. (b) Colloid carcinoma, with T2-hyperintensity within cystic areas. (c) UOGC imaging shows a large well-circumscribed lesion. (d) Adenosquamous carcinoma shows cystic areas, possibly representing necrosis

imaging characteristics of adenosquamous carcinoma of the pancreas highlight that compared to the conventional type PDCA which demonstrated irregular borders, AdSCa tends to be rounder and more lobulated with extensive central necrosis and often found to be associated with the presence of tumor thrombi within the porto-venous system (Fig. 5.2d). Most of the differences between the variants and the conventional type PDCA are quite subtle due to overlap in the imaging findings [11]. Thus, the identification of unique radiologic features that can distinguish the different variants continues to remain a challenge.

Although radiologic imaging has furthered our understanding of pancreatic neoplasms, a definitive diagnosis is usually rendered with fine needle aspiration cytology or core needle biopsies. In conjunction with endoscopic ultrasound, the sensitivity and specificity of fine needle aspiration in making a diagnosis range from 92% to 98% (Fig. 5.1c) [9]. The diagnosis of pancreatic ductal adenocarcinoma can be straightforward if a systematic approach is used in evaluating smear preparations. Important features to consider include the background, cellularity, the organization of the epithelial groups, and the assessment for nuclear atypia [9, 15, 16]. The cytologic and histologic features along with the differential and ancillary/molecular studies for each pancreatic ductal adenocarcinoma variant are discussed below.

Pancreatic Cancer Precursors: Pancreatic Intraepithelial Neoplasia (PanIN)

The development of pancreatic ductal adenocarcinoma and its associated variants represents a stepwise progression that begins with the common precursor known as pancreatic intraepithelial neoplasia or PanIN. PanIN is a relatively common finding in about 50% of older adults and represents an atypical intraductal precursor that exists on a histologic spectrum [3]. The dysplastic precursor begins as low-grade or PanIN-1A and PanIN-1B and progresses to an intermediate grade or PanIN-2 and eventually becomes high-grade PanIN-3 (Fig. 5.3a–d). PanIN-3 is more likely to be associated with invasive adenocarcinoma compared to the lower and intermediate grades (Fig. 5.4). Given that the process is primarily

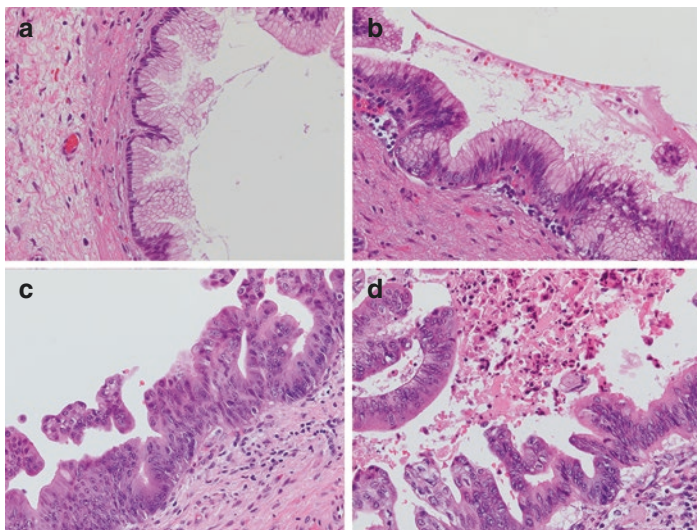


Fig. 5.3 Histologic spectrum of pancreatic intraepithelial neoplasia (PanIN). (a, b) PanIN-1A shows cells with voluminous mucinous cytoplasm, low-grade nuclei without any pseudostratification, which starts to appear with PanIN-1B. (c) PanIN-2 is an intermediate-grade lesion with mild to moderate nuclear atypia and pseudostratification. (d) PanIN-3 shows significant nuclear atypia and architectural complexity along with mucin depletion

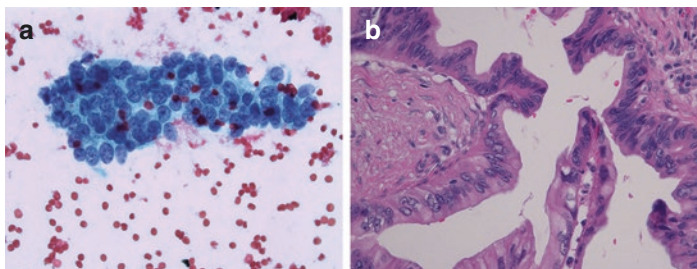


Fig. 5.4 PanIN-3 cytology and histology. (a) Fine needle aspiration demonstrates cohesive ductal groups with disorganization, nuclear crowding, and increased nuclear to cytoplasmic ratio in a clean background. (b) Histology highlights an intraductal proliferation with mucin depletion, increased nuclear to cytoplasmic ratio, significant pseudostratification, and disorganization of ductal cells

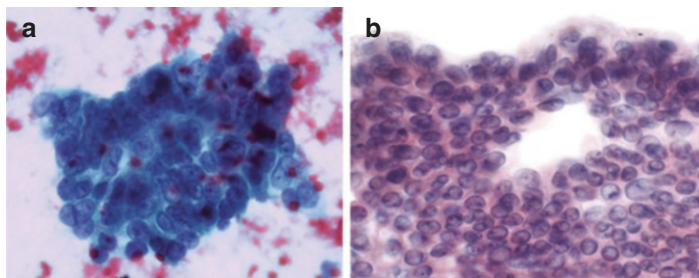


Fig. 5.5 Distinguishing PanIN-3 from a well-differentiated pancreatic ductal adenocarcinoma can be challenging on cytology. (a) PanIN-3 cytology (Papanicolaou stain, $\times 40$). (b) Well-differentiated pancreatic ductal adenocarcinoma (Papanicolaou stain, $\times 40$). Both can show anisonucleosis and a clean background. Although PanIN-3 is more cohesive than a well-differentiated pancreatic ductal adenocarcinoma, the findings should be interpreted judiciously along with clinical history and the radiologic findings

intraductal, a true mass may or may not be identifiable on imaging. However, given the degree of atypia in PanIN-3, this can lead to a diagnostic false positive interpretation of the smear as ductal adenocarcinoma (Fig. 5.5). Thus, caution is needed and the findings should be interpreted in the context of both clinical and radiologic findings [2, 3, 15, 17, 18].

Important Cytologic Features

The key cytologic features of PanIN include:

- Scantly cellular tightly cohesive ductal cell groups with anisonucleosis, disorganization, and nuclear crowding.
- Nuclei may show mild enlargement with hypochromasia, nuclear irregularities, and increased nuclear to cytoplasmic ratio in the early stages of PanIN.
- Smears from late stages of PanIN, such as PanIN-3, can be challenging as the cytologic features show remarkable similarity to conventional PDAC that is further discussed below, but includes anisonucleosis, crowding, and disorganization similar to a “drunken honeycomb” [17, 18].

- Background may show underlying features of the surrounding pancreatic parenchyma, such as chronic or autoimmune pancreatitis if present.

Histologic Correlation

The key histologic features of PanIN include:

- PanIN is an intraductal proliferation and grading depends on architectural and cytologic atypia [3].
- PanIN-1A is a replacement of the cuboidal ductal epithelium with tall, columnar cells with mucinous cytoplasm. Little to no atypia is identifiable in this PanIN subtype.
- PanIN-1B shows additional architectural complexity compared to PanIN-1A with papillary tufting of the mucinous epithelium into the luminal space.
- PanIN-2 shows a greater degree of cytologic atypia compared to PanIN-1A and PanIN-1B with crowded hyperchromatic nuclei with pseudostratification and loss of polarization with mitoses primarily restricted to the base of the cells.
- In cases of PanIN-3, there is a greater degree of nuclear atypia with mitoses extending to the luminal aspect. Cribriform architecture and necrosis may also occur (Figs. 5.3 and 5.4).

Differential Diagnosis (Cytology and Histology)

Table 5.2 outlines the differential diagnosis for PanIN.

Ancillary Testing and Molecular Signature

Currently, given that PanIN exists as a gradient and represents the precursor of invasive PDCA, similar molecular alterations may be present. For instance, low-grade PanIN-1 may harbor KRAS changes, whereas PanIN-2 and PanIN-3 may show additional alterations in CDKN2A, SMAD4, and TP53 [3].

Table 5.2 Differential diagnosis of pancreatic intraepithelial neoplasia (PanIN)

Chronic pancreatitis	Variable cellularity, ductal and acinar cells, stromal fragments, and inflammation Mild cytologic atypia compatible with reactive changes present
Intraductal papillary mucinous neoplasm (IPMN)	Larger in diameter compared to PanINs, involve main ducts, cystically dilated ~ > 1 cm Can be challenging to distinguish both lesions on cytology
Well-differentiated pancreatic ductal adenocarcinoma (PDCA)	Distinct mass on imaging Can be extremely challenging to distinguish well-differentiated PDCA and PanIN on cytology due to the subtle cytologic atypia that can occur in both cases

Immunohistochemical markers are also likely to pose similar challenges as well, as there is no definitive way to separate between the different PanIN subtypes and given the lack of architecture on fine needle aspirates. Thus, an integration of both imaging and cytology findings will be important as PanIN alone is not likely to cause a mass lesion [2, 3, 17, 18].

Ductal Adenocarcinoma, Conventional Type

The most common type of pancreatic ductal adenocarcinoma is the conventional type that accounts for >80% of pancreatic cancer cases [2, 3]. Most patients present in the sixth or seventh decade of life, although younger patients may present if underlying hereditary factors are also present [4, 5]. Generalized abdominal symptoms are common and imaging demonstrates a pancreatic mass [1]. A definitive diagnosis relies on fine needle aspiration. Smears should be assessed for cellularity, architectural features, cytoplasmic contents, and nuclear features. Distinct differences can be seen between well-differentiated and high-grade pancreatic ductal adenocarcinoma, such as the presence of necrosis and single cells that are associated with high-grade lesions. The key in

both diagnoses is the disorganization of the ductal sheets with cellular crowding and three-dimensionality with nuclear enlargement and membrane irregularities. Equally important is the evaluation of the cytoplasmic contents that may reveal the presence of mucin that should not typically be seen in benign ductal cells. Thus, with a systematic approach, the diagnosis of PDCA can be straightforward [9, 15, 16].

Important Cytologic Features

The key cytologic features for PDCA include well-differentiated and high-grade PDCA.

Well-Differentiated PDCA

- Clean background with either high or low cellularity but uncommon to see single cells [15].
- Cohesive ductal cells in glandular architecture.
- Crowding and disorganization within the ductal groups, characterized as a “drunken” honeycomb (Fig. 5.6).
- Increase in nuclear to cytoplasmic ratio with a columnar shape, mucinous cytoplasm, and nuclei oriented at the basal aspect.
- Anisonucleosis (at least fourfold variation in nuclear size in cells of the same group).
- Nuclei will display chromatin clearing with mildly irregular nuclear membranes.

High-Grade PDCA

- Dirty background with necrotic debris (Fig. 5.7).
- Dyshesive single neoplastic cells or loose sheets with significant nuclear crowding or overlap.
- Glandular architecture is not apparent in the three-dimensional fragments, although cytoplasmic mucin vacuoles may be apparent.
- Nuclear pleomorphism or anisonucleosis between adjacent nuclei is striking, with abnormal chromatin distribution and mitotic figures.

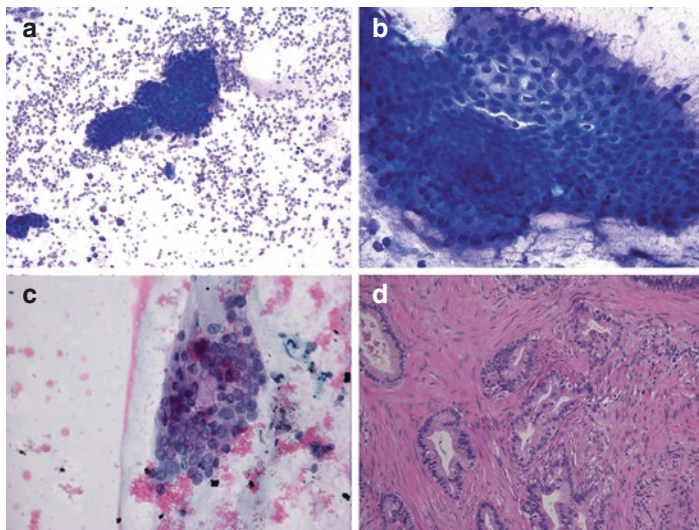


Fig. 5.6 Low-grade pancreatic ductal adenocarcinoma. (a–c) Fine needle aspiration shows cohesive clusters of ductal cells with a “drunken honeycomb” appearance with nuclear hypochromasia and mild enlargement in a clean background (Diff-Quik and Papanicolaou stains, $\times 20$, $\times 40$). (d) A surgical resection specimen shows infiltrating well-formed glands in a desmoplastic stroma without significant nuclear pleomorphism

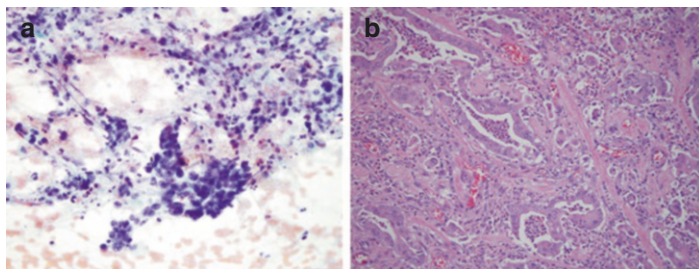


Fig. 5.7 High-grade pancreatic ductal adenocarcinoma. (a). Fine needle aspiration shows poorly cohesive cells with anisonucleosis in a “dirty” background of necrosis and acute inflammatory debris (Diff-Quik stain $\times 20$, $\times 40$). (b). A corresponding biopsy shows small infiltrative glands and single cells with significant nuclear pleomorphism in a desmoplastic stroma, consistent with high-grade pancreatic ductal adenocarcinoma (H&E stain $\times 20$, $\times 40$)

Histologic Correlation

The key histologic features of PDCA include:

- Small, incomplete, disorganized irregular glands in an infiltrative pattern (Figs. 5.6 and 5.7).
- Lobular configuration and ductal branching are absent.
- Perineural invasion, invasion into preexisting ducts, or may be present adjacent to large, thick, muscular vessels.
- Presence of bare ducts within fibroadipose tissue or single infiltrating cells in desmoplastic stroma is also diagnostic of carcinoma.
- Well-differentiated conventional type PDCA: little nuclear variability and architectural atypia with an infiltrative pattern are key [2, 3, 15].
- Higher-grade PDCA: greater nuclear variability, necrosis may be present [2, 3].
- Histologic types:
 - Clear cell type PDCA: >75% of tumor cells with cleared-out cytoplasm that does not contain glycogen or mucin. No prognostic impact.
 - Cystic change in PDCA is typically admixed with the conventional type PDCA with numerous cysts lined with tall columnar mucinous cells in a complex papillary architecture; however, this pattern of growth lacks elastin staining that distinguishes it from intraductal papillary mucinous neoplasm (IPMN). No prognostic impact.
 - Foamy gland pattern: Tumor cells show microvacuolated cytoplasm with low nuclear to cytoplasmic ratio, prominent cell borders, and hyperchromatic wrinkled nuclei resembling koilocytic change. Anisonucleosis with loss of honeycomb arrangement is appreciated (Fig. 5.8a–c). On histology, the tumor is infiltrative with minimal or no desmoplasia and cells demonstrate abundant foamy cytoplasm with raisinoid nuclei (Fig. 5.8d). The differential diagnosis includes metastatic clear cell renal cell carcinoma (Fig. 5.9). A chromophilic brush-border-like zone (BBLZ) is visible on the apical aspect with strong reactivity with

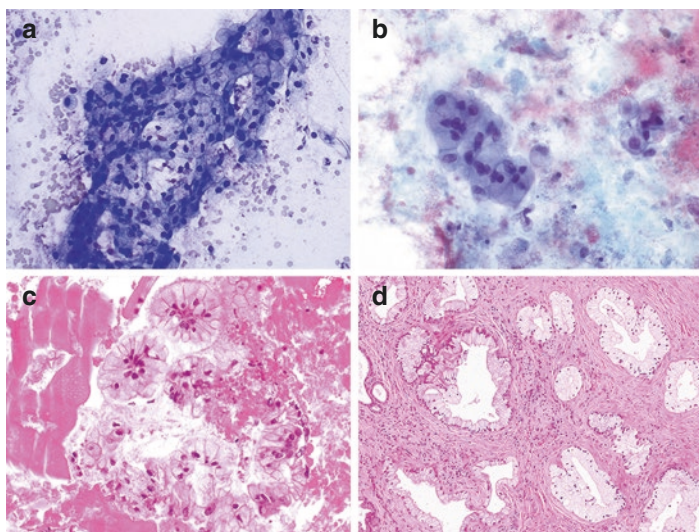


Fig. 5.8 Pancreatic ductal adenocarcinoma, foamy cell pattern. (a, b) Fine needle aspiration shows cells with abundant clear and vacuolated cytoplasm, low nuclear to cytoplasmic ratio, and raisinoid hyperchromatic nuclei (Diff-Quik and Papanicolaou stains, $\times 40$). (c) Cell block preparation highlights the voluminous cytoplasm and the presence of a brush border-like zone at the apical aspect (H&E stain, $\times 10$). (d) A surgical resection shows glands with voluminous cytoplasm, with basally oriented raisinoid hyperchromatic nuclei, and the brush border-like zone (H&E stain, $\times 10$) (All images courtesy of Carlie Sigel, Memorial Sloan Kettering)

mucicarmine, Alcian Blue, CEA, and CK8. Focal positivity can be seen with Ber-EP4, B72.3, cathepsin D, and CK20, whereas MUC2, CK5/6, and calretinin stains are negative. DPC4 is absent in tumor cells. Nuclear p53 can be demonstrated in a subset of tumors with a low proliferative Ki67 index ranging from 1 to 10%. From a molecular standpoint, similar to the conventional pancreatic ductal adenocarcinoma, tumors with foamy gland pattern can harbor a KRAS G12 codon mutation in the few cases reported thus far in the literature. There is no prognostic impact [2, 3, 22–24].

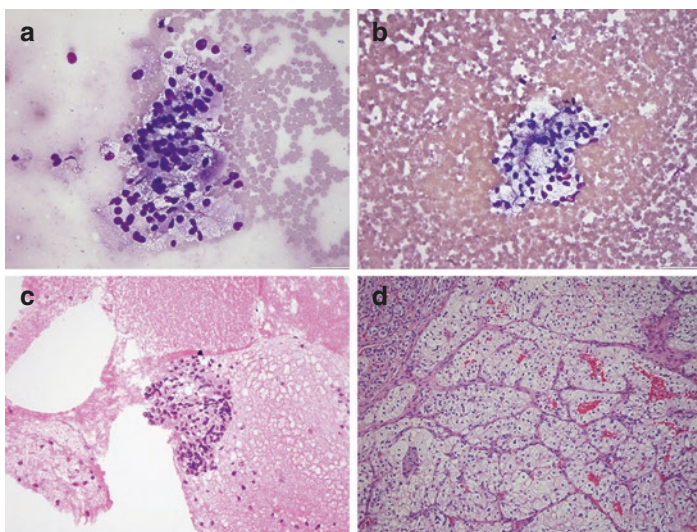


Fig. 5.9 Metastatic clear cell carcinoma. (a, b) Fine needle aspiration shows polygonal cells with clear and vesicular cytoplasm and small nuclei (Diff-Quik stain $\times 40$). (c) A cell block preparation showed scant cell clusters with clear cytoplasm (H&E stain $\times 40$). (d) Surgical resection shows nests of cells with clear cell cytoplasm, small nuclei, and intervening delicate vasculature, confirming the diagnosis of metastatic renal cell carcinoma (H&E stain $\times 10$)

Differential Diagnosis

Table 5.3 outlines the differential diagnosis of ductal adenocarcinoma, conventional type.

Ancillary Testing and Molecular Signature

Immunohistochemical markers can be helpful in distinguishing reactive processes from ductal adenocarcinoma. PDCA is typically positive for multiple cytokeratin proteins including CK7, CK8, CK18, and CK19. CK20 is at most focally positive in the conventional type of PDCA. Other notable markers positive in PDCA include EMA, CA 19–9, TAG72, and CA125. Mucicarmine

Table 5.3 Differential diagnosis for ductal adenocarcinoma, conventional type

Chronic pancreatitis	Lobular architecture with tubular or oval-shaped ducts Stromal fragments and inflammation No perineural invasion No anisonucleosis Nucleoli may be moderately enlarged, compatible with reactive changes
Lymphoplasmacytic sclerosing pancreatitis	Prominent lymphoplasmacytic infiltrate No infiltrative pattern of ducts Increased serum IgG4 and >30 IgG4+ plasma cells per hpf
Pancreatoblastoma	Prominent acinar differentiation with only focal ductal differentiation Squamoid nests May have primitive round cell component
Acinar cell carcinoma	Granular cytoplasm with round basally placed nuclei and purplish granules Single large central nucleolus Solid or acinar architecture No desmoplastic reaction Immunohistochemistry positive for trypsin and chymotrypsin
Islet aggregation in chronic pancreatitis	Islet clusters in small irregular cords Lack of glandular architecture Uniform cells with round nuclei “Salt-and-pepper” neuroendocrine-type chromatin Immunohistochemistry positive for synaptophysin and chromogranin

will highlight the cytoplasmic mucin, and tumor cells also show positivity for various mucin proteins including MUC1, MUC3, MUC4, and MUC5AC. MUC2 is not expressed in the conventional type PDCA, whereas MUC6 is expressed in only a fraction of PDCA_s [2, 3, 9, 15].

A multitude of studies have characterized the molecular landscape of the conventional type of pancreatic ductal adenocarcinoma. Both the well-differentiated and high-grade types of conventional PDCA_s harbor similar genetic changes. These include mutations in KRAS (90% of all PDCA cases), TP53 (in

50% of the cases), and SMAD4 (55% of the cases). Loss of CDKN2A through mutation or promoter hypermethylation is also common. Immunohistochemistry demonstrating a loss of SMAD4 or aberrant p53 expression may help provide supporting evidence [2, 3, 19–21].

Undifferentiated (Anaplastic) Carcinoma

Undifferentiated carcinoma (UC) is also a rare subtype comprising 2–7% of all PDACs [2, 3, 22]. It is also referred to as pleomorphic carcinoma, pleomorphic giant cell carcinoma, pleomorphic large cell carcinoma, and sarcomatoid carcinoma in the literature. UC is typically seen in older males in the fifth to the seventh decades of life and is predominantly located in the head of the pancreas. This variant is aggressive and most patients show distant metastases at the time of presentation. Not surprisingly, patients with UC have a dismal prognosis of several months in most cases.

Important Cytologic Features and Histologic Correlation

The key cytologic and histologic features of UC ((Figs. 5.10 and 5.11) include:

- High cellularity comprising of small clusters or dispersed single medium-to-large spindle and ovoid cells with increased nuclear/cytoplasmic ratio in a necrotic background [2, 3, 23–27].
- Nuclei are pleomorphic, multinucleate, and bizarre with coarse chromatin, prominent nucleoli, and brisk mitotic activity [23–27].
- Cytoplasmic mucin vacuoles are not distinct.
- Osteoclast-like giant cells are not identifiable.
- Irregularly shaped clusters or pseudoglandular structures with cytomorphologic features similar to the conventional PDAC may be present.

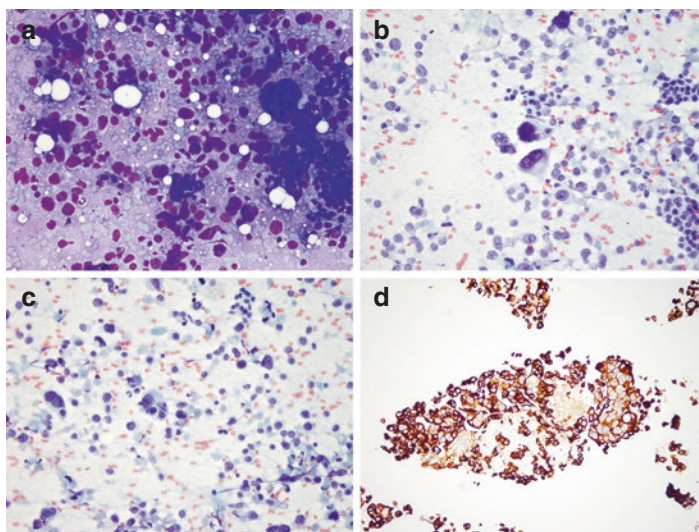


Fig. 5.10 Undifferentiated (anaplastic) carcinoma of the pancreas, cytology. (a–c) Fine needle aspirates demonstrate large pleomorphic and bizarre cells in a necrotic background (Diff-Quik and Papanicolaou stains, $\times 40$). (d) Cell block preparation shows large pleomorphic cells that are strongly positive with a pan-cytokeratin immunostain

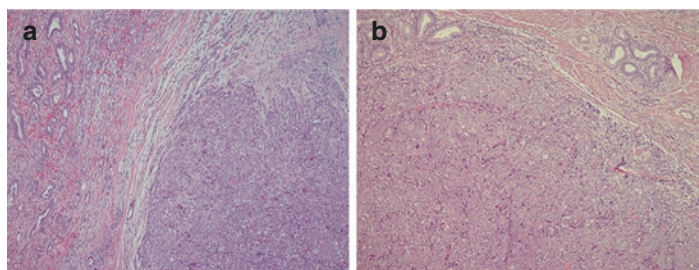


Fig. 5.11 Undifferentiated (anaplastic) carcinoma of the pancreas, surgical pathology. (a–d) A surgical resection specimen demonstrates sheets of large cells with an adjacent conventional type pancreatic ductal adenocarcinoma. On higher magnification, cells appear loosely cohesive without architecture and with pleomorphic nuclei and prominent nucleoli (H&E stain, $\times 10$, $\times 20$, $\times 40$)

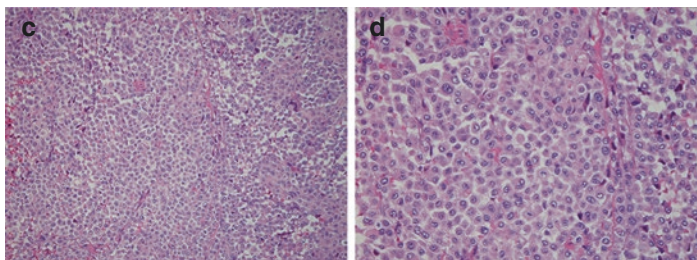


Fig. 5.11 (continued)

- On histology, carcinomatous component may predominate with spindle cells and may show focal areas of squamous differentiation.
- Significant necrosis and brisk mitotic activity.
- Perineural invasion, lymphatic invasion, and vascular invasion may be identified in most cases.

Differential Diagnosis

Table 5.4 outlines the differential diagnosis for UC.

Ancillary Testing and Molecular Signature

The immunohistochemical panel can help distinguish between the pleomorphic dispersed single cells and the irregular conventional type PDCA glandular components. UC tumor cells are cytokeratin and vimentin positive, while negative for E-cadherin. Conversely, the conventional PDCA glandular component retains E-cadherin expression and is negative for vimentin [22–27].

There is limited sequencing data available for UC in the literature. Among the cases sequenced thus far, 75–100% of UC tumors show the canonical KRAS activating G12D mutation, whereas up to 25% of the tumors can have wild-type KRAS. However, the KRAS mutational status does not appear to have a significant

Table 5.4 Differential diagnosis for undifferentiated (anaplastic) carcinoma

Metastatic carcinoma	Usually lacks associated glandular component
Malignant melanoma	May show spindled or epithelioid morphology and single prominent nucleoli Melanoma is negative for histiocytic and epithelial markers and positive for S100, melan A, and HMB45
Metastatic sarcoma	Negative or focally positive for epithelial markers
Undifferentiated (anaplastic) carcinoma with osteoclast-like giant cells	Osteoclast-like giant cells are identifiable

prognostic impact in these patients as the survival is not significantly different for patients with KRAS mutated UC tumors in comparison to patients with KRAS wild-type UC tumors [22].

Undifferentiated Carcinoma with Osteoclast-Like Giant Cells

First described in 1954 by Sommers and Meissner, this rare variant of PDAC shows stark resemblance to other tumors with similar morphologic features [28–34]. Undifferentiated carcinoma with osteoclast-like giant cells (UOC) is a rare variant of PDAC, accounting for approximately 1.4% of resected PDACs. UOC tends to have a slight female predominance, tends to occur more in the body/tail of the pancreas, and occurs over a wide range of ages, but primarily in the elderly. As the name suggests, these tumors contain a significant number of osteoclastic giant cells resembling osteoclasts of the bone admixed with neoplastic cells. Yet, despite the significant morphologic differences between UOC and PDAC, these two tumor types surprisingly share a similar genetic landscape, highlighting that UOC is in fact a related variant of PDAC. Although studies thus far have utilized small cohorts, overall survival in patients with UOC tumors (59%) has been recently shown to be better as compared to the conventional PDAC (16%) [32]. Additionally, UOC associated with a PDAC component have

a worse prognosis as compared to pure UOC [6, 22, 30, 32]. For this reason, pure UOC tumors have to be extensively sampled to exclude the presence of a PDAC component that can impact the prognosis.

Important Cytologic Features

Figure 5.12 highlights key cytologic features of UOC including:

- Moderate cellularity with an admixture of uniform mononuclear cells, atypical pleomorphic spindled or epithelioid cells, and osteoclast-like giant cells [28, 29, 31, 33].
- Clusters or single pleomorphic giant tumor cells (PGCs) in a necrotic background and neutrophilia.

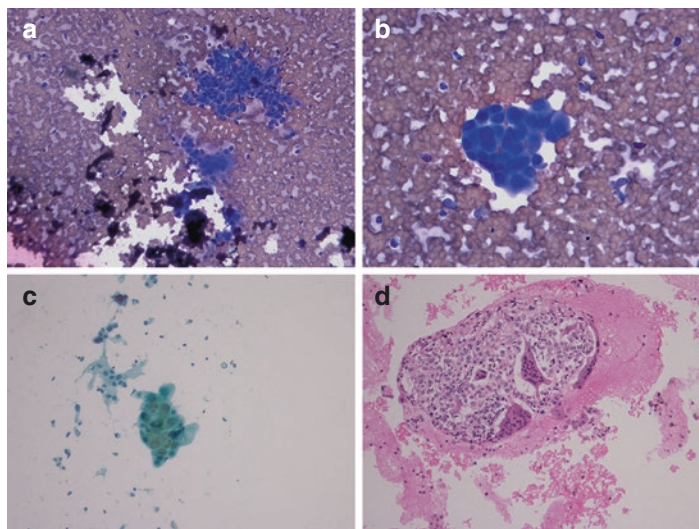


Fig. 5.12 Undifferentiated carcinoma of the pancreas with osteoclast-like giant cells, cytology. (a–c) Several clusters and sheets of pleomorphic bizarre cells with scattered osteoclast-like giant cells with multiple nuclei and voluminous cytoplasm are present on smear preparations (Diff-Quik and Papanicolaou stain, $\times 20$, $\times 40$). (d) A cell block preparation demonstrates pleomorphic cells admixed with osteoclast-like giant cells (H&E stain, $\times 20$)

- Osteoclast-like giant cells (OGCs) demonstrate multiple oval, bland nuclei with indistinct nucleoli, and abundant pale eosinophilic to grey cytoplasm.
- Histiocyte-like sarcomatoid carcinoma cells (HSCs) showed variable long slender to round morphology, and PGCs show marked pleomorphic nuclei with lobations, hyperchromasia, and macronucleoli. Both HSCs and PGCs have a high N:C ratio.
- A component of conventional PDAC type may be present.
- Cell block preparations are also useful in identifying OGCs and necrosis.

Histologic Correlation

Figure 5.13 highlights key histologic features of UOC including:

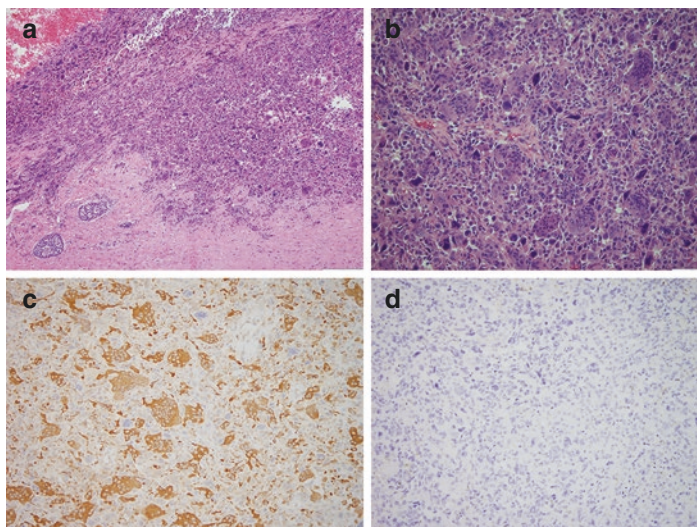


Fig. 5.13 Undifferentiated carcinoma of the pancreas with osteoclast-like giant cells, surgical pathology. (a, b) On resection, sheets of large bizarre and spindled cells are noted admixed with osteoclast-like giant cells (H&E stain, $\times 10$, $\times 20$). (c, d) The osteoclast-like giant cells are positive for CD68 (KP1 clone) and negative for CAM5.2 on immunohistochemistry (IHC, $\times 40$)

- As in cytology, three different cell populations are noted [32, 33].
- First, osteoclast-like giant cells (OGCs) resembling osteoclasts are present. Areas of UOC with a significant number of OGCs tend to be more nodular with abundant extravasated red blood cells. OGCs may also show phagocytosis.
- Second population present is the histiocyte-like sarcomatoid carcinoma (HSC) cells that are relatively small, round to ovoid, dyshesive, and resembling histiocytes.
- Third component of UOCs is the pleomorphic giant cell carcinoma cells (PGCs) which are highly atypical cells with large irregular hyperchromatic nuclei.
- Intraductal/intracystic growth of tumor cells.
- Perineural invasion and lymph node metastases are not as common compared to PDACs.
- Large proportion of UOCs can have an associated invasive PDAC component or high-grade PanIN, making extensive sampling imperative.
- Can show heterologous elements (for instance, osteoid) similar to carcinosarcomas in other organ systems.

Differential Diagnosis

Table 5.5 outlines the differential diagnosis for undifferentiated carcinoma with osteoclast-like giant cells.

Ancillary Testing and Molecular Signature

The three tumor cell populations noted on histology have a unique immunohistochemical signature. Both OGCs and HSCs express CD68, whereas PGCs are negative for this marker. Variable pancytokeratin staining, CD163 positivity, and aberrant p53 expression can be seen with PGCs and HSCs; however, OGCs are negative for cytokeratin, CD163, p53, and EMA. All three components were negative for S100 and retain INI-1. Finally, both HSCs and PGCs have a high rate of Ki67 proliferation index in comparison to OGCs which is much lower [28–34].

Table 5.5 Differential diagnosis for undifferentiated carcinoma with osteoclast-like giant cells

Chronic pancreatitis with associated granulation tissue	Foamy histiocytoid cells, giant cells, and capillaries can mimic UOC No cytologic pleomorphism or significant atypia EMA is negative
Micropapillary pattern of pancreatic ductal adenocarcinoma	Micropapillae can mimic appearance of osteoclast-like giant cells CD68 negative
Undifferentiated pancreatic rhabdoid carcinoma	Eosinophilic rhabdoid cells with pleomorphic nuclei and prominent nucleoli SMARCB1-deficient and shows INI-1 loss on immunohistochemistry
Malignant melanoma	May show spindled or epithelioid morphology and single prominent nucleoli Melanoma is negative for histiocytic and epithelial markers and positive for S100, melan A, and HMB45
Metastatic sarcoma	Rare Bland OGCs are not identifiable Negative or focally positive for epithelial markers
Undifferentiated (anaplastic) carcinoma	Osteoclast-like giant cells are absent

Surprisingly, although UOC tumors are morphologically distinct compared to the other subtypes of PDACs, they seem to show a significant overlap at the genetic level [30, 34]. Whole exome sequencing of small UOC cohorts shows consistent classic genetic changes that one may observe in conventional PDAC, including activating KRAS mutations, SMAD4 inactivation, TP53 mutations, and CDKN2A biallelic inactivation. While other unique somatic mutations have been noted at lower frequency, the clinical significance of these mutations is unclear and is not discussed here. Given the similarity in the genetic landscape, one may speculate that epigenetic mechanisms, including noncoding RNAs or histone modifications, may contribute to significant morphologic differences between UOC and PDAC [22, 30, 34].

Colloid (Mucinous Noncystic) Carcinoma

Making up 1–3% of all resected exocrine pancreatic carcinomas, colloid carcinoma (CC), both by the WHO and AFIP definitions, should be composed of large pools of extracellular mucin comprising at least 80% of the volume [2, 3, 7, 8, 35, 36]. CC occurs in older patients in their sixth/seventh decade of life with an equal distribution in men and women. The tumor localizes predominantly in the head of the pancreas. Most patients with CC do not appear to present with distal metastases in comparison to PDCA. Moreover, most patients with CC do well after surgical resection, chemoradiation therapy with a 5-year survival of 57% in comparison to the poor 12% survival for patients with conventional type PDCA [2, 3, 7, 8, 35]. CC tumors are most commonly seen in conjunction with a neoplastic IPMN in the surrounding parenchyma. In rare instances, CC patients may also develop pseudomyxoma peritonei as a sequela.

Important Cytologic Features

Figure 5.14a–c highlights key cytologic features of CC:

- Scant to moderate cellularity with thick mucin on Diff-Quik smears.
- Degenerative changes are identifiable including histiocytes and neutrophils admixed with the mucin.
- Three-dimensional tumor cell clusters floating in mucin show atypia with overlapping enlarged nuclei, moderate nuclear size variation, and increased nuclear to cytoplasmic ratio [36].
- A combination of cytologic atypia and presence of thick mucin should be sufficient to raise concern for the possibility of colloid carcinoma.

Histologic Correlation

On histology, key features of CC (Fig. 5.14d) include:

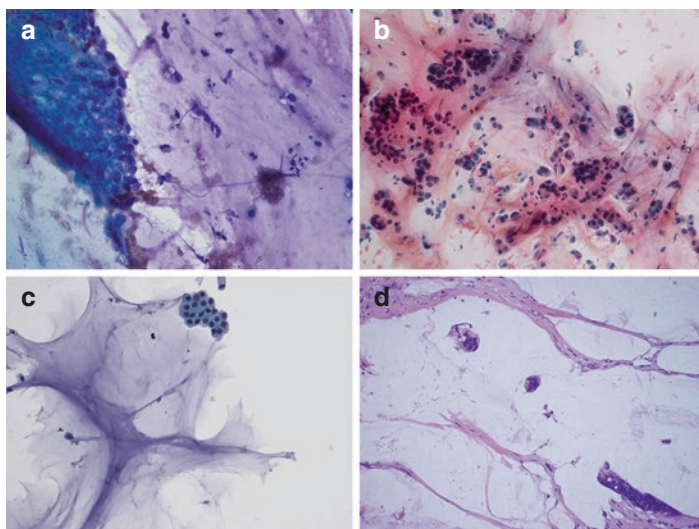


Fig. 5.14 Colloid carcinoma of the pancreas. (a–c) Smear preparations from fine needle aspirates show adenocarcinoma within abundant mucin (Papanicolaou stain, $\times 40$). (d) Surgical resection specimens demonstrate pools of mucin with either scattered tumor cell clusters or with an attenuated malignant epithelial lining (H&E stain, $\times 10$, $\times 20$)

- Nodular appearance composed of pools of mucin with scant intervening stroma.
- Tumor cells either absent or in different morphologic patterns in mucin lakes [3, 7, 8, 35]. When present, cells can occur in cribriform morphology, strips clinging to the surrounding walls of the mucin lake, gland-forming clusters, and signet ring like, or be dispersed as single cells. With respect to signet ring morphology, unlike signet ring cell carcinoma (SRCC, discussed below), these signet ring cells are restricted to the mucin lakes and not infiltrating the surrounding stroma.
- Eosinophilic cytoplasm with minimal to moderate nuclear size variation with occasional prominent nucleoli and mild nuclear irregularities.
- Inflammatory debris with polymorphonuclear leukocytes and microscopic calcifications can be seen.

Table 5.6 Differential diagnosis of colloid (mucinous noncystic) carcinoma

Mucinous cystic neoplasm (MCN) of pancreas	<p>Clinically presents as a cystic lesion in pancreas with or without a solid component</p> <p>Moderate cellularity with cystic background</p> <p>Scant to moderate extracellular thick mucin</p> <p>Small clusters of bland mucin-containing epithelial cells and muciphages</p> <p>Nuclei without significant atypia with regular membranes, fine chromatin, small nucleoli in low-grade dysplasia</p> <p>Cytology for high-grade atypia and invasion similar to PDCA</p> <p>No necrosis and atypical mitoses</p> <p>No communication with the ducts (vs IPMN)</p> <p>Nearly all the patients are women</p>
Mucocele-like lesion	<p>Pools of mucin lacking epithelial lining and floating mucinous cells</p> <p>Marked inflammation</p> <p>Restricted to periductal region</p>
Intraductal papillary mucinous neoplasm (IPMN)	<p>Cytologic features similar to MCN</p> <p>Cystic communication with main pancreatic ducts or side branches with or without solid component</p> <p>Histology evaluation needed to definitively assess invasion</p>

- Most resections of CC show a component of IPMN with at least focal severe atypia and also intermixed with the invasive CC.

Differential Diagnosis

Table 5.6 outlines the differential diagnosis of colloid (mucinous noncystic) carcinoma.

Ancillary Testing and Molecular Signature

CC tumor cells express B72.3, CEA, and CA19–9. MUC2 and CDX2, notably associated with intestinal differentiation, are also positive in this tumor. A unique feature of colloid carcinoma is the

strong diffuse CK20 staining that is lacking in conventional type PDCA and the other variants. Mucin lakes and mucin-containing tumor cells are highlighted strongly with mucicarmine and Alcian Blue [3, 7, 8, 35, 36].

With respect to the molecular signature of CC, sequencing of small cohorts has identified KRAS activating mutations and TP53 mutations similar to that seen in PDCA. Yet, predominantly most CC cases are either wild-type p53 or KRAS (about 67%). In addition, CC tumors retain DPC4 expression and do not show microsatellite instability with unaffected MLH1, MSH2, MSH6, and PMS2 expression. However, it remains unclear whether the lack of these canonical mutations contributes to the improved overall 5-year survival seen in CC patients [8].

Signet Ring Cell Carcinoma

Signet ring cell carcinoma (SRCC) of the pancreas is an extremely rare variant comprising <1% of all PDACs and is named due to the presence of intracytoplasmic mucin vacuoles that impart a signet ring morphology [6, 37–41]. The diagnosis of SRCC requires at least 50% signet ring morphology and exclusion of metastases from another site [2, 3]. SRCC tends to occur in elderly patients with a predilection for males. Predominantly occurring in the head of the pancreas, similar to conventional type PDAC, SRCC has a dismal prognosis with an overall 5-year survival rate of 4–6%, attributed to distant disease at the time of presentation [2, 3, 42].

Important Cytologic Features

The key cytologic features of SRCC include:

- Few dispersed clusters or singly scattered round malignant cells with large nuclei with nuclear membrane irregularities and prominent nucleoli in “signet ring”-like morphology, with low N:C ratio and nuclei eccentrically placed [41].

- Cytoplasm may show mucin vacuoles.
- Conventional type PDCA may be identified.
- Signet ring features best appreciated on cell block studies.

Histologic Correlation

The key histologic features of SRCC include:

- Poorly cohesive, single, “signet ring”-like tumor cells diffusely scattered with an infiltrative pattern in a desmoplastic stroma.
- Round cells with intracytoplasmic mucin and a peripheral flattened nucleus, imparting the characteristic signet ring appearance [2, 3, 37–41].

Differential Diagnosis

Table 5.7 outlines the differential diagnosis of signet ring cell carcinoma.

Ancillary Testing and Molecular Signature

On immunohistochemistry, malignant signet ring cells are strongly CEA and cytokeratin 7 positive and negative for CDX2, CK20, CD68, and synaptophysin. Mucicarmine and PAS stains help highlight the intracytoplasmic mucin vacuoles [37, 39–41].

Table 5.7 Differential diagnosis of signet ring cell carcinoma

Metastatic signet ring cell carcinoma	Immunohistochemical panel to rule out other primary sites Needs correlation with clinical history and radiologic findings
Colloid carcinoma	Mucin pools/lakes with scant malignant cells Although tumor cells can take on signet ring morphology, they are not infiltrative

To date, no unique molecular signatures have been identified for SRCC [3].

Adenosquamous Carcinoma

Adenosquamous carcinoma of the pancreas is a rare variant representing about 0.4–4% of all ductal adenocarcinomas and is characterized by a biphasic admixture of malignant glandular and squamous components [2, 3, 43]. The diagnosis is primarily made on histologic examination because as per AFIP guidelines, at least 30% of the tumor has to have either keratinizing or non-keratinizing squamous differentiation. AdSCa is most often seen in patients in their sixth decade of life with a slight male predominance and occurs most commonly in the head of the pancreas. The prognosis of adenosquamous carcinoma is poor and similar if not worse compared to the usual variant of pancreatic ductal adenocarcinoma [43–48]. Secondary metastases arising from a pancreatic AdSCa may purely be ductal adenocarcinoma.

Important Cytologic Features

The key cytologic features of AdSCa (Fig. 5.15a–c) include:

- Depends on primary component sampled [49–51].
- High cellularity in a background of necrotic debris, blood, or mucin.
- High-grade tumor cells may show either glandular or squamous differentiation or both.
- Squamous component will show single cells and small clusters with central hyperchromatic and pleomorphic nuclei, dense cytoplasm, and distinct cell borders.
- If keratinization is present, cells will be deeply orangeophilic on Papanicolaou-stained smears.
- Squamous cells from AdSCa may also show basaloid features with minimal keratinization.

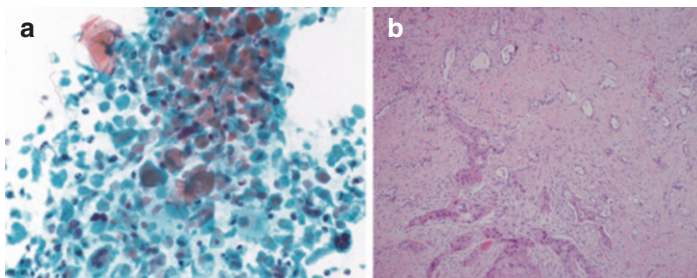


Fig. 5.15 Adenosquamous carcinoma of the pancreas. (a) Smear preparations may either show a glandular component, a squamous component, which may or may not be keratinizing, or both depending on sampling (Papanicolaou staining $\times 20$, *image courtesy of Martha Pitman, Massachusetts General Hospital*). (b) A surgical resection specimen of adenosquamous carcinoma highlights the admixture of glandular and squamous components within a desmoplastic stroma (H&E stain, $\times 20$)

- Conversely, when the malignant glandular component is sampled, the cytomorphic features resemble the conventional type PDAC with anisonucleosis, disorganization of the honeycomb pattern, and cytoplasmic mucin vacuoles.

Histologic Correlation

The key histologic features of AdSCa (Fig. 5.15d) include:

- Two defining populations—a glandular component and a squamous component [2, 3, 46].
- The malignant glandular component will resemble the conventional type PDCA with infiltrating irregular glands in a desmoplastic stroma.
- Squamous component, at least 30%, in cohesive infiltrative fragments or sheets with well-defined cell borders, intercellular bridges, and may show keratinization.
- Areas of necrosis will be present.

Table 5.8 Differential diagnosis for adenosquamous carcinoma

Squamous contamination	Cytomorphology shows benign features Squamous cells with very low N:C ratio with small, round bland nuclei with abundant cytoplasm and well-defined borders Lymphocytes are absent
Lymphoepithelial cyst of pancreas	Similar to squamous contamination Lymphocytes and keratinaceous material may be present on smears No cytologic atypia Cell block preparation may also show cholesterol crystals, macrophages, and granulomas
Squamous metaplasia	Can occur in the setting of stent placement, chronic pancreatitis, or mucin-producing neoplastic cysts Squamous cells are scant Atypia not amounting to the atypia identified in the malignant squamous population in AdSCa
Metastatic squamous cell carcinoma (Fig. 5.16)	Lacks the focal adenocarcinoma component History or clinical findings of a squamous primary
Primary squamous cell carcinoma of the pancreas	Extremely rare Extensive sampling to ensure that glandular component is absent

Differential Diagnosis

Table 5.8 outlines the differential diagnosis for adenosquamous carcinoma. See also Fig. 5.16.

Ancillary Testing and Molecular Signature

The two components in AdSCa have distinct immunoprofiles that enable easy identification. The IHC profile of the malignant glandular component mirrors the conventional type PDCA with positive CKAE1/3, CEA, and CA19–9 staining in most tumors, and the squamous component can be highlighted with p63 or p40.

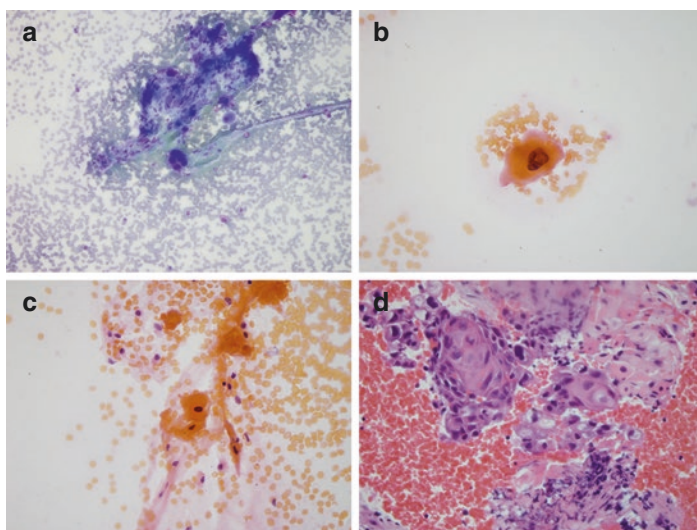


Fig. 5.16 Metastatic squamous cell carcinoma. (a–c) Fine needle aspiration only demonstrates squamous cells with pleomorphic, hyperchromatic nuclei indicative of malignancy (Diff-Quik and Papanicolaou stain, $\times 20$, $\times 40$). (d) A cell block study showed similar findings with a keratinizing squamous cell carcinoma (H&E stain, $\times 20$). Although adenosquamous carcinoma could be considered on the differential, the patient had a known prior history of metastatic squamous cell carcinoma

AdSCa has also been reported to have increased EGFR expression, reduced or lost E-cadherin, aberrant p53 expression, and a complete loss of p16 (CDKN2A pathway).

Recent studies sequencing both the glandular and the squamous components within AdSCa have demonstrated that their mutational landscape shows significant overlap with the conventional type PDCA [20, 52–57]. AdSCa has been reported to harbor mutations in KRAS, DPC4 and SMAD4, and CDKN2A/p16 exome deletions. In addition, more recent work has identified mutations in the UPF1 gene in approximately 78% of AdSCa that is involved in regulating splicing and nonsense-mediated RNA decay. Dysregulation or loss of UPF1 has been suggested to lead to the accumulation of mRNAs of other mutant proteins such as

mutated p53 that can lead to tumorigenesis; however, its precise role in the context of the development of adenosquamous carcinoma remains to be delineated [58].

Mixed Ductal-Endocrine Carcinoma

Mixed ductal-endocrine carcinomas (MDECs) of the pancreas go by multiple synonyms including mixed adenoneuroendocrine carcinoma, mixed carcinoid-adenocarcinoma, mucinous carcinoid tumor, and mixed endocrine-exocrine tumors. MDEC comprises only about 0.2% of all cases of PDCA; thus, like most other nonconventional PDCA subtypes, it is rare to encounter. MDECs are typically seen in middle-aged to elderly patients without gender predilection and are most commonly found in the head of the pancreas [59]. As the name suggests, the tumor is an admixture of endocrine and exocrine components, and by definition, each component should represent >30% of tumor cellularity in order to be classified into this category [2, 3]. Although the number of reported MDEC cases in the literature is small, patients with MDECs appear to have the same prognosis as the conventional type of PDCA [59–66].

Important Cytologic Features

The key cytologic features of MDEC include:

- Challenging due to possible sampling bias of the predominant tumor component.
- Smears of the endocrine component show loose clusters of monomorphic; round to oval cells, with indistinct borders; and abundant granular cytoplasm. The nuclei are round and monomorphic with salt-and-pepper chromatin and a plasmacytoid orientation. Nucleoli may be present [59, 62, 64].
- The exocrine ductal component cytomorphology is similar to other ductal variants.
- Cell block studies may show both components.

Histologic Correlation

The key histologic features of MDEC include:

- Cellular neoplasm with two infiltrating nodular populations [2, 59–62, 64, 66].
- The exocrine component is typically a conventional ductal adenocarcinoma.
- The endocrine component recapitulates the histologic features seen within a pancreatic neuroendocrine tumor (see Chap. 6).

Differential Diagnosis

Table 5.9 outlines the differential diagnosis for mixed ductal-endocrine carcinoma.

Table 5.9 Differential diagnosis for mixed ductal-endocrine carcinoma

Pancreatoblastoma with prominent ductal and endocrine differentiation	More common in children but can occur in adults in mid-30s Prominent acinar differentiation in addition to both neuroendocrine and ductal differentiation Acinar component is positive for trypsin, chymotrypsin, and BCL10 Squamoid nests May have primitive round cell component
Peri-islet invasion by pancreatic ductal adenocarcinoma	Neuroendocrine cells are rare and account for <30% of the tumor
Ductulo-insular neuroendocrine tumors	Entrapped ductal component does not show any cytologic atypia Immunohistochemical and molecular profiles seen in PDCA, including KRAS, CDKN2A, SMAD4, and TP53, are not identified, indicating nonneoplastic nature of ductal component Only the neuroendocrine component metastasizes compared to MDEC where either or both components can metastasize

Ancillary Testing and Molecular Signature

As described by the name, the tumor is an admixture of both an exocrine ductal component and an endocrine component. Each component has its own distinct immunoprofile. Similar to pancreatic neuroendocrine tumors, the neuroendocrine component of MDEC is synaptophysin and chromogranin positive. In a large proportion of cases with a poorly differentiated neuroendocrine component, alterations in p53 and Rb can be detected [2, 3].

On the other hand, the immunoprofile for the ductal component is akin to conventional and variant types of PDCA that are described above (see Sect. 5.4), including CKAE1/3, CA19–9, CK7, and mucicarmine, among others. If the ductal component is poorly differentiated, loss of SMAD4 and aberrant p53 expression may be seen. In addition, the ductal component is negative for neuroendocrine markers [59, 60].

Very little is known about the genetic underpinning in MDECs. The molecular alterations in the two different components can be extrapolated based on the known genetic makeup of the conventional type PDCA and neuroendocrine tumors. The molecular landscape of the conventional type PDCA is discussed extensively above but includes the canonical alterations in KRAS, CDKN2A, SMAD4, and TP53 (see Sect. 5.4).

Poorly differentiated neuroendocrine tumors are more likely to be associated with mutations in TP53 and Rb (95% and 74% of the cases, respectively). When Rb expression is retained, p16 expression tends to be lost. Lastly, proteins involved in the DNA damage response pathway including ATRX and DAXX are retained as well. This is in contrast to well-differentiated neuroendocrine tumors, where TP53, Rb, and p16 are retained; however, mutations in ATRX and DAXX are commonly found [3]. However, whether mutations are retained in true MDECs remains to be determined [59].

Medullary Carcinoma

Medullary carcinoma of the pancreas represents a distinct entity among the different subtypes of pancreatic ductal adenocarcinoma with characteristic clinicopathologic, immuno-

histochemical, genetic, and morphologic signatures. This tumor type has been reported in up to 4% of pancreatic ductal adenocarcinomas in various studies with a particular enrichment in patients with hereditary nonpolyposis colorectal cancer (HNPCC)/Lynch syndrome. In fact, medullary carcinoma is now included as an HNPCC-associated tumor in the revised Bethesda criteria [67, 68]. Conversely, patients presenting with pancreatic medullary carcinoma are also more likely to have first-degree relatives with a history of malignancy or with HNPCC. Although the prognostic significance of the medullary carcinoma requires additional studies, so far, the overall 2-year and 5-year survival rates have been reported to be 29% and 13%, respectively, similar to low-stage pancreatic ductal adenocarcinoma [67–71].

Important Cytologic Features

The key cytologic features of medullary carcinoma include:

- Syncytial fragments of cells with poorly defined borders and eosinophilic cytoplasm.
- Enlarged round to oval nuclei with prominent nucleoli, but with smooth nuclear membrane contours without significant irregularities.
- Background may show lymphocytes, plasma cells, and necrosis [6].

Histologic Correlation

The key histologic features of medullary carcinoma include:

- Poorly differentiated tumor in syncytial sheets without gland formation or apparent mucin.
- Expansive pushing borders are key.
- Neoplastic cells have abundant basophilic or eosinophilic cytoplasm without well-defined cell borders.
- Nuclei show marked pleomorphism and prominent nucleoli.

- Extensive necrosis is present in most cases, and tumors may also have additional focal areas of clear cell change or adeno-squamous differentiation.
- Variable numbers of intra-tumoral lymphocytes and Crohn's-like lymphoid infiltrates are not apparent.

Differential Diagnosis

Table 5.10 outlines the differential diagnosis for medullary carcinoma.

Ancillary Testing and Molecular Signature

Immunohistochemical markers for identifying medullary carcinoma show significant overlap with other morphotypes. Medullary carcinomas of the pancreas show CK7 and pan-cytokeratin reactivity, but are negative for lipase, CK20, CEA, chromogranin, S100, and CD45. Mucicarmine highlights focal to diffuse mucin in tumors [67, 69–71].

Rarely, a variant of a medullary carcinoma with lymphoepithelial-like features may occur in the context of harboring a latent EBV virus. In such cases, testing for EBV RNA in situ hybridization would be prudent to support the diagnosis [70].

Medullary carcinoma of the pancreas appears to be a genetically distinct entity in two ways compared to other morphologic patterns of pancreatic ductal adenocarcinoma. First, 69% of medullary carcinomas of the pancreas described thus far are wild-type for KRAS. In comparison, other morphotypes of ductal adenocar-

Table 5.10 Differential diagnosis for medullary carcinoma

Poorly differentiated PDCA	Infiltrative borders Distinct cell borders No microsatellite instability
Poorly differentiated acinar cell carcinoma of the pancreas	Prominent central nucleoli Lipase and trypsin positive No microsatellite instability

cinoma harbor KRAS G12 codon mutations. Second, 22% of medullary carcinomas show microsatellite instability, which is rarely ever identified in other types of pancreatic ductal adenocarcinoma. Given the known development of pancreatic medullary carcinoma in the context of the HNPCC/Lynch syndrome, the current body of work suggests that immunohistochemistry with a panel of markers for MLH1, PMS2, MSH2, and MSH6 is warranted as an initial method for predictive screening for an underlying germline mutation [67, 69, 70]. Thus, the differences in the morphologic pattern and the molecular landscape should prove useful in diagnosing medullary carcinoma from other types of pancreatic ductal adenocarcinoma.

Hepatoid Carcinoma of the Pancreas

Hepatoid carcinoma (HC) of the pancreas is an uncommon histologic variant of PDCA and comprises a heterogeneous group of tumors that may exist either in a pure form or mixed with either a neuroendocrine or conventional ductal component [72]. From a clinical standpoint, HC tends to occur more frequently in men in the fifth to sixth decades of life. Similar to conventional type PDCA, patients with HC present with symptoms of obstructive jaundice; however, unique to HC, several patients have been reported to have elevated serum levels of alpha-fetoprotein (AFP) [72–74]. Given the aggressive nature of HC, patients with this variant have an unfavorable survival outcome with most presenting at a late stage with liver and lymph node metastases. In addition, although more studies are needed, the presence of a mixed or a pure histologic pattern does not appear to have a significant prognostic impact [72–78].

Important Cytologic Features

The key cytologic features of hepatoid carcinoma of the pancreas [72, 73] include:

- Sheets and clusters of large, epithelioid cells.
- Abundant foamy cytoplasm.
- Enlarged nuclei with irregular nuclear membranes, coarse chromatin, and prominent nucleoli.
- Transgressing vessels may be identified.

Histologic Correlation

The key histologic features of hepatoid carcinoma of the pancreas [72–76, 78] include:

- Solid, nested, or trabecular architecture.
- Polygonal cells with granular, eosinophilic, clear, or foamy cytoplasm.
- Distinct cell borders.
- Centrally located nuclei and prominent nucleoli.
- Bile pigment may be present.

Differential Diagnosis

Table 5.11 outlines the differential diagnosis for HC.

Table 5.11 Differential diagnosis for hepatoid carcinoma of the pancreas

Acinar cell carcinoma of the pancreas	Trypsin, chymotrypsin, lipase and amylase positive Heppar1 negative on IHC
Pancreatoblastoma	Small acinar structures Mesenchymal component Characteristic squamoid morules Beta-catenin positive
Intraductal oncocytic papillary neoplasm	Papillary architecture Stratified oncocytic cells with mucin production and goblet cells CEA, HepPar1 positive in >50% cases and not useful
Metastatic hepatocellular carcinoma	Clinical correlation is necessary

Ancillary Testing and Molecular Signature

The hepatoid carcinoma of the pancreas demonstrates immunohistochemical patterns similar to that seen in the native liver. Hepatocyte paraffin 1 (HepPar1) and arginase are expressed in these tumors highlighting the hepatocellular differentiation. In addition, polyclonal CEA and CD10 show a canalicular staining pattern. Alpha-fetoprotein (AFP) and alpha-1-antitrypsin may also be identifiable in these tumors [3, 72–76, 78].

Given the rarity of hepatoid carcinoma of the pancreas, the genomic landscape of this variant remains unclear. In the literature, thus far, next-generation sequencing data has been reported only on two cases of hepatoid carcinoma of the pancreas. In one case, a frameshift mutation Q590fs in exon 14 of BAP1 (BRCA1-associated protein 1) was identified, whereas in the second case, no mutations were identified. Interestingly, however, in both cases, mutations in the canonical pathways known to be involved in the pathogenesis of PDCA, including KRAS, TP53, and SMAD4, were not identified, and both cases reported microsatellite stability [75, 78]. Thus, although the data is limited, the molecular signature of hepatoid carcinoma of the pancreas appears to be distinct from conventional type and other variants of PDCA.

References

1. De La Cruz MS, Young AP, Ruffin MT. Diagnosis and management of pancreatic cancer. *Am Fam Physician*. 2014;89(8):626–32.
2. Bosman FT, Carneiro F, Hruban RH, Theise ND, editors. WHO classification of tumors of the digestive system. Lyon, IARC2010.
3. Odze RD, Goldblum JR. Odze and Goldblum surgical pathology of the GI tract, liver, biliary tract, and pancreas. Philadelphia: Saunders/Elsevier; 2015.
4. Matsubayashi H, Takaori K, Morizane C, Maguchi H, Mizuma M, Takahashi H, et al. Familial pancreatic cancer: concept, management and issues. *World J Gastroenterol*. 2017;23(6):935–48.
5. Rustgi AK. Familial pancreatic cancer: genetic advances. *Genes Dev*. 2014;28(1):1–7.
6. Centeno BA, Stelow EB, Pitman MB. In: Geisinger KP, Campion MB, editors. *Pancreatic cytohistology*: Cambridge University Press; 2015.

7. Adsay NV, Merati K, Nassar H, Shia J, Sarkar F, Pierson CR, et al. Pathogenesis of colloid (pure mucinous) carcinoma of exocrine organs—coupling of gel-forming mucin (MUC2) production with altered cell polarity and abnormal cell-stroma interaction may be the key factor in the morphogenesis and indolent behavior of colloid carcinoma in the breast and pancreas. *Am J Surg Pathol.* 2003;27(5):571–8.
8. Adsay NV, Pierson C, Sarkar F, Abrams J, Weaver D, Conlon KC, et al. Colloid (mucinous noncystic) carcinoma of the pancreas. *Am J Surg Pathol.* 2001;25(1):26–42.
9. Jang DK, Lee SH, Lee JK, Paik WH, Chung KH, Lee BS, et al. Comparison of cytological and histological preparations in the diagnosis of pancreatic malignancies using endoscopic ultrasound guided fine needle aspiration. *Hepatob Pancreat Dis.* 2017;16(4):418–23.
10. Lee ES, Lee JM. Imaging diagnosis of pancreatic cancer: a state-of-the-art review. *World J Gastroenterol.* 2014;20(24):7864–77.
11. Toshima F, Inoue D, Yoshida K, Yoneda N, Minami T, Kobayashi S, et al. Adenosquamous carcinoma of pancreas: CT and MR imaging features in eight patients, with pathologic correlations and comparison with adenocarcinoma of pancreas. *Abdom Radiol.* 2016;41(3):508–20.
12. Tummala P, Junaidi O, Agarwal B. Imaging of pancreatic cancer: an overview. *J Gastrointest Oncol.* 2011;2(3):168–74.
13. Yang KY, Choi JI, Choi MH, Park MY, Rha SE, Byun JY, et al. Magnetic resonance imaging findings of undifferentiated carcinoma with osteoclast-like giant cells of pancreas. *Clin Imag.* 2016;40(1):148–51.
14. Yoon MA, Lee JM, Kim SH, Lee JY, Han JK, Choi BI, et al. MRI features of pancreatic colloid carcinoma. *Am J Roentgenol.* 2009;193(4):W308–W13.
15. Lin F, Staerckel G. Cytologic criteria for well differentiated adenocarcinoma of the pancreas in fine-needle aspiration biopsy specimens. *Cancer Cytopathol.* 2003;99(1):44–50.
16. Mitchell ML, Carney CN. Cytologic criteria for the diagnosis of pancreatic-carcinoma. *Am J Clin Pathol.* 1985;83(2):171–6.
17. Jarboe EA, Layfield LJ. Cytologic features of pancreatic intraepithelial neoplasia and pancreatitis: potential pitfalls in the diagnosis of pancreatic ductal carcinoma. *Diagn Cytopathol.* 2011;39(8):575–81.
18. Layfield LJ, Jarboe EA. Cytopathology of the pancreas: neoplastic and nonneoplastic entities. *Ann Diagn Pathol.* 2010;14(2):140–51.
19. Bailey P, Chang DK, Nones K, Johns AL, Patch AM, Gingras MC, et al. Genomic analyses identify molecular subtypes of pancreatic cancer. *Nature.* 2016;531(7592):47.
20. Dreyer SB, Jamieson NB, Upstill-Goddard R, Bailey PJ, McKay CJ, Biankin AV, et al. Defining the molecular pathology of pancreatic body and tail adenocarcinoma. *Brit J Surg.* 2018;105(2):E183–E91.
21. Mulder BGS, Mieog JSD, Handgraaf HJM, Sarasqueta AF, Vasen HFA, Potjer TP, et al. Targeted next-generation sequencing of FNA-derived DNA in pancreatic cancer. *J Clin Pathol.* 2017;70(2):174–8.

22. Hoorens A, Prenzel K, Lemoine NR, Kloppel G. Undifferentiated carcinoma of the pancreas: analysis of intermediate filament profile and Ki-ras mutations provides evidence of a ductal origin. *J Pathol.* 1998;185(1):53–60.
23. Ergun M, Aydog G, Kayacetin E, Sasmaz N. A case of anaplastic carcinoma of pancreas diagnosed with endoscopic ultrasound-guided fine needle aspiration cytology. *Turk J Gastroenterol.* 2012;23(6):828–9.
24. Khashab MA, Emerson RE, DeWitt JM. Endoscopic ultrasound-guided fine-needle aspiration for the diagnosis of anaplastic pancreatic carcinoma: a single-center experience. *Pancreas.* 2010;39(1):88–91.
25. Naito Y, Kawahara A, Taira T, Takase Y, Murata K, Ishida Y, et al. Cytopathological and immunocytochemical findings of pancreatic anaplastic carcinoma with ZEB1 expression by means of touch imprint cytology. *Diagn Cytopathol.* 2018;46(2):198–203.
26. Oka K, Inoue K, Sugino S, Harada T, Tsuji T, Nakashima S, et al. Anaplastic carcinoma of the pancreas diagnosed by endoscopic ultrasound-guided fine-needle aspiration: a case report and review of the literature. *J Med Case Rep.* 2018;12(1):152.
27. Pinto MM, Monteiro NL, Tizol DM. Fine needle aspiration of pleomorphic giant-cell carcinoma of the pancreas. Case report with ultrastructural observations. *Acta Cytol.* 1986;30(4):430–4.
28. Chopra S, Wu MLC, Imagawa DK, Lee J, Gu M. Endoscopic ultrasound-guided fine-needle aspiration of undifferentiated carcinoma with osteoclast-like giant cells of the pancreas: a report of 2 cases with literature review. *Diagn Cytopathol.* 2007;35(9):601–6.
29. Layfield LJ, Bentz J. Giant-cell containing neoplasms of the pancreas: an aspiration cytology study. *Diagn Cytopathol.* 2008;36(4):238–44.
30. Luchini C, Pea A, Lionheart G, Mafficini A, Nottegar A, Veronese N, et al. Pancreatic undifferentiated carcinoma with osteoclast-like giant cells is genetically similar to, but clinically distinct from, conventional ductal adenocarcinoma. *J Pathol.* 2017;243(2):148–54.
31. Mullick SS, Mody DR. “Osteoclastic” giant cell carcinoma of the pancreas—report of a case with aspiration cytology. *Acta Cytol.* 1996;40(5):975–9.
32. Muraki T, Reid MD, Basturk O, Jang KT, Bedolla G, Bagci P, et al. Undifferentiated carcinoma with osteoclastic giant cells of the pancreas clinicopathologic analysis of 38 cases highlights a more protracted clinical course than currently appreciated. *Am J Surg Pathol.* 2016;40(9):1203–16.
33. Reid MD, Muraki T, HooKim K, Memis B, Graham RP, Allende D, et al. Cytologic features and clinical implications of undifferentiated carcinoma with osteoclastic giant cells of the pancreas: an analysis of 15 cases. *Cancer Cytopathol.* 2017;125(7):563–75.
34. Westra WH, Sturm P, Drillenburger P, Choti MA, Klimstra DS, Albores-Saavedra J, et al. K-ras oncogene mutations in osteoclast-like giant cell

- tumors of the pancreas and liver—genetic evidence to support origin from the duct epithelium. *Am J Surg Pathol*. 1998;22(10):1247–54.
35. Adsay NV, Conlon KC, Zee SY, Brennan MF, Klimstra DS. Intraductal papillary–mucinous neoplasms of the pancreas—an analysis of in situ and invasive carcinomas in 28 patients. *Cancer*. 2002;94(1):62–77.
 36. Sigel CS, Santos-Zabala L, Basturk O. Fine-needle aspiration cytology of colloid carcinoma of the pancreas. *Ajcp-Rev Rep*. 2015;20(4):169–74.
 37. Gheza F, Cervi E, Pulcini G, Villanacci V, Giuliani SM, Schiavo-Lena M, et al. Signet ring cell carcinoma of the ampulla of Vater demonstration of a pancreatobiliary origin. *Pancreas*. 2011;40(5):791–3.
 38. Radojkovic M, Ilic D, Ilic I. Primary signet ring cell carcinoma of the pancreas with a good response to chemotherapy: case report and literature review. *Tumori*. 2017;103(Suppl. 1):e50–e2.
 39. Sakai T, Koshita S, Ito K, Kanno Y, Ogawa T, Kusunose H, et al. Signet-ring cell carcinoma derived from a Main duct-type Intraductal papillary mucinous neoplasm of the pancreas: a case report with long-term follow-up. *Intern Med*. 2018;57(8):1093–9.
 40. Terada T. Primary signet-ring cell carcinoma of the pancreas diagnosed by endoscopic retrograde pancreatic duct biopsy: a case report with an immunohistochemical study. *Endoscopy*. 2012;44:E141–E2.
 41. Zhang YT, Soofi Y, Cheng JRA. Case of primary signet ring cell carcinoma of the pancreas. *Am J Clin Pathol*. 2018;149:S55.
 42. Patel M, Hans HS, Pan K, Khan H, Donath E, Caldera H. The impact of epidemiological factors and treatment interventions on survival in patients with signet ring cell carcinoma of the pancreas. *Am J Clin Oncol*. 2018.
 43. Kardon DE, Thompson LDR, Przygodzki RM, Heffess CS. Adenosquamous carcinoma of the pancreas: a clinicopathologic series of 25 cases. *Modern Pathol*. 2001;14(5):443–51.
 44. Imaoka H, Shimizu Y, Mizuno N, Hara K, Hijioka S, Tajika M, et al. Clinical characteristics of Adenosquamous carcinoma of the pancreas a matched case-control study. *Pancreas*. 2014;43(2):287–90.
 45. Katz MHG, Taylor TH, Al-Refaie WB, Hanna MH, Imagawa DK, Anton-Culver H, et al. Adenosquamous versus adenocarcinoma of the pancreas: a population-based outcomes analysis. *J Gastrointest Surg*. 2011;15(1):165–74.
 46. Komatsu H, Egawa S, Motoi F, Morikawa T, Sakata N, Naitoh T, et al. Clinicopathological features and surgical outcomes of adenosquamous carcinoma of the pancreas: a retrospective analysis of patients with resectable stage tumors. *Surg Today*. 2015;45(3):297–304.
 47. Okabayashi T, Hanazaki K. Surgical outcome of adenosquamous carcinoma of the pancreas. *World J Gastroentero*. 2008;14(44):6765–70.
 48. Hester CA, Augustine MM, Choti MA, Mansour JC, Minter RM, Polanco PM, et al. Comparative outcomes of adenosquamous carcinoma of the

- pancreas: an analysis of the National Cancer Database. *J Surg Oncol.* 2018;118(1):21–30.
49. Olson MT, Siddiqui MT, Ali SZ. The differential diagnosis of squamous cells in Pancreatic aspirates: from contamination to Adenosquamous carcinoma. *Acta Cytol.* 2013;57(2):139–46.
 50. Rahemtullah A, Misdraji J, Pitman MB. Adenosquamous carcinoma of the pancreas—Cytologic features in 14 cases. *Cancer Cytopathol.* 2003;99(6):372–8.
 51. Rahemtullah A, Misdraji J, Pitman MB. Adenosquamous carcinoma of the pancreas: cytological and clinical features in a series of 15 cases. *Modern Pathol.* 2003;16(1):78a–9a.
 52. Borazanci E, Millis SZ, Korn R, Han HY, Whatcott CJ, Gatalica Z, et al. Adenosquamous carcinoma of the pancreas: molecular characterization of 23 patients along with a literature review. *World J Gastro Oncol.* 2015;7(9):132–40.
 53. Brody JR, Costantino CL, Potoczek M, Cozzitorto J, McCue P, Yeo CJ, et al. Adenosquamous carcinoma of the pancreas harbors KRAS2, DPC4 and TP53 molecular alterations similar to pancreatic ductal adenocarcinoma. *Modern Pathol.* 2009;22(5):651–9.
 54. Fang Y, Su Z, Xie J, Xue RD, Ma Q, Li YM, et al. Genomic signatures of pancreatic adenosquamous carcinoma (PASC). *J Pathol.* 2017;243(2):155–9.
 55. Marcus R, Maitra A, Roszik J. Recent advances in genomic profiling of adenosquamous carcinoma of the pancreas. *J Pathol.* 2017;243(3):271–2.
 56. Murakami Y, Yokoyama T, Yokoyama Y, Kanehiro T, Uemura K, Sasaki M, et al. Adenosquamous carcinoma of the pancreas: preoperative diagnosis and molecular alterations. *J Gastroenterol.* 2003;38(12):1171–5.
 57. Silvestris N, Brunetti O, Pinto R, Petriella D, Argentiero A, Fucci L, et al. Immunological mutational signature in adenosquamous cancer of pancreas: an exploratory study of potentially therapeutic targets. *Expert Opin Ther Tar.* 2018;22(5):453–61.
 58. Liu C, Karam R, Zhou Y, Su F, Ji Y, Li G, et al. The UPF1 RNA surveillance gene is commonly mutated in pancreatic adenosquamous carcinoma. *Nat Med.* 2014;20(6):596–8.
 59. Reid MD, Akkas G., Basturk O., Adsay V. Mixed adenoneuroendocrine carcinoma of the pancreas. In: La Rosa S, Sessa F, Pancreatic neuroendocrine neoplasms. Cham: Springer; 2015. p. 155–165.
 60. Ballas KD, Rafailidis SF, Demertzidis C, Alatsakis MB, Pantzaki A, Sakadamis AK. Mixed exocrine-endocrine tumor of the pancreas. *JOP: Journal of the pancreas.* 2005;6(5):449–54.
 61. Hirano H, Terada N, Yamada N, Yamanegi Y, Oyama H, Nishigami T, et al. A case of mixed ductal-endocrine carcinoma of the pancreas. *Med Mol Morphol.* 2011;44(1):58–62.

62. Kaji K, Seishima J, Yamato M, Miyazawa M, Komura T, Marukawa Y, et al. Clinical utility of endoscopic ultrasound-guided fine-needle aspiration in mixed adenoneuroendocrine carcinoma with signet-ring cells of the pancreas: a case report and review of the literature. *Clin J Gastroenterol.* 2016;9(1):43–8.
63. La Rosa S, Marando A, Sessa F, Capella C. Mixed Adenoneuroendocrine carcinomas (MANECs) of the gastrointestinal tract: an update. *Cancers (Basel).* 2012;4(1):11–30.
64. Lennerz JKM, Fernandez-Del Castillo C, Pitman MB. Mixed ductal-endocrine carcinoma of the pancreas metastatic to the liver. *Pancreas.* 2011;40(2):319–21.
65. Leteurtre E, Brami F, Kerr-Conte J, Quandalle P, Lecomte-Houcke M. Mixed ductal-endocrine carcinoma of the pancreas—a case study with mixed ductal-endocrine metastasis double labeled for cytokeratin 19 and synaptophysin. *Arch Pathol Lab Med.* 2000;124(2):284–6.
66. Zehani A, Chelly I, Azouz H, Makni A, Haouet S, Kchir N. Mixed ductal endocrine carcinoma of the pancreas. *Ann Pathol.* 2012;32(4):296–8.
67. Banville N, Geraghty R, Fox E, Leahy DT, Green A, Keegan D, et al. Medullary carcinoma of the pancreas in a man with hereditary nonpolyposis colorectal cancer due to a mutation of the MSH2 mismatch repair gene. *Hum Pathol.* 2006;37(11):1498–502.
68. Cumplido Buron JD, Toral Pena JC. The medullary carcinoma of the pancreas. A relative new entity. *Rev Esp Enferm Dig.* 2011;103(6):335–6.
69. Goggins M, Offerhaus GJ, Hilgers W, Griffin CA, Shekher M, Tang D, et al. Pancreatic adenocarcinomas with DNA replication errors (RER+) are associated with wild-type K-ras and characteristic histopathology. Poor differentiation, a syncytial growth pattern, and pushing borders suggest RER+. *Am J Pathol.* 1998;152(6):1501–7.
70. Wilentz RE, Goggins M, Redston M, Marcus VA, Adsay NV, Sohn TA, et al. Genetic, immunohistochemical, and clinical features of medullary carcinoma of the pancreas: a newly described and characterized entity. *Am J Pathol.* 2000;156(5):1641–51.
71. Yago A, Furuya M, Mori R, Yabushita Y, Sawada Y, Kumamoto T, et al. Medullary carcinoma of the pancreas radiologically followed up as a cystic lesion for 9 years: a case report and review of the literature. *Surg Case Rep.* 2018;4(1):80.
72. Marchegiani G, Gareer H, Parisi A, Capelli P, Bassi C, Salvia R. Pancreatic hepatoid carcinoma: a review of the literature. *Dig Surg.* 2013;30(4–6):425–33.
73. Hameed O, Xu H, Saddeghi S, Maluf H. Hepatoid carcinoma of the pancreas: a case report and literature review of a heterogeneous group of tumors. *Am J Surg Pathol.* 2007;31(1):146–52.
74. Paner GP, Thompson KS, Reyes CV. Hepatoid carcinoma of the pancreas. *Cancer.* 2000;88(7):1582–9.

75. Chang JM, Katariya NN, Lam-Himlin DM, Haakinson DJ, Ramanathan RK, Halfdanarson TR, et al. Hepatoid carcinoma of the pancreas: case report, next-generation tumor profiling, and literature review. *Case Rep Gastroenterol.* 2016;10(3):605–12.
76. Hughes K, Kelty S, Martin R. Hepatoid carcinoma of the pancreas. *Am Surg.* 2004;70(11):1030–3.
77. Kuo PC, Chen SC, Shyr YM, Kuo YJ, Lee RC, Wang SE. Hepatoid carcinoma of the pancreas. *World J Surg Oncol.* 2015;13:185.
78. Vanoli A, Argenti F, Vinci A, La Rosa S, Viglio A, Riboni R, et al. Hepatoid carcinoma of the pancreas with lymphoid stroma: first description of the clinical, morphological, immunohistochemical, and molecular characteristics of an unusual pancreatic carcinoma. *Virchows Arch.* 2015;467(2):237–45.



Pancreatic Neuroendocrine Tumors and Other Solid Tumors of Pancreas

Jacob Sweeney and Rema Rao

Introduction

This chapter reviews the key features that define pancreatic neuroendocrine neoplasia (PNEN), acinar cell carcinoma (ACC), solid pseudopapillary neoplasm (SPN), and pancreatoblastoma (PB) on cytology specimens with cytologic-histologic correlations. These four tumors often share overlapping clinical, morphologic, and immunohistochemical features and consequently must often be considered together within the same differential diagnosis. At the time of initial sampling, all four tumors often present as solid pancreatic masses that yield highly cellular aspirates, comprised of large polygonal cells with round nuclei, arranged as single cells or aggregates. This potential for overlapping cytomorphology necessitates the use of immunohistochemical panels to effectively diagnose these entities (Table 6.3). From a molecular pathogenesis standpoint,

J. Sweeney (✉) · R. Rao

Department of Pathology and Laboratory Medicine, Weill-Cornell Medicine, New York Presbyterian Hospital, New York, NY, USA
e-mail: jas9275@nyp.org

© Springer Nature Switzerland AG 2019

A. Goyal et al. (eds.), *Pancreas and Biliary Tract Cytohistology*,
Essentials in Cytopathology 28,
https://doi.org/10.1007/978-3-030-22433-2_6

these tumors do not show the characteristic alterations of pancreatic ductal adenocarcinoma (PDA). The tumors in this chapter are generally associated with variable genetic abnormalities, with the exception of SPN, which is invariably associated with gain-of-function mutations in the CTNNB1 gene leading to nuclear accumulation of the β [beta]-catenin protein within the nucleus. ACC and PB can possess similar molecular alterations, emphasizing the potential overlap between these tumors [1]. Despite the overlapping features, effective diagnosis of these entities is critical as each diagnosis portends dramatically different prognosis and treatment. This chapter will review the key clinical, morphologic, and immunohistochemical features required to effectively work through this challenging differential diagnosis.

Pancreatic Neuroendocrine Neoplasia

Background

PNEN includes well-differentiated pancreatic neuroendocrine tumor (PNET) and poorly differentiated pancreatic neuroendocrine carcinoma (PNEC). While PNEN as a group are rare, PNET is much more common than the vanishingly rare PNEC. PNET and PNEC are distinct in that, clinically, PNEC are more aggressive than even high grade PNET, and require different treatment options. Morphologically, PNEC are distinct from PNET and are histologically similar to either small cell carcinoma or large cell neuroendocrine carcinoma of the lung.

PNET can be stratified into three different grades—G1, G2, and G3—which correlate with prognosis and response to chemotherapy (Table 6.1). Grading of PNET can be performed on both aspirates and surgical resections. In surgical specimens, PNET can be graded by counting mitotic figures or measuring the Ki67 proliferation index. In aspirate specimens, only Ki67 proliferation index should be used to determine the grade. The fragmented

Table 6.1 WHO 2017 classification of well-differentiated pancreatic neuroendocrine tumors [2]

Grade	Ki67 proliferation index (%)	Mitotic index (per 10 hpf)
1	<3	<2
2	3–20	2–20
3	>20	>20

nature of aspirate specimens makes counting mitotic figures in consecutive high-power fields a challenge. The grading accuracy of Ki67 proliferation index increases as the number of counted cells increases; it has been shown that grading accuracy on aspirate specimens decreases significantly when less than 200 cells are counted [2].

Grossly, PNET are usually solid and well-circumscribed; however, larger lesions may show cystic degeneration (Fig. 6.1). They can present at any age but are more common in adults [1, 3–5]. They are more common in the body and tail but can occur at any location in the pancreas. On imaging, PNET are hypervascular with increased enhancement relative to the surrounding pancreatic parenchyma [6] (Fig. 6.2). A minority of PNET are functional and may present with clinical syndromes as a result of increased serum hormone levels. Insulinomas and gastrinomas are the most common functional PNET [7, 8]. However, the majority of PNET are nonfunctional and are identified incidentally on abdominal radiographs [5]. Histologically, functional and nonfunctional PNET are indistinguishable from one another [1].

PNET may occur in association with several different inherited syndromes including multiple endocrine neoplasia type 1 (MEN1), von Hippel-Lindau syndrome (vHL), tuberous sclerosis complex type 1 and 2 (TSC 1 and 2), and less commonly neurofibromatosis type 1 (NF1). Sporadic PNET are associated with multiple different somatic alterations with MEN1, DAXX, and ATRX mutations being the most common. In contrast, PNEC typically show TP53 and RB alterations that are not observed in PNET [1, 9].



Fig. 6.1 Gross photographs of PNET showing well-circumscribed tumors, which are characteristically solid (a), however, may show cystic degeneration (b) especially in large tumors



Fig. 6.2 MRI image showing a well-circumscribed mass arising in the pancreatic uncinate region, which shows increased enhancement relative to surrounding pancreas

Key Cytologic Features

- Cellular aspirates comprised of monotonous polygonal and plasmacytoid cells [1, 3–5, 8, 10–13] (Fig. 6.3).
- Tumor cells commonly present as single cells, naked nuclei, and pseudorosettes [1, 3–5, 8, 10–13] (Fig. 6.4).
- Nuclei with smooth nuclear contours and “salt and pepper” chromatin [1, 3–5, 8, 10–13] (Fig. 6.5).
- Eccentric plasmacytoid nuclei are common [5, 10] (Fig. 6.6).
- Nucleoli are typically inconspicuous or absent; however, prominent nucleoli may be seen in rare cases [1, 3–5, 8, 10–13].
- Cytoplasm is finely granular and can be amphophilic to basophilic [1, 3–5, 8, 10–13] (Figs. 6.6 and 6.7).

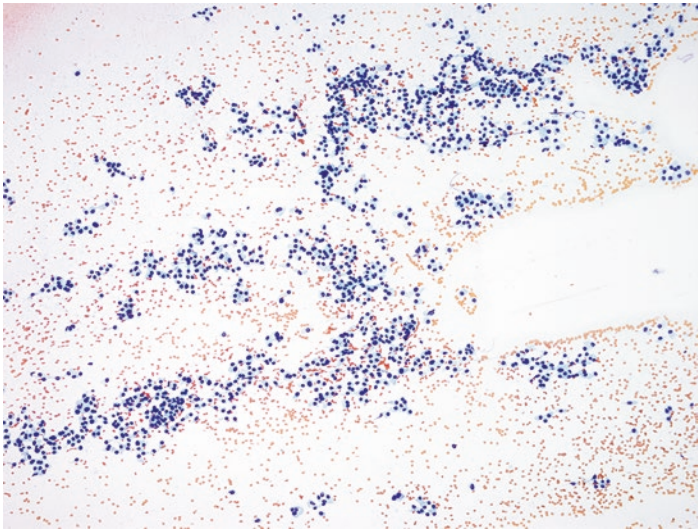


Fig. 6.3 PNET on an alcohol-fixed Papanicolaou-stained smear shows a cellular sample with a bloody background comprised of monotonous polygonal and plasmacytoid cells present as sheets of single cells and small aggregates

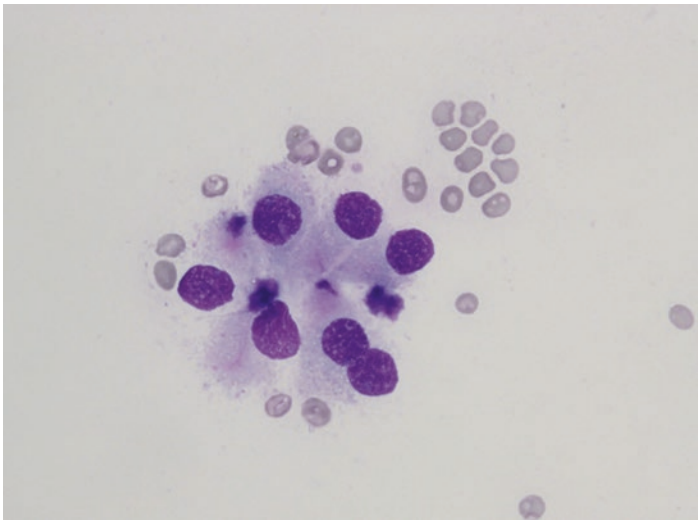


Fig. 6.4 PNET on an air-dried Diff-Quick preparation showing a pseudorosette formation

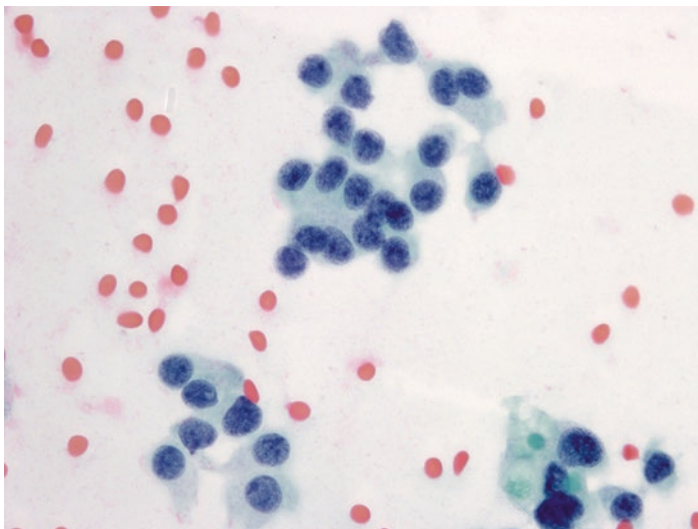


Fig. 6.5 PNET on an alcohol-fixed Papanicolaou-stained smear showing smooth nuclear contours, small inconspicuous nucleoli, and granular “salt and pepper” neuroendocrine chromatin

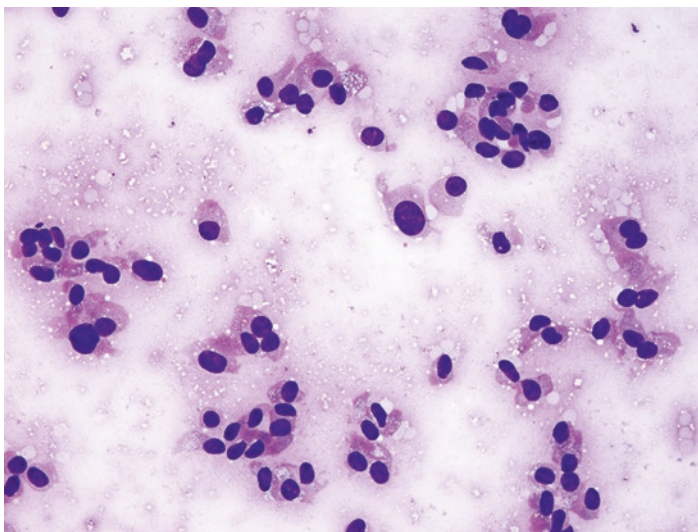


Fig. 6.6 PNET on an air-dried Diff-Quick preparation showing eccentric nuclei giving a “plasmacytoid” appearance and granular cytoplasm

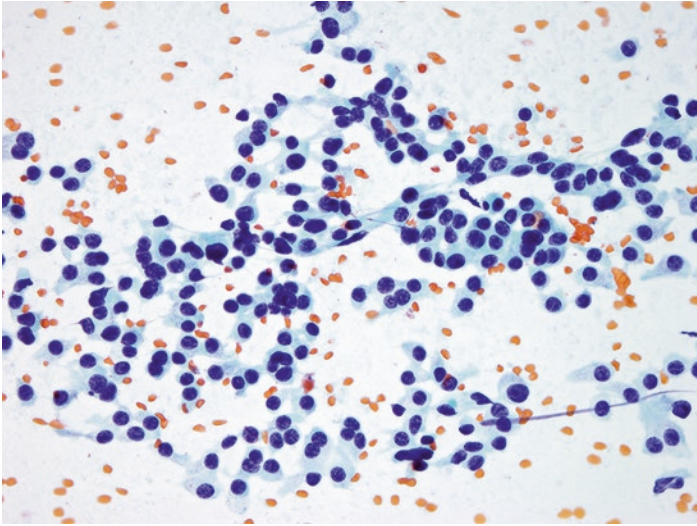


Fig. 6.7 PNET on an air-dried Diff-Quick preparation showing monotonous ovoid cells with eccentric nuclei, “salt and pepper” chromatin, and abundant finely granular cytoplasm

- Scattered binucleate cells as well as occasional large “bizarre” cells (endocrine atypia) [5, 10].
- Spindled, vacuolated, and oncocyctic cytomorphologies can be observed but are rare [3–5].
- The presence of increased mitotic figures and necrosis is associated with higher grade and aggressive tumor behavior [3, 4].
- PNEC are extraordinarily rare and are cytologically indistinguishable from small cell carcinoma or large cell neuroendocrine carcinoma of the lung [4, 5] (Fig. 6.8).

Key Histologic Features

- A wide variety of architectural patterns may be observed including nested, trabeculated, and gland forming [4].

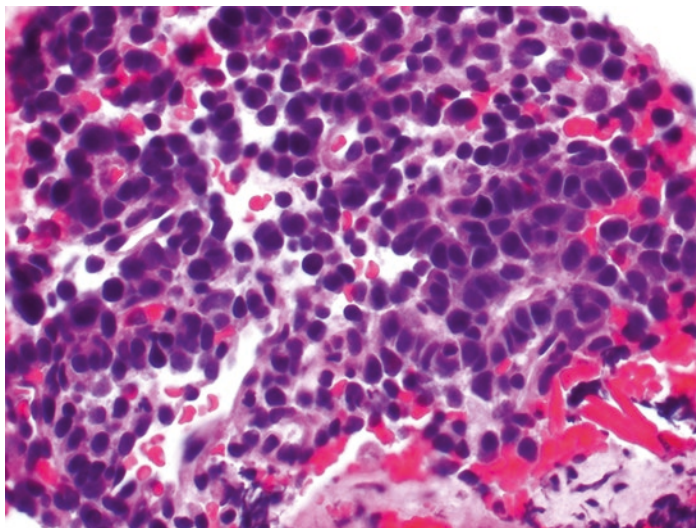


Fig. 6.8 In contrast to PNET, tumor cells in this small cell carcinoma of pancreas show high N:C ratio and molding similar to that seen in small cell carcinoma of the lung. (Image credit: Carlie Sigel, MD, Memorial Sloan Kettering Cancer Center, NY)

- Tumor cell groups are often separated by thin vasculature [4] (Fig. 6.9).
- Absent desmoplastic stroma [4].
- Hyalinized stroma is common [4] (Fig. 6.10).
- PNEC are histologically similar to small cell carcinoma or large cell neuroendocrine carcinoma of the lung and characteristically show abundant mitotic activity and necrosis [4] (Fig. 6.8).

Differential Diagnosis

Please refer to Table 6.2 for review of key cytomorphologic features and molecular alterations and Table 6.3 for review of key

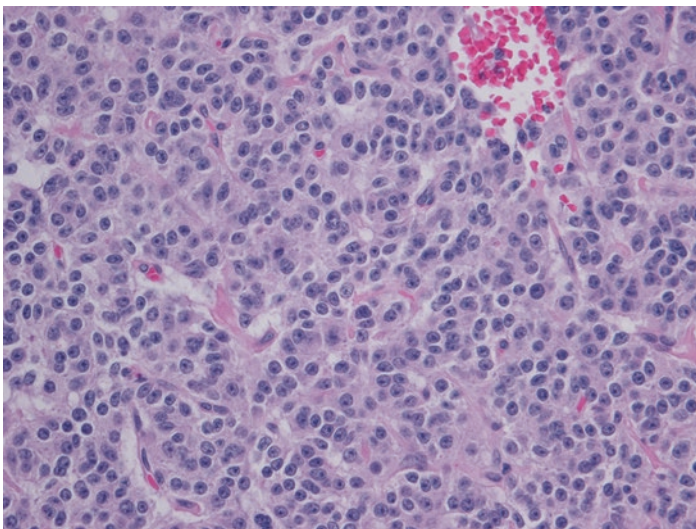


Fig. 6.9 H&E stained slide from a PNET resection specimen, showing prominent capillary network between tumor cell groups

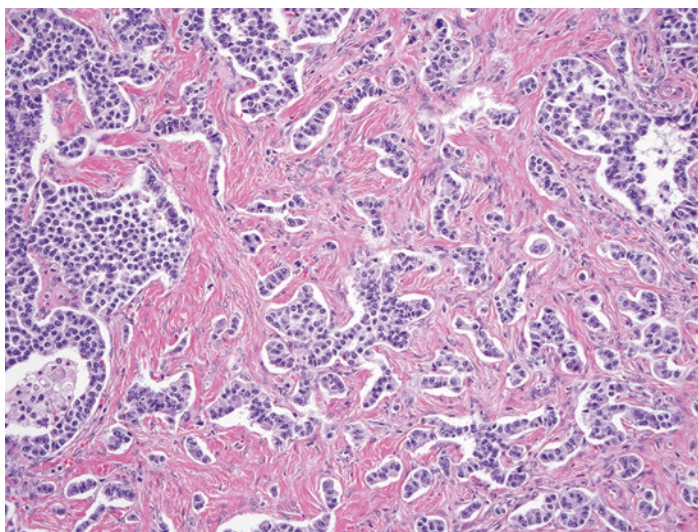


Fig. 6.10 H&E stained slide from a PNET resection specimen, showing abundant hyalinized stroma. This feature is not commonly seen in ACC. (Image credit: Carlie Sigel, MD, Memorial Sloan Kettering Cancer Center, NY)

Table 6.2 Defining features of well-differentiated pancreatic neuroendocrine tumors, acinar cell carcinoma, pancreatoblastoma, and solid pseudopapillary tumors

Tumor type	Clinical features	Cytologic feature	Histologic feature	Molecular alterations
PNET	Adults Body/tail Islet cell hypersecretion syndrome MEN1, VHL, TSC1 and 2, NF1	Cellular aspirate Ovoid cells Round smooth nuclear contours 'Salt and pepper' chromatin Inconspicuous nucleoli Fine cytoplasmic granules	Highly cellular Hyalinized stroma Nested and trabeculated architecture	MEN1 DAXX ATRX
ACC	Older men Head Lipase hypersecretion syndrome	Cellular aspirate Ovoid cells Round smooth nuclear contours Coarse chromatin Prominent nucleoli Large cytoplasmic granules	Highly cellular Scant stroma Solid and acini forming architecture	Loss of 11p APC/ β [beta]-catenin alterations in minority of cases
PB	Children Any location Beckwith-Wiedemann syndrome and familial adenomatous polyposis	Squamoid nests Epithelial component indistinguishable from ACC or PNET Mesenchymal component +/- pleomorphism and heterologous elements	Highly cellular Cellular stroma forms thick fibrous bands and a lobulated architecture	Loss of 11p APC/ β [beta]-catenin alterations in many cases
SPN	Middle-aged women Body/tail	Irregular nuclear contours and grooves Indistinct nucleoli Pseudopapillary structures Extracellular hyaline globules	Highly cellular Discohesive neoplastic cells Tumoral degeneration and pseudopapillary structures Variable stromal hyalinization	APC/ β [beta]-catenin pathway mutations in nearly 100%

Table 6.3 Immunohistochemical features of well-differentiated pancreatic neuroendocrine tumors, acinar cell carcinoma, and solid pseudopapillary neoplasms [31–33] (refer to Chap. 12)

	Chromogranin	Synaptophysin	CD56	Trypsin	Chymotrypsin	BCL10	β [beta]-catenin ^a	CD10	Progesterone receptor
PNET	P	P	P/N	N	N	N	N	P/N	P/N
ACC	R	R	R	P	P	P	P/N	N	N
SPN	N	P/N	P	N	N	N	P	P	P

P positive, *N* negative, *P/N* positive or negative, *R* rare positive

^aNuclear and cytoplasmic staining

ancillary studies including immunohistochemical profiles that separate PNET from other solid pancreatic non-ductal neoplasia.

Clinical Management

PNET are treated surgically as well as with chemotherapy in some cases. The prognosis is generally excellent following complete surgical excision. When complete surgical excision is not possible, treatment with somatostatin analogue chemotherapy is often employed. As was mentioned previously, prognosis correlates with tumor size and grade [1–4]. PNEC are associated with poor prognosis and require treatment with platinum-based chemotherapy [4].

Acinar Cell Carcinoma

Background

ACC is a rare pancreatic tumor that predominantly occurs in older men; however, it may present at any age. Presenting symptoms are generally nonspecific and often include abdominal pain. Jaundice is uncommon. Rarely patients present with peripheral fat necrosis and arthralgias as a result of increased serum lipase levels [1, 3, 4]. The presence of these symptoms often correlates with metastatic disease [1, 14]. ACC typically presents as a large solid tumor in the head of the pancreas [1, 3, 12, 15]. On gross examination, ACCs are typically large and well circumscribed with pushing borders. They can often show necrosis and cystic degeneration [1, 3, 4] (Fig. 6.11). Similarly, on imaging, ACCs are large, well-circumscribed solid tumors, with necrosis and cystic degeneration. The solid areas show homogeneous enhancement on both CT and MRI [1, 6] (Fig. 6.12).

The somatic mutations characteristically observed in PDA are not seen in ACC. Additionally, recurrent somatic mutations in single genes are uncommon in ACC with the one exception, which is the gain-of-function or loss-of-function mutations in the APC/



Fig. 6.11 Gross photograph of ACC. ACC are typically large bulky tumors that frequently show necrosis

β [beta]-catenin pathway, which occurs in 20–25% of ACC. These tumors therefore may show positive staining for β [beta]-catenin IHC [4, 16]. While somatic single gene mutations are relatively rare in ACC, chromosomal instability with allele loss and gain is common. Loss of chromosome 11p is one of the more common large chromosomal deletions and occurs in 50% of ACCs. ACC is not associated with any germline alterations [4, 17].

Key Cytologic Features

- Highly cellular aspirate comprised of single cells, naked nuclei, and small to large loose clusters forming acini-like structures [3, 4, 18] (Figs. 6.13, 6.14, and 6.15).
- Clean background, which may show small eosinophilic granules and abundant naked nuclei [3, 4, 18].



Fig. 6.12 ACC on CT imaging, showing a large, exophytic, lobulated, well-margined, fairly homogenous mass, in the pancreatic tail

- Prominent capillary network coursing through larger aggregates visible on aspirate smears [4] (Fig. 6.13).
- Prominent amphophilic to eosinophilic intracytoplasmic granules [3, 4, 14] (Fig. 6.14).
- Nuclei generally have clumped chromatin and prominent nucleoli [1, 3–5, 12, 14] (Fig. 6.15).
- Nuclei are typically uniform with round smooth contours but may also show pleomorphism and anisonucleosis [3, 19].
- Abundant mitotic figures and tumoral necrosis may be present [17].

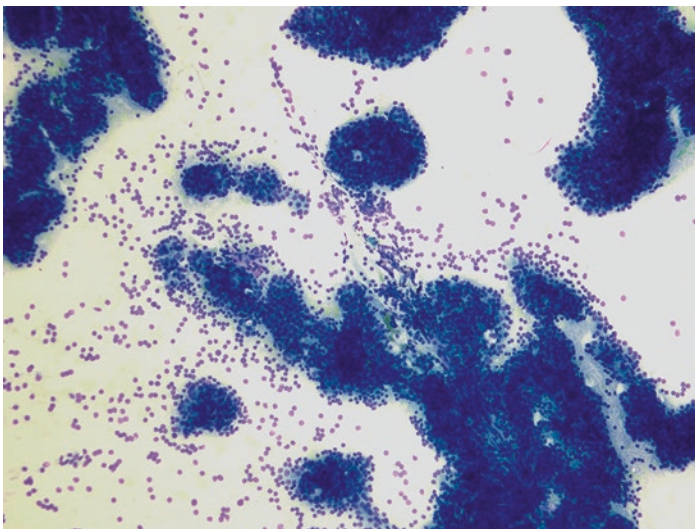


Fig. 6.13 ACC on an air-dried Diff-Quick preparation showing a highly cellular aspirate comprised of monotonous single cells, abundant naked nuclei, as well as larger aggregates against a clear background

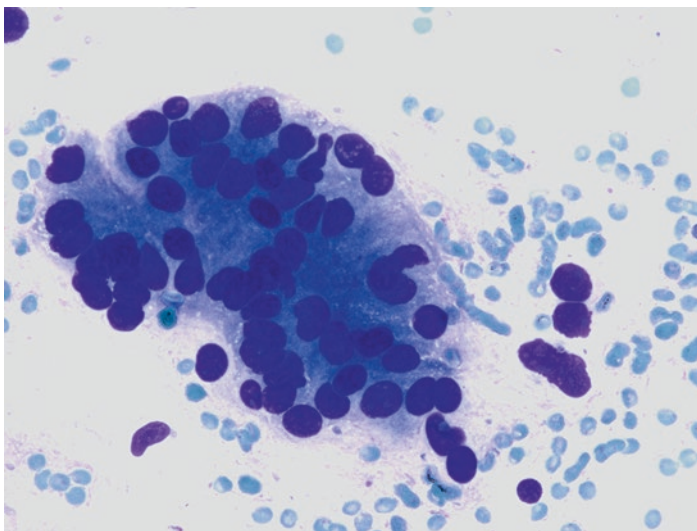


Fig. 6.14 ACC on an air-dried Diff-Quick preparation showing prominent acini formation with amphiphilic to eosinophilic intracytoplasmic granules

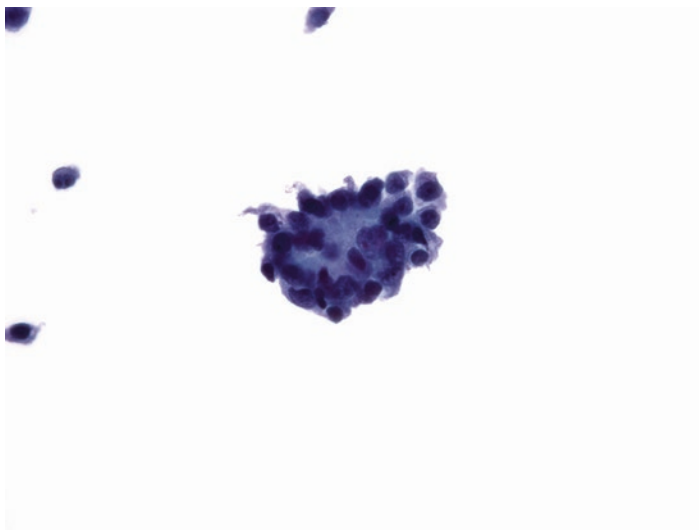


Fig. 6.15 ACC on a liquid-based preparation (ThinPrep) showing acini formation and single cells

Key Histologic Features

- Highly cellular [4] (Figs. 6.15, 6.16, and 6.17)
- Basally located nuclei [4] (Fig. 6.16)
- Solid, trabeculated, and acini forming architectures [4]
- Scant stroma [4] (Figs. 6.16 and 6.17)
- Absent desmoplastic stroma response [4]

Differential Diagnosis

It is important to distinguish benign pancreatic acini from ACC on aspirate samples. Benign acini typically show lower N:C ratio with smaller nuclei and small nucleoli (nuclear size is similar to that of red blood cells, Fig. 6.18) than ACC tumor cells, which tend to show enlarged nuclei and prominent nucleoli. Benign acinar cells are also more cohesive and form uniform cell aggregates in contrast to ACCs which present as small clusters, single cells, and naked nuclei. Mixed tumors

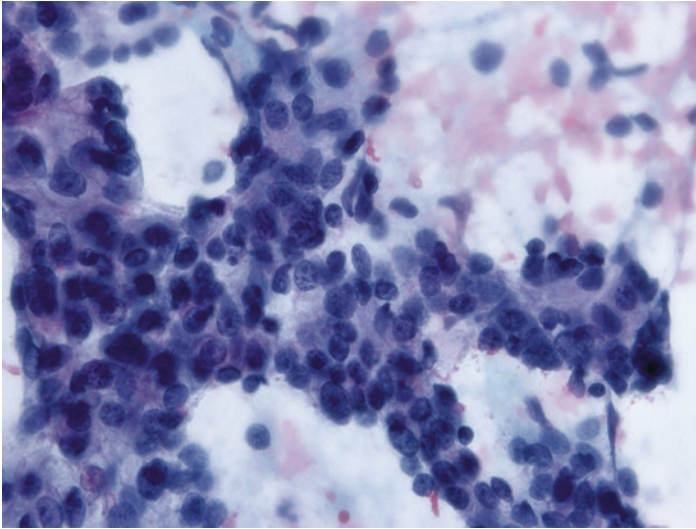


Fig. 6.16 ACC on aspirate sample with alcohol-fixed Papanicolaou-stained preparation shows tumor cells with large nuclei, coarse clumped chromatin, prominent nucleoli, granular eosinophilic cytoplasm, and high N:C ratio

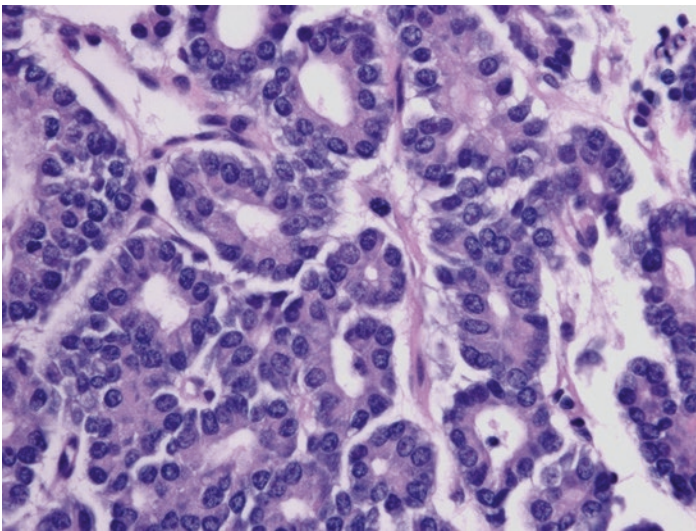


Fig. 6.17 H&E stained slide of ACC from a cell block showing prominent acini formation, basally located nuclei, mitotic activity, and scant stroma

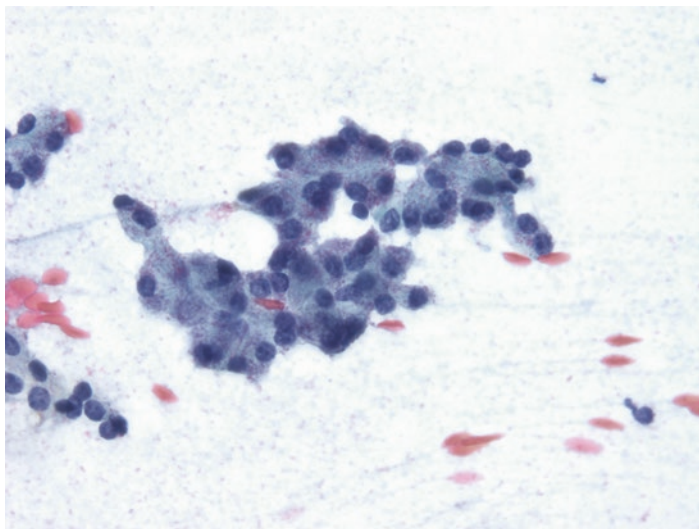


Fig. 6.18 Aspirate sample of benign acini on an alcohol-fixed Papanicolaou-stained preparation showing smaller nuclei (same as neighboring red blood cells) and small nucleoli

that include an ACC component are also possible. Mixed tumors are comprised of ACC as well as a PNET and or PDA component wherein the individual components comprise at least 25% of the tumor. The ACC component is predominant in most mixed tumors. Clinically, mixed tumors behave similarly to pure ACC. It is important to perform immunohistochemical stains specific to both ACC and PNET in order to rule out the possibility of a mixed tumor [4]. It is also important to emphasize that mixed tumors require a minor component that comprises at least 25% of the tumor mass. This is important to note as pure ACC can show positive staining for neuroendocrine markers such as chromogranin and synaptophysin in rare scattered cells.

Please refer to Table 6.2 for review of key cytomorphologic features and molecular alterations and Table 6.3 for review of key ancillary studies including immunohistochemical profiles that separate ACC from other solid pancreatic non-ductal neoplasia.

Clinical Management

Long-term survival is poor in ACC, and patients often present with metastatic disease involving lymph nodes and the liver [3, 4]. Distinguishing ACC from PNET is important as each requires different lines of chemotherapy. Surgical resection is the only curative treatment for ACC and is usually only employed for low-stage tumors [3]. Tumor size, lymph node involvement, and the presence of distant metastasis are all associated with poor prognosis [1, 15].

Pancreatoblastoma

Background

PB is an extremely rare pancreatic tumor that predominantly occurs in young children under the age of 10 [1, 14]. Patients usually present with nonspecific symptoms such as abdominal pain, weight loss, nausea, and diarrhea. A palpable abdominal mass can sometimes be appreciated on physical exam. Jaundice is uncommon. A minority of patients may present with elevated serum AFP [1, 3, 20, 21]. Grossly, PB are typically large, well-circumscribed, lobulated masses, with prominent necrosis. This tumor is not associated with a specific location and can occur anywhere in the pancreas. On imaging, PB are large, well-circumscribed and heterogeneous with internal septation. Calcification may be observed at the tumor margin [1, 6]. The characteristic molecular alterations in PDA are not observed in PB. The most common genetic abnormality in this tumor is loss of 11p [1]. Like ACC and SPN, both gain-of-function and loss-of-function somatic mutations in the APC/ β [beta]-catenin pathway can occur in PB [1, 4]. PB has been associated with both Beckwith-Wiedemann syndrome and familial adenomatous polyposis [4, 5].

Key Cytologic Features

- Highly cellular aspirates with cells present in large clusters, loosely cohesive three-dimensional groups, solid sheets, and occasional single cells [1, 4, 5, 14, 21–23].
- The tumor can have different appearances with both epithelial and mesenchymal components in some cases [1, 4, 5, 14, 21–24].
- Epithelial tumor cells most commonly show acinar cell differentiation but can also show organoid islands and ductal formation [1, 4, 5, 14, 21–23] (Fig. 6.19).

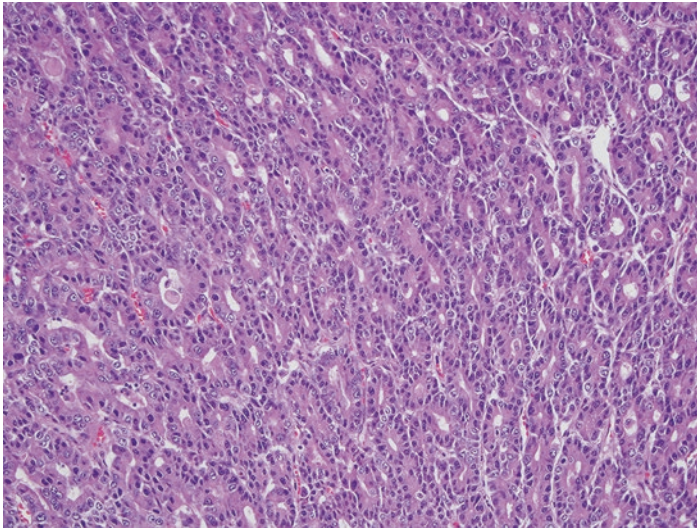


Fig. 6.19 H&E stained slide from ACC surgical resection specimen shows highly cellular tumor with acini forming architecture, basally oriented nuclei, and scant stroma. (Image credit: Carlie Sigel, MD, Memorial Sloan Kettering Cancer Center, NY)

- The presence of squamoid nests is a defining characteristic of PB [1, 4, 5, 14, 21–23].
- Squamoid nests are formed by squamous cells with oval nuclei and clear chromatin and may or may not be associated with keratinization [1, 4, 5, 14, 21–23].
- The squamous component showing swirling eddies is usually best appreciated on cell block preparations [1, 4, 5, 14, 21–23].
- A mesenchymal component, if present, is hypercellular and comprised of atypical pleomorphic spindle cells. Rarely, heterologous elements such as cartilage can also be observed [1, 4, 5, 14, 21–24].

Key Histologic Features

- The identification of squamoid nests is required for this diagnosis [4] (Figs. 6.20, 6.21 and 6.22).

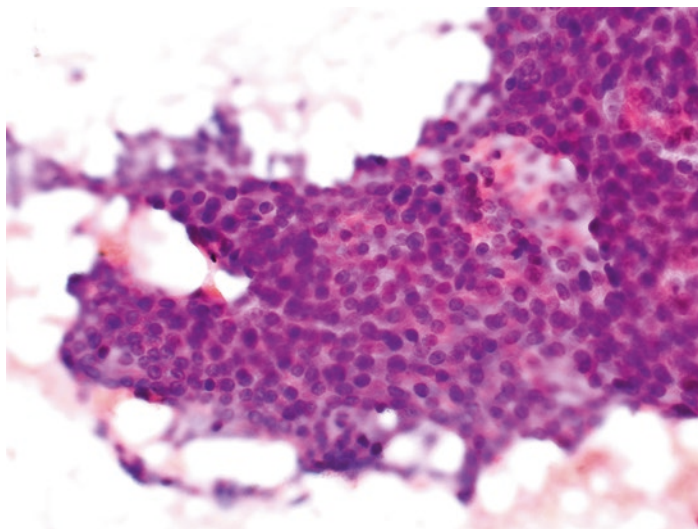


Fig. 6.20 H&E stained slide of PB on an aspirate specimen showing round pale nuclei in these epithelial groups with even chromatin and prominent nucleoli. (Image credit: Carlie Sigel, MD, Memorial Sloan Kettering Cancer Center, NY)

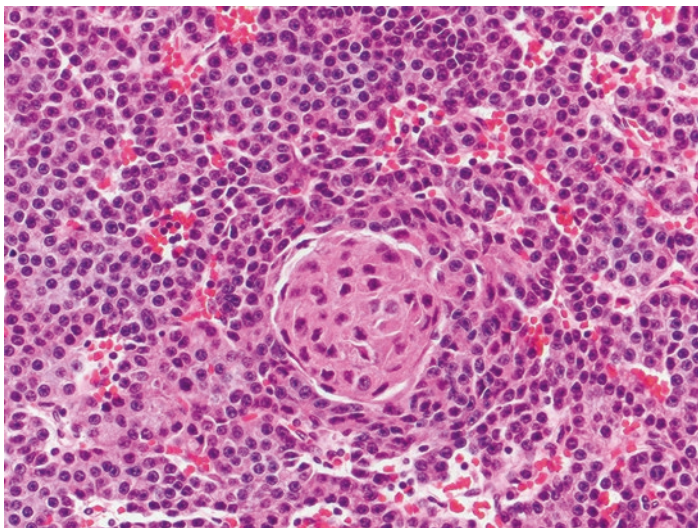


Fig. 6.21 H&E stained slide from PB surgical resection specimen shows cellular tumor with both acinar cell differentiation and squamoid nest formation. (Image credit: Meredith Pittman, MD, Weill Cornell Medicine, NY)

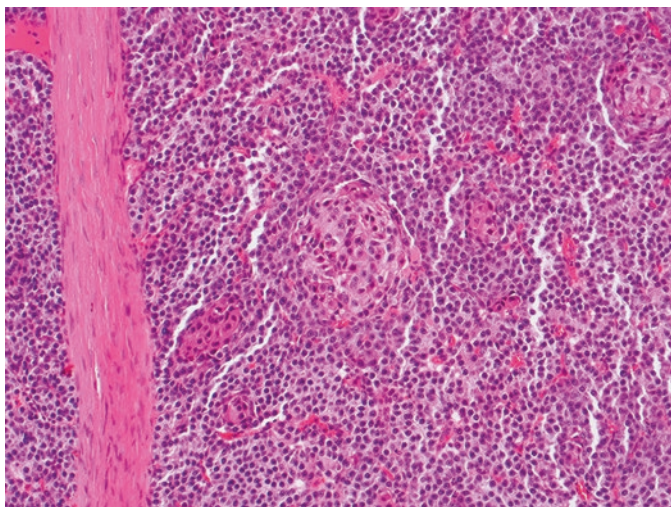


Fig. 6.22 H&E stained slide from PB surgical resection specimen shows cellular tumor with acinar cell differentiation, squamoid nest formation, as well as thick fibrous bands. (Image credit: Meredith Pittman, MD, Weill Cornell Medicine, NY)

- The histologic and cytologic appearance of the epithelial component may be indistinguishable from ACC or less commonly PNET or PDA [4].
- Thick and cellular stromal bands create a lobulated architecture [4].

Differential Diagnosis

Please refer to Table 6.2 for review of key cytomorphologic features and molecular alterations and Table 6.3 for review of key ancillary studies including immunohistochemical profiles that separate PB from other solid pancreatic non-ductal neoplasia.

Unfortunately, IHC cannot discriminate between PB with acinar cell differentiation and ACC, as both entities will stain positively for pancreatic exocrine enzymes such as trypsin, chymotrypsin, and lipase. Similarly, PB with neuroendocrine differentiation may also show similar cytomorphology and IHC staining characteristics as that seen in PNET. The diagnosis of PB depends on the identification of squamoid nests. Wilms tumor, hepatoblastoma, and neuroblastoma must also be considered in certain clinical contexts [1].

Clinical Management

Surgical resection is the primary treatment for PB. In pediatric patients, PB without metastatic disease is associated with a good prognosis. In pediatric patients with metastatic disease and in adult patients, the prognosis is poor [3–5]. In adults, PB behave similarly to ACC even when resected at an earlier stage [5].

Solid Pseudopapillary Neoplasm

Background

SPN is a rare tumor that occurs in adolescent and middle-aged women but is rare in men, children, and the elderly. Patients may

present with nonspecific abdominal pain, nausea, and vomiting. Many SPN are painless and discovered incidentally on abdominal imaging. SPN are often large at the time of diagnosis. Jaundice is an uncommon presenting symptom [1, 3, 25, 26].

Grossly, SPN are usually well-circumscribed solid lesions but frequently undergo cystic degeneration (Fig. 6.23). These tumors most commonly arise in the body and tail of the pancreas but can occur at any location. Calcification, encapsulation, cyst formation, and septations are all characteristically observed on imaging studies [27, 28] (Fig. 6.24). SPN show gain-of-function mutations in the CTNNB1 gene leading to nuclear accumulation of the β [beta]-catenin protein in nearly 100% of cases [1]. Other somatic mutations are uncommon in SPN. SPN are not associated with any germline alterations [4].

Key Cytologic Features

- Aspirate samples are typically highly cellular but may be paucicellular if cystic areas are sampled [3–5, 26] (Fig. 6.25).

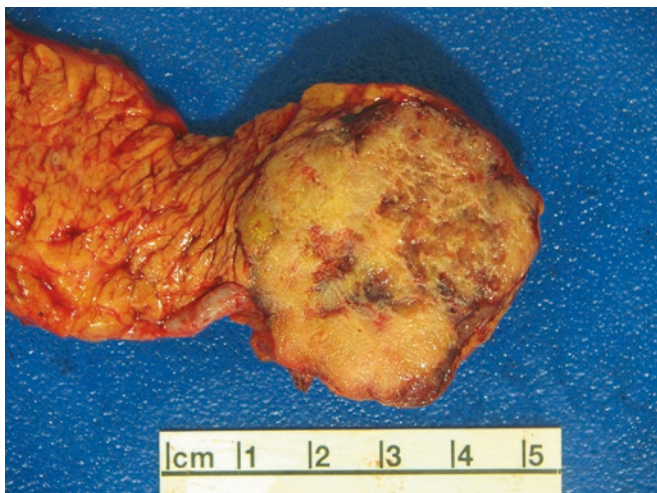


Fig. 6.23 Gross photograph of SPN showing a well-circumscribed solid mass with hemorrhage and cystic degeneration

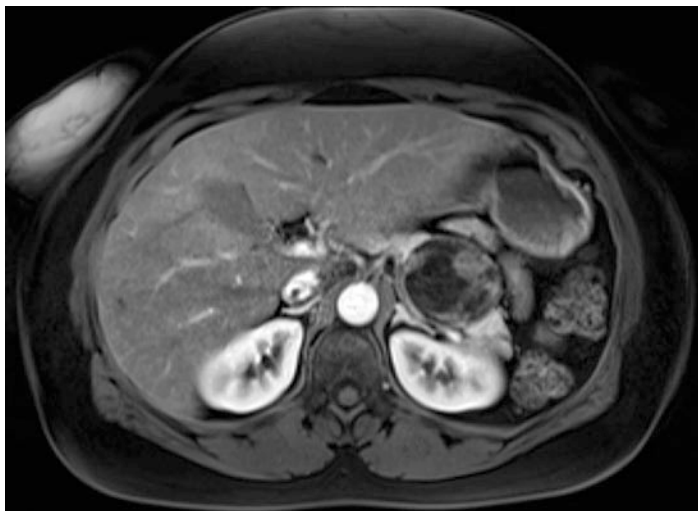


Fig. 6.24 SPN on MRI imaging, showing a large T2 heterogenous, well-circumscribed mass, in the distal body/tail of the pancreas

- The aspirate background commonly shows proteinaceous and necrotic debris [3–5, 26].
- Cytoplasm is delicate to finely granular [4, 5, 26, 29].
- Nuclei are bland with granular chromatin, small indistinct nucleoli, and nuclear grooves [4, 5, 26, 29] (Fig. 6.26).
- Mitotic figures are uncommon [4, 5, 26, 29].
- Pseudopapillary structures are comprised of a central capillary, a middle layer of myxoid stroma, and an outer cellular lining [4, 5, 26, 29] (Fig. 6.27).
- Tumor cells are present both as single cells and in association with branching pseudopapillary structures [4, 5, 26, 29] (Figs. 6.27, 6.28 and 6.29).
- PAS-positive hyaline globules are often observed in extracellular space [3–5, 26].

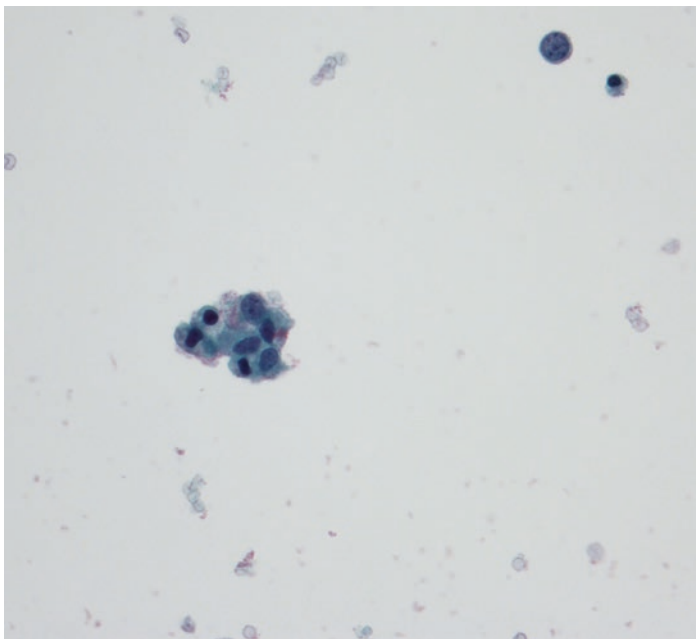


Fig. 6.25 Aspirate sample of a predominantly cystic SPN on a Papanicolaou-stained liquid-based preparation (ThinPrep) showing a paucicellular sample with rare to occasional tumor cell clusters

Key Histologic Features

- Solid highly cellular and vascular tumor comprised of discohesive neoplastic cells [4].
- Degeneration of tumor cells distant from vasculature leads to the formation of pseudopapillary architecture [4].
- Pseudopapillary structures are characterized by a rim of tumor cells surrounding blood vessels [4] (Fig. 6.30).

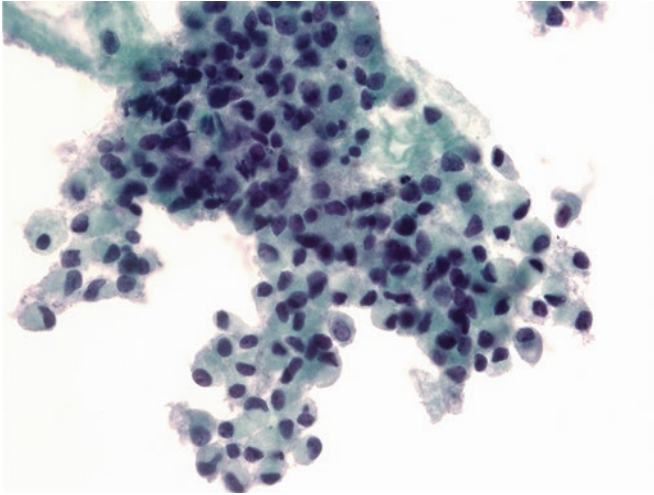


Fig. 6.26 Aspirate sample of a SPN on an alcohol-fixed Papanicolaou-stained preparation showing ovoid nuclei, irregular nuclear contours, nuclear grooves, and delicate cytoplasm

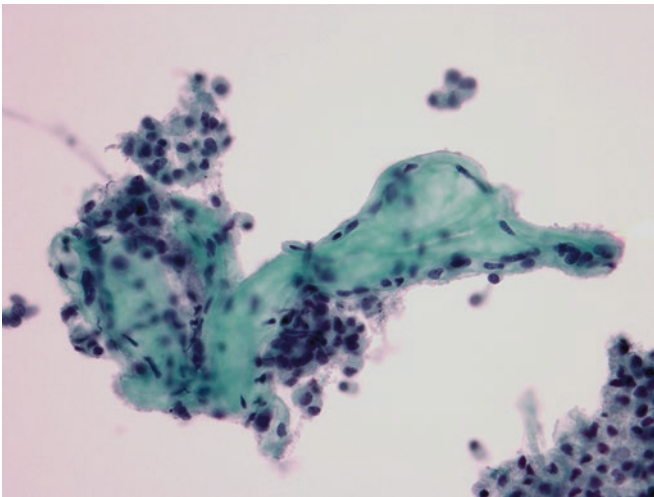


Fig. 6.27 Aspirate sample of an SPN on a Papanicolaou-stained liquid-based preparation (ThinPrep) showing the central capillary and stroma and an outer layer of cells

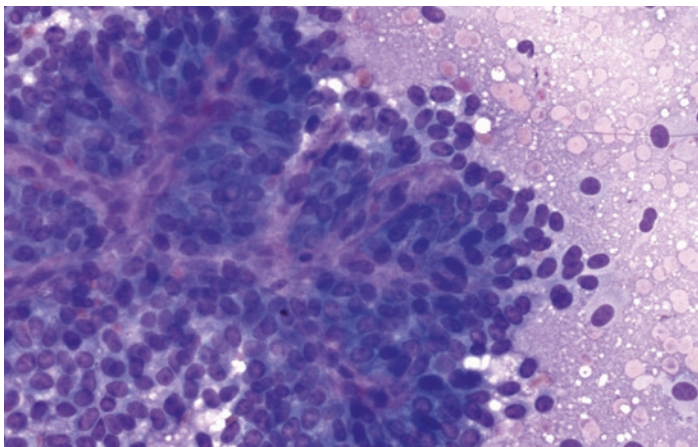


Fig. 6.28 Aspirate sample of a SPN on an air-dried Diff-Quik preparation showing a central vascular core of capillary admixed with myxoid stroma and an outer lining of tumor cells

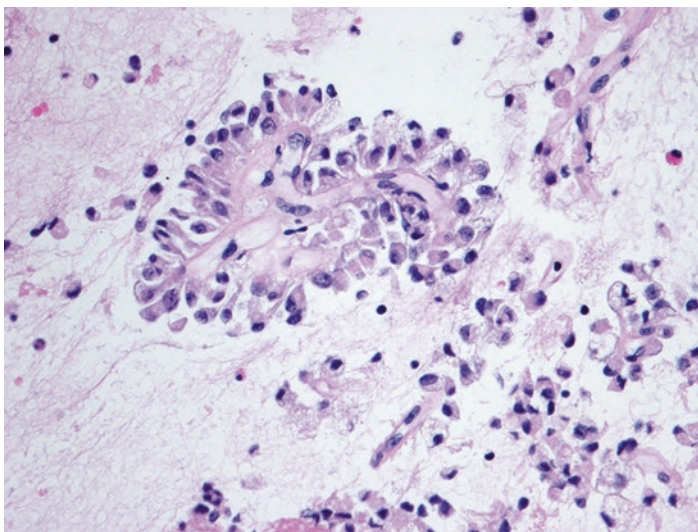


Fig. 6.29 SPN on aspirate sample with cell block preparation shows single cells as well as pseudopapillary structure

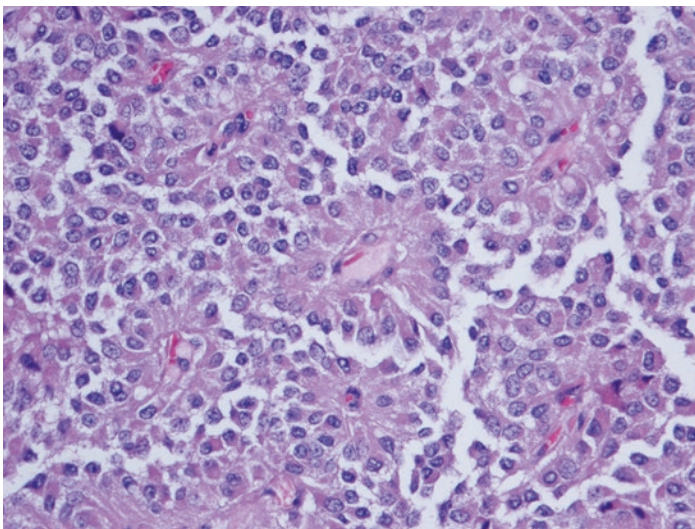


Fig. 6.30 H&E stained slide from SPN surgical resection specimen shows pseudopapillary structures

- Stromal hyalinization may be seen in some cases.
- PAS-positive hyaline globules are often observed in the extracellular space [4] (Fig. 6.31).

Differential Diagnosis

The differential diagnosis for SPN includes PNET, ACC, PB, as well as IPMN. Like IPMN, SPN may form cysts and papillary structures. However, it is important not to confuse myxoid stroma in SPN with the thick extracellular mucin observed in IPMN (see Chap. 2). In contrast to SPN, neoplastic cells in IPMNs are more often columnar, contain intracellular mucin, and may show greater degrees of nuclear pleomorphism [3, 29].

Please refer to Table 6.2 for review of key cytomorphologic features and molecular alterations and Table 6.3 for review of key ancillary studies including immunohistochemical profiles that separate SPN from other solid pancreatic non-ductal neoplasia.

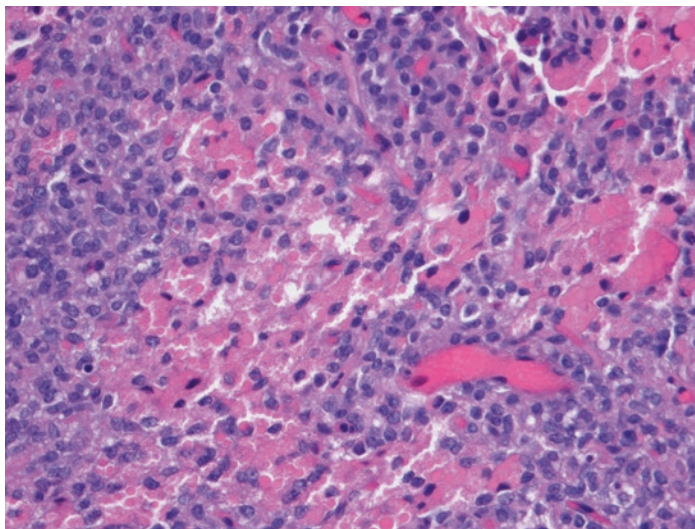


Fig. 6.31 H&E stained slide from SPN surgical resection specimen showing solid areas with occasional hyaline globules (PAS-positive diastase resistant)

It is worth emphasizing that SPN often show positive staining for synaptophysin and CD56, a fact which underlines the importance of utilizing a panel of immunohistochemical markers when considering this differential diagnosis.

Clinical Management

The prognosis for SPN is good even when metastatic disease is present. The treatment for SPN is surgical excision [3, 5, 26, 28, 30].

References

1. Bosman FT, Carneiro F, Hruban RH, Theise ND, editors. WHO classification of tumors of the digestive system. Lyon: IARC; 2010.
2. Sigel CS. Advances in the cytologic diagnosis of gastroenteropancreatic. *Cancer Cytopathol.* 2018. Epub ahead of print. Available from: <https://onlinelibrary.wiley.com/doi/full/10.1002/ency.22073>.

3. Chhieng DC, Stelow EB. *Pancreatic cytopathology*. New York: Springer; 2007.
4. Odze RD, Goldblum JR. *Surgical pathology of the GI tract, liver, biliary tract, and pancreas*. Philadelphia: Saunders/Elsevier; 2015.
5. Bellizzi AM, Stelow EB. Pancreatic cytopathology: a practical approach and review. *Arch Pathol Lab Med*. 2009;133(3):388–404.
6. Shah S, Morteale KJ. Uncommon solid pancreatic neoplasms: ultrasound, computed tomography, and magnetic resonance imaging features. *Semin Ultrasound CT MR*. 2007;28(5):357–70.
7. Milan SA, Yeo CJ. Neuroendocrine tumors of the pancreas. *Curr Opin Oncol*. 2012;24(1):46–55.
8. Jahan A, Yusuf MA, Loya A. Fine-needle aspiration cytology in the diagnosis of pancreatic neuroendocrine tumors: a single-center experience of 25 cases. *Acta Cytol*. 2015;48(3):163–8.
9. Inzani F, Petrone G, Rindi G. The New World Health Organization classification for pancreatic neuroendocrine neoplasia. *Endocrinol Metab Clin N Am*. 2018;47(3):463–70.
10. Jiménez-Heffernan JA, Vicandi B, López-Ferrer P, González-Peramato P, Pérez-Campos A, Viguer JM. Fine needle aspiration cytology of endocrine neoplasms of the pancreas. Morphologic and immunocytochemical findings in 20 cases. *Acta Cytol*. 2004;48(3):295–301.
11. Gu M, Ghafari S, Lin F, Ramzy I. Cytological diagnosis of endocrine tumors of the pancreas by endoscopic ultrasound-guided fine-needle aspiration biopsy. *Diagn Cytopathol*. 2005;32(4):204–10.
12. Labate AM, Klimstra DL, Zakowski MF. Comparative cytologic features of pancreatic acinar cell carcinoma and islet cell tumor. *Diagn Cytopathol*. 1997;16(2):112–6.
13. Paschalis C, Charitini S, Panagiotis K, Ioannis K, Stratigoula S, Irini D. Endoscopic ultrasound-guided fine-needle aspiration cytology of pancreatic neuroendocrine tumors: a study of 48 cases. *Cancer Cytopathol*. 2008;114(4):255–62.
14. Wood LD, Klimstra DS. Pathology and genetics of pancreatic neoplasms with acinar differentiation. *Semin Diagn Pathol*. 2014;31(6):491–7.
15. La Rosa S, Adsay V, Albarello L, Asioli S, Casnedi S, Franzi F, et al. Clinicopathologic study of 62 acinar cell carcinomas of the pancreas: insights into the morphology and immunophenotype and search for prognostic markers. *Am J Surg Pathol*. 2012;36(12):1782–95.
16. Serra S, Chetty R. Revision 2: an immunohistochemical approach and evaluation of solid pseudopapillary tumour of the pancreas. *J Clin Pathol*. 2008;61(11):1153–9.
17. La Rosa S, Sessa F, Capella C. Acinar cell carcinoma of the pancreas: overview of clinicopathologic features and insights into the molecular pathology. *Front Med (Lausanne)*. 2015;2(41). Available from: <https://www.ncbi.nlm.nih.gov/pmc/articles/PMC4469112/>.
18. Simmons S, Eltoum IA. Acinar cell carcinoma of the pancreas: cytologic, immunohistochemical, and ultrastructural features. *Pathol Case Rev*. 2015;20(4):192–5.

19. Stelow EB, Bardales RH, Shami VM, Woon C, Presley A, Mallery S, et al. Cytology of pancreatic acinar cell carcinoma. *Diagn Cytopathol.* 2006;34(4):367–72.
20. Das S, Ghosh R, Sen A, Das RN, Saha K, Chatterjee U. Fine needle aspiration cytology diagnosis of a pancreatoblastoma in an infant: case report with a summary of prior published cases. *Cytopathology.* 2016;27(6):479–82.
21. Klimstra DS, Wenig BM, Adair CF, Heffess CS. Pancreatoblastoma. A clinicopathologic study and review of the literature. *Am J Surg Pathol.* 1995;19(12):1371–89.
22. Sidhu GS, Cassai ND, Yang GCH. Fine-needle aspiration cytology of pancreatoblastoma in a young woman: report of a case and review of the literature. *Diagn Cytopathol.* 2005;33(4):258–62.
23. Henke AC, Kelley CM, Jensen CS, Timmerman TG. Fine-needle aspiration cytology of pancreatoblastoma. *Diagn Cytopathol.* 2001;25(2):118–21.
24. Pitman MB, Faquin WC. The fine-needle aspiration biopsy cytology of pancreatoblastoma. *Diagn Cytopathol.* 2004;31(6):402–6.
25. Huang HL, Shih SC, Chang WH, Wang TE, Chen MJ, Chan YJ. Solid-pseudopapillary tumor of the pancreas: clinical experience and literature review. *World J Gastroenterol.* 2005;11(9):1403–9.
26. Ersen A, Agalar AA, Ozer E, Agalar C, Unek T, Egeli T, et al. Solid-Pseudopapillary neoplasm of the pancreas: a clinicopathological review of 20 cases including rare examples. *Pathol Res Pract.* 2016;212(11):1052–8.
27. Salvia R, Bassi C, Festa L, Falconi M, Crippa S, Butturini G, et al. Clinical and biological behavior of pancreatic solid pseudopapillary tumors: report on 31 consecutive patients. *J Surg Oncol.* 2007;95(4):304–10.
28. Vassos N, Agaimy A, Klein P, Hohenberger W, Croner RS. Solid-pseudopapillary neoplasm (SPN) of the pancreas: case series and literature review on an enigmatic entity. *Int J Clin Exp Pathol.* 2013;6(6):1051–9.
29. Bardales RH, Centeno B, Mallery JS, Lai R, Pochapin M, Guiter G, Stanley MW. Endoscopic ultrasound-guided fine-needle aspiration cytology diagnosis of solid-pseudopapillary tumor of the pancreas: a rare neoplasm of elusive origin but characteristic cytomorphologic features. *Am J Clin Pathol.* 2004;121(5):654–62.
30. Papavramidis T, Papavramidis S. Solid pseudopapillary tumors of the pancreas: review of 718 patients reported in English literature. *J Am Coll Surg.* 2005;200(6):965–72.
31. Klimstra DS, Adsay V. Acinar neoplasms of the pancreas-A summary of 25 years. *Semin Diagn Pathol.* 2016;33(5):307–18.
32. Lin F, Chen ZE, Wang HL. Utility of immunohistochemistry in the pancreaticobiliary tract. *Arch Pathol Lab Med.* 2015;139(1):24–38.
33. Ohara Y, Oda T, Hashimoto S, Akashi Y, Miyamoto R, Enomoto T, Satomi K. Pancreatic neuroendocrine tumor and solid-pseudopapillary neoplasm: key immunohistochemical profiles for differential diagnosis. *World J Gastroenterol.* 2016;22(38):8596–604.



Intraductal Papillary Mucinous Neoplasms

Lorene Yoxtheimer and Abha Goyal

Introduction

With ever-increasing use of cross-sectional abdominal imaging, there has been a rise in the number of asymptomatic pancreatic cysts that are detected incidentally, the management of which poses a major issue. In a series of 2832 consecutive outpatients who underwent multidetector computed tomography (MDCT) scan for nonpancreatic causes, the prevalence of pancreatic cysts was found to be 2.6% [1]. In another study of 2803 individuals, de Jong et al. reported the prevalence of pancreatic cysts to be 2.4% on magnetic resonance imaging (MRI) [2]. Lee et al. reported the prevalence of incidentally detected pancreatic cysts on MRI to be 13.5% [3]. In all the above series, the prevalence of pancreatic cysts correlated with increasing age.

The most common cysts of the pancreas include nonneoplastic pseudocysts and neoplastic cysts, i.e., intraductal papillary mucinous neoplasms (IPMNs), serous cystadenomas (SCAs), and

L. Yoxtheimer · A. Goyal (✉)

Department of Pathology and Laboratory Medicine, Weill-Cornell Medicine, New York Presbyterian Hospital, New York, NY, USA
e-mail: abg9017@med.cornell.edu

mucinous cystic neoplasms (MCNs). A large proportion of the asymptomatic pancreatic cysts that are detected on imaging are believed to comprise of branch duct IPMNs [4].

IPMNs and MCNs are considered premalignant lesions that can demonstrate atypia ranging from low-grade dysplasia to invasive carcinoma. The goal of preoperative diagnostic procedures is primarily to differentiate between nonmucinous cysts (SCAs and pseudocysts) and premalignant neoplastic mucinous cysts (IPMNs and MCNs) that may require continued surveillance or resection. This chapter discusses the clinical, imaging, and pathologic features, molecular genetics, and management aspects of IPMNs.

Clinical Features

IPMNs are more common in the elderly, the median age at diagnosis being 66 years. Though traditionally they have been considered to be more common in men, multiple prevalence studies for pancreatic cysts (including surgical series) have reported no significant difference in terms of gender [1–5].

Most of the IPMNs that are diagnosed these days are detected incidentally and are asymptomatic. However, they may present with symptoms such as abdominal pain, weight loss, acute pancreatitis, and jaundice. In a series of 454 resected IPMNs, the prevalence of diabetes mellitus among the patients was 34%. Preoperative diabetes mellitus has been found to be associated with a significantly increased risk for high-grade dysplasia and invasive carcinoma that is independent of cyst size and pancreatic duct dilatation [6].

Imaging Findings

As per the 2017 revision of international consensus Fukuoka guidelines, cysts of the pancreas that are greater than 5 mm in size should be evaluated by a pancreatic protocol CT scan or a gadolinium-enhanced MRI with MRCP (magnetic resonance

cholangiopancreatography) [7]. MRI/MRCP may be preferred over CT scan for its higher spatial and contrast resolution, its ability to determine communication of the cyst with the main duct, an increased sensitivity for detecting intramural nodules, and lack of ionizing radiation [8].

Endoscopic modalities can assist further in characterizing pancreatic cysts. Upper endoscopy occasionally reveals a “fish mouth” patulous papilla extruding mucin that is characteristic of an IPMN with main duct involvement. Endoscopic ultrasound (EUS) is comparable to or better than MRI/MRCP because it permits detailed evaluation of the architecture of the cysts, including wall thickness, septa, and mural nodules. In addition, EUS offers the capability to perform fine needle aspiration (FNA) for cyst fluid analysis [9]. Contrast-enhanced harmonic EUS has better ability to discriminate between mural nodules from mucous clots in IPMNs [10]. But the test is invasive, operator-dependent, and less available as compared to the cross-sectional imaging studies. In most situations in clinical practice, EUS is not the initial imaging modality for evaluating pancreatic cysts; rather it is complementary to CT/MRI.

IPMNs can be subdivided into branch duct IPMN (BD-IPMN) with cystic dilatation of one or more branch ducts without macroscopic or microscopic involvement of the main duct, main duct IPMN (MD-IPMN) with main duct involvement only, and mixed- or combined-type IPMN with involvement of both the main duct and the branch ducts.

Radiologically, as per the Fukuoka guidelines, MD-IPMNs are defined as segmental or diffuse dilation of the main duct >5 mm in the absence of other causes of obstruction. BD-IPMNs are cysts >5 mm in size that are not associated with the dilation of main duct but communicate with it. They are frequently located in the uncinate process although they can occur anywhere in the pancreas. On imaging, they appear as a cluster of small cysts with lobulated margins or as a single, unilocular cystic lesion. Complex features include thick enhancing wall, septa, and mural nodules. Mixed-type IPMNs exhibit features of both MD-IPMN and BD-IPMN.

The mean frequency of invasive carcinoma in resected MD-IPMN is high, i.e., 61.6%. In contrast, resected BD-IPMNs have

a much smaller risk of malignancy—mean of 25.5% [11]. Recent evidence indicates that the risk of invasive carcinoma in mixed-type IPMNs is more than BD-IPMNs but less than MD-IPMNs and may depend on the degree of involvement of the main duct [4].

Pathologic Features

Gross Findings

IPMNs are characterized by a grossly visible (≥ 1.0 cm) lesion in the main pancreatic duct and/or its branches. MD-IPMNs are associated with diffuse or segmental dilatation of the main duct. BD-IPMNs form multicystic grapelike structures and are commonly located in the uncinate process of the pancreas. When associated with an invasive carcinoma, the invasive component may result in irregularly thickened cyst walls or nodules. Colloid carcinoma can form gelatinous stromal masses. Extensive histologic sampling of IPMNs is essential to exclude an invasive component [12].

Histology

The epithelium of the IPMNs can be flat or it can form papillae with fibrovascular cores. Based on the highest degree of architectural and cytologic atypia, the epithelial dysplasia is graded as low, intermediate, and high. Low-grade dysplasia reveals a single layer of cells with small nuclei and minimal cytologic atypia (Fig. 7.1). Intermediate-grade dysplasia shows nuclear stratification with crowding and loss of polarity (Fig. 7.2). High-grade dysplasia is characterized by marked architectural and cytologic atypia with complex branching papillae or cribriform growth pattern. Nuclei tend to be hyperchromatic, pleomorphic, and stratified (Fig. 7.3). Mitotic figures are frequent.

Four distinct histologic subtypes of IPMNs are recognized based on the type of epithelial lining: gastric, intestinal, pancreatobiliary, and oncocytic. If more than one type of lining epithelium is identified, the categorization is based on the predominant subtype. The gastric-type is frequently seen in BD-IPMNs and reveals columnar mucinous cells resembling gastric foveolar-type epithelium. Majority of the BD-IPMNs are associated with

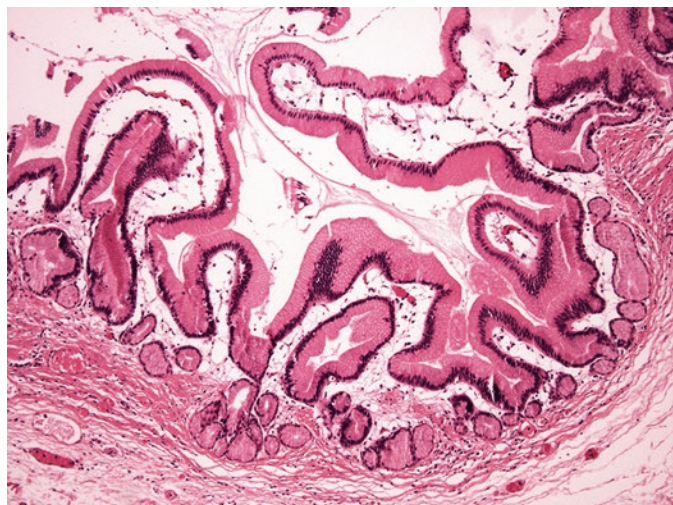


Fig. 7.1 Intraductal papillary mucinous neoplasm with low-grade dysplasia with gastric-type foveolar epithelium with abundant cytoplasm and basally located nuclei (hematoxylin-eosin, 200 \times)

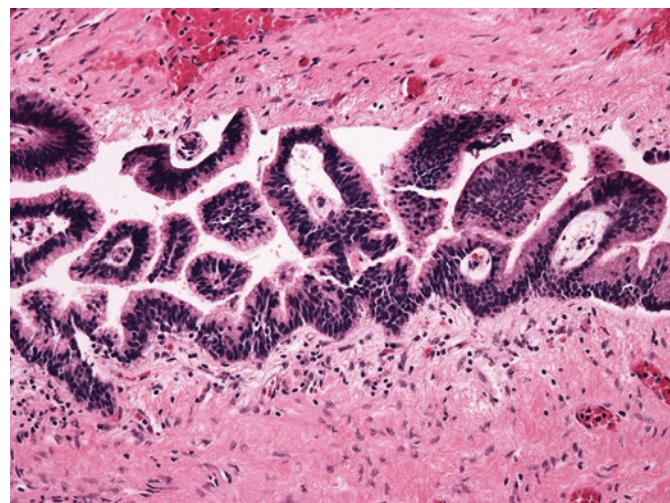


Fig. 7.2 Intraductal papillary mucinous neoplasm with intermediate-grade dysplasia with nuclear stratification with crowding and loss of polarity (hematoxylin-eosin, 200 \times)

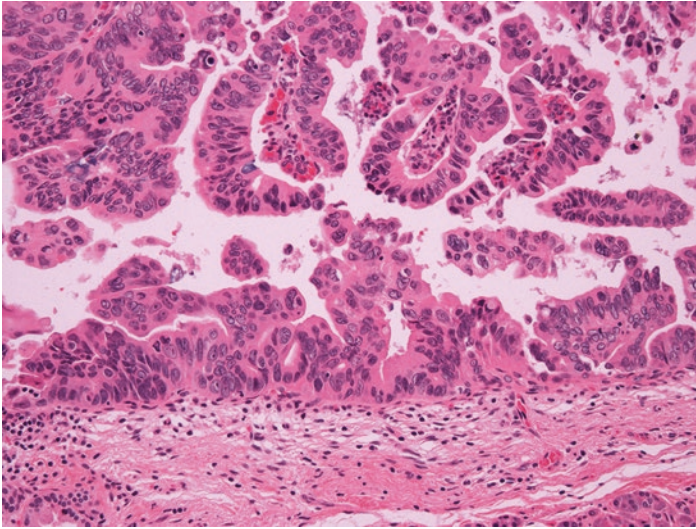


Fig. 7.3 Intraductal papillary mucinous neoplasm with high-grade dysplasia with marked architectural and cytologic atypia. Nuclei are hyperchromatic, pleomorphic, and stratified (hematoxylin-eosin, 400 \times)

low-grade dysplasia. The invasive component when present in the gastric-type IPMNs is of the tubular type that is morphologically similar to pancreatic ductal adenocarcinoma (Fig. 7.4).

The intestinal type IPMN is mainly seen in MD-IPMNs. The epithelium shows tall columnar cells with stratified cigar-shaped nuclei. It usually exhibits intermediate- to high-grade dysplasia. The invasive carcinoma that is usually seen in this type is colloid carcinoma. Colloid carcinomas have a more favorable prognosis as compared to the tubular-type.

The pancreatobiliary type of IPMN is the least common type. It usually involves the main duct and shows high-grade dysplasia. The cells tend to be cuboidal with moderate amounts of cytoplasm with significant nuclear atypia. The invasive component is of the tubular-type that behaves aggressively.

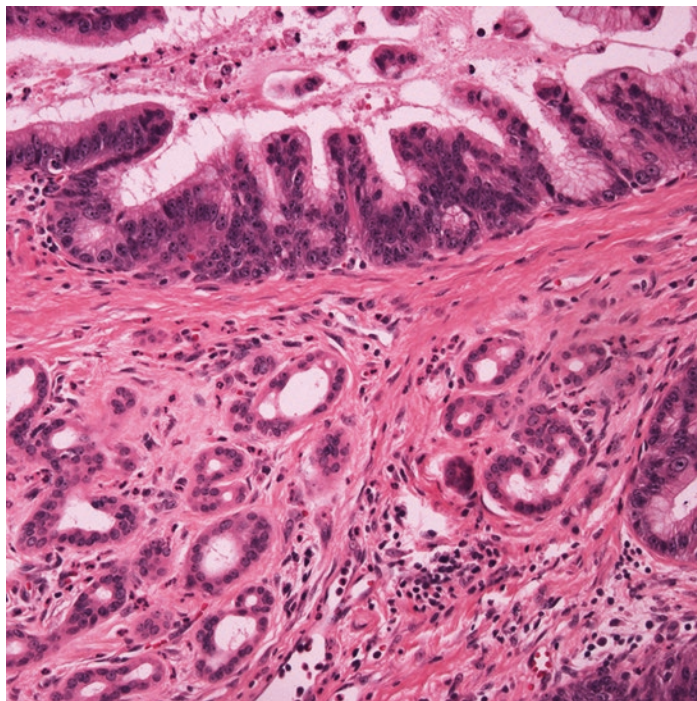


Fig. 7.4 Intraductal papillary mucinous neoplasm with high-grade dysplasia with associated invasive carcinoma (tubular type). The carcinoma is indistinguishable from a pancreatic ductal adenocarcinoma (hematoxylin-eosin, 400 \times)

The oncocytic type is infrequent. It typically involves the main duct and is associated with high-grade dysplasia and/or invasive carcinoma. It features complex arborizing papillae with cuboidal to columnar cells with oncocytic cytoplasm and enlarged, round nuclei with prominent nucleoli. The invasive carcinoma is of the oncocytic type which has a favorable prognosis [4, 12].

Cytology

The two important questions that the cytologist has to answer upon the evaluation of a pancreatic cyst are: is the cyst mucinous and is there any high-grade epithelial atypia or worse. The overall accuracy of cytology in diagnosing mucinous cysts is limited—around 50–58% [13, 14]. The cytology specimen shows variable amounts of extracellular thick mucin and/or neoplastic mucinous epithelium. Thick, colloid-like mucin is diagnostic of a neoplastic mucinous cyst, even in the absence of lesional epithelium. The presence of degenerated cells within the mucin is also supportive of a mucinous neoplasm (Fig. 7.5). On liquid-based preparations, the mucin may get attenuated and be challenging to differentiate from gastrointestinal tract contamination (Fig. 7.6).

The lining epithelium may exhibit varying degrees of dysplasia and the cytology sample may not be representative of the

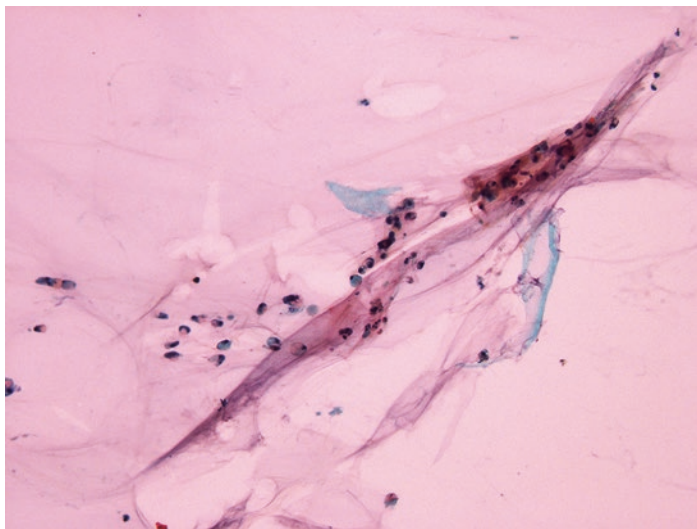


Fig. 7.5 Fine needle aspiration of an intraductal papillary mucinous neoplasm reveals thick colloid-type mucin. The presence of degenerated cells in the mucin supports its derivation from a neoplasm (Papanicolaou stain, 200 \times)

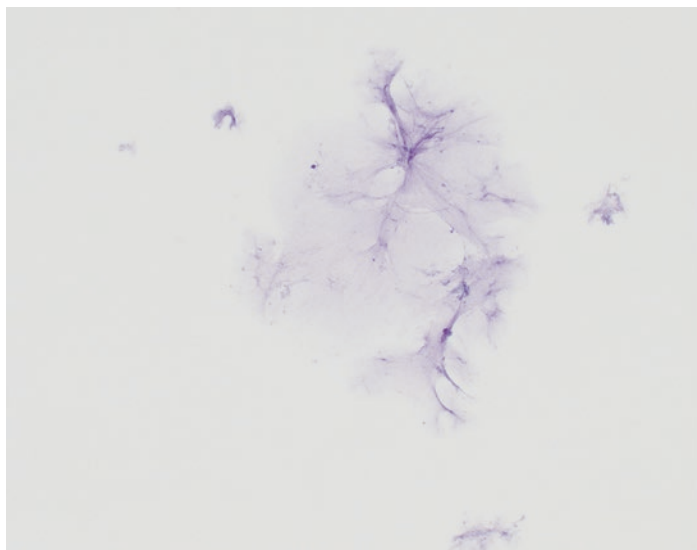


Fig. 7.6 Fine needle aspiration of an intraductal papillary mucinous neoplasm. The mucin gets attenuated and more difficult to reliably identify on liquid-based preparations (ThinPrep, Papanicolaou stain, 200 \times)

severity of dysplasia in the lesion. The concept of cytology as a predictor of the grade of dysplasia and/or invasive carcinoma for pancreatic mucinous neoplasms has developed over time. Layfield and Cramer reported that an increasing degree of nuclear atypia, nuclear molding, prominence of nucleoli, nuclear irregularity, and cell crowding are associated with a higher grade of dysplasia/invasive carcinoma in pancreatic mucinous neoplasms [15]. Stelow et al. showed that cytologic features such as nuclear crowding, loss of nuclear uniformity, chromatin abnormalities, and nucleolar prominence became more pronounced in mucinous neoplasms with an increasing grade of dysplasia. They identified necrotic material only in cases with significant cytologic atypia or frank malignancy [16]. Michaels et al. reported that cytologic features could be used to predict the histologic grade of a mucinous neoplasm in many instances. They showed that tight epithelial clusters with hyperchromatic nuclei and a high

nuclear-cytoplasmic ratio were significantly associated with at least moderate dysplasia. Pale nuclei with parachromatin clearing and significant background inflammation correlated with at least carcinoma in situ, while necrosis was significantly associated with invasion [17]. Subsequent to these studies, Pitman et al. demonstrated that high-grade atypical epithelial cells that were qualitatively and quantitatively insufficient for a malignant diagnosis or “positive” cytology were a more sensitive and accurate predictor of high-grade dysplasia [18].

Given the considerable significance of high-grade epithelial atypia in pancreatic cyst aspirates, what is a good approach to qualify this atypia? The Papanicolaou Society of Cytopathology (Pap Society) has recommended a two-tiered approach of low-grade and high-grade for characterizing the atypia in pancreatic mucinous cysts on EUS-FNA. Low-grade atypia on cytology encompasses the atypia associated with low-grade and intermediate-grade dysplasia, whereas high-grade atypia correlates with at least high-grade dysplasia in most instances [19]. An international interobserver concordance study has shown better agreement for grading atypia with a two-tiered approach [20].

Low-grade dysplasia is characterized by cells with abundant mucinous cytoplasm, low nuclear-cytoplasmic ratio, and fine nuclear chromatin (Fig. 7.7). It can be difficult to ascertain if this epithelium is derived from a mucinous neoplasm or if it is a gastric contaminant. Intranuclear cytoplasmic inclusions have been identified as a specific morphologic feature that can be seen in up to a third of low-grade IPMNs but are absent in gastric foveolar epithelium (Fig. 7.8) [21].

High-grade dysplasia is often seen as tight epithelial clusters or singly lying cells with high nuclear-cytoplasmic ratio and abnormal chromatin distribution (Fig. 7.9). They may also show irregular nuclear membranes. The cytologic criteria for the recognition of high-grade epithelial atypia have been better defined recently, the most accurate being the presence of background necrosis, chromatin pattern changes, and an increased nuclear-cytoplasmic ratio (Fig. 7.10) [22]. Intermediate-grade dysplasia shows cytologic features that fall in between those of low-grade and high-grade dysplasia (Fig. 7.11). At times, intermediate-grade

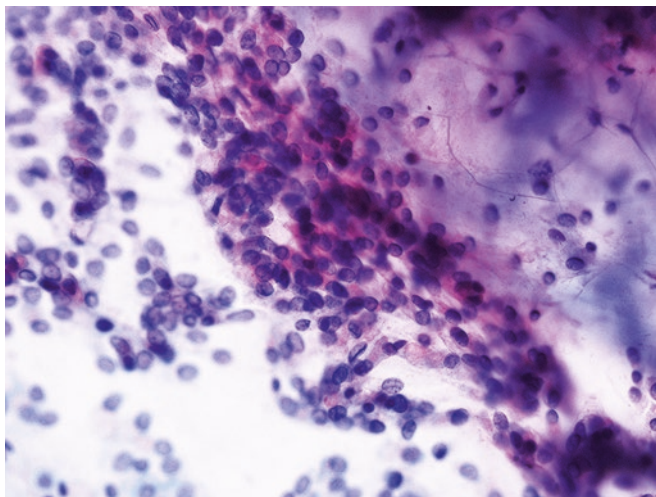


Fig. 7.7 Low-grade dysplasia in intraductal papillary mucinous neoplasm on cytologic preparations reveals cells with abundant mucinous neoplasm and fine chromatin. The nuclei may exhibit grooves (Papanicolaou stain, 400 \times)

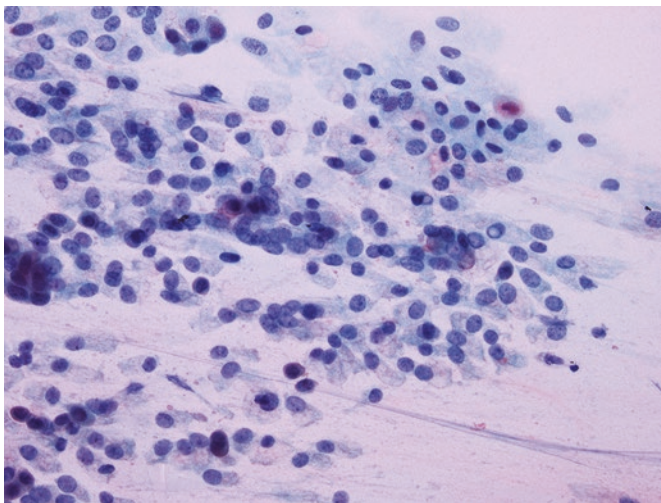


Fig. 7.8 Intranuclear cytoplasmic inclusions have been found be associated with neoplastic mucinous epithelium in pancreatic cyst aspirates (Papanicolaou stain, 400 \times)

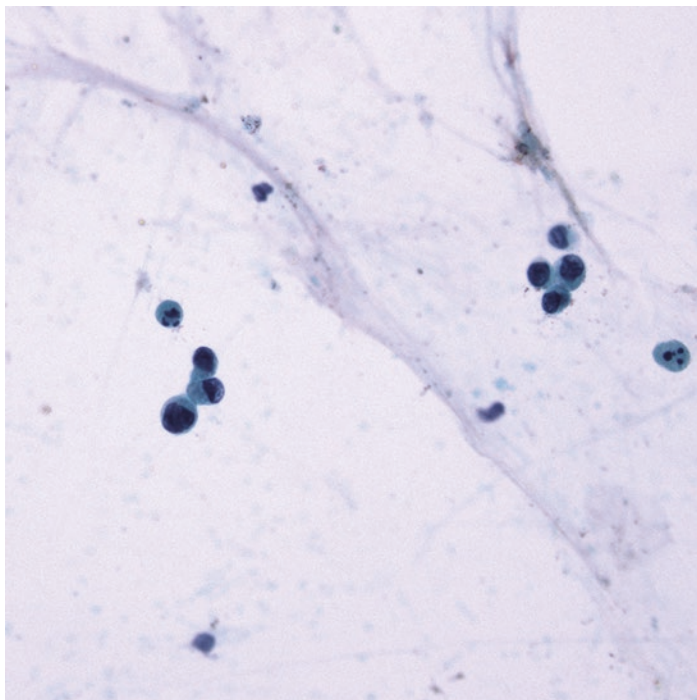


Fig. 7.9 High-grade dysplasia in intraductal papillary mucinous neoplasms on cytologic preparations reveals singly lying cells or cells in small groups with high nuclear-cytoplasmic ratio and abnormal chromatin distribution (Papanicolaou stain, 400 \times)

dysplasia may be difficult to distinguish from high-grade dysplasia on cytology [18].

After the publication of the Pap Society guidelines for reporting of pancreatobiliary cytology, some studies have evaluated the interobserver variability in grading atypia in neoplastic mucinous cysts on cytology. In a study of 54 cases, Sigel et al. demonstrated fair interobserver agreement for grading mucinous neoplasms and low interobserver agreement for identifying neoplastic mucin [23]. In a study of 20 cases, Goyal and colleagues showed that the

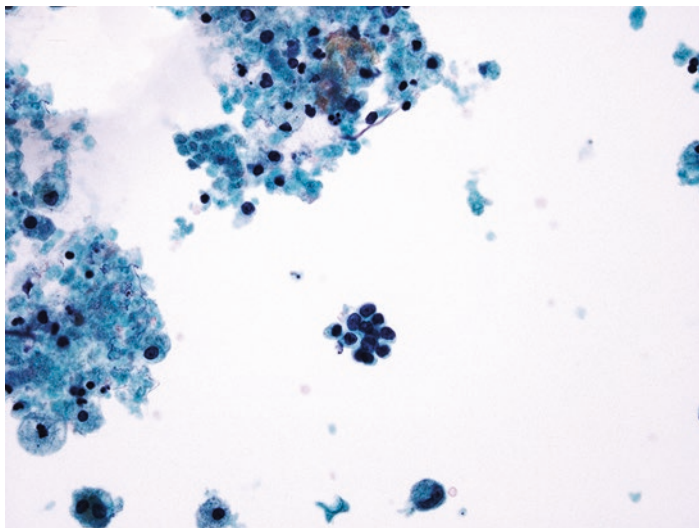


Fig. 7.10 Cytologic high-grade epithelial atypia in pancreatic mucinous cysts is characterized by high nuclear-cytoplasmic ratio, abnormal chromatin distribution, and background necrosis (Papanicolaou stain, 200 \times)

cytologic recognition of high-grade dysplasia or worse as high-grade atypia in pancreatic mucinous cysts has a good degree of interobserver reproducibility among cytopathologists. However, the cytologic recognition of low-grade and intermediate-grade dysplasia as low-grade atypia appeared to be problematic with a lack of agreement [24].

Microforceps Pancreatic Cyst Biopsy

A novel cyst wall tissue sampling technique has shown promise in procuring histologic samples for pathologic diagnosis. It is the Moray microforceps biopsy device (US Endoscopy, Mentor, Ohio) that enables the sampling from cysts that can be accessed with a 19-gauge EUS-FNA needle. The microforceps biopsy

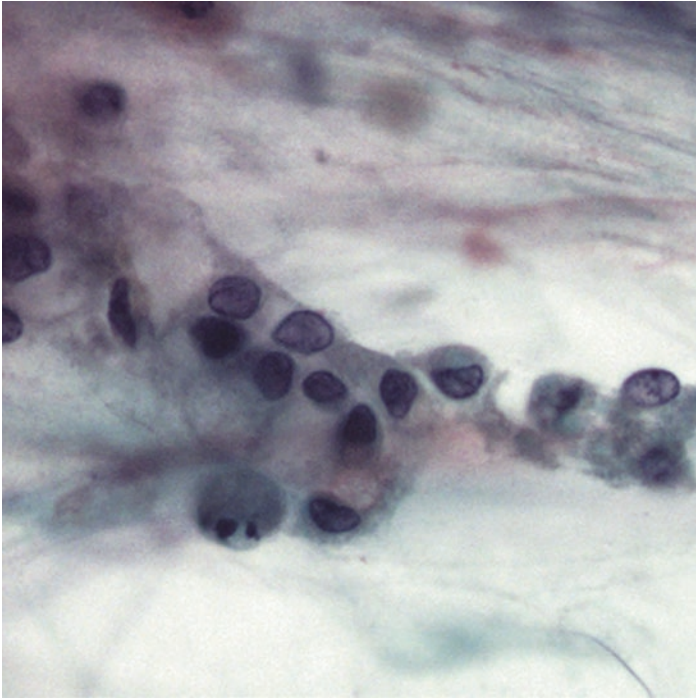


Fig. 7.11 Intermediate-grade dysplasia can be problematic to accurately classify on cytology. The cytologic features are in between that of low-grade and high-grade dysplasia (Papanicolaou stain, 400 \times)

device is introduced through the 19-gauge EUS-FNA needle to obtain histologic samples from the cyst wall, septations, nodules, or adjacent masses. A multicenter study involving 42 patients who underwent both EUS-FNA and microforceps biopsy showed that the cytologic analysis of cyst fluid and microforceps biopsy were comparable in distinguishing mucinous and nonmucinous cysts and in detecting high-risk cysts. However, microforceps biopsy was far superior to cytology in terms of providing a specific cyst diagnosis (Fig. 7.12) [25].

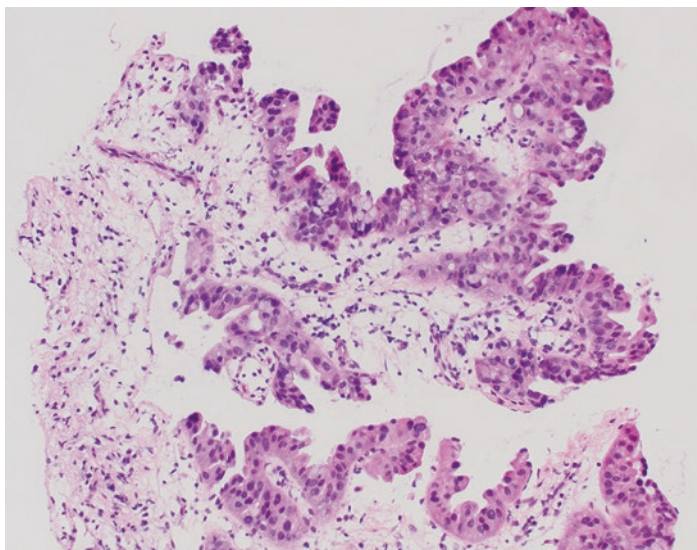


Fig. 7.12 Microforceps biopsy of intraductal papillary mucinous neoplasm reveals oncocytic-type epithelium with high-grade dysplasia (hematoxylin-eosin, 400 \times)

Cyst Fluid Biochemistry

Carcinoembryonic antigen (CEA) is the most commonly used cyst fluid marker for distinction between mucinous and nonmucinous cysts. In 2004, a multicenter prospective study demonstrated that cyst fluid concentration of CEA alone was more accurate than a combination of EUS morphology, cytology, and other tumor markers (CEA, CA 72-4, CA 125, CA 19-9, and CA 15-3). At a cutoff value of 192 ng/mL, the cyst fluid CEA demonstrated a sensitivity of 73%, a specificity of 84%, and an accuracy of 79% for diagnosis of pancreatic mucinous cysts [26]. A 2011 study reported that a CEA cutoff value of 109.9 ng/ml is more accurate

(86%) in the diagnosis of a mucinous cyst. At this value, CEA had a sensitivity of 81% and a specificity of 98%. CEA levels, however, cannot distinguish between benign cysts and those with high-grade dysplasia or invasive carcinoma [27]. The cut-off value may vary among different laboratories. Approximately, 0.2–1.0 mL of cyst fluid is needed to run the test [28].

Cyst fluid amylase levels do not help distinguish between an IPMN and a mucinous cystic neoplasm [29].

Molecular Genetics

Somatic mutations of *KRAS* gene are found in 30–80% of IPMNs. *GNAS* oncogene somatic mutations are found in greater than 60% of IPMNs and are more frequent in intestinal-type IPMN. Somatic mutations in *RNF43*, a gene encoding an E3 ubiquitin ligase, are detected in 75% of IPMNs. *TP53* mutations can be seen in foci of high-grade dysplasia. Loss of *p16* expression can be seen in both noninvasive and invasive components. Loss of *SMAD4* expression occurs more frequently in invasive carcinomas associated with IPMN [30].

GNAS testing is a highly specific test for IPMNs with most studies reporting 100% specificity of *GNAS* mutation for the diagnosis of IPMN [31, 32]. Only rare instances of *GNAS* mutation in other pancreatic cysts (including two serous cystadenomas and one pseudocyst) have been reported [33, 34]. The combination of *KRAS* and *GNAS* mutation analyses has shown a high sensitivity for the diagnosis of IPMNs. Singhi and colleagues found that with the combination of *GNAS* and *KRAS* testing, mutation in either gene had 84% sensitivity and 98% specificity for IPMNs [31]. A recent multicenter study involving 94 IPMNs revealed that 91% of IPMN samples had a mutation in *KRAS* or *GNAS*, and 47% had a mutation in both genes [35].

Molecular analysis of limited samples is revolutionizing the classification and risk stratification of pancreatic cysts. Jones and colleagues showed that next-generation sequencing of pancreatic cyst fluid can provide valuable information regarding the nature of the cyst and its risk of malignancy. A cyst was defined as mucinous

based on the presence of *KRAS* or *GNAS* mutations even when the CEA was low. *TP53* mutation or loss of *CDKN2A* or *SMAD4* helped in the identification of high-risk cysts [36]. miRNAs also hold promise as biomarkers for characterization of pancreatic cysts. Matthaei et al. showed that a logistic regression model using nine miRNAs could differentiate between cysts requiring resection (high-grade IPMNs, pancreatic neuroendocrine tumors, and solid pseudopapillary neoplasms) and cysts that are managed conservatively (low-grade IPMNs and serous cystadenomas) with a sensitivity of 89% and a specificity of 100% [37].

Management

The 2017 revisions of international consensus Fukuoka guidelines for the management of IPMNs define certain parameters for the risk stratification of these neoplasms. *High-risk stigmata* are considered as obstructive jaundice in a patient with a cystic lesion of the pancreatic head, enhanced mural nodule ≥ 5 mm, and MPD size of ≥ 10 mm. All cysts with *high-risk stigmata* should be resected in surgically fit patients. *Worrisome features* are defined as cyst size of ≥ 3 cm, enhancing mural nodule < 5 mm, thickened enhanced cyst walls, MPD size of 5–9 mm, abrupt change in the MPD caliber with distal pancreatic atrophy, lymphadenopathy, an elevated serum level of carbohydrate antigen (CA)19–9, and a rapid rate of cyst growth ≥ 5 mm/2 years. As per these guidelines, all cysts with *worrisome features* should undergo EUS for further evaluation. If on EUS, the cyst shows a definite mural nodule ≥ 5 mm in size or exhibits main duct features suspicious for involvement or has a cytology diagnosis of high-grade dysplasia or worse, surgical resection should be considered if clinically appropriate. If no *worrisome features* are present, surveillance is recommended based on the size of the lesion.

BD-IPMNs often occur in elderly patients and are associated with a relatively low (1.4–6.9%) annual rate of progression to high-grade dysplasia or invasive carcinoma. As a result, these lesions should be conservatively followed unless they exhibit features that predict high-grade dysplasia or invasive carcinoma. As per

the 2017 international consensus guidelines for management of IPMNs, the absolute indications for the resection of a BD-IPMN are cytology with high-grade dysplasia or worse or the presence of a mural nodule ≥ 5 mm in size. The cutoff for the size of mural nodule at 5 mm meets acceptable sensitivity and specificity for the detection of high-grade dysplasia or invasive carcinoma. Cyst size alone is not considered an appropriate indication of surgery. The indications for surgical resection also depend upon the patient's age, comorbidities, and location of the cyst. BD-IPMNs that lack *high-risk stigmata* and *worrisome features* (as previously defined) should be monitored for stability by short interval (3–6 months) imaging, if prior studies are unavailable [11].

The American Gastroenterological Association (AGA) also published guidelines regarding the diagnosis and management of asymptomatic neoplastic pancreatic cysts in 2015. The salient aspects of these guidelines include that patients with pancreatic cysts < 3 cm without a solid component or a dilated pancreatic duct should undergo MRI for surveillance in 1 year and then every 2 years for a total of 5 years if there is no change in size or characteristics. The AGA suggests against continued surveillance of pancreatic cysts if there has been no significant change in the characteristics of the cyst after 5 years of surveillance or if the patient is no longer a surgical candidate. Pancreatic cysts with at least two high-risk features (size ≥ 3 cm, a dilated main pancreatic duct, or the presence of an associated solid component) should be examined with EUS-FNA. Patients with both a solid component and a dilated pancreatic duct and/or concerning features on EUS and FNA should undergo surgery to reduce the risk of mortality from carcinoma [38].

References

1. Laffan TA, Horton KM, Klein AP, Berlanstein B, Siegelman SS, Kawamoto S, et al. Prevalence of unsuspected pancreatic cysts on MDCT. *AJR Am J Roentgenol.* 2008;191:802–7. <https://doi.org/10.2214/AJR.07.3340>.
2. de Jong K, Nio CY, Hermans JJ, Dijkgraaf MG, Gouma DJ, van Eijck CH. High prevalence of pancreatic cysts detected by screening magnetic resonance imaging examinations. *Clin Gastroenterol Hepatol.* 2010;8:806–11. <https://doi.org/10.1016/j.cgh.2010.05.017>.

3. Lee KS, Sekhar A, Rofsky NM, Pedrosa I. Prevalence of incidental pancreatic cysts in the adult population on MR imaging. *Am J Gastroenterol.* 2010;105:2079–84. <https://doi.org/10.1038/ajg.2010.122>.
4. Morales-Oyarvide V, Fong ZV, Fernández-Del Castillo C, Warshaw AL. Intraductal papillary mucinous neoplasms of the pancreas: strategic considerations. *Visc Med.* 2017;33:466–76. <https://doi.org/10.1159/000485014>.
5. Pergolini I, Sahara K, Ferrone CR, Morales-Oyarvide V, Wolpin BM, Mucci LA, et al. Long-term risk of pancreatic malignancy in patients with branch duct intraductal papillary mucinous neoplasm in a Referral Center. *Gastroenterology.* 2017;153:1284–1294.e1. <https://doi.org/10.1053/j.gastro.2017.07.019>.
6. Morales-Oyarvide V, Mino-Kenudson M, Ferrone CR, Sahani DV, Pergolini I, Negreros-Osuna AA, et al. Diabetes mellitus in intraductal papillary mucinous neoplasm of the pancreas is associated with high-grade dysplasia and invasive carcinoma. *Pancreatology.* 2017;17:920–6. <https://doi.org/10.1016/j.pan.2017.08.073>.
7. Tanaka M, Fernández-Del Castillo C, Kamisawa T, Jang JY, Levy P, Ohtsuka T, et al. Revisions of international consensus Fukuoka guidelines for the management of IPMN of the pancreas. *Pancreatology.* 2017;17:738–53. <https://doi.org/10.1016/j.pan.2017.07.007>.
8. Berland LL, Silverman SG, Gore RM, Mayo-Smith WW, Megibow AJ, Yee J, et al. Managing incidental findings on abdominal CT: white paper of the ACR incidental findings committee. *J Am Coll Radiol.* 2010;7:754–73. <https://doi.org/10.1016/j.jacr.2010.06.013>.
9. Efthymiou A, Podas T, Zacharakis E. Endoscopic ultrasound in the diagnosis of pancreatic intraductal papillary mucinous neoplasms. *World J Gastroenterol.* 2014;20:7785–93. <https://doi.org/10.3748/wjg.v20.i24.7785>.
10. Kitano M, Sakamoto H, Komaki T, Kudo M. New techniques and future perspective of EUS for the differential diagnosis of pancreatic malignancies: contrast harmonic imaging. *Dig Endosc.* 2011;23(Suppl 1):46–50. <https://doi.org/10.1111/j.1443-1661.2011.01146.x>.
11. Tanaka M, Fernández-del Castillo C, Adsay V, Chari S, Falconi M, Jang JY, et al. International consensus guidelines 2012 for the management of IPMN and MCN of the pancreas. *Pancreatology.* 2012;12:183–97. <https://doi.org/10.1016/j.pan.2012.04.004>.
12. Adsay NV, Fukushima N, Furukawa T, Hruban RH, Klimstra DS, Klöppel G, et al. Intraductal neoplasms of the pancreas. In: Bosman FT, Carneiro F, Hruban RH, Theise ND, editors. *WHO classification of tumors of the digestive system.* 4th ed. Lyon: IARC; 2010. p. 304–13.
13. Pitman MB, Lewandrowski K, Shen J, Sahani D, Brugge W, Fernandez-del Castillo C. Pancreatic cysts: preoperative diagnosis and clinical management. *Cancer Cytopathol.* 2010;118:1–13. <https://doi.org/10.1002/cncy.20059>.

14. Smith AL, Abdul-Karim FW, Goyal A. Cytologic categorization of pancreatic neoplastic mucinous cysts with an assessment of the risk of malignancy: a retrospective study based on the Papanicolaou Society of Cytopathology guidelines. *Cancer Cytopathol.* 2016;124:285–93. <https://doi.org/10.1002/cncy.21657>.
15. Layfield LJ, Cramer H. Fine-needle aspiration cytology of intraductal papillary-mucinous tumors: a retrospective analysis. *Diagn Cytopathol.* 2005;32:16–20.
16. Stelow EB, Stanley MW, Bardales RH, Mallery S, Lai R, Linzie BM, et al. Intraductal papillary-mucinous neoplasm of the pancreas. The findings and limitations of cytologic samples obtained by endoscopic ultrasound-guided fine-needle aspiration. *Am J Clin Pathol.* 2003;120:398–404.
17. Michaels PJ, Brachtel EF, Bounds BC, Brugge WR, Pitman MB. Intraductal papillary mucinous neoplasm of the pancreas: cytologic features predict histologic grade. *Cancer.* 2006;108:163–73.
18. Pitman MB, Genevay M, Yaeger K, Chebib I, Turner BG, Mino-Kenudson M, et al. High-grade atypical epithelial cells in pancreatic mucinous cysts are a more accurate predictor of malignancy than “positive” cytology. *Cancer Cytopathol.* 2010;118:434–40. <https://doi.org/10.1002/cncy.20118>.
19. Pitman MB, Layfield LJ. Guidelines for pancreaticobiliary cytology from the Papanicolaou Society of Cytopathology: a review. *Cancer Cytopathol.* 2014;122:399–411. <https://doi.org/10.1002/cncy.21427>.
20. Pitman MB, Centeno BA, Genevay M, Fonseca R, Mino-Kenudson M. Grading epithelial atypia in endoscopic ultrasound-guided fine-needle aspiration of intraductal papillary mucinous neoplasms: an international interobserver concordance study. *Cancer Cytopathol.* 2013;121:729–36. <https://doi.org/10.1002/cncy.21334>.
21. Lee PJ, Fischer AH, Owens CL, Hutchinson L. Intranuclear cytoplasmic inclusions are a specific diagnostic feature distinguishing low-grade pancreatic intraductal papillary mucinous neoplasms from contaminating gastric epithelium. *J Am Soc Cytopathol.* 2013;2:S66–7. <https://doi.org/10.1016/j.jasc.2013.08.182>.
22. Pitman MB, Centeno BA, Daglilar ES, Brugge WR, Mino-Kenudson M. Cytological criteria of high-grade epithelial atypia in the cyst fluid of pancreatic intraductal papillary mucinous neoplasms. *Cancer Cytopathol.* 2014;122:40–7. <https://doi.org/10.1002/cncy.21344>.
23. Sigel CS, Edelweiss M, Tong LC, Magda J, Oen H, Sigel KM, et al. Low interobserver agreement in cytology grading of mucinous pancreatic neoplasms. *Cancer Cytopathol.* 2015;123:40–50. <https://doi.org/10.1002/cncy.21492>.
24. Goyal A, Abdul-Karim FW, Yang B, Patel JB, Brainard JA. Interobserver agreement in the cytologic grading of atypia in neoplastic pancreatic mucinous cysts with the 2-tiered approach. *Cancer Cytopathol.* 2016;124:909–16. <https://doi.org/10.1002/cncy.21767>.

25. Zhang ML, Arpin RN, Brugge WR, Forcione DG, Basar O, Pitman MB. Moray micro forceps biopsy improves the diagnosis of specific pancreatic cysts. *Cancer Cytopathol.* 2018;126:414–20. <https://doi.org/10.1002/ency.21988>.
26. Brugge WR, Lewandrowski K, Lee-Lewandrowski E, Centeno BA, Szydlo T, Regan S, et al. Diagnosis of pancreatic cystic neoplasms: a report of the cooperative pancreatic cyst study. *Gastroenterology.* 2004;126:1330–6.
27. Cizginer S, Turner BG, Bilge AR, Karaca C, Pitman MB, Brugge WR. Cyst fluid carcinoembryonic antigen is an accurate diagnostic marker of pancreatic mucinous cysts. *Pancreas.* 2011;40:1024–8. <https://doi.org/10.1097/MPA.0b013e31821bd62f>.
28. Rockacy M, Khalid A. Update on pancreatic cyst fluid analysis. *Ann Gastroenterol.* 2013;26:122–7.
29. Oh HC, Kang H, Brugge WR. Cyst fluid amylase and CEA levels in the differential diagnosis of pancreatic cysts: a single-center experience with histologically proven cysts. *Dig Dis Sci.* 2014;59:3111–6. <https://doi.org/10.1007/s10620-014-3254-8>.
30. Reid MD, Saka B, Balci S, Goldblum AS, Adsay NV. Molecular genetics of pancreatic neoplasms and their morphologic correlates: an update on recent advances and potential diagnostic applications. *Am J Clin Pathol.* 2014;141:168–80. <https://doi.org/10.1309/AJCP0FKDP7ENVKEV>.
31. Singhi AD, Nikiforova MN, Fasanella KE, McGrath KM, Pai RK, Ohori NP, et al. Preoperative GNAS and KRAS testing in the diagnosis of pancreatic mucinous cysts. *Clin Cancer Res.* 2014;20:4381–9. <https://doi.org/10.1158/1078-0432.CCR-14-0513>.
32. Wu J, Matthaei H, Maitra A, Dal Molin M, Wood LD, Eshleman JR, et al. Recurrent GNAS mutations define an unexpected pathway for pancreatic cyst development. *Sci Transl Med.* 2011;3:92ra66. <https://doi.org/10.1126/scitranslmed.3002543>.
33. Kadayifci A, Atar M, Wang JL, Forcione DG, Casey BW, Pitman MB, et al. Value of adding GNAS testing to pancreatic cyst fluid KRAS and carcinoembryonic antigen analysis for the diagnosis of intraductal papillary mucinous neoplasms. *Dig Endosc.* 2017;29:111–7. <https://doi.org/10.1111/den.12710>.
34. Lee LS, Doyle LA, Houghton J, Sah S, Bellizzi AM, Szafranska-Schwarzbach AE, et al. Differential expression of GNAS and KRAS mutations in pancreatic cysts. *JOP.* 2014;15:581–6. <https://doi.org/10.6092/1590-8577/2432>.
35. Springer S, Wang Y, Dal Molin M, Masica DL, Jiao Y, Kinde I, et al. A combination of molecular markers and clinical features improve the classification of pancreatic cysts. *Gastroenterology.* 2015;149:1501–10. <https://doi.org/10.1053/j.gastro.2015.07.041>.
36. Jones M, Zheng Z, Wang J, Dudley J, Albanese E, Kadayifci A, et al. Impact of next-generation sequencing on the clinical diagnosis of

- pancreatic cysts. *Gastrointest Endosc.* 2016;83:140–8. <https://doi.org/10.1016/j.gie.2015.06.047>.
37. Matthaei H, Wylie D, Lloyd MB, Dal Molin M, Kemppainen J, Mayo SC, et al. miRNA biomarkers in cyst fluid augment the diagnosis and management of pancreatic cysts. *Clin Cancer Res.* 2012;18:4713–24. <https://doi.org/10.1158/1078-0432.CCR-12-0035>.
 38. Vege SS, Ziring B, Jain R, Moayyedi P, Clinical Guidelines Committee; American Gastroenterology Association. American gastroenterological association institute guideline on the diagnosis and management of asymptomatic neoplastic pancreatic cysts. *Gastroenterology.* 2015;148:819–22. ; quiz12–3. <https://doi.org/10.1053/j.gastro.2015.01.015>.



Mucinous Cystic Neoplasms

8

Lorene Yoxtheimer and Abha Goyal

Clinical Features

Mucinous cystic neoplasm (MCN) is an uncommon tumor of the pancreas that is characterized by the presence of subepithelial ovarian-type stroma. Although most of these tumors are benign, they are considered to be premalignant as they can develop dysplasia and invasive carcinoma. The prevalence of invasive carcinoma has been reported to range from 3.9% to 34.4% in these lesions [1].

They occur almost exclusively in women in the fifth to sixth decades of life; the mean age being 48 years. Though patients may present with symptoms including abdominal pain, recurrent pancreatitis, abdominal mass, or weight loss, an increasing number of MCNs are asymptomatic, being incidentally detected on imaging [2].

L. Yoxtheimer · A. Goyal (✉)

Department of Pathology and Laboratory Medicine, Weill-Cornell Medicine, New York Presbyterian Hospital, New York, NY, USA
e-mail: abg9017@med.cornell.edu

© Springer Nature Switzerland AG 2019

A. Goyal et al. (eds.), *Pancreas and Biliary Tract Cytohistology*,
Essentials in Cytopathology 28,
https://doi.org/10.1007/978-3-030-22433-2_8

203

Pathogenesis

The expression of the estrogen receptor (ER) and progesterone receptor (PR) and steroidogenic enzymes by the ovarian-type stroma in MCNs suggests a role of female sex steroids in their pathogenesis [3, 4]. Also, these tumors are mostly seen in women and are histologically similar to tumors arising in the liver and biliary tract and in the retroperitoneum. One possibility is that MCNs may originate from the ovarian primordium. This is supported by their similar morphology and immunophenotype and the presence of luteinized cells.

Another hypothesis is that they are derived from ectopic ovarian-type stroma in the distal pancreas which by producing hormones and growth factors may cause endodermally derived epithelium to proliferate and form cystic neoplasms. However, such mechanisms do not explain the occasional occurrence of MCNs in men [3].

Imaging Findings

Majority (>95%) of MCNs are located in the body or tail of the pancreas [5]. On imaging, they usually appear as macrocystic lesions that may have a solid component. Unlike side-branch intraductal papillary mucinous neoplasms (IPMNs), there is usually no communication with the pancreatic duct.

MCNs, especially if small in size, may be indistinguishable from pseudocysts, serous cystadenomas, and IPMNs on imaging. Lesion shape on computed tomography (CT) scan has been reported to be a helpful discriminating feature between oligocystic serous adenomas, MCNs, and IPMNs. Serous cystadenomas tend to have a multicystic or lobulated contour with or without septation, while MCNs have a smooth contour with or without septation, and IPMNs either have a pleomorphic or a clubbed fingerlike cystic shape [6]. In a study of 33 patients with unilocular pancreatic cystic lesions, Cohen-Scali reported that location in the pancreatic head, lobulated contour, and lack of wall enhancement were specific for serous cystadenomas in comparison to MCNs

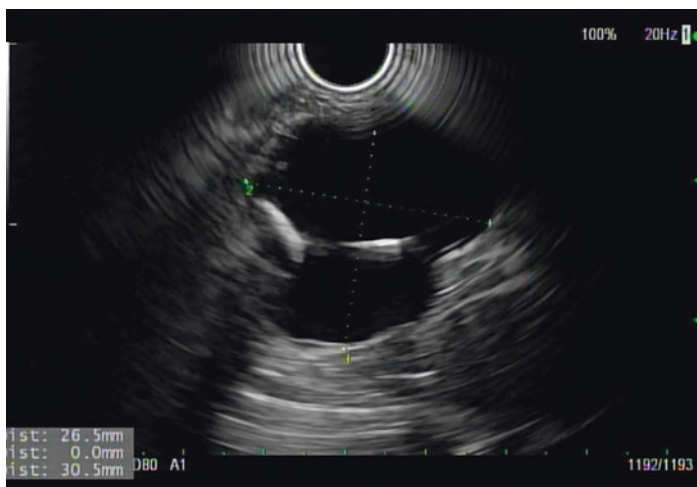


Fig. 8.1 Endoscopic ultrasound of mucinous cystic neoplasm (MCN) shows a septated cyst in the body of the pancreas with calcifications in the wall. Histologic follow-up revealed a MCN with low-grade dysplasia

[7]. Endoscopic ultrasound (EUS) can help visualize septations, thick cyst walls, and mural nodules better than CT and/or magnetic resonance imaging (MRI) (Fig. 8.1). Also, it can allow the aspiration of the cyst contents and biopsy of the cyst wall for a tissue diagnosis [8].

The predictors of malignancy in MCNs on imaging have been variably reported. A retrospective study of 52 patients by Procacci and colleagues showed that the presence of septal or wall calcifications, septations, and a thick wall on CT scan was associated with malignancy in 95% of cases [9]. In a study of 90 MCNS, Park et al. found that the presence of mural nodules on CT scan was a significant predictor of malignancy [2]. A study of 32 resected MCNs with preoperative MDCT or MRI showed that MCN size (>8.5 cm) and volume were the only features that correlated with high-grade dysplasia/carcinoma. A cyst size of >8.5 cm was associated with 60% sensitivity and 97% specificity for the presence of high-grade dysplasia/carcinoma [10].

Pathologic Features

Gross Findings

MCNS are usually solitary, large, multilocular or unilocular cysts with a thick fibrotic capsule and a mean diameter of 6.5 cm [1]. The cysts contain abundant mucus and cloudy brown fluid. Solid areas may be seen in the cysts that should be sampled extensively for histologic examination. Typically, there is no communication with the pancreatic duct system.

Histology

MCNs are characterized by mucinous epithelium with varying degrees of dysplasia. The epithelium may be mostly bland with tall columnar to cuboidal cells with basally located nuclei in a flat or papillary architecture (Fig. 8.2). Although scattered goblet cells

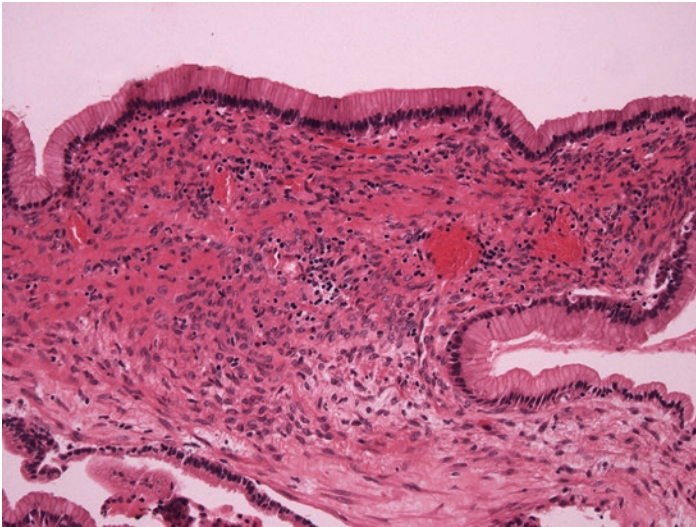


Fig. 8.2 Mucinous cystic neoplasm (MCN) with low-grade dysplasia. The epithelium is composed of tall, columnar mucinous cells with basally located nuclei. It overlies a characteristic spindled ovarian-type stroma that is a prerequisite for the diagnosis of MCN (hematoxylin-eosin stain, 400 \times)

may be present, intestinal differentiation is not a usual feature of MCNs [11]. Some foci of the epithelium may be lined by a single layer of pancreatobiliary-type, non-mucinous cuboidal cells [12].

The subepithelial ovarian-type stroma is essential for the diagnosis of MCN and should be present at least focally in the tumor. At times, the epithelium may be denuded; but the ovarian-type stroma may still be identifiable, providing an important clue to the diagnosis. The spindle cell stroma may also contain nests of epithelioid cells with features suggestive of luteinization. The stroma can also exhibit degenerative changes such as hyalinization, calcification, and cholesterol clefts.

As per the 2010 World Health Organization classification, the dysplasia in MCN is graded as low, intermediate, or high, based on the most severely dysplastic focus [13]. It is critical that the tumor is extensively, if not completely, sampled for histologic examination as high-grade dysplasia may be present only focally in the tumor. In low-grade dysplasia, the lining epithelium is cytologically bland with minimal architectural complexity. Intermediate-grade dysplasia is characterized by loss of nuclear polarity, moderate atypia, and mild architectural complexity. High-grade dysplasia is associated with marked cytologic atypia and mitotic figures with significant architectural complexity.

Invasive carcinomas arising in MCNs are usually of the tubular type, resembling conventional pancreatic ductal adenocarcinomas. Adenosquamous carcinoma and undifferentiated carcinoma (with or without osteoclast-like giant cells) may rarely occur in MCNs [3, 14].

Cytology

On FNA specimens, MCNs and IPMNs cannot be distinguished from one another based on cytologic features [15, 16]. The subepithelial ovarian-type stroma that is considered a prerequisite for the diagnosis of MCNs cannot be visualized on cytologic samples.

The cytologic diagnosis for a neoplastic mucinous cyst is based on the presence of extracellular thick mucin and/or neoplastic mucinous epithelium that can show a range of atypias (Figs. 8.3 and 8.4). The aspirates of MCNs are usually paucicellular. In an analysis of 61 MCNs, Scourtas et al. reported lack of epithelial

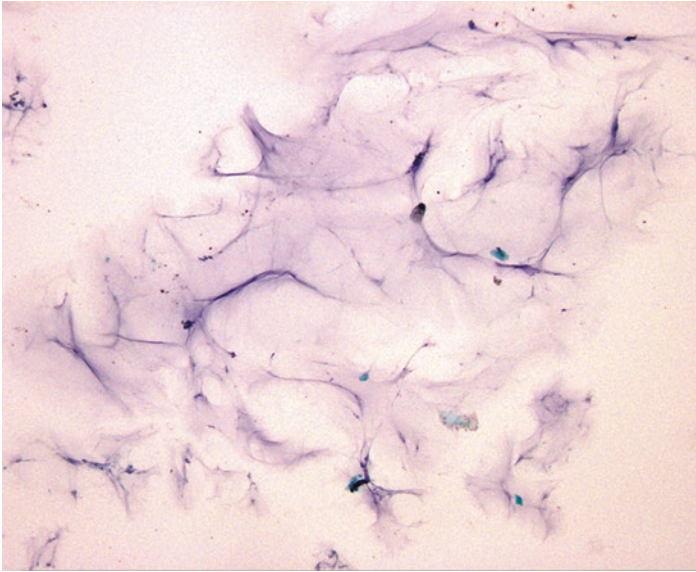


Fig. 8.3 Thick mucin on cytology is indicative of a neoplastic mucinous cyst by itself (ThinPrep, Papanicolaou stain, 200 \times)

cells in 74% of cases. Extracellular mucin was seen in 39% of low-risk cysts and 33% of high-risk cysts. Necrosis or cellular debris were identified in 31% of low-risk cysts and 50% of high-risk cysts. The presence of mucin or necrosis/cellular debris was not found to be significantly associated with the degree of dysplasia on histology. Inflammation and/or histiocytes were more frequently seen in low-risk cysts in contrast to high-risk cysts [8].

A purely cytologic approach is inferior to an integrated approach of cytology with ancillary testing in diagnosing a neoplastic mucinous cyst of the pancreas. Until recently, there had been no standardized guidelines for the cytopathologist to report pancreatico-biliary cytology. The Papanicolaou Society of Cytopathology (Pap Society) advocates a multidisciplinary approach for the diagnosis of pancreatic lesions and recommends the incorporation of all available relevant ancillary data to make a cytologic diagnosis. In addition, they support a two-tiered approach for grading cytologic

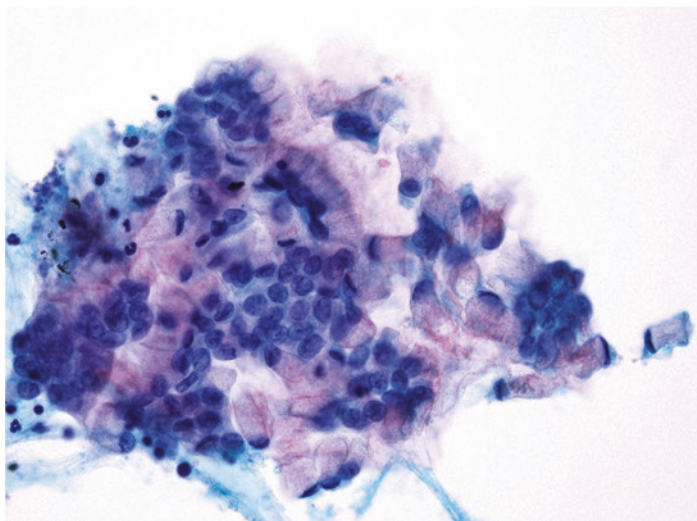


Fig. 8.4 Low-grade atypia characterizes the majority of mucinous cystic neoplasms on cytology. The low-grade epithelium reveals abundant mucinous cytoplasm with a low nuclear-cytoplasmic ratio and finely distributed nuclear chromatin (ThinPrep, Papanicolaou stain, 400 \times)

atypia in mucinous cysts when features suspicious or unequivocal for malignancy are not seen: low-grade atypia (usually correlates with low-grade or intermediate-grade dysplasia on histology) and high-grade atypia (usually correlates with high-grade dysplasia or worse on follow-up) [15, 16].

Scourtas et al. reported the finding of high-grade atypia in 33% of high-risk MCNs with available cytology. Though the sensitivity of cytology was limited in the detection of high-risk cysts, its specificity was 100% and accuracy 95% [8].

Immunohistochemistry

The lining epithelium of MCNs is typically positive for MUC5AC and negative for MUC1. MUC2 expression is restricted to goblet cells that are dispersed within the epithelium [14]. The stromal

cells are positive for estrogen and progesterone receptors; and the luteinized cells exhibit positivity for inhibin, tyrosine hydroxylase, and calretinin.

p53 positivity increases with the grade of dysplasia and can also be seen in the invasive component [3]. Loss of DPC4 protein expression is a frequent event in invasive MCNs in contrast to noninvasive ones [17].

Cyst Fluid Biochemistry

Amylase levels are variable in MCNs and may not be helpful in differentiating them from IPMNs [18].

See also Cyst Fluid Biochemistry section in Chap. 7.

Molecular Genetics

Whole-exome sequencing of MCNs has revealed 16 ± 7.6 nonsynonymous somatic mutations per tumor. Mutations have been identified in *RNF43* (which codes for a protein with intrinsic E3 ubiquitin ligase activity), *KRAS*, *TP53*, *SMAD4*, and *CDKN2A*. *KRAS* mutation is an early event, while tumor suppressor gene mutations (*TP53*, *SMAD4*, and *CDKN2A*) occur in MCNs with high-grade dysplasia or associated invasive carcinomas [19, 20]. *GNAS* mutations are not found in MCNs, in contrast to IPMNs [21]. *PIK3CA* mutations have also been detected in MCNs with high-grade dysplasia and may contribute to tumor progression [22].

Management

As per the 2012 Fukuoka consensus guidelines, surgical resection is recommended for all surgically fit patients with MCNs. Surgical resection has been the traditional management for MCNs due to their potential for malignant transformation, their location in the distal pancreas, and the relatively young age of the patients. MCNs are usually located in the pancreatic body and tail and

therefore require distal pancreatectomy. Furthermore, there is no definitive method to determine preoperatively whether the tumor is benign or malignant, and conservative management would require years of surveillance with high-resolution imaging that is associated with high costs [23].

Although surgical resection has been the treatment of choice, more conservative management options are being explored for the management of MCNs. A study of 90 patients with MCNs showed that regardless of histologic grade, long-term outcome was excellent in MCNs. In this study, only 10% of MCNs were malignant. The overall 5-year disease-free survival was 98.8% for all patients, 100% for MCNs with high-grade dysplasia, and 75% for those with invasive carcinoma. Based on the results of this study, MCNs which are smaller than 3 cm that lack mural nodules and elevated serum carbohydrate antigen 19-9 are very likely to be benign. Therefore, the authors suggested that MCNs that met the aforementioned criteria could be followed conservatively [2].

In a study of 168 MCNs, Crippa et al. identified a low risk of cancer in these tumors (11% invasive and 6% in situ) and thereby indicated that nonoperative management could potentially be allowed in MCNs that are asymptomatic, <4 cm in size, and without solid components [24].

As per the 2018 European evidence-based guidelines on pancreatic cystic neoplasms, MCNs ≥ 40 mm should undergo surgical resection. Resection is also recommended for MCNs which are symptomatic or have risk factors (i.e., mural nodule) irrespective of their size. MCNs measuring <40 mm without a mural nodule or symptoms may undergo surveillance with MRI, endoscopic ultrasound (EUS), or a combination of both [25].

Prognosis

The complete resection of a noninvasive MCN is curative, requiring no postoperative surveillance with a 5-year disease-specific survival rate of 100% [26, 27]. However, the 5-year disease-specific survival rate drops to 20% to 60% for patients with MCNs with advanced invasive carcinoma [24, 28, 29].

Minimally invasive carcinomas (<0.5 cm) as well as MCNs with invasion limited to ovarian-like stroma or intratumoral septa reportedly have a good prognosis [13, 30]. Another study showed that MCN with T1a (≤ 0.5 cm) and T1b (>0.5 cm and <1.0 cm) carcinomas had an excellent prognosis similar to MCNs with low-grade or high-grade dysplasia after complete tumor sampling for histologic examination. These studies suggest that for such tumors, close follow-up may be a better approach as compared to aggressive systemic therapy [31].

References

1. Fukushima N, Zamboni G. Mucinous cystic neoplasms of the pancreas: update on the surgical pathology and molecular genetics. *Semin Diagn Pathol.* 2014;31:467–74. <https://doi.org/10.1053/j.semdp.2014.08.007>.
2. Park JW, Jang JY, Kang MJ, Kwon W, Chang YR, Kim SW. Mucinous cystic neoplasm of the pancreas: is surgical resection recommended for all surgically fit patients? *Pancreatol.* 2014;14:131–6. <https://doi.org/10.1016/j.pan.2013.12.006>.
3. Zamboni G, Scarpa A, Bogina G, Iacono C, Bassi C, Talamini G, et al. Mucinous cystic tumors of the pancreas: clinicopathological features, prognosis, and relationship to other mucinous cystic tumors. *Am J Surg Pathol.* 1999;23:410–22.
4. Ishida K, Sasano H, Moriya T, Takahashi Y, Sugimoto R, Mue Y, et al. Immunohistochemical analysis of steroidogenic enzymes in ovarian-type stroma of pancreatic mucinous cystic neoplasms: comparative study of sub-epithelial stromal cells in intraductal papillary mucinous neoplasms of the pancreas. *Pathol Int.* 2016;66:281–7. <https://doi.org/10.1111/pin.12406>.
5. Thompson LD, Becker RC, Przygodzki RM, Adair CF, Heffess CS. Mucinous cystic neoplasm (mucinous cystadenocarcinoma of low-grade malignant potential) of the pancreas: a clinicopathologic study of 130 cases. *Am J Surg Pathol.* 1999;23:1–16.
6. Kim SY, Lee JM, Kim SH, Shin KS, Kim YJ, An SK, et al. Macroscopic neoplasms of the pancreas: CT differentiation of serous oligocystic adenoma from mucinous cystadenoma and intraductal papillary mucinous tumor. *AJR Am J Roentgenol.* 2006;187:1192–8.
7. Cohen-Scali F, Vilgrain V, Brancatelli G, Hammel P, Vullierme MP, Sauvanet A, et al. Discrimination of unilocular macrocystic serous cystadenoma from pancreatic pseudocyst and mucinous cystadenoma with CT: initial observations. *Radiology.* 2003;228:727–33.

8. Scourtas A, Dudley JC, Brugge WR, Kadayifci A, Mino-Kenudson M, Pitman MB. Preoperative characteristics and cytological features of 136 histologically confirmed pancreatic mucinous cystic neoplasms. *Cancer Cytopathol.* 2017;125:169–77. <https://doi.org/10.1002/cncy.21806>.
9. Procacci C, Carbognin G, Accordini S, Biasiutti C, Guarise A, Lombardo F, et al. CT features of malignant mucinous cystic tumors of the pancreas. *Eur Radiol.* 2001;11:1626–30.
10. Garces-Descovich A, Beker K, Castillo-Angeles M, Brook A, Resnick E, Shinagare S, et al. Mucinous cystic neoplasms of the pancreas: high-resolution cross-sectional imaging features with clinico-pathologic correlation. *Abdom Radiol (NY).* 2018;43:1413–22. <https://doi.org/10.1007/s00261-017-1326-x>.
11. Baker ML, Seeley ES, Pai R, Suriawinata AA, Mino-Kenudson M, Zamboni G, et al. Invasive mucinous cystic neoplasms of the pancreas. *Exp Mol Pathol.* 2012;93:345–9. <https://doi.org/10.1016/j.yexmp.2012.07.005>.
12. Albores-Saavedra J, Manivel C, Dorantes-Heredia R, Chablé-Montero F, Godoy-Valdés C, Chan-Núñez C, et al. Nonmucinous cystadenomas of the pancreas with pancreatobiliary phenotype and ovarian-like stroma. *Am J Clin Pathol.* 2013;139:599–604. <https://doi.org/10.1309/AJCPHSV7TV2WOJFE>.
13. Zamboni G, Fukushima N, Hruban RH, Klöppel G. Mucinous cystic neoplasms of the pancreas. In: Bosman FT, Carneiro F, Hruban RH, Theise ND, editors. *WHO classification of tumors of the digestive system.* 4th ed. Lyon: IARC; 2010. p. 300–3.
14. Lüttges J, Feyerabend B, Buchelt T, Pacena M, Klöppel G. The mucin profile of noninvasive and invasive mucinous cystic neoplasms of the pancreas. *Am J Surg Pathol.* 2002;26:466–71.
15. Pitman MB, Centeno BA, Ali SZ, Genevay M, Stelow E, Mino-Kenudson M, et al. Standardized terminology and nomenclature for pancreatobiliary cytology: the Papanicolaou Society of Cytopathology guidelines. *Diagn Cytopathol.* 2014;42:338–50. <https://doi.org/10.1002/dc.23092>.
16. Pitman MB, Layfield LJ. Guidelines for pancreaticobiliary cytology from the Papanicolaou Society of Cytopathology: a review. *Cancer Cytopathol.* 2014;122:399–411. <https://doi.org/10.1002/cncy.21427>.
17. Iacobuzio-Donahue CA, Wilentz RE, Argani P, Yeo CJ, Cameron JL, Kern SE, et al. Dpc4 protein in mucinous cystic neoplasms of the pancreas: frequent loss of expression in invasive carcinomas suggests a role in genetic progression. *Am J Surg Pathol.* 2000;24:1544–8.
18. Oh HC, Kang H, Brugge WR. Cyst fluid amylase and CEA levels in the differential diagnosis of pancreatic cysts: a single-center experience with histologically proven cysts. *Dig Dis Sci.* 2014;59:3111–6. <https://doi.org/10.1007/s10620-014-3254-8>.

19. Wu J, Jiao Y, Dal Molin M, Maitra A, de Wilde RF, Wood LD, et al. Whole-exome sequencing of neoplastic cysts of the pancreas reveals recurrent mutations in components of ubiquitin-dependent pathways. *Proc Natl Acad Sci U S A*. 2011;108:21188–93. <https://doi.org/10.1073/pnas.1118046108>.
20. Wood LD, Hruban HR. Genomic landscapes of pancreatic neoplasia. *J Pathol Transl Med*. 2015;49:13–22. <https://doi.org/10.4137/jptm.2014.12.26>.
21. Singhi AD, Nikiforova MN, Fasanella KE, McGrath KM, Pai RK, Ohori NP, et al. Preoperative GNAS and KRAS testing in the diagnosis of pancreatic mucinous cysts. *Clin Cancer Res*. 2014;20:4381–9. <https://doi.org/10.1158/1078-0432.CCR-14-0513>.
22. Garcia-Carracedo D, Chen ZM, Qiu W, Huang AS, Tang SM, Hruban RH, et al. PIK3CA mutations in mucinous cystic neoplasms of the pancreas. *Pancreas*. 2014;43:245–9. <https://doi.org/10.1097/MPA.0000000000000034>.
23. Tanaka M, Fernández-del Castillo C, Adsay V, Chari S, Falconi M, Jang JY, et al. International consensus guidelines 2012 for the management of IPMN and MCN of the pancreas. *Pancreatology*. 2012;12:183–97. <https://doi.org/10.1016/j.pan.2012.04.004>.
24. Crippa S, Salvia R, Warshaw AL, Domínguez I, Bassi C, Falconi M, et al. Mucinous cystic neoplasm of the pancreas is not an aggressive entity: lessons from 163 resected patients. *Ann Surg*. 2008;247:571–9. <https://doi.org/10.1097/SLA.0b013e31811f4449>.
25. European Study Group on Cystic Tumours of the Pancreas. European evidence-based guidelines on pancreatic cystic neoplasms. *Gut*. 2018;67:789–804. <https://doi.org/10.1136/gutjnl-2018-316027>.
26. Wilentz RE, Albores-Saavedra J, Zahurak M, Talamini MA, Yeo CJ, Cameron JL. Pathologic examination accurately predicts prognosis in mucinous cystic neoplasms of the pancreas. *Am J Surg Pathol*. 1999;23:1320–7.
27. Xourafas D, Tavakkoli A, Clancy TE, Ashley SW. Noninvasive intra-ductal papillary mucinous neoplasms and mucinous cystic neoplasms: recurrence rates and postoperative imaging follow-up. *Surgery*. 2015;157:473–83. <https://doi.org/10.1016/j.surg.2014.09.028>.
28. Suzuki Y, Atomi Y, Sugiyama M, Isaji S, Inui K, Kimura W, et al. Cystic neoplasm of the pancreas: a Japanese multiinstitutional study of intra-ductal papillary mucinous tumor and mucinous cystic tumor. *Pancreas*. 2004;28(3):241–6.
29. Testini M, Gurrado A, Lissidini G, Venezia P, Greco L, Piccinni G. Management of mucinous cystic neoplasms of the pancreas. *World J Gastroenterol*. 2010;16:5682–92.

30. Lewis GH, Wang H, Bellizzi AM, Klein AP, Askin FB, Schwartz LE, et al. Prognosis of minimally invasive carcinoma arising in mucinous cystic neoplasms of the pancreas. *Am J Surg Pathol*. 2013;37:601–5. <https://doi.org/10.1097/PAS.0b013e318273f3b0>.
31. Hui L, Rashid A, Foo WC, Katz MH, Chatterjee D, Wang H, et al. Significance of T1a and T1b carcinoma arising in mucinous cystic neoplasm of pancreas. *Am J Surg Pathol*. 2018;42:578–86. <https://doi.org/10.1097/PAS.0000000000001040>.



Other Cystic Lesions of the Pancreas

Abha Goyal

Introduction

Pancreatic cyst lesions encompass a wide variety of entities ranging from nonneoplastic to neoplastic lesions with cystic degeneration (Table 9.1). The cysts can show significant overlap in terms of imaging findings as well as clinical features. Cytology along with cyst fluid analysis plays a pivotal role in the preoperative characterization of these lesions. However, some lesions, especially the uncommon ones, may not be diagnosed accurately resulting in unnecessary surgery. This chapter will discuss the various aspects of pancreatic cystic lesions (other than the neoplastic mucinous cysts) including the clinical features, imaging findings, pathologic features, molecular genetics, and management.

A. Goyal (✉)

Department of Pathology and Laboratory Medicine, Weill-Cornell Medicine, New York Presbyterian Hospital, New York, NY, USA
e-mail: abg9017@med.cornell.edu

© Springer Nature Switzerland AG 2019

A. Goyal et al. (eds.), *Pancreas and Biliary Tract Cytohistology*,
Essentials in Cytopathology 28,
https://doi.org/10.1007/978-3-030-22433-2_9

217

Table 9.1 Pancreatic cyst classification

<i>Neoplastic cysts</i>
Intraductal papillary mucinous neoplasm
Mucinous cystic neoplasm
Serous cystic neoplasm
Neoplasms with cystic degeneration
Solid pseudopapillary neoplasm
Pancreatic neuroendocrine tumor
Pancreatic ductal adenocarcinoma
Acinar cell carcinoma
<i>Nonneoplastic cysts</i>
Pseudocyst
Lymphoepithelial cyst
Epidermoid cyst of the accessory spleen
Dermoid cyst
Squamoid cyst of the pancreatic ducts
Retention cyst
Enterogenous duplication cyst
Endometriotic cyst
<i>Other</i>
Acinar cell cystadenoma (cystic acinar transformation)

Other Neoplastic Cysts of the Pancreas

Serous Cystadenoma

Clinical Features

Though uncommon, serous cystadenomas (SCAs) constitute one of the most frequent benign cystic neoplasms of the pancreas. They mostly occur in the body or tail of the pancreas. The mean age of presentation is 60 years, and the majority (67–80%) of patients are women. They also occur in 35–90% of patients with von Hippel-Lindau (VHL) syndrome. Multifocality or diffuse involvement of the pancreas is typically seen in VHL syndrome. Many are asymptomatic and are discovered incidentally.

Symptoms may include abdominal pain, palpable mass, nausea and vomiting, and weight loss [1, 2]. With lesions that are >4 cm in size, symptoms are reportedly more frequent [3].

Imaging Findings

Serous adenomas can be microcystic, macrocystic, oligocystic (<10% of cases), mixed (micro-macrocystic), or solid. Microcystic serous cystadenoma (SCA) typically appears as an isolated, lobulated, well-marginated, multilocular lesion on computed tomography scan/magnetic resonance imaging (MRI). It comprises of a cluster of multiple small cysts separated by thin septa. The typical imaging finding of a honeycomb appearance with a central stellate scar with sunburst pattern of calcifications is seen in only 20% of cases. Branch duct intraductal papillary mucinous neoplasms (BD-IPMNs) may also present in a polycystic pattern, simulating the microcystic SCAs.

Macrocystic SCAs are characterized by fewer cysts that are larger in size (>2 cm in diameter) or even one single cyst. The macrocystic SCAs can be particularly difficult to distinguish from mucinous cystic neoplasms and BD-IPMNs. If the patient has a history of pancreatitis, another differential diagnostic consideration is a pseudocyst.

The mixed micro-macrocystic type shows a combination of features of both microcystic and macrocystic types. The solid SCAs consist of small cysts which are separated by multiple, thick fibrous septa [4, 5].

Pathologic Features

Gross Findings Typically, SCAs are single masses that are well circumscribed and average 6 cm in diameter. They do not communicate with the pancreatic ducts. Classically, the cut surface is sponge-like with numerous small cysts (just few mm in diameter) filled with clear, serous fluid. The center of the neoplasm may show a dense fibrous scar with thin septa radiating to the periphery. The scar may also be calcified. Unlike the microcystic SCAs, the macrocystic ones tend to be located in the head of the pancreas.

Histology The cysts are lined by a single layer of cuboidal or flat epithelium with clear cytoplasm. The cytoplasm is clear due to the presence of abundant intracellular glycogen. Occasionally, the epithelial lining cells can exhibit eosinophilic granular cytoplasm. The nuclei are round to ovoid with inconspicuous nucleoli. The lining epithelium is closely associated with underlying fibrovascular stroma with a rich capillary network (Fig. 9.1). Intracystic papillae may develop that lack fibrovascular cores.

Solid serous adenomas show similar cytology, but the cells tend to be arranged in small acini. Solid serous adenomas may be difficult to distinguish from metastatic renal cell carcinoma, pancreatic neuroendocrine tumor (PanNET), and clear cell sugar tumor. In patients with VHL, the neuroendocrine tumors can exhibit clear cells and closely mimic SCAs [1, 2].

Cytology Usually, the cytologic interpretation is descriptive or nondiagnostic due to lack of sufficient cellularity. When present,

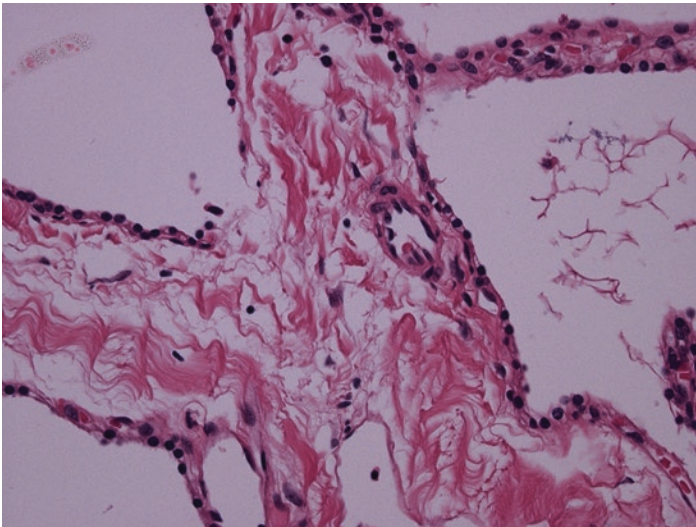


Fig. 9.1 Histology of serous cystadenoma reveals bland cuboidal epithelium with interspersed fibrovascular septa (hematoxylin-eosin stain, 400 \times)

the neoplastic cells are cuboidal with moderately abundant granular to clear, non-mucinous cytoplasm and round nuclei with fine chromatin (Fig. 9.2). The background is usually hemorrhagic and may contain hemosiderin-laden macrophages. A close mimicker of the SCA is a cystic PanNET. In contrast to the SCA, the PanNET cells tend to exhibit a finely stippled “salt and pepper” chromatin. SCAs can also be mistaken for pseudocysts and for neoplastic mucinous cysts owing to contaminating gastrointestinal epithelium and mucin [6, 7].

Although periodic acid-Schiff (PAS) and PAS/diastase stains could help identify the glycogen in SCA cells and inhibin immunohistochemistry is reportedly helpful in their identification, the aspirates are mostly paucicellular and inadequate for additional studies [8]. Another diagnostic pitfall is that inhibin can show positive staining in PanNETs with clear cell features [9].

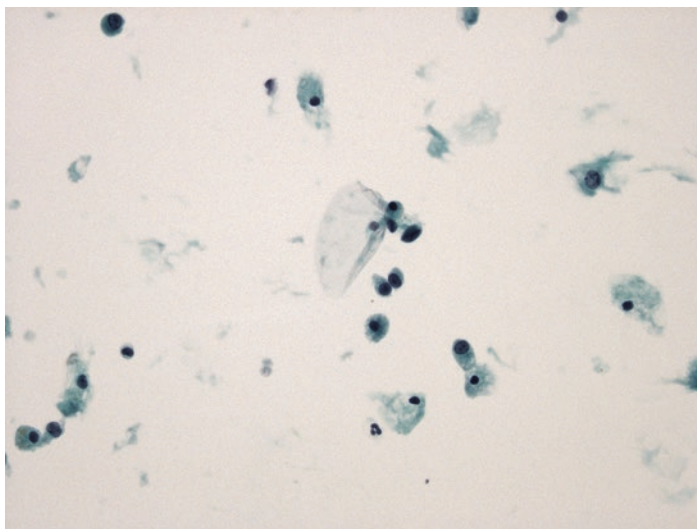


Fig. 9.2 Fine needle aspirate of serous cystadenoma is usually paucicellular. The lesional epithelium is composed of cuboidal cells with non-mucinous cytoplasm and round nuclei with fine chromatin (Papanicolaou stain, ThinPrep, 400×)

Cyst Fluid Biochemistry

SCAs typically have low carcinoembryonic antigen (CEA) (<5 ng/ml) and amylase (<250 IU/L) levels [6].

Molecular Genetics

Mutations or loss of heterozygosity in the *VHL* gene has been identified in 67% of SCAs [10].

Management

Majority of SCAs follow a benign course, and risk of malignant transformation is minimal. Most patients can be followed by serial imaging. The usual indications for resecting SCAs are to alleviate symptoms or when the diagnosis is uncertain and a malignant process/transformation cannot be excluded [2].

Solid Pseudopapillary Neoplasm

Clinical Features

Solid pseudopapillary neoplasm (SPN) of the pancreas is a neoplasm of uncertain lineage that tends to undergo hemorrhagic cystic degeneration. It is predominantly seen in young women (mean age being 28 years). They can be asymptomatic and found incidentally on imaging performed for other indications. If symptomatic, the presenting symptoms include abdominal pain, early satiety, nausea, and vomiting [11].

Imaging Findings

On imaging, the tumor is well demarcated and variably solid and cystic. It typically appears as a mixed-density lesion with solid component peripherally and cystic component more centrally. Calcification may be seen at the periphery of the lesion. On MRI, SPNs usually have variable signal intensity on T1-weighted images, high signal intensity on T2-weighted images, and a hypointense rim on both T1- and T2-weighted images. Hemorrhage appears as areas of high signal on T1-weighted images and low signal on T2-weighted images [12].

Pathologic Features

Gross Findings SPNs appear as solitary masses that are well demarcated from the surrounding pancreas. Cut surface is yellow to brown with solid and cystic areas and zones of hemorrhage.

Histology and Cytology SPNs are characterized by loosely cohesive tumor cells that surround hyalinized to myxoid stroma containing thin-walled blood vessels (Fig. 9.3). There are foci of hemorrhage, and solid areas may contain tumor cell aggregates with cholesterol clefts surrounded by foreign body giant cells. The tumor cells show moderately abundant eosinophilic or clear cytoplasm. The nuclei are indented or grooved and exhibit fine chromatin (Fig. 9.4). Intracellular and/or extracellular hyaline globules may be present. Histologic features such as perineural invasion, vascular invasion, and infiltration of the surrounding structures do not appear to correlate with the biologic behavior of the neoplasm [11].

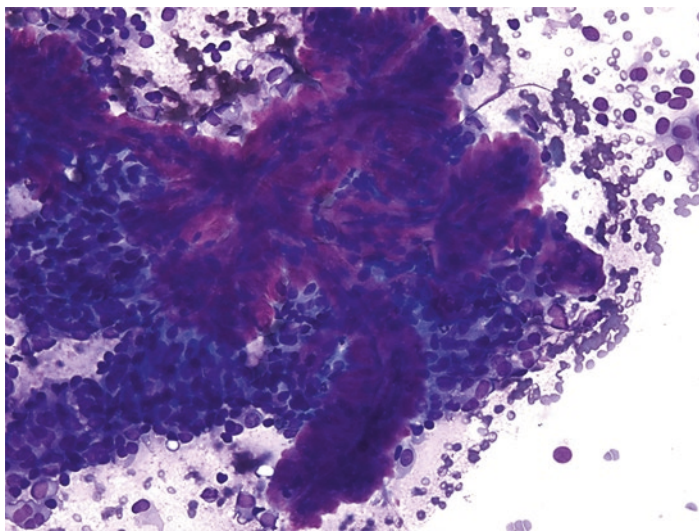


Fig. 9.3 Solid pseudopapillary neoplasm with metachromatic hyalinized fibrovascular cores surrounded by loosely cohesive monotonous neoplastic cells (Diff-Quik stain, 200 \times)

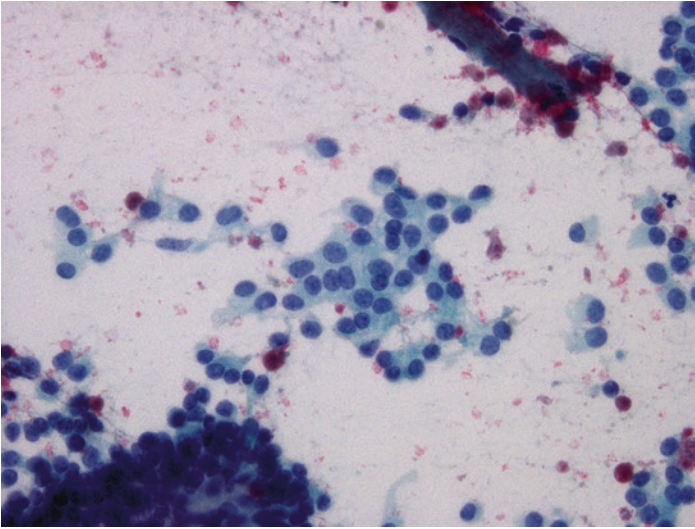


Fig. 9.4 Neoplastic cells of solid pseudopapillary neoplasm exhibit moderate amount of cytoplasm with round to oval nuclei with fine chromatin. Nuclear grooves may not be conspicuous (Papanicolaou stain, 400 \times)

Immunohistochemistry

The tumor cells characteristically reveal nuclear and cytoplasmic staining with β -catenin (Fig. 9.5). Due to alterations of the catenin-cadherin complex, the tumor cells do not demonstrate a membranous expression pattern with E-cadherin. Instead, there is either complete loss of staining or cytoplasmic/nuclear staining [13, 14]. Another recently described immunohistochemical marker for SPN is lymphoid enhancer binding factor 1 (LEF1). LEF1 shows strong and diffuse nuclear expression in SPNs (Fig. 9.6) [15].

Other markers that are helpful in the diagnosis of SPNs are CD10 and PR (Fig. 9.7). CD10 and PR may be expressed in a minority of pancreatic neuroendocrine tumors, but their expression tends to be focal in these tumors. SPNs may show focal and weak reactivity with cytokeratin in 10–74% of cases. They are usually positive for CD56 and may exhibit focal and weak reactivity with synaptophysin but are negative for chromogranin [13, 14].

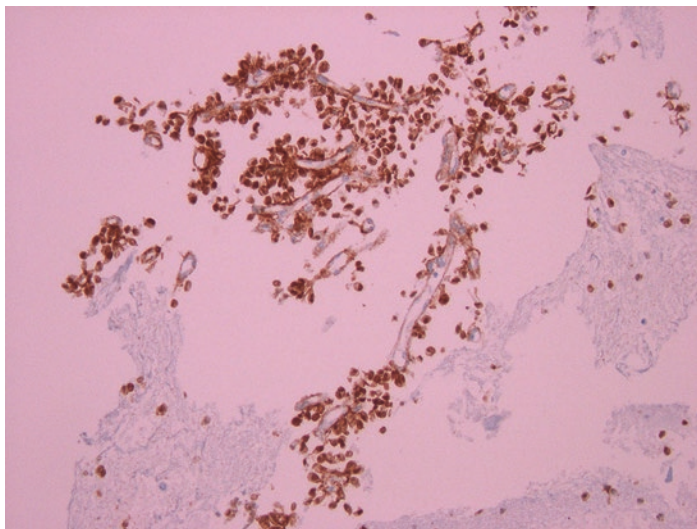


Fig. 9.5 Beta-catenin immunohistochemistry in solid pseudopapillary neoplasm reveals nuclear and cytoplasmic staining (200 \times)

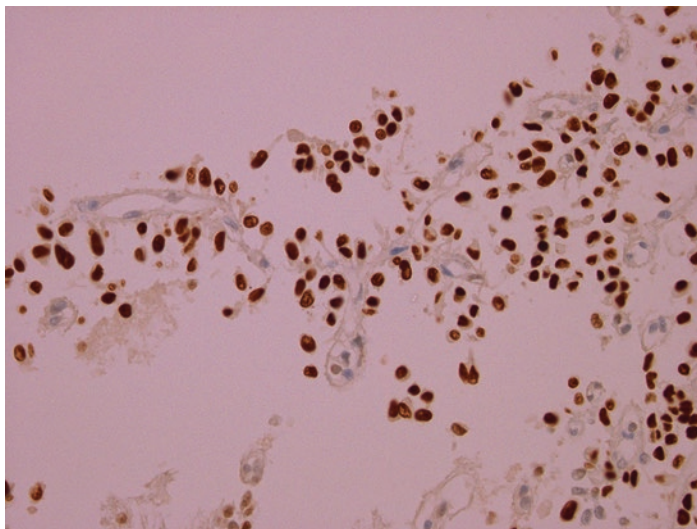


Fig. 9.6 LEF1 immunohistochemistry in solid pseudopapillary neoplasm reveals nuclear staining (400 \times)

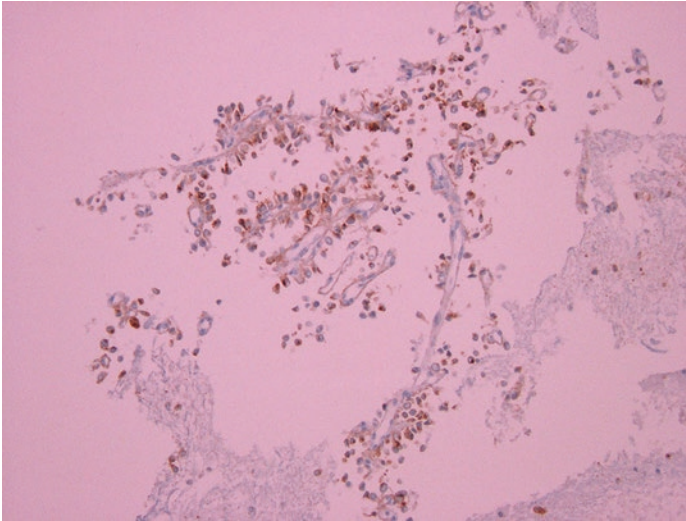


Fig. 9.7 CD10 immunohistochemistry in solid pseudopapillary neoplasm reveals cytoplasmic staining (200 \times)

Molecular Genetics

SPNs exhibit somatic mutations in the β -catenin (CTNNB1) gene in 95% of cases [10].

Management

SPNs are considered as low-grade malignancies. Complete surgical resection can cure as many as 95% of patients. Metastasis to the peritoneum or liver may be encountered in 5–15% of cases [11].

Cystic Pancreatic Neuroendocrine Tumor (PanNET)

Cystic PanNETs are similar in sex distribution and can occur over a wide age range (23–91 years; mean, 52 years) just like their solid counterparts. Cystic PanNETs are mostly located in the tail of the pancreas. On imaging, these are unilocular cysts which can be difficult to differentiate from other pancreatic cysts [16]. On EUS, these tend to be thick-walled cysts [17].

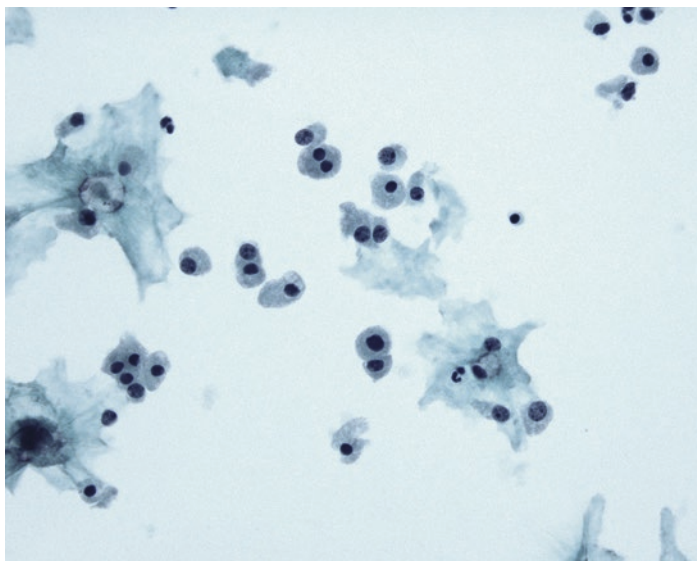


Fig. 9.8 Fine needle aspirate of cystic pancreatic neuroendocrine tumor reveals polygonal neoplastic cells with eccentrically placed nuclei and coarsely stippled chromatin in a background of histiocytes (Papanicolaou stain, ThinPrep, 400 \times)

Histologically, the cystic PanNETs are well demarcated and surrounded by a thin to thick fibrous capsule. The individual cells are typical of neuroendocrine morphology being characterized by monotonous polygonal cells with amphiphilic to eosinophilic cytoplasm and eccentrically placed nuclei with stippled chromatin. Mitotic figures tend to be rare, and tumor necrosis is unusual [16]. Cytology can make a specific diagnosis of cystic PanNET in as many as 71% of instances (Fig. 9.8). Immunohistochemistry for chromogranin and synaptophysin can assist in the differential diagnosis with SCAs and cystic acinar cell tumors [18]. A Ki-67 proliferation index is usually low in these tumors (range, 0.2–11%; mean, 1.8%) [16].

Cyst fluid CEA (range, 0.2 to >500 ng/mL; mean, 29.5 ng/mL) and amylase (mostly <500 U/L) levels are typically low in cystic PanNETs [18]. In terms of biologic behavior, several studies have

shown that cystic PanNETs have less aggressive biologic behavior as compared to the solid ones [16, 19, 20].

Nonneoplastic Cysts

Pseudocyst

Clinical Features and Imaging Findings

Most patients with pseudocysts have a history of prior pancreatitis. On imaging, it is a thin-walled unilocular cyst that frequently has internal debris and lacks a mural nodule. The adjoining pancreas may show features of pancreatitis. It should be emphasized that patients with IPMNs and other neoplastic pancreatic cysts can also present with acute pancreatitis.

Cytology

The aspirate mostly contains neutrophils and histiocytes (which could be hemosiderin laden). Extracellular yellow pigment has been reported in as many as 31% of pseudocyst samples and is considered to be a combination of hematoidin and bile pigment (Fig. 9.9). Occasionally, necrotic fat cells can be identified.

The cytologic findings in a pseudocyst can be associated with several diagnostic pitfalls. Contaminating gastrointestinal tract epithelium can result in a false interpretation of a neoplastic mucinous cyst. Additionally, a pseudocyst can reveal the presence of Alcian blue- and mucicarmine-positive material that can result in the misinterpretation of a neoplastic mucinous cyst. Clusters of ductal epithelium with reactive atypia can also be encountered which may be mistaken for malignancy. These cells may have enlarged nuclei with nuclear overlap but usually lack anisonucleosis to the extent of 1:4, and nuclear membranes tend to be smooth (Figs. 9.10 and 9.11).

The cytologic findings in a pseudocyst tend to be nonspecific and can overlap many a time with a neoplastic mucinous cyst.

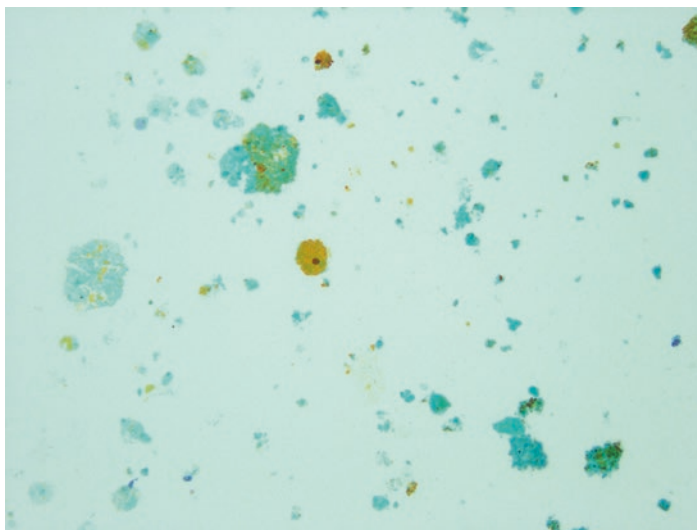


Fig. 9.9 Fine needle aspirate of pseudocyst usually reveals nonspecific findings. The presence of a yellow pigment is suggested as a surrogate marker for pseudocysts (Papanicolaou stain, ThinPrep, 200 \times)

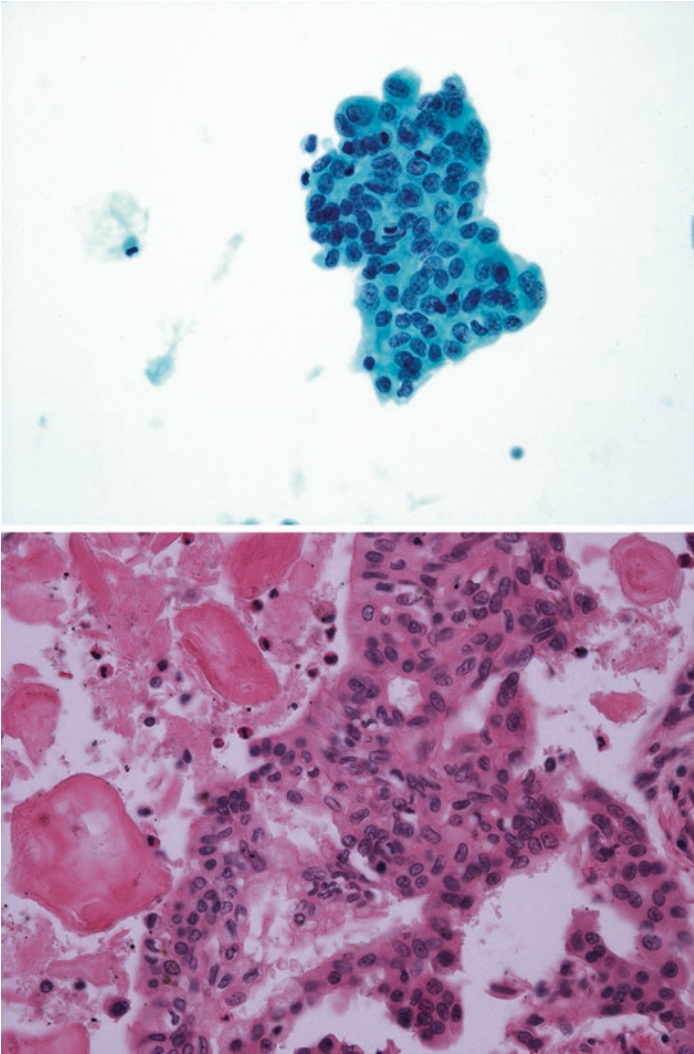
However, when interpreted in conjunction with appropriate clinical findings (a prior history of pancreatitis), imaging studies, and cyst fluid biochemistry, they support the diagnosis of a pseudocyst. The primary role of cytology in such instances is to exclude malignancy.

Ancillary Studies

The amylase level is >250 IU/ml in pseudocysts, and CEA tends to be low [21].

Management

Pseudocysts mostly resolve spontaneously. However, when they are associated with complications and large size, drainage is indicated. Drainage could be endoscopic, percutaneous, or surgical [22].



Figs. 9.10 and 9.11 Reactive ductal atypia in fine needle aspirate and excision of pseudocyst. The ductal epithelial cells show mild crowding with mild degree of anisonucleosis, fine chromatin, and smooth nuclear membranes (Papanicolaou stain, ThinPrep, 400 \times) (hematoxylin-eosin stain, 400 \times)

Lymphoepithelial Cyst (LEC)

Clinical Features and Imaging Findings

Lymphoepithelial cysts of the pancreas are rare, benign cysts that are lined by keratinizing squamous epithelium with adjoining lymphoid tissue. They usually occur in older men with male to female ratio of 4:1. The patients may be asymptomatic or may present with abdominal pain.

They can be intrapancreatic or peripancreatic and can be exophytic. On CT, a multilocular cyst on the surface of the pancreas with decreased attenuation is supportive of a lymphoepithelial cyst. LECs demonstrate hypointensity on T2 imaging and a high signal intensity on T1-weighted images. On EUS, these can appear as predominantly solid or multilocular or unilocular cysts. The imaging findings can be nonspecific and can overlap with other pancreatic cysts including pseudocysts and neoplastic mucinous cysts.

Cytology

The aspirate may be viscous, thick milky, creamy, or frothy. The cytologic smears are predominantly composed of keratinous debris and a variable number of anucleated and nucleated squamous cells. Plate-like cholesterol crystals may also be seen. Lymphocytes are usually sparse (Figs. 9.12 and 9.13). The differential diagnosis includes epidermoid cyst of the accessory spleen and dermoid cyst. The presence of contaminating gastrointestinal tract epithelium may be mistaken for neoplastic mucinous epithelium, and these cysts may be erroneously diagnosed as neoplastic mucinous cysts.

Ancillary Studies

The CEA level can be markedly elevated in lymphoepithelial cysts, and this is probably due to the expression of CEA by the squamous epithelium and presence of mucous cells in the lining epithelium of the cyst. As a result, lymphoepithelial cysts may be difficult to distinguish from neoplastic mucinous cysts.

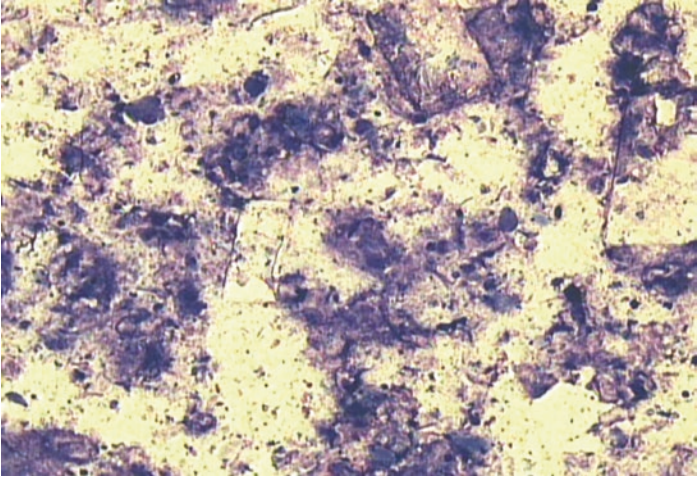


Fig. 9.12 Fine needle aspirate of lymphoepithelial cyst showing keratinous debris and cholesterol crystals (Diff-Quik stain, 100 \times)

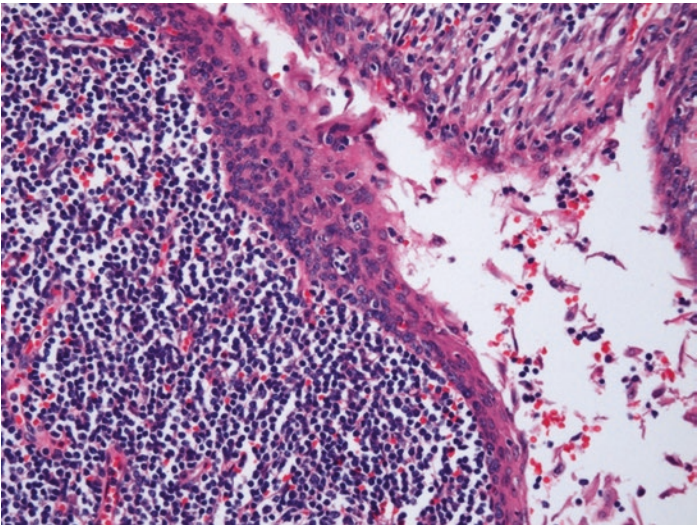


Fig. 9.13 Histology of lymphoepithelial cyst showing benign stratified squamous epithelial lining with an accompanying lymphoid infiltrate (hematoxylin-eosin stain, 200 \times)

Management

Asymptomatic patients are managed conservatively. It may be difficult to make a definitive diagnosis of lymphoepithelial cyst preoperatively. The cyst may be surgically resected due to the patient's symptoms or to exclude a premalignant/malignant cyst [23, 24].

Epidermoid Cyst of the Accessory Spleen

An epidermoid cyst arising within an intrapancreatic accessory spleen is a rare occurrence. These are almost exclusively located in the tail of the pancreas with size ranging from 1.5 to 11.5 cm and can be unilocular or multilocular. It has been hypothesized that these cysts may arise due to mesothelial inclusion with squamous metaplasia, as a by-product of a teratoma, or due to communication between the pancreatic ducts and an intrapancreatic accessory spleen.

On contrast-enhanced CT scan, the periphery of these lesions may show the same enhancement as that of the spleen in the arterial phase. On MRI, the cystic contents show high signal intensity on both T1- and T2-weighted images.

Histologically, the cyst is lined by keratinizing or non-keratinizing stratified squamous epithelium and is surrounded by normal splenic tissue. A fine needle aspiration (FNA) of an epidermoid cyst within an intrapancreatic accessory spleen can yield only inflammatory debris, but the presence of mature squamous epithelial cells with lack of malignant-appearing cells can assist in the differential diagnosis [25–27].

Retention Cyst

Obstruction and fibrosis of the pancreatic duct can result in upstream dilatation resulting in a retention cyst. The cyst lining epithelium is composed of low cuboidal or attenuated mucinous epithelium. The finding of an obstruction of the pancreatic duct can aid in the diagnosis of a retention cyst.

Squamoid Cyst of the Pancreatic Ducts (SCOP)

In 2007, Othman et al. reported a distinct type of squamous-lined pancreatic cyst termed squamoid cyst of the pancreatic ducts (SCOP). These are unilocular cystic dilatation of the ducts that usually contain muco-proteinaceous acidophilic acinar secretions forming concretions that suggests the role of a localized obstruction in their pathogenesis. No evidence of pancreatitis is present, however. The epithelial lining ranges from attenuated, flat squamoid to transitional to stratified squamous cells without keratinization. On immunohistochemistry, the cells forming the basal/parabasal region express p63, and the surface cells are positive for MUC-1 and MUC-6 (which are also expressed by intercalated duct cells). SCOP is thought to be a metaplastic cystic transformation beginning in the intercalated ducts [28]. Recently, Hanson et al. reported that SCOPs could be associated with elevated CEA levels and may be difficult to distinguish preoperatively from mucinous cysts [29].

Acinar Cell Cystadenoma

Acinar cell cystadenoma is a rare, benign cystic lesion of the pancreas. It may be detected incidentally or can present with abdominal pain. Imaging reveals a unilocular or multilocular cyst that may be located anywhere in the pancreas. Whether it is neoplastic or nonneoplastic is not clearly understood. Some authors have suggested alternative terminology, that is, cystic acinar transformation, for this entity.

Histologically, the cysts are lined by acinar cells (with apical bright-red zymogen granules) and ductal epithelium. No cytologic atypia, mitoses, necrosis, infiltrative growth, or associated invasive carcinoma is identified. Mucinous epithelium, akin to gastric foveolar-type epithelium, can also be seen.

On cytology, the acinar cells could be misinterpreted as PanNET cells derived from a neoplastic mucinous cyst or an adenocarcinoma. PAS with diastase stain can help highlight the apical cytoplasmic granules of an acinar cell cystadenoma. On immunohistochemistry, the acinar cells are positive for trypsin

and chymotrypsin and negative for neuroendocrine markers (synaptophysin, chromogranin, and CD56). Ki-67 labeling index is reportedly low (1–2%).

Cyst fluid CEA levels may be elevated and are probably due to the presence of mucinous epithelium in acinar cystadenomas. Amylase levels are elevated with a reported range of 73–252,788 U/L and a mean of 45,847.5 U/L [30, 31].

References

1. Terris B, Fukushima N, Hruban RH. Serous neoplasms of the pancreas. In: Bosman FT, Carneiro F, Hruban RH, Theise ND, editors. WHO classification of tumors of the digestive system. 4th ed. Lyon: IARC; 2010. p. 296–9.
2. Zhang XP, Yu ZX, Zhao YP, Dai MH. Current perspectives on pancreatic serous cystic neoplasms: diagnosis, management and beyond. *World J Gastrointest Surg.* 2016;8:202–11.
3. Tseng JF, Warshaw AL, Sahani DV, Lauwers GY, Rattner DW, Fernandez-del Castillo C. Serous cystadenoma of the pancreas: tumor growth rates and recommendations for treatment. *Ann Surg.* 2005;242:413–9.
4. Ishigami K, Nishie A, Asayama Y, Ushijima Y, Takayama Y, Fujita N, et al. Imaging pitfalls of pancreatic serous cystic neoplasm and its potential mimickers. *World J Radiol.* 2014;6:36–47. <https://doi.org/10.4329/wjr.v6.i3.36>.
5. Choi JY, Kim MJ, Lee JY, Lim JS, Chung JJ, Kim KW, et al. Typical and atypical manifestations of serous cystadenoma of the pancreas: imaging findings with pathologic correlation. *AJR Am J Roentgenol.* 2009;193:136–42. <https://doi.org/10.2214/AJR.08.1309>.
6. Belsley NA, Pitman MB, Lauwers GY, Brugge WR, Deshpande V. Serous cystadenoma of the pancreas: limitations and pitfalls of endoscopic ultrasound-guided fine-needle aspiration biopsy. *Cancer.* 2008;114:102–10. <https://doi.org/10.1002/cncr.23346>.
7. Lilo MT, VandenBussche CJ, Allison DB, Lennon AM, Younes BK, Hruban RH, et al. Serous cystadenoma of the pancreas: potentials and pitfalls of a preoperative cytopathologic diagnosis. *Acta Cytol.* 2017;61:27–33. <https://doi.org/10.1159/000452471>.
8. Salomao M, Remotti H, Allendorf JD, Poneris JM, Sethi A, Gonda TA, et al. Fine-needle aspirations of pancreatic serous cystadenomas: improving diagnostic yield with cell blocks and α -inhibin immunohistochemistry. *Cancer Cytopathol.* 2014;122:33–9.
9. Kaur G, Bakshi P, Singla V, Verma K. Clear cell neuroendocrine tumor of pancreas: endoscopic ultrasound-guided fine needle aspiration diagnosis of an uncommon variant. *Cytojournal.* 2016;13:7. <https://doi.org/10.4103/1742-6413.178995>.

10. Reid MD, Saka B, Balci S, Goldblum AS, Adsay NV. Molecular genetics of pancreatic neoplasms and their morphologic correlates: an update on recent advances and potential diagnostic applications. *Am J Clin Pathol*. 2014;141:168–80.
11. Kloppel G, Hruban RH, Klimstra DS, Maitra A, Morohoshi T, Notohara, et al. Solid pseudopapillary neoplasm of the pancreas. In: Bosman FT, Carneiro F, Hruban RH, Theise ND, editors. *WHO classification of tumors of the digestive system*. 4th ed. Lyon: IARC; 2010. p. 327–30.
12. Sunkara S, Williams TR, Myers DT, Kryvenko ON. Solid pseudopapillary tumours of the pancreas: spectrum of imaging findings with histopathological correlation. *Br J Radiol*. 2012;85:e1140–4. <https://doi.org/10.1259/bjr/20695686>.
13. Ohara Y, Oda T, Hashimoto S, Akashi Y, Miyamoto R, Enomoto T, et al. Pancreatic neuroendocrine tumor and solid-pseudopapillary neoplasm: key immunohistochemical profiles for differential diagnosis. *World J Gastroenterol*. 2016;22:8596–604.
14. Burford H, Baloch Z, Liu X, Jhala D, Siegal GP, Jhala N. E-cadherin/beta-catenin and CD10: a limited immunohistochemical panel to distinguish pancreatic endocrine neoplasm from solid pseudopapillary neoplasm of the pancreas on endoscopic ultrasound-guided fine-needle aspirates of the pancreas. *Am J Clin Pathol*. 2009;132:831–9.
15. Singhi AD, Lilo M, Hruban RH, Cressman KL, Fuhrer K, Seethala RR. Overexpression of lymphoid enhancer-binding factor 1 (LEF1) in solid-pseudopapillary neoplasms of the pancreas. *Mod Pathol*. 2014;27:1355–63.
16. Singhi AD, Chu LC, Tatsas AD, Shi C, Ellison TA, Fishman EK, et al. Cystic pancreatic neuroendocrine tumors: a clinicopathologic study. *Am J Surg Pathol*. 2012;36:1666–73. <https://doi.org/10.1097/PAS.0b013e31826a0048>.
17. Yoon WJ, Daglilar ES, Pitman MB, Brugge WR. Cystic pancreatic neuroendocrine tumors: endoscopic ultrasound and fine-needle aspiration characteristics. *Endoscopy*. 2013;45:189–94. <https://doi.org/10.1055/s-0032-1325990>.
18. Morales-Oyarvide V, Yoon WJ, Ingkakul T, Forcione DG, Casey BW, Brugge WR, et al. Cystic pancreatic neuroendocrine tumors: the value of cytology in preoperative diagnosis. *Cancer Cytopathol*. 2014;122:435–44. <https://doi.org/10.1002/cncy.21403>.
19. Cloyd JM, Kopecky KE, Norton JA, Kunz PL, Fisher GA, Visser BC, et al. Neuroendocrine tumors of the pancreas: degree of cystic component predicts prognosis. *Surgery*. 2016;160:708–13. <https://doi.org/10.1016/j.surg.2016.04.005>.
20. Ridiitiid W, Halawi H, DeWitt JM, Sherman S, LeBlanc J, McHenry L, et al. Cystic pancreatic neuroendocrine tumors: outcomes of preoperative endosonography-guided fine needle aspiration, and recurrence during long-term follow-up. *Endoscopy*. 2015;47:617–25. <https://doi.org/10.1055/s-0034-1391712>.

21. Gonzalez Obeso E, Murphy E, Brugge W, Deshpande V. Pseudocyst of the pancreas: the role of cytology and special stains for mucin. *Cancer*. 2009;117:101–7.
22. Aghdassi AA, Mayerle J, Kraft M, Sielenkämper AW, Heidecke CD, Lerch MM. Pancreatic pseudocysts—when and how to treat? *HPB (Oxford)*. 2006;8:432–41. <https://doi.org/10.1080/13651820600748012>.
23. Policarpio-Nicolas ML, Shami VM, Kahaleh M, Adams RB, Mallery S, Stanley MW, et al. Fine-needle aspiration cytology of pancreatic lymphoepithelial cysts. *Cancer*. 2006;108:501–6.
24. Raval JS, Zeh HJ, Moser AJ, Lee KK, Sanders MK, Navina S, et al. Pancreatic lymphoepithelial cysts express CEA and can contain mucous cells: potential pitfalls in the preoperative diagnosis. *Mod Pathol*. 2010;23:1467–76. <https://doi.org/10.1038/modpathol.2010.144>.
25. Adsay NV, Hasteh F, Cheng JD, Klimstra DS. Squamous-lined cysts of the pancreas: lymphoepithelial cysts, dermoid cysts (teratomas), and accessory-splenic epidermoid cysts. *Semin Diagn Pathol*. 2000;17:56–65.
26. Zavras N, Machairas N, Foukas P, Lazaris A, Patapis P, Machairas A. Epidermoid cyst of an intrapancreatic accessory spleen: a case report and literature review. *World J Surg Oncol*. 2014;12:92. <https://doi.org/10.1186/1477-7819-12-92>.
27. Horn AJ, Lele SM. Epidermoid cyst occurring within an intrapancreatic accessory spleen. A case report and review of the literature. *JOP*. 2011;12:279–82.
28. Othman M, Basturk O, Groisman G, Krasinskas A, Adsay NV. Squamoid cyst of pancreatic ducts: a distinct type of cystic lesion in the pancreas. *Am J Surg Pathol*. 2007;31:291–7.
29. Hanson JA, Salem RR, Mitchell KA. Squamoid cyst of pancreatic ducts: a case series describing novel immunohistochemistry, cytology, and quantitative cyst fluid chemistry. *Arch Pathol Lab Med*. 2014;138:270–3. <https://doi.org/10.5858/arpa.2012-0667-CR>.
30. Singhi AD, Norwood S, Liu TC, Sharma R, Wolfgang CL, Schulick RD, et al. Acinar cell cystadenoma of the pancreas: a benign neoplasm or non-neoplastic ballooning of acinar and ductal epithelium? *Am J Surg Pathol*. 2013;37:1329–35. <https://doi.org/10.1097/PAS.0b013e3182a1ad72>.
31. Chen AL, Misdraji J, Brugge WR, Ferrone CR, Pitman MB. Acinar cell cystadenoma: a challenging cytology diagnosis, facilitated by moray[®] micro-forceps biopsy. *Diagn Cytopathol*. 2017;45:557–60. <https://doi.org/10.1002/dc.23693>.



Metastases to the Pancreas

10

Momin T. Siddiqui

Introduction

Metastasis to the pancreas is an uncommon occurrence with an incidence on fine needle aspiration (FNA) cytology ranging from 0.7% to 11.1% and comprising 1.8–10.8% of all pancreatic malignancies [1–16]. The primary tumors can arise from a diverse and wide group of organs which can include most commonly the kidney and the lung and less commonly the gastrointestinal tract, liver, breast, ovaries, and thyroid [17, 18]. In addition, metastatic melanomas, malignant lymphomas, and neuroendocrine tumors arising from different primary sources have also been diagnosed in the pancreas [17, 18]. A cytopathologist should be aware that even with these diverse groups of tumors, renal cell carcinoma and tumors arising from the lung remain the largest groups of tumors which have been reported to metastasize to the pancreas. In most instances of patient clinical workup, metastatic disease to the pancreas is usually found to be part of widespread and disseminated disease rather than being a solitary presentation [9, 14]. However, metastasis to the pancreas can also present as a solitary tumor many years after the primary malignancy was initially diagnosed [9, 14]. Hence, some of these diagnoses are rendered after a long latency period, after the primary diagnosis

M. T. Siddiqui (✉)

Department of Pathology and Laboratory Medicine, Weill-Cornell Medicine, New York Presbyterian Hospital, New York, NY, USA
e-mail: mos9084@med.cornell.edu

was rendered. Radiographic studies, which can include CT scan or, more commonly, endoscopic ultrasound-guided fine needle aspiration (EUS-FNA), are currently the mainstay to evaluate and diagnose these tumors [18]. EUS-FNA ensures a high degree of safety for the patients, is cost-effective, and leads to minimal morbidity in patients. EUS-FNA in experienced hands also ensures accuracy in diagnosing metastatic disease to the pancreas, which is extremely important for clinical staging and appropriate management of the patient [17, 18].

Metastatic Renal Cell Carcinoma

Renal cell carcinoma has been cited as one of the most common tumors to metastasize to the pancreas [1–16]. The prevalence rate has been found to be wide from 8% to 64% of metastatic tumors to the pancreas [2–16]. It can have a long latency period after the primary renal malignancy diagnosis and can be noted as long as 36 years after the primary diagnosis was rendered [18]. Hematogenous spread is most likely involved in metastatic renal cell carcinoma to the pancreas. The key features of metastatic renal cell carcinoma include large polygonal cells with clear, foamy, granular, or vacuolated cytoplasm (Figs. 10.1 and 10.2). The nuclei are round to oval with prominent nucleoli present (Fig. 10.3). Immunohistochemical staining (IHCS) is helpful in separating metastatic renal cell carcinoma from adenocarcinoma of primary pancreatobiliary origin. CD10 [9, 10, 14], RCC [7, 9, 11], PAX-8 [14, 16], and CAIX [16] are helpful immunohistochemical markers which will help highlight metastatic malignant cells (Figs. 10.4 and 10.5).

Metastatic Pulmonary Non-small Cell Carcinoma

The literature has initially indicated that the lung was the most common primary site of pancreatic metastases, followed by metastases from the kidney [1–18]. However, other studies have indicated that the lung as the primary site has been surpassed by the kidney [9, 13, 14]. Pulmonary non-small cell carcinomas metastasizing to the pancreas can range from well- to poorly differentiated adenocarcinomas and squamous cell carcinomas, which may make it difficult to differentiate them from primary pancreatobiliary adenocarcino-

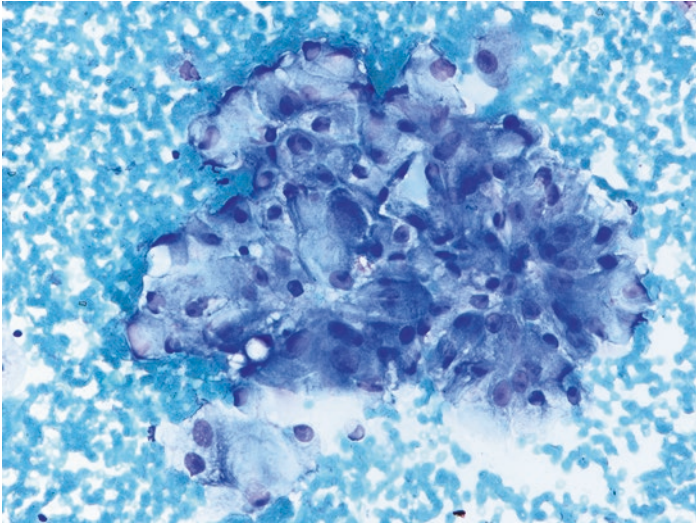


Fig. 10.1 Metastatic renal cell carcinoma with large polygonal cells with clear and granular cytoplasm (Diff-Quik stain $\times 40$)

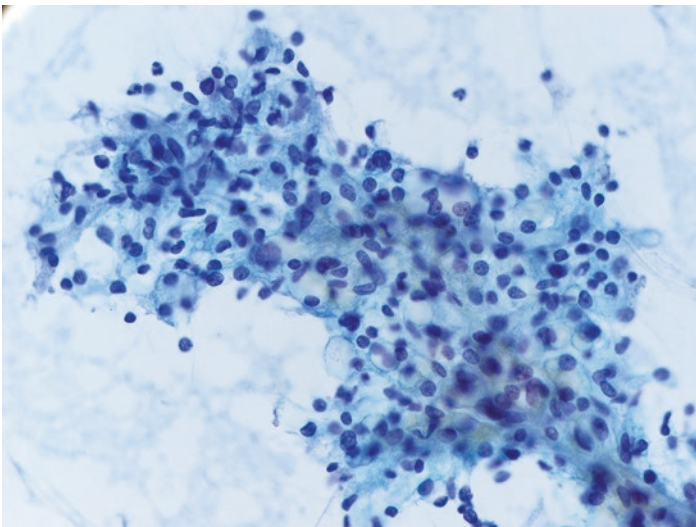


Fig. 10.2 The tumor cells show clear cytoplasm with large nuclei. Blood vessels are seen traversing in between the tumor cells (Papanicolaou stain $\times 40$)

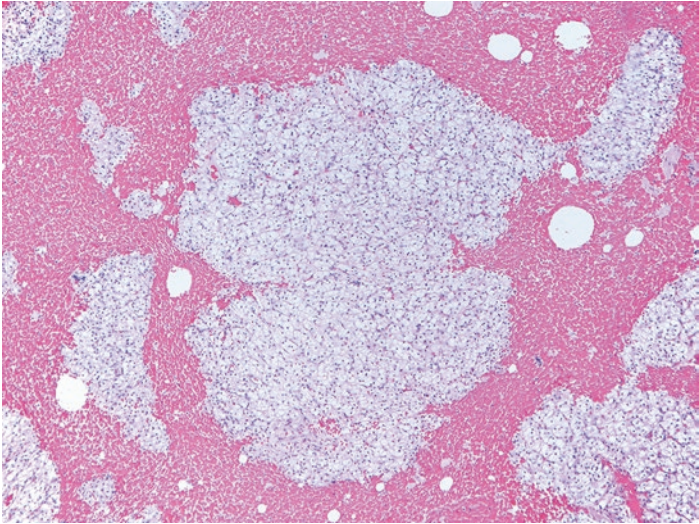


Fig. 10.3 Numerous sheets of cells representing metastatic renal cell carcinoma with clear cytoplasm in a cell block (H&E stain $\times 10$)

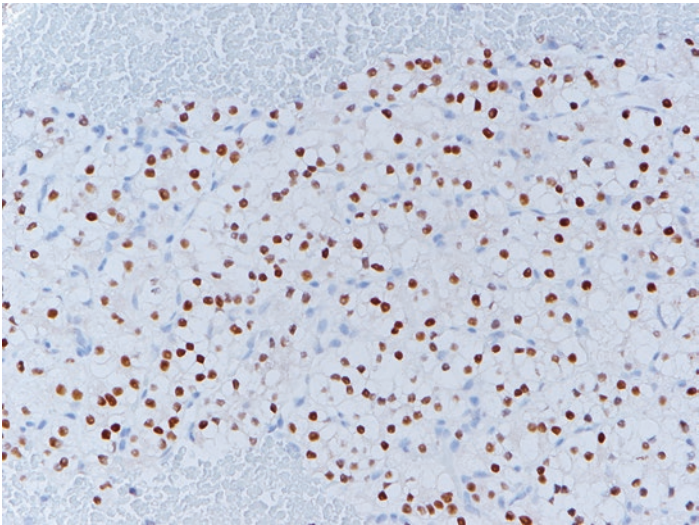


Fig. 10.4 Metastatic renal cell carcinoma showing positive nuclear staining with PAX-8 (IHCS $\times 40$)

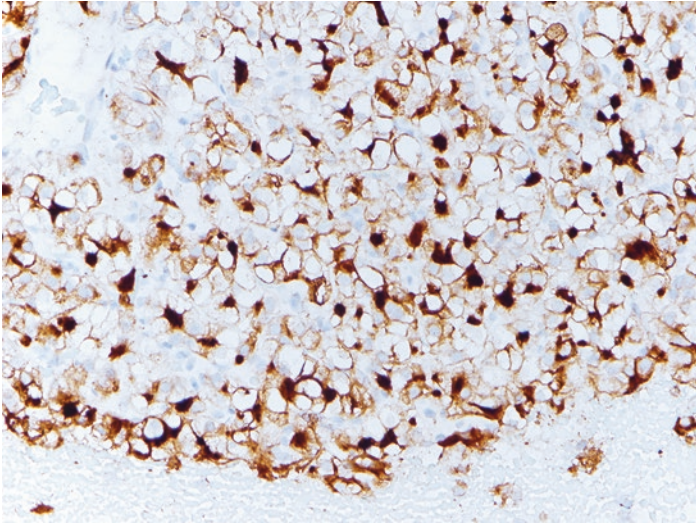


Fig. 10.5 CD10 staining shows cytoplasmic staining for metastatic renal cell carcinoma (IHCs $\times 40$)

mas on morphology alone [3, 8, 13]. The smears will show a wide range of cytomorphologic features depending on the differentiation of the primary tumor. Well- and moderately differentiated adenocarcinoma would exhibit features of glandular differentiation, while poorly differentiated adenocarcinoma would comprise malignant cells with high nuclear to cytoplasmic ratio and prominent nucleoli (Figs. 10.6, 10.7, 10.8, and 10.9). Similarly, metastatic squamous cell carcinoma would show keratinization in well-differentiated metastases, while poorly differentiated tumors would lack keratinization and would comprise tumor cells with indistinct borders, pleomorphic nuclei, and markedly irregular nuclear membranes (Figs. 10.10, 10.11, 10.12, and 10.13). Immunohistochemical staining will be helpful in confirming the diagnosis. TTF-1 and napsin A staining will confirm a diagnosis of metastatic lung adenocarcinoma, whereas p40 staining will confirm a diagnosis of metastatic squamous cell carcinoma (Figs. 10.9 and 10.13) [8, 11, 16, 19]. It is important to recognize that the primary features of these metastatic tumors may overlap with primary pancreatobiliary malignancy; and this requires a review of clinical history, radiologic findings, and

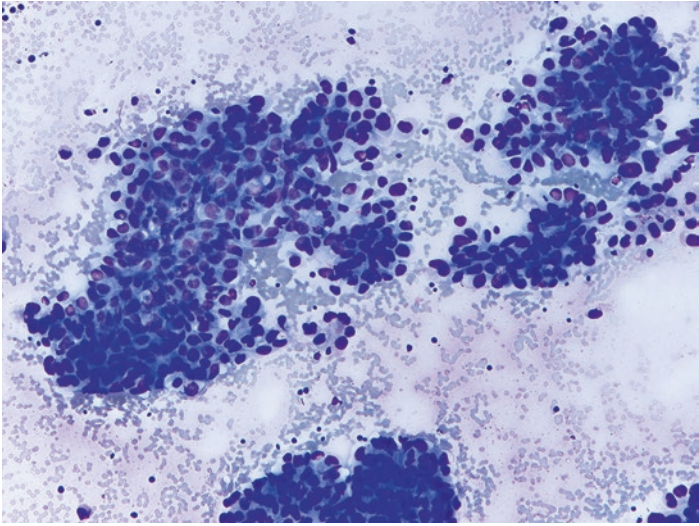


Fig. 10.6 Metastatic lung adenocarcinoma exhibiting focal gland formation and high nuclear to cytoplasmic ratio (Diff-Quik stain $\times 20$)

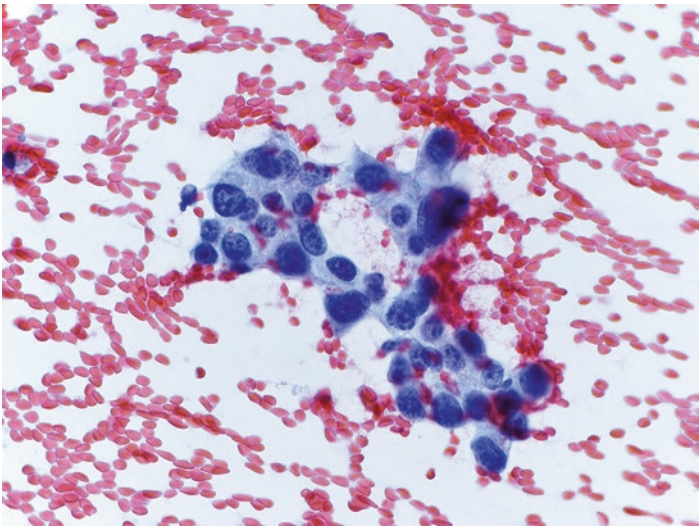


Fig. 10.7 Metastatic lung adenocarcinoma with delicate cytoplasm and high nuclear to cytoplasmic ratio. The tumor cells show nuclear hyperchromasia and prominent nucleoli (Papanicolaou stain $\times 40$)

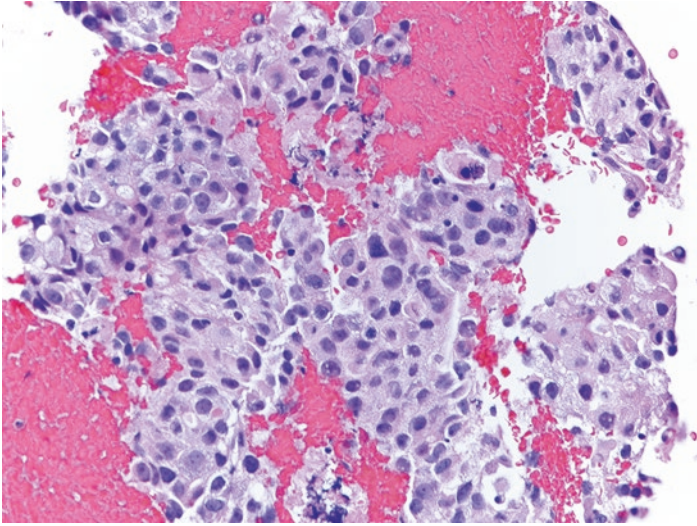


Fig. 10.8 A cell block from an aspirate with metastatic lung adenocarcinoma showing focal cytoplasmic vacuolation (H&E stain $\times 40$)

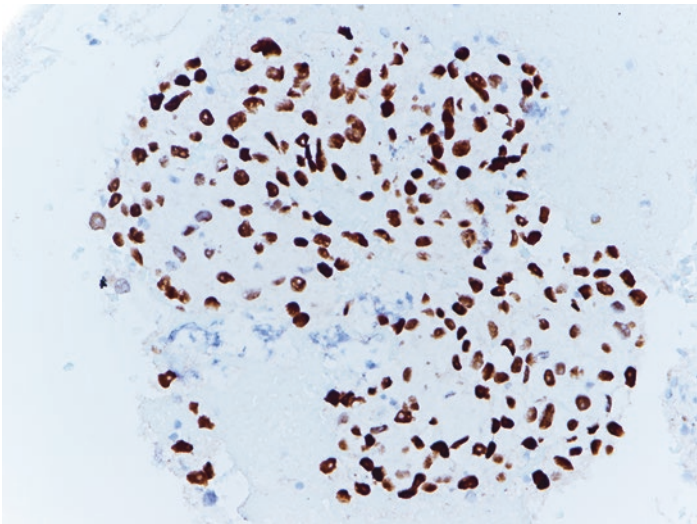


Fig. 10.9 TTF-1 staining confirms the diagnosis of metastatic adenocarcinoma. The patient had a known lung primary tumor which was also positive for TTF-1 staining (IHCS $\times 40$)

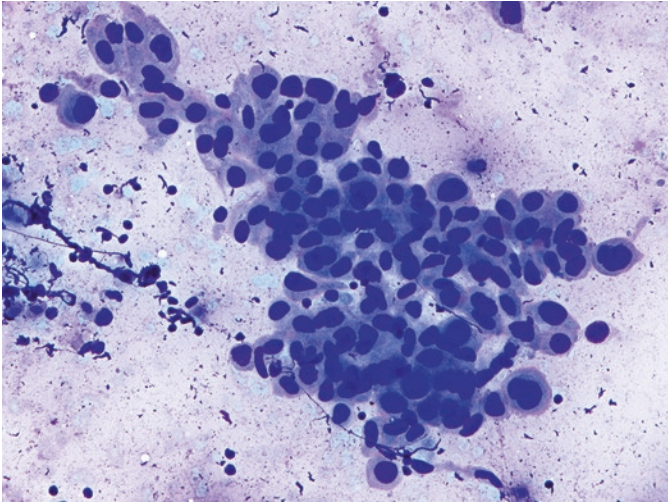


Fig. 10.10 A patient with known history of lung squamous cell carcinoma with metastatic tumor cells in the pancreas. The tumor cells show dense cytoplasm and hyperchromatic nuclei with irregular nuclear membranes. (Diff-Quik stain $\times 40$)

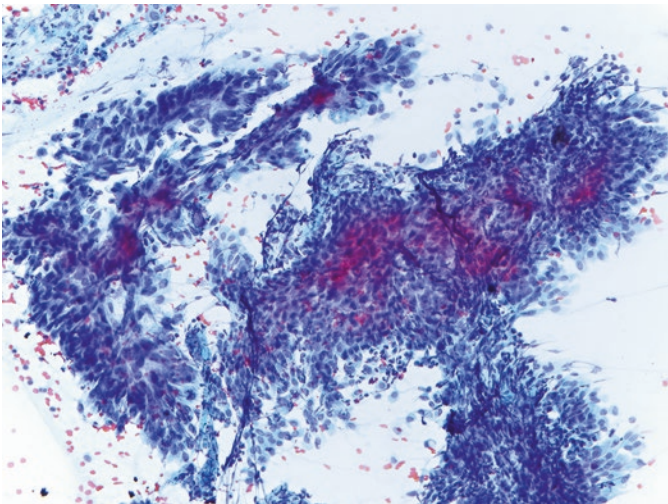


Fig. 10.11 Poorly differentiated metastatic squamous cell carcinoma lacking keratinization would comprise tumor cells with indistinct borders, pleomorphic nuclei, and markedly irregular nuclear membranes (Papanicolaou stain $\times 20$)

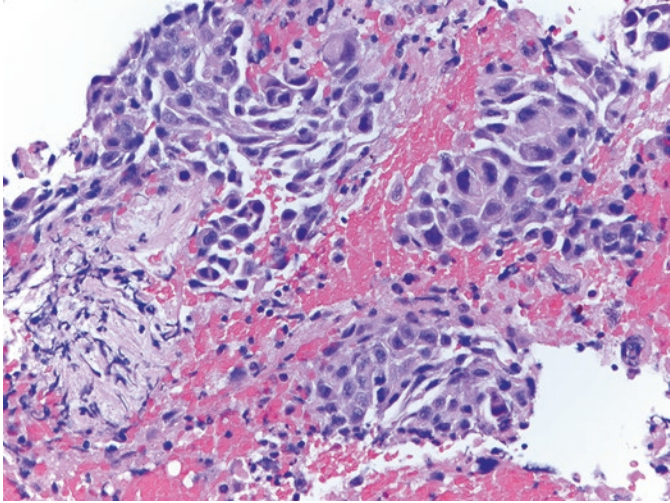


Fig. 10.12 A cell block from an aspirate with metastatic lung squamous cell carcinoma. The tumor cells are arranged in sheets with intercellular bridges apparent in between a few cells. The nuclei display characteristic hyperchromasia (H&E $\times 40$)

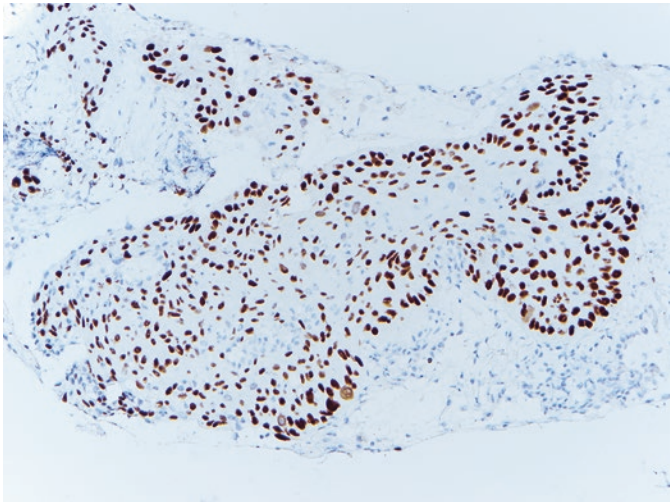


Fig. 10.13 A p40-positive nuclear stain would confirm a diagnosis of squamous cell carcinoma in a cell block (IHCS $\times 20$)

performance of immunohistochemical staining to separate the metastasis from a primary pancreatic malignancy.

Metastatic Neuroendocrine Carcinoma

Metastatic neuroendocrine carcinoma is also a malignancy that can be encountered in the pancreas. The majority of them are small cell neuroendocrine carcinomas arising from the lung (Figs. 10.14, 10.15, 10.16, 10.17, and 10.18) [4–14, 16]. The smears will show small- to intermediate-size cells with high nuclear to cytoplasmic ratio and hyperchromatic nuclei and frequently present crush artifact due to the fragility of the cells (Figs. 10.14 and 10.15). It is difficult to distinguish metastatic lung neuroendocrine carcinoma from a primary pancreatobiliary neuroendocrine carcinoma based on cytomorphol-

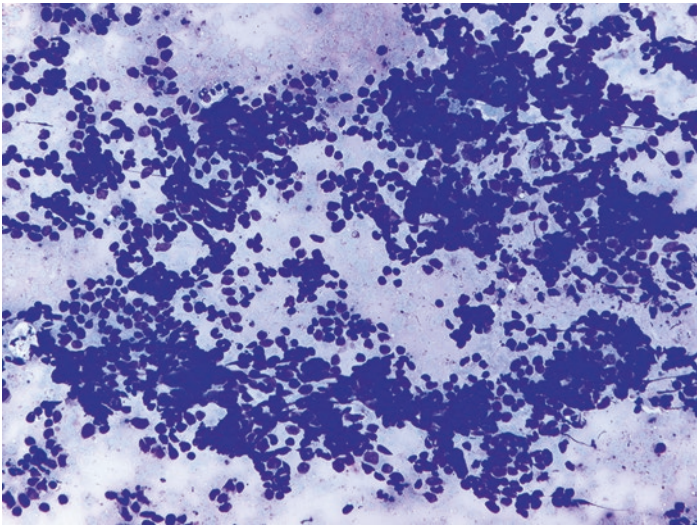


Fig. 10.14 The smears from a metastatic small cell carcinoma will show small- to intermediate-size cells with high nuclear to cytoplasmic ratio. The small cells are two to three times the size of a mature lymphocyte with rare intermediate-size cells being three to four times larger than a mature lymphocyte (Diff-Quik stain $\times 20$)

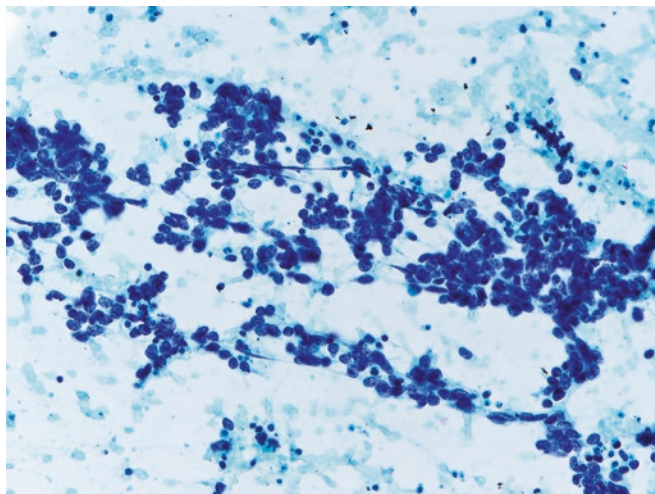


Fig. 10.15 Metastatic small cell carcinoma showing tumor cell molding and scant cytoplasm, with salt and pepper chromatin (Papanicolaou stain $\times 20$)

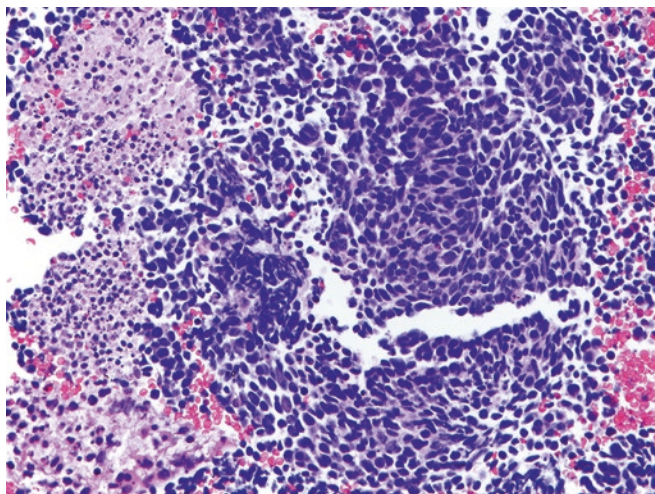


Fig. 10.16 A cell block from an aspirate showing metastatic small cell neuroendocrine carcinoma with nuclear molding and scant cytoplasm. Extensive necrosis in the background is also identified (H&E $\times 20$)

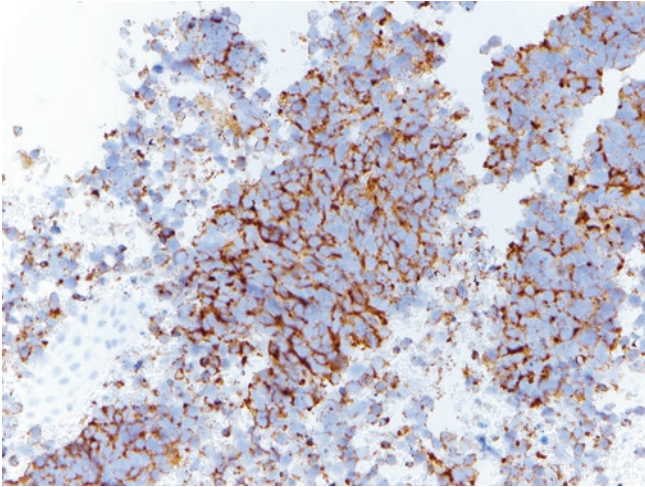


Fig. 10.17 Synaptophysin cytoplasmic staining of tumor cells from a patient with metastatic small cell neuroendocrine carcinoma from the lung (IHCS $\times 20$)

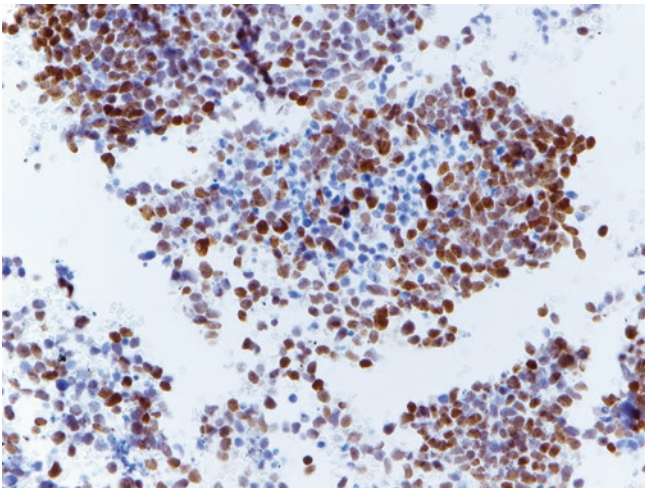


Fig. 10.18 TTF-1 nuclear staining is noted in approximately 90% of small cell neuroendocrine carcinomas of the lung. TTF-1 staining cannot be reliably used to confirm lung metastasis and would require clinical and radiologic confirmation of a primary lung tumor, since a small percentage of primary pancreatic small cell neuroendocrine carcinomas can also express it (IHCS $\times 20$)

ogy alone. Neuroendocrine carcinoma would show a variable amount of immunoreactivity for synaptophysin, chromogranin, and CD56 staining; and these stains will help in confirming the diagnosis (Fig. 10.17) [5, 16, 17, 18]. The main cytomorphologic challenge with these tumors is distinguishing metastatic from primary neuroendocrine carcinoma of the pancreas. Lung and pancreatic neuroendocrine malignancies are sensitive to different chemotherapeutic agents due to which accurately identifying the primary site of origin is very important. TTF-1 is noted in approximately 90% of small cell neuroendocrine carcinomas of the lung; however, a small percentage of primary pancreatic small cell neuroendocrine carcinomas of the pancreas are also known to show TTF-1 immunoreactivity (Fig. 10.18) [9, 13, 14, 17, 18]. Hence, TTF-1 staining cannot be reliably used to confirm lung metastasis and would require clinical and radiologic confirmation of a primary lung tumor.

Metastatic Gastrointestinal and Hepatocellular Carcinoma

Tumors arising from the gastrointestinal tract have also been diagnosed on pancreatic fine needle aspirations [16–18]. Typically, these comprise adenocarcinomas which can arise from sites including the stomach and colon. The aspirate will comprise abundant mucin with variable cellularity [4, 5, 11]. The tumor cells can be single and signet ring-shaped in the case of a primary gastric origin, whereas colonic primary tumor cells will show sheets and clusters with a variable degree of differentiation. CDX-2 staining can be helpful in characterizing these metastatic tumors, but can lack both sensitivity and specificity [17, 18]. Clinical history and radiology features play an important role in separating these metastatic tumors from those of primary pancreatobiliary origin. Hepatocellular carcinoma can also be rarely identified in pancreatic aspirates (Figs. 10.19, 10.20, and 10.21). The tumor cells are polygonal and show a variable degree of differentiation. The cytoplasm tends to be granular with large nuclei and prominent nucleoli. A positive arginase-1 immunohistochemical staining will confirm the diagnosis of metastatic hepatocellular carcinoma in most pancreatic aspirations (Fig. 10.22).

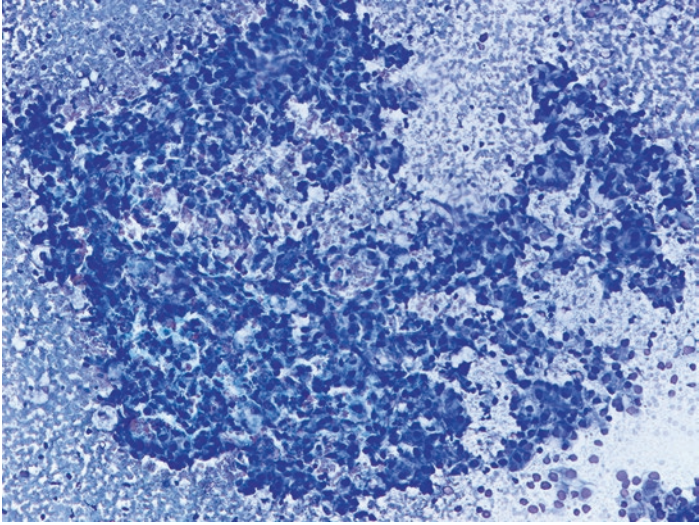


Fig. 10.19 Metastatic hepatocellular carcinoma with polygonal cells with granular cytoplasm (Diff-Quik stain $\times 20$)

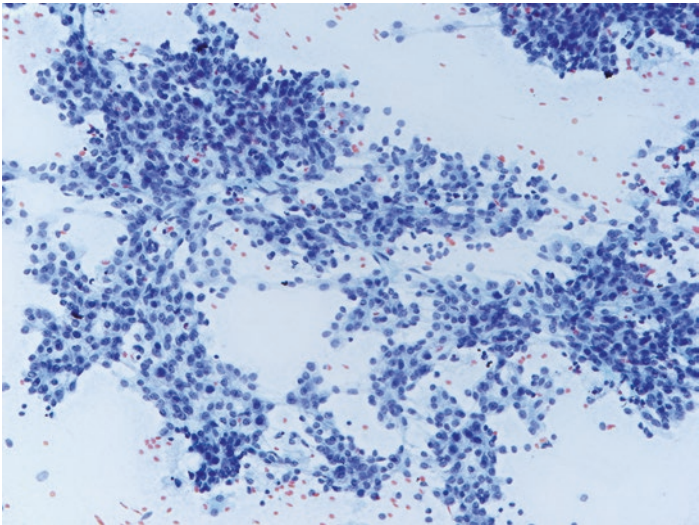


Fig. 10.20 Fine capillaries are seen separating the tumor cells from a patient with metastatic hepatocellular carcinoma. The cytoplasm of the tumor cells is granular with round and oval nuclei (Papanicolaou stain $\times 20$)

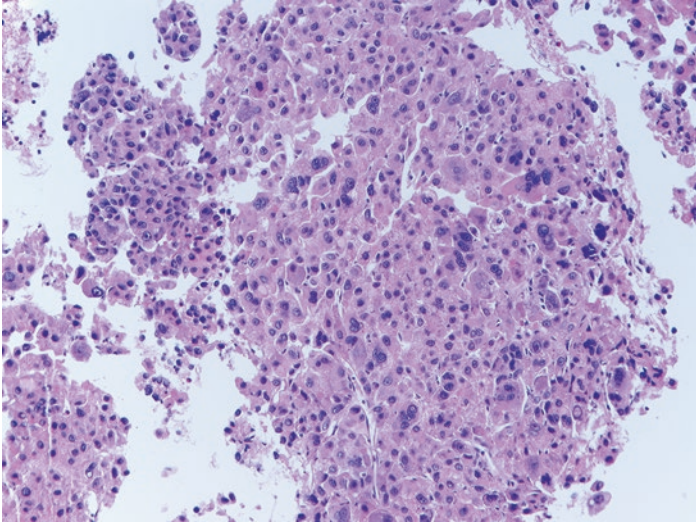


Fig. 10.21 A cell block from an aspirate with metastatic hepatocellular carcinoma. The tumor cells are intermediate to large in size. The nuclei display prominent nuclei and focal inclusions (H&E $\times 20$)

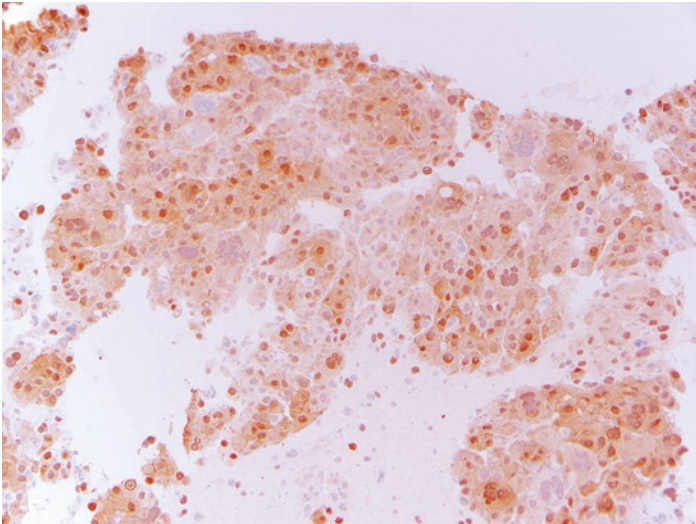


Fig. 10.22 Staining with arginase-1 will confirm a diagnosis of metastatic hepatocellular carcinoma (IHCS $\times 20$)

Metastatic Malignant Melanoma

Metastatic malignant melanoma has also been identified as a common metastatic tumor to the pancreas [5–7, 13]. On fine needle aspiration, metastatic malignant melanomas are hypercellular and comprise dyscohesive cells, which may range from plasmacytoid to pleomorphic and round to spindle (Fig. 10.23). Large nuclei with prominent nucleoli are also present (Fig. 10.24). Intranuclear cytoplasmic pseudoinclusions can also be identified and can be helpful in diagnosing metastatic malignant melanoma. The tumor cells may also show abundant melanin pigment which may also be dispersed in the background. These cytomorphologic features and additional ancillary immunohistochemical staining with HMB-45, S-100 protein, melan-A, MART-1, and SOX-10 will help in confirming the diagnosis [6–8, 12–14, 20].

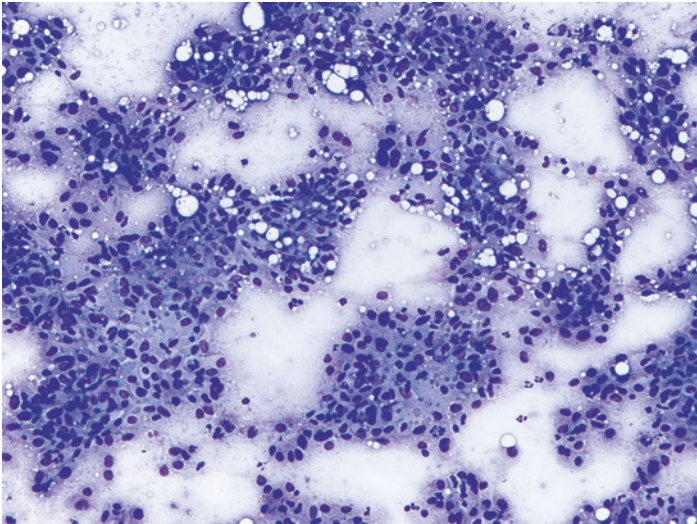


Fig. 10.23 Metastatic malignant melanoma will exhibit a variety of cell shapes and sizes. The tumor cells are round, oval, and spindle (Diff-Quik $\times 20$)

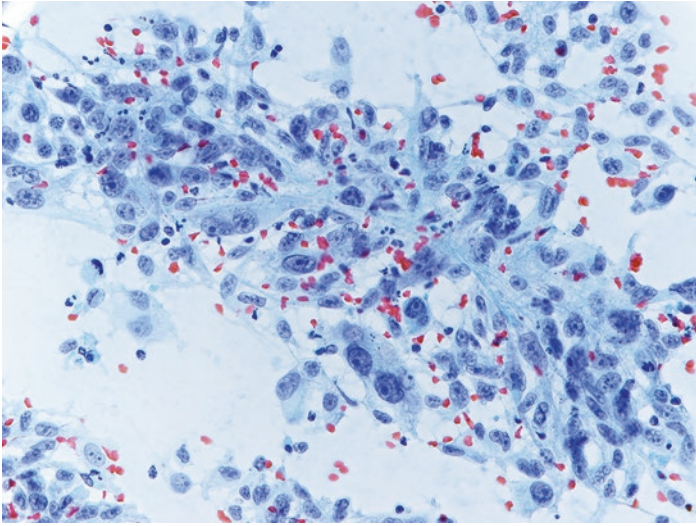


Fig. 10.24 Metastatic malignant melanoma with large prominent nuclei with enlarged prominent nucleoli is noted in this aspirate with an unknown primary site. Immunohistochemical staining with HMB-45, S-100 protein, and SOX-10 can confirm the diagnosis (IHCS $\times 40$)

References

1. Benning TL, Silverman JF, Berns LA, Geisinger KR. Fine needle aspiration of metastatic and hematologic malignancies clinically mimicking pancreatic carcinoma. *Acta Cytol.* 1992;36:471–6.
2. Carson HJ, Green LK, Castelli MJ, Reyes CV, Prinz RA, Gattuso P. Utilization of fine-needle aspiration biopsy in the diagnosis of metastatic tumors to the pancreas. *Diagn Cytopathol.* 1995;12:8–13.
3. Fritscher-Ravens A, Sriram PV, Krause C, et al. Detection of pancreatic metastases by EUS-guided fine-needle aspiration. *Gastrointest Endosc.* 2001;53:65–70.
4. Mesa H, Stelow EB, Stanley MW, Mallery S, Lai R, Bardales RH. Diagnosis of non-primary pancreatic neoplasms by endoscopic ultrasound-guided fine-needle aspiration. *Diagn Cytopathol.* 2004;31:313–8.

5. Volmar KE, Jones CK, Xie HB. Metastases in the pancreas from Non-hematologic neoplasms: report of 20 cases evaluated by fine needle aspiration. *Diagn Cytopathol.* 2004;31:216–20.
6. DeWitt J, Jewell P, Leblanc J, et al. EUS-guided FNA of pancreatic metastases: a multicenter experience. *Gastrointest Endosc.* 2005;61:689–96.
7. Gilbert CM, Monaco SE, Cooper ST, Khalbuss WE. Endoscopic ultrasound-guided fine-needle aspiration of metastases to the pancreas: a study of 25 cases. *Cytojournal.* 2011;8:7.
8. Hijioka S, Matsuo K, Mizuno N, et al. Role of endoscopic ultrasound and endoscopic ultrasound-guided fine-needle aspiration in diagnosing metastasis to the pancreas: a tertiary center experience. *Pancreatol.* 2011;11:390–8.
9. Layfield LJ, Hirschowitz SL, Adler DG. Metastatic disease to the pancreas documented by endoscopic ultrasound guided fine-needle aspiration: a seven-year experience. *Diagn Cytopathol.* 2012;40:228–33.
10. Ardengh JC, Lopes CV, Kemp R, Venco F, de Lima-Filho ER, dos Santos JS. Accuracy of endoscopic ultrasound-guided fine-needle aspiration in the suspicion of pancreatic metastases. *BMC Gastroenterol.* 2013;13:63.
11. Atiq M, Bhutani MS, Ross WA, et al. Role of endoscopic ultrasonography in evaluation of metastatic lesions to the pancreas: a tertiary cancer center experience. *Pancreas.* 2013;42:516–23.
12. El Hajj II, LeBlanc JK, Sherman S, et al. Endoscopic ultrasound guided biopsy of pancreatic metastases: a large single-center experience. *Pancreas.* 2013;42:524–30.
13. Olson MT, Wakely PE Jr, Ali SZ. Metastases to the pancreas diagnosed by fine-needle aspiration. *Acta Cytol.* 2013;57:473–80.
14. Waters L, Si Q, Caraway N, Mody D, Staerkel G, Sneige N. Secondary tumors of the pancreas diagnosed by endoscopic ultrasound guided fine-needle aspiration: a 10-year experience. *Diagn Cytopathol.* 2014;42:738–43.
15. Smith AL, Odronic SI, Springer BS, Reynolds JP. Solid tumor metastases to the pancreas diagnosed by FNA: a single-institution experience and review of the literature. *Cancer Cytopathol.* 2015;123:347–55.
16. Alomari AK, Ustun B, Aslanian HR, Ge X, Chhieng D, Cai G. Endoscopic ultrasound-guided fine-needle aspiration diagnosis of secondary tumors involving the pancreas: an institution's experience. *Cytojournal.* 2016;13:1.
17. Raymond SLT, Yugawa D, Chang KHF, Ena B, Tauchi-Nishi PS. Metastatic neoplasms to the pancreas diagnosed by fine needle aspiration/biopsy cytology: a 15-year retrospective analysis. *Diagn Cytopathol.* 2017;45:771–83.
18. Hou Y, Rulong S, Tonkovich D, Li Z. Endoscopic ultrasound guided fine needle aspiration diagnosis of secondary tumors involving pancreas: an institution's experience. *J Am Soc Cytopathol.* 2018;7:261–7.

19. Vogt AP, Cohen C, Siddiqui MT. p40 (Δ Np63) is more specific than p63 and cytokeratin 5 in identifying squamous cell carcinoma of bronchopulmonary origin: a review and comparative analysis. *Diagn Cytopathol.* 2014;42(5):453–8.
20. Ko HM, Saieg MA, da Cunha Santos G, Kamel-Reid S, Boerner SL, Geddie WR. Use of cytological samples of metastatic melanoma for ancillary studies. *Cytopathology.* 2017;28(3):221–7.



Abha Goyal

Introduction

The majority of biliary strictures are malignant, the most common malignancies being pancreatic ductal adenocarcinomas, cholangiocarcinomas, and peri-ampullary carcinomas. Benign etiologies for bile duct strictures include chronic pancreatitis, choledocholithiasis, primary sclerosing cholangitis, IgG4-related sclerosing cholangitis, and iatrogenic bile duct injury (following cholecystectomy and liver transplantation) [1, 2].

The malignancies of the pancreatico-biliary tract, ductal adenocarcinomas and cholangiocarcinomas, are associated with a very poor prognosis. Based on the most recent Surveillance, Epidemiology, and End Results data, the overall 5-year survival for pancreatic cancer is 8.5%. However, for cancer which is localized, that is, confined to the pancreas, the 5-year survival is 34.3% [3]. The prognosis for extrahepatic biliary cancer is similar with the 5-year survival being approximately 30% if the cancer is resectable. A definitive diagnosis of malignancy aids in early treatment if the tumor is resectable and, if not, helps in planning palliative care [4].

A. Goyal (✉)

Department of Pathology and Laboratory Medicine, Weill-Cornell Medicine, New York Presbyterian Hospital, New York, NY, USA
e-mail: abg9017@med.cornell.edu

The determination of biliary strictures as benign or malignant is challenging in clinical practice. Several imaging modalities have been studied for the differentiation between benign and malignant biliary strictures. Endoscopic retrograde cholangiopancreatography (ERCP) has shown comparable sensitivity (85%) and specificity (75%) to magnetic resonance cholangiopancreatography (MRCP) (sensitivity 85%, specificity 71%) in the diagnosis of malignant biliary strictures. ERCP not only provides the location and extent of the biliary stricture but has the added advantage of allowing sampling for pathologic examination. Histologic sampling in this area is difficult due to high rate of complications and is also associated with significant artifacts from tissue crushing and distortion. For evaluation of pancreatic duct and bile duct strictures, endoscopic retrograde cholangiopancreatography (ERCP)-guided brush cytology is considered the preferred method. The brushings sample a much larger area as compared to a biopsy and are associated with fewer complications [5]. Bile duct brush cytology has special value in the surveillance of patients with primary sclerosing cholangitis. This condition incurs a high risk of developing cholangiocarcinoma with the lifetime occurrence varying from 5% to 36%. The early detection of malignancy in these patients may improve survival by enabling a liver transplantation [6].

The specificity of brush cytology for the diagnosis of pancreatobiliary tract malignancy is >95%, but the sensitivity is suboptimal, ranging from 30% to 85% [7–11]. A 2015 meta-analysis of nine studies found that the sensitivity of brush cytology and intraductal biopsy in diagnosing malignancy was 45% and 48%, respectively. A combination of the two techniques resulted in a modest increase in sensitivity to 59.4%. However, the specificity of both techniques approached 100% [12].

The distinct advantage of biopsies lies in their ability to provide subepithelial stroma that can help in recognizing stromal invasion. Mucosal atypia can be difficult to categorize as reactive or neoplastic, especially with a history of an indwelling stent. The value of biliary biopsies has been variably reported. Different approaches for tissue acquisition have been found useful including combined brushing and biopsy, biopsy follow-

ing negative cytology, and biopsy only. The varying results could be related to differences in sampling and interpretation [13–16].

Role of EUS-FNA

Radiologically evident pancreatic masses are usually sampled by fine needle aspiration under endoscopic ultrasound guidance. For bile duct strictures, the sensitivity of EUS-FNA is much higher for diagnosing distal malignant bile duct strictures as compared to that for proximal ones. The overall sensitivity of EUS-FNA for the diagnosis of cholangiocarcinoma has been shown to be 73%, being significantly higher in distal compared to proximal cholangiocarcinoma (81% vs. 59%, respectively). It is also superior to ERCP in tissue sampling, especially for pancreatic masses with an overall accuracy and sensitivity of 94% and 94% for EUS-FNA and 53% and 50% for ERCP sampling, respectively [17].

EUS-FNA may provide a diagnosis of malignancy when ERCP sampling is negative or indeterminate and in patients in whom cross-sectional imaging does not reveal a mass. It is also important in sampling of lymph node metastases. Therefore, EUS-FNA can also prove useful to the diagnostic armamentarium in patients with suspected cholangiocarcinoma [18].

Sample Preparation Methods

Typically, the brush is guided through a stricture over a wire and positioned across the stricture. The brush scrapes material from the superficial mucosa, and it is retracted into a sheath. To retrieve material from the brush, the brush is opened outside of the sheath to expose the bristles. The brush may be placed against a glass slide to prepare direct smears. Thereafter, the brush is cut from the catheter and placed in a fixative solution. In the laboratory, the sample is agitated, and usually a ThinPrep preparation is prepared. Any residual material may be employed for cell block preparation following fixation in formalin [19].

The main advantage of the ThinPrep over direct smears has been the elimination of air-drying artifact and diminished effect of obscuring blood elements and inflammation that are frequently encountered with smears. In addition, it results in a greater diagnostic cell yield; and due to enhanced alcohol fixation, the cells are better preserved with improved chromatin detail [20].

Cytologic Features

Normal Bile Duct Epithelium

Normal biliary epithelium is composed of cohesive groups of cuboidal to columnar cells with retained polarity, that is, basally located nuclei. The cells are seen in an orderly arrangement in flat honeycomb sheets or in a picket fence arrangement. The cytoplasmic borders are well defined. The nuclear-cytoplasmic ratio is low. The nuclear membranes are smooth, and the chromatin is finely distributed with indistinct nucleoli.

Reactive Bile Duct Epithelium

As a consequence of inflammatory changes as in the presence of stones, stent, and primary sclerosing cholangitis, the biliary epithelium can demonstrate reactive changes that can be very pronounced. These changes can be present to a varying degree in the epithelium, resulting in a spectrum of cell populations. The background may show acute inflammation and even necrosis. The cells are seen in flat to mildly disorganized groups. Mild degree of nuclear enlargement and anisonucleosis may be seen; however, the nuclear-cytoplasmic ratio is usually low. The chromatin is finely distributed, the nuclear membranes are smooth, and nucleoli may be prominent (Figs. 11.1, 11.2, 11.3, and 11.4) [21].

We frequently receive bile duct brushings for evaluation from patients with an indwelling stent or a history of stent placement in our practice. In such an instance, the cytomorphologic features that are associated with malignancy include anisonucleosis (with at least sixfold variation in nuclear size), three-dimensional archi-

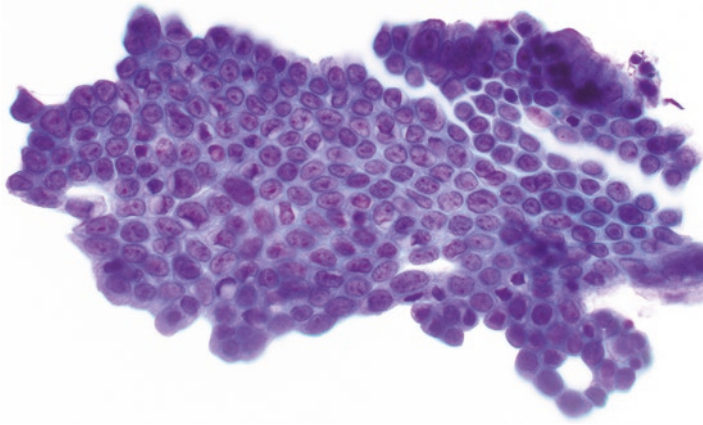


Fig. 11.1 Reactive bile duct epithelium reveals flat to mildly disorganized groups with mild degree of anisonucleosis, fine chromatin, and smooth nuclear membranes (ThinPrep, Papanicolaou stain, 600 \times)



Fig. 11.2 The reactive features can be pronounced in the setting of a stent and of primary sclerosing cholangitis. Anisonucleosis can exceed 1:3. However, there is usually only mild disorganization of architecture, nuclear membranes are smooth, and chromatin is finely distributed (ThinPrep, Papanicolaou stain, 600 \times)

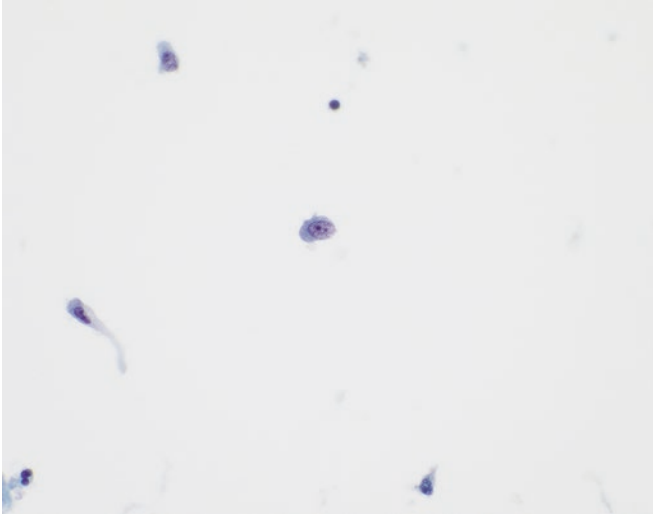


Fig. 11.3 Single atypical cells with enlarged nuclei can occasionally be seen in primary sclerosing cholangitis with reactive changes (ThinPrep, Papanicolaou stain, 600 \times)

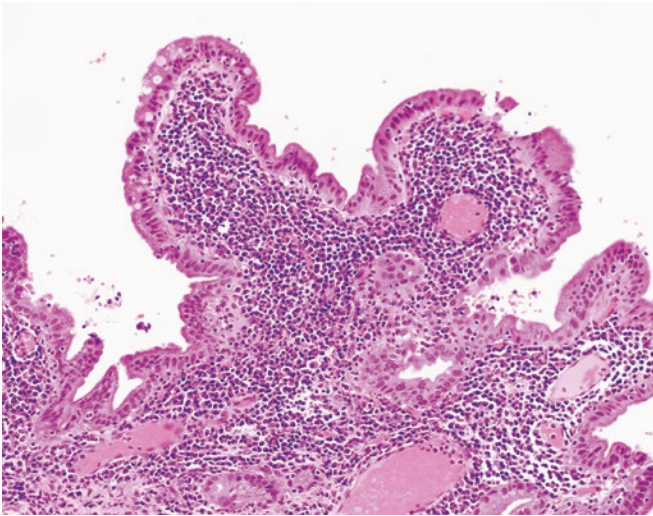


Fig. 11.4 Bile duct biopsy in primary sclerosing cholangitis with reactive, inflamed epithelium (hematoxylin-eosin, 200 \times)

tecture, coarse chromatin distribution, and the presence of single malignant cells [22].

Dysplasia

Cytologic criteria for biliary intraepithelial neoplasia (BiIN) are not well defined. The biliary epithelium shows cytologic atypia, ranging from low grade to high grade. Low-grade dysplasia results in nuclear stratification with mild nuclear crowding and hyperchromatic and elongated nuclei. While there is nuclear enlargement in these cells, the overall nuclear-cytoplasmic ratio remains low. High-grade dysplasia, in contrast, reveals three-dimensional cell arrangement, nuclear enlargement, irregular nuclear membranes, and coarse chromatin distribution. High-grade dysplasia can be indistinguishable from adenocarcinoma on cytology [23, 24].

Adenocarcinoma

Several studies have attempted to identify cytologic criteria that can better predict malignancy in bile duct brushings. Cohen et al. showed that nuclear molding, chromatin clumping, and increased nuclear-cytoplasmic ratio were key cytologic features that were associated with malignancy. The presence of two of these features resulted in 83% sensitivity and 98% specificity for carcinoma detection [25]. Renshaw and colleagues demonstrated that an overall assessment of malignancy or the criteria of chromatin clumping, increased nuclear-cytoplasmic ratio, and either nuclear molding or loss of honeycombing accurately predicted malignancy in bile duct brushings [26]. Fritcher et al. examined cytologic criteria associated with malignancy in pancreatobiliary brushings with corresponding positive fluorescence in situ hybridization (FISH) and found that abnormal single cells, nuclear membrane irregularity, and nuclear enlargement were independent predictors of malignancy on logistic regression. Their study also showed that the presence of single abnormal cells (defined

as single cells with at least one atypical nuclear feature) was the most significant finding on multivariate and univariate analysis (76.9% in malignant vs. 10.0% in benign samples) [7]. Salomao et al. also reported that on multivariate exact logistic regression, only the finding of single vacuolated cells was predictive of malignancy in biliary strictures (70.58% in malignant vs. 16.07% in benign samples) [27]. In a recent study, Avadhani et al. reported that 11 cytologic characteristics were significantly associated with malignancy on statistical analysis in bile duct brushings. These included three-dimensional clusters, pleomorphism, two-cell population, chromatin pattern changes, high nuclear-cytoplasmic ratio, cytoplasmic vacuoles, nuclear irregularity, cellular dis-cohesion, hypercellularity, nuclear molding, and prominent nucleoli. They found that the identification of 3 of these 11 features improved the pathologists' performance greatly in predicting malignancy [28].

As is depicted above, different studies have highlighted various key features for diagnosing malignancy in bile duct brushings. My approach toward diagnosing malignancy in bile duct brushings is based on the constellation of cytologic features identified in the specimen. Renshaw et al. have also shown that an overall cytologic assessment of malignancy was a better predictor of malignancy as compared to any other criteria with a sensitivity of 36.2% and a specificity of 95% [26].

The bile duct brushings from adenocarcinoma usually reveal two distinct cell populations—benign and malignant. However, one can see a spectrum of malignant cells in the sample when the tumor exhibits a range of differentiation. The malignant groups show nuclear crowding to a varying degree, ranging from mild nuclear overlap to more pronounced three-dimensionality. Nuclei are enlarged with a greater variation ($\geq 1:3$) in nuclear size within the same cell group. Nuclear membranes can be irregular, chromatin distribution is abnormal (mostly coarse but can be hypochromatic), and nucleoli may be prominent. An important finding that points toward malignancy is the presence of single malignant cells in the background. Necrosis and inflammation are nonspecific findings that can also be identified in benign samples (Figs. 11.5, 11.6, 11.7, 11.8, and 11.9).

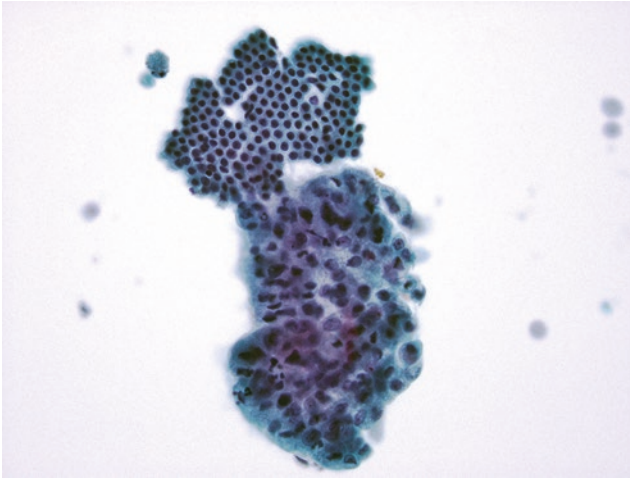


Fig. 11.5 Two contrasting populations are typical of malignant non-stented bile duct brushings. The well-organized group of normal biliary epithelium shows a striking contrast to the three-dimensional malignant group (ThinPrep, Papanicolaou stain, 400 \times)

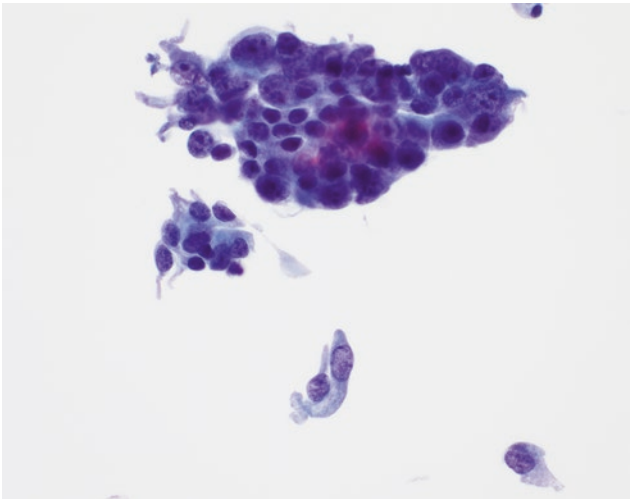


Fig. 11.6 Adenocarcinomas in bile duct brushings show irregular chromatin distribution, significant nuclear crowding, and anisonucleosis (at least to the extent of $\geq 1:3$) (ThinPrep, Papanicolaou stain, 600 \times)

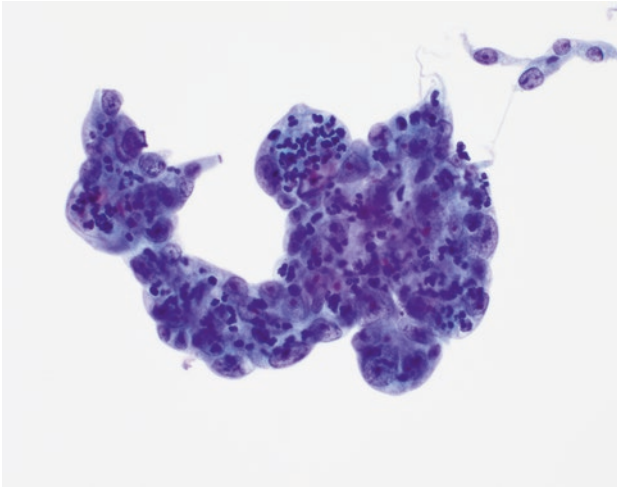


Fig. 11.7 Malignant groups in bile duct brushings can show hypochromatic nuclei with markedly prominent nucleoli and presence of intracytoplasmic neutrophils. However, the presence of neutrophils has not been observed as a specific feature of malignancy (ThinPrep, Papanicolaou stain, 600 \times)

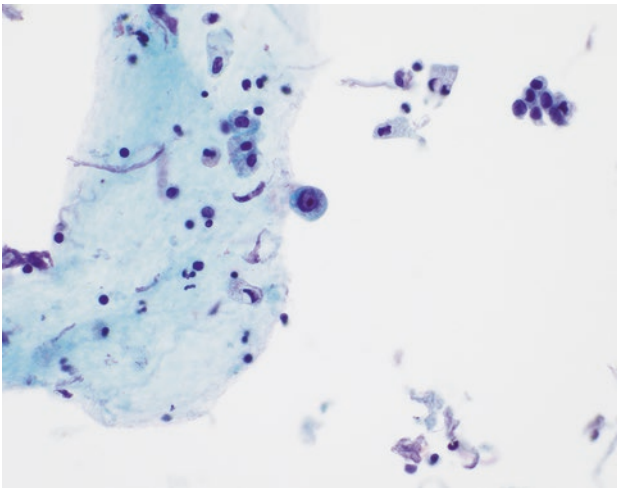


Fig. 11.8 Single malignant cells in the background are a helpful clue to the diagnosis of malignancy. However, the overall morphology of the lesion should be considered to make a diagnosis of malignancy (ThinPrep, Papanicolaou stain, 600 \times)

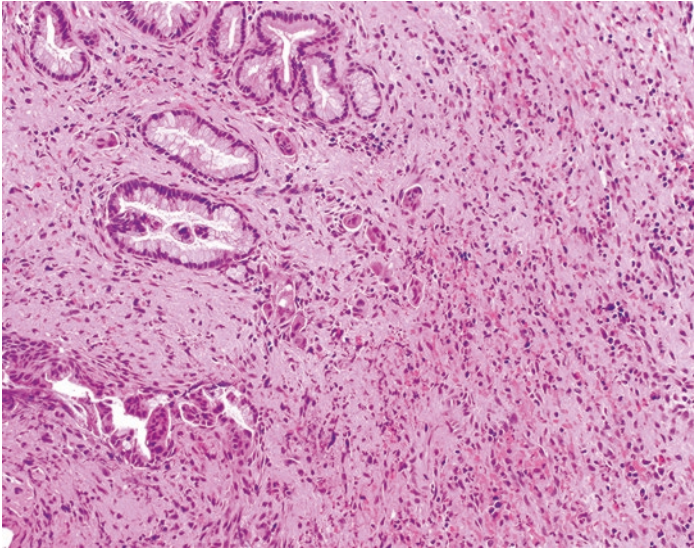


Fig. 11.9 Intraductal forceps biopsy aids in the diagnosis of malignancy as it can demonstrate the presence of stromal invasion (hematoxylin-eosin, 400 \times)

Intraductal Papillary Neoplasm of the Bile Ducts (IPN-B)

Intraductal papillary neoplasm of the bile ducts (IPN-B) is a rare disease that is seen primarily in patients from Far Eastern areas, such as Taiwan, Japan, and Korea, where hepatolithiasis and clonorchiasis are endemic. Majority of the patients are between 50 and 70 years of age [29].

It is characterized by an intraductal, predominantly papillary proliferation with a distinct fibrovascular stalk. The lining cells usually show intracellular mucin production. Many authors have considered IPN-B to represent the biliary counterpart of IPMN. Also similar to IPMN, four histologic subtypes of IPN-B have been recognized: pancreatobiliary, intestinal, gastric, and oncocytic. Approximately 40–80% of IPN-Bs contain a component of invasive carcinoma—tubular or mucinous adenocarcinoma—suggesting that IPN-B is a disease with a high potential for malignancy. It

is difficult to make an accurate diagnosis of IPN-B preoperatively due to its low incidence and lack of a specific clinical manifestation. Computed tomography (CT) scan and magnetic resonance imaging (MRI) usually fail to detect minor tumors and mucin. Therefore, cholangiography and cholangioscopy are needed for pathologic confirmation by biopsy and to demonstrate the extent of the lesions. In multifocal disease, different foci may be at different stages, indicating that the pathologic diagnosis by biopsy cannot reflect the actual stage in many cases. An approach for the cytologic evaluation of these neoplasms has not been established [30, 31].

Diagnostic Challenges

The low sensitivity of BDB cytology is mainly attributed to sampling difficulties, interpretation errors, and suboptimal slide preparations. In a retrospective analysis of 1832 pancreatobiliary brushings, Logrono and colleagues found that sampling errors were the major cause of false-negative diagnoses (67%), followed by interpretation errors (17%) and technical issues (17%) [10]. In an assessment of 267 bile duct brushings, Kocjan and Smith also concluded that improved sampling, preparation, and interpretation could result in better diagnostic accuracy of bile duct brushings [32].

Interpretation can be difficult due to limited cellularity specimens, well-differentiated adenocarcinomas, mucinous carcinomas, and cytologic atypia that falls short of a malignant diagnosis and in the presence of confounding factors such as primary sclerosing cholangitis and stent-related changes. Primary sclerosing cholangitis with marked reactive atypia of the biliary epithelium and scant cellularity with degenerative atypia can result in a false-positive diagnosis of malignancy [33]. Therefore, the threshold for malignant diagnosis is generally high in BDB cytology.

Ancillary Studies

Fluorescence in situ hybridization (FISH) has shown promise as an adjunct in improving the sensitivity of cytology for the detection of malignant biliary strictures. Using the UroVysion probe

set (Abbott Molecular Inc., Des Plaines, IL), it has been shown to enhance the sensitivity of BDB cytology to 42.9–63.89% for detection of malignancy [27, 34]. The FISH probes detect aneuploidy in the centromeric regions of chromosomes 3, 7, and 17 and homozygous or heterozygous deletion of locus 9p21. The results of FISH testing need to be correlated with clinical and imaging findings in patients with primary sclerosing cholangitis. Polysomy in the presence of a dominant stricture has a higher positive predictive value for cholangiocarcinoma in patients with PSC [34]. More recently, Fritcher et al. reported that a different set of FISH probes 1q21, 7p12, 8q24, and 9p21 identified malignancy in pancreatobiliary samples with a higher sensitivity (64.7%) as compared to the UroVysion probes (45.9%) or routine cytology analysis (18.8%) [35].

In terms of immunohistochemistry, various markers have been studied to assist in the identification of malignancy in bile duct brushings including p53, S100P, maspin, and claudin-18. Maspin is a mammary serine protease inhibitor that potentially plays a role in cell growth, invasion, and metastases and is overexpressed in cholangiocarcinomas. S100P is a calcium-binding protein that belongs to the S100 protein family and is overexpressed in biliary dysplastic epithelium and cholangiocarcinoma. Claudins are tight junction transmembrane proteins present in epithelial and endothelial cells. Claudin-18 immunohistochemical expression reportedly has a sensitivity of 89% for the detection of pancreatobiliary carcinomas [36, 37].

Recently, targeted next-generation sequencing along with cytology revealed a sensitivity of 85% for the detection of malignancy in bile duct brushings by revealing driver mutations in 30% of cases, including *KRAS*, *TP53*, *SMAD4*, and *CDKN2A* [38].

References

1. Singh A, Gelrud A, Agarwal B. Biliary strictures: diagnostic considerations and approach. *Gastroenterol Rep (Oxf)*. 2015;3:22–31. <https://doi.org/10.1093/gastro/gou072>.
2. Costamagna G, Bošković I. Current treatment of benign biliary strictures. *Ann Gastroenterol*. 2013;26:37–40.

3. Cassani L, Lee JH. Management of malignant distal biliary obstruction. *Gastrointest Interv.* 2015;4:15–20. <https://doi.org/10.1016/j.gii.2015.02.001>.
4. National Cancer Institute: Surveillance, Epidemiology and End Results Program. <https://seer.cancer.gov/statfacts/html/pancreas.html> (2018). Accessed 24 April 2018.
5. Rösch T, Hofrichter K, Frimberger E, Meining A, Born P, Weigert N, et al. ERCP or EUS for tissue diagnosis of biliary strictures? A prospective comparative study. *Gastrointest Endosc.* 2004;60:390–6.
6. Moff SL, Clark DP, Maitra A, Pandey A, Thuluvath PJ. Utility of bile duct brushings for the early detection of cholangiocarcinoma in patients with primary sclerosing cholangitis. *J Clin Gastroenterol.* 2006;40:336–41.
7. Barr Fritcher EG, Caudill JL, Blue JE, Djuric K, Feipel L, Maritim BK, et al. Identification of malignant cytologic criteria in pancreatobiliary brushings with corresponding positive fluorescence in situ hybridization results. *Am J Clin Pathol.* 2011;136:442–9. <https://doi.org/10.1309/AJCPDULIOEOTUZ5H>.
8. Volmar KE, Vollmer RT, Routbort MJ, Creager AJ. Pancreatic and bile duct brushing cytology in 1000 cases: review of findings and comparison of preparation methods. *Cancer.* 2006;108:231.
9. Stewart CJ, Mills PR, Carter R, O'Donohue J, Fullarton G, Imrie CW, et al. Brush cytology in the assessment of pancreatobiliary strictures: a review of 406 cases. *J Clin Pathol.* 2001;54:449–55.
10. Kocjan G, Smith AN. Bile duct brushings cytology: potential pitfalls in diagnosis. *Diagn Cytopathol.* 1997;16:358–63.
11. Burnett AS, Calvert TJ, Chokshi RJ. Sensitivity of endoscopic retrograde cholangiopancreatography standard cytology: 10-y review of the literature. *J Surg Res.* 2013;184:304–11. <https://doi.org/10.1016/j.jss.2013.06.028>.
12. Navaneethan U, Njei B, Lourdasamy V, Konjeti R, Vargo JJ, Parsi MA. Comparative effectiveness of biliary brush cytology and intraductal biopsy for detection of malignant biliary strictures: a systematic review and meta-analysis. *Gastrointest Endosc.* 2015;81:168–76. <https://doi.org/10.1016/j.gie.2014.09.017>.
13. Pugliese V, Conio M, Nicolò G, Saccomanno S, Gatteschi B. Endoscopic retrograde forceps biopsy and brush cytology of biliary strictures: a prospective study. *Gastrointest Endosc.* 1995;42:520526.
14. Kawashima H, Itoh A, Ohno E, Goto H, Hirooka Y. Transpapillary biliary forceps biopsy to distinguish benign biliary stricture from malignancy: how many tissue samples should be obtained? *Dig Endosc.* 2012;24(Suppl 1):22–7. <https://doi.org/10.1111/j.1443-1661.2012.01253.x>.
15. Ponchon T, Gagnon P, Berger F, Labadie M, Liaras A, Chavaillon A, et al. Value of endobiliary brush cytology and biopsies for the diagnosis of malignant bile duct stenosis: results of a prospective study. *Gastrointest Endosc.* 1995;42:565–72.

16. Kubota Y, Takaoka M, Tani K, Ogura M, Kin H, Fujimura K, et al. Endoscopic transpapillary biopsy for diagnosis of patients with pancreaticobiliary ductal strictures. *Am J Gastroenterol.* 1993;88:1700–4.
17. DeWitt J, Misra VL, Leblanc JK, McHenry L, Sherman S. EUS-guided FNA of proximal biliary strictures after negative ERCP brush cytology results. *Gastrointest Endosc.* 2006;64:325–33.
18. Ohshima Y, Yasuda I, Kawakami H, Kuwatani M, Mukai T, Iwashita T, et al. EUS-FNA for suspected malignant biliary strictures after negative endoscopic transpapillary brush cytology and forceps biopsy. *J Gastroenterol.* 2011;46:921–8. <https://doi.org/10.1007/s00535-011-0404-z>.
19. Brugge W, Dewitt J, Klapman JB, Ashfaq R, Shidham V, Chhieng D, et al. Techniques for cytologic sampling of pancreatic and bile duct lesions. *Diagn Cytopathol.* 2014;42:333–7. <https://doi.org/10.1002/dc.23096>.
20. Siddiqui MT, Gokaslan ST, Saboorian MH, Carrick K, Ashfaq R. Comparison of ThinPrep and conventional smears in detecting carcinoma in bile duct brushings. *Cancer.* 2003;99:205–10.
21. Heath JE, Goicochea LB, Staats PN. Biliary stent related alterations can be distinguished from adenocarcinoma on bile duct brushings using a limited number of cytologic features. *J Am Soc Cytopathol.* 2015;4:282–9.
22. Goyal A, Sharaiha RZ, Alperstein SA, Siddiqui MT. Cytologic diagnosis of adenocarcinoma on bile duct brushings in the presence of stent associated changes: A retrospective analysis. *Diagn Cytopathol.* 2018;46:826–32. <https://doi.org/10.1002/dc.24052>.
23. Layfield LJ, Wax TD, Lee JG, Cotton PB. Accuracy and morphologic aspects of pancreatic and biliary duct brushings. *Acta Cytol.* 1995;39:11–8.
24. Pitman MB, Centeno BA, Ali SZ, Genevay M, Stelov E, Mino-Kenudson M, et al. Standardized terminology and nomenclature for pancreatobiliary cytology: the Papanicolaou Society of Cytopathology guidelines. *Diagn Cytopathol.* 2014;42(4):338–50. <https://doi.org/10.1002/dc.23092>.
25. Cohen MB, Wittchow RJ, Johlin FC, Bottles K, Raab SS. Brush cytology of the extrahepatic biliary tract: comparison of cytologic features of adenocarcinoma and benign biliary strictures. *Mod Pathol.* 1995;8:498–502.
26. Renshaw AA, Madge R, Jiroutek M, Granter SR. Bile duct brushing cytology: statistical analysis of proposed diagnostic criteria. *Am J Clin Pathol.* 1998;110:635–40.
27. Salomao M, Gonda TA, Margolskee E, Eguia V, Remotti H, Poneris JM, et al. Strategies for improving diagnostic accuracy of biliary strictures. *Cancer Cytopathol.* 2015;123:244–52. <https://doi.org/10.1002/cncy.21509>.
28. Avadhani V, Hachisanoglu E, Memis B, Pehlivanoglu B, Hanley KZ, Krishnamurti U, et al. Cytologic predictors of malignancy in bile duct brushings: a multi-reviewer analysis of 60 cases. *Mod Pathol.* 2017;30:1273–86. <https://doi.org/10.1038/modpathol.2017.51>.

29. Lee SS, Kim MH, Lee SK, Jang SJ, Song MH, Kim KP, et al. Clinicopathologic review of 58 patients with biliary papillomatosis. *Cancer*. 2004;100:783–93.
30. Ohtsuka M, Kimura F, Shimizu H, Yoshidome H, Kato A, Yoshitomi H, et al. Similarities and differences between intraductal papillary tumors of the bile duct with and without macroscopically visible mucin secretion. *Am J Surg Pathol*. 2011;35:512–21. <https://doi.org/10.1097/PAS.0b013e3182103f36>.
31. Wan XS, Xu YY, Qian JY, Yang XB, Wang AQ, He L, et al. Intraductal papillary neoplasm of the bile duct. *World J Gastroenterol*. 2013;19:8595–604. <https://doi.org/10.3748/wjg.v19.i46.8595>.
32. Logrono R, Kurtycz DF, Molina CP, Trivedi VA, Wong JY, Block KP. Analysis of false-negative diagnoses on endoscopic brush cytology of biliary and pancreatic duct strictures: the experience at 2 university hospitals. *Arch Pathol Lab Med*. 2000;124:387–92.
33. Layfield LJ, Cramer H. Primary sclerosing cholangitis as a cause of false positive bile duct brushing cytology: report of two cases. *Diagn Cytopathol*. 2005;32:119–24.
34. Fritcher EG, Kipp BR, Halling KC, Oberg TN, Bryant SC, Tarrell RF, et al. A multivariable model using advanced cytologic methods for the evaluation of indeterminate pancreatobiliary strictures. *Gastroenterology*. 2009;136:2180–6. <https://doi.org/10.1053/j.gastro.2009.02.040>.
35. Barr Fritcher EG, Voss JS, Brankley SM, Campion MB, Jenkins SM, Keeney ME, et al. An optimized set of fluorescence in situ hybridization probes for detection of pancreatobiliary tract Cancer in cytology brush samples. *Gastroenterology*. 2015;149:1813–1824.e1. <https://doi.org/10.1053/j.gastro.2015.08.046>.
36. Kanzawa M, Sanuki T, Onodera M, Fujikura K, Itoh T, Zen Y. Double immunostaining for maspin and p53 on cell blocks increases the diagnostic value of biliary brushing cytology. *Pathol Int*. 2017;67:91–8. <https://doi.org/10.1111/pin.12505>.
37. Tokumitsu T, Sato Y, Yamashita A, Moriguchi-Goto S, Kondo K, Nanashima A, et al. Immunocytochemistry for Claudin-18 and Maspin in biliary brushing cytology increases the accuracy of diagnosing pancreatobiliary malignancies. *Cytopathology*. 2017;28:116–21. <https://doi.org/10.1111/cyt.12368>.
38. Dudley JC, Zheng Z, McDonald T, Le LP, Dias-Santagata D, Borger D, et al. Next-generation sequencing and fluorescence in situ hybridization have comparable performance characteristics in the analysis of pancreatobiliary brushings for malignancy. *J Mol Diagn*. 2016;18:124–30. <https://doi.org/10.1016/j.jmoldx.2015.08.002>.



Ancillary Studies in the Cytologic Diagnosis of Pancreatico-biliary Lesions

Jonas J. Heymann

Pancreatic Ductal Adenocarcinoma and Cholangiocarcinoma

Pancreatic ductal adenocarcinoma (PDACA) demonstrates a complex molecular landscape that may include both somatic and germline alterations [1]. Characteristic somatic alterations include both gene-level and whole chromosomal arm-level copy number aberrations. The most frequent mutations are encountered in *KRAS* (93%), *TP53* (72%), *SMAD4*, *CDKN2A*, and *GNAS*; and loss of heterozygosity (LoH) is identified in *CDKN2A* (9p21.3), *SMAD4*, *ARID1A*, and *PTEN*. The most frequent germline mutations are encountered in genes involved in deoxyribonucleic acid (DNA) repair, such as *BRCA1*, *BRCA2*, *ATM*, and *PALB2* [2–6]; and tumors harboring alterations in such genes may respond to various therapeutic agents, including poly-(adenosine diphosphate-ribose) polymerase-1 (PARP) inhibitors [7].

J. J. Heymann (✉)

Department of Pathology and Laboratory Medicine, Weill-Cornell
Medicine, New York Presbyterian Hospital, New York, NY, USA
e-mail: jjh7002@med.cornell.edu

Cholangiocarcinoma (ChACA) demonstrates a molecular landscape similar in complexity to that of PDACA, although characteristic alterations differ between cases of intrahepatic and extrahepatic ChACA, as well as between those cases that are associated with liver flukes and those that are not [8]. Characteristic alterations include change-of-function mutations in either *IDH1* or *IDH2*, and identified mutant alleles (Arg132Cys in *IDH1* and Arg172Lys and Arg172Ser in *IDH2*) are distinct from those more commonly identified in glioma and acute myeloid leukemia (enriched for Arg132His in *IDH1* and Arg140Gln in *IDH2*). *IDH* mutations are predominantly associated with intrahepatic tumors, as are potentially targetable *FGFR2* fusions. Loss-of-function alterations in *PBRM1* and *BAP1* are also common. Elevated copy number and expression of several mitochondrial genes, as well as hypermethylation and decreased expression of genes involved in chromatin modification, including *ARID1A*, are significantly associated with *IDH* and *PBRM1* mutant samples; low expression of those same mitochondrial genes is associated with *FGFR2*-fused samples. Interestingly, *CDKN2A* is mutated, deleted, or epigenetically silenced at a very high rate, while *KRAS*, *TP53*, and *SMAD4* are altered at significantly lower rates than in PDACA.

In order to optimize utilization and triage of limited biopsy specimen tissue, the Papanicolaou Society of Cytopathology (Pap Society) has published guidelines for pancreatico-biliary cytology [9]. Pap Society guidelines include separate sections for specimens derived from solid lesions, cystic lesions, and strictures; and the guidelines highlight important molecular testing regimens available for each of several diagnostic entities.

Immunohistochemistry

Among multiple studies regarding immunohistochemical (IHC) markers of pancreatico-biliary adenocarcinoma, few have differentiated between PDACA and ChACA. Those that have specifically differentiated the two entities from one another have included a relatively low number of cases of ChACA, particularly intrahepatic ChACA.

Pancreatic Ductal Adenocarcinoma

The protein product of the *SMAD4* gene is SMAD4, and its expression is lost upon deletion or loss of *SMAD4* function. IHC analysis of SMAD4 expression has been studied as a marker of PDACA both alone [10] and in combination with expression of pVHL, insulin-like growth factor mRNA-binding protein-3 (IMP3), S100P, and maspin [11]. In the latter study, the authors concluded that a panel including pVHL, maspin, S100P, and IMP3 is optimal for confirming a diagnosis of PDACA. In the absence of an immunostaining panel, loss of SMAD4 expression independently supports a malignant diagnosis, but retention of signal does not prove that a lesion is benign.

Mesothelin is a *MUC16* (CA-125) ligand that may be overexpressed in PDACA [12]. IHC analysis of mesothelin expression has been studied as a marker of PDACA both alone [13] and in combination with expression of IMP3 [14] and S100P [15]. The best evidence of the value of IHC analysis of mesothelin expression comes from a meta-analysis of 12 studies, in which its sensitivity and specificity for malignancy were estimated to be 71% and 88%, respectively [16].

The protein product of the *TP53* gene is p53, and it demonstrates changes in expression upon genetic alteration. Specifically, loss-of-function mutations—typically missense mutations—in the DNA-binding domain lead to overexpression, while deletion or truncating mutations lead to complete loss of expression. IHC analysis of p53 expression has been infrequently studied as a marker of PDACA in endoscopic ultrasound-guided fine needle aspiration (EUS-FNA) biopsy-derived cell block material in combination with expression of S100P and claudin-4 [17]. Limited evidence suggests that expression of p53 is a specific but insensitive marker of malignancy.

Multiple other IHC stains have been investigated as markers of PDACA, but they need further validation before their routine use in the diagnosis of PDACA in a cytology laboratory [18, 19]. Our group has also studied the efficacy of performing IHC analysis on EUS-FNA-derived cell block material. We observed loss of SMAD4 expression in 30/37 samples of PDACA compared to 2/30 samples of benign ductal epithelium. Positivity for at least

two out of three IHC markers (SMAD4, IMP3, and S100P) was sensitive (92%) and highly specific (100%) for PDACA (Fig. 12.1) [20]. Potential IHC markers of PDACA, along with their expected expression profiles, are presented in Table 12.1.

Cholangiocarcinoma

Multiple antibodies have been developed such that IHC analysis has broad utility in detecting *IDH* mutations. It is important to note that each antibody has been developed against a specific epitope in the *IDH* protein products isocitrate dehydrogenase 1 (IDH1) and IDH2 such that, in the absence of genetic sequencing

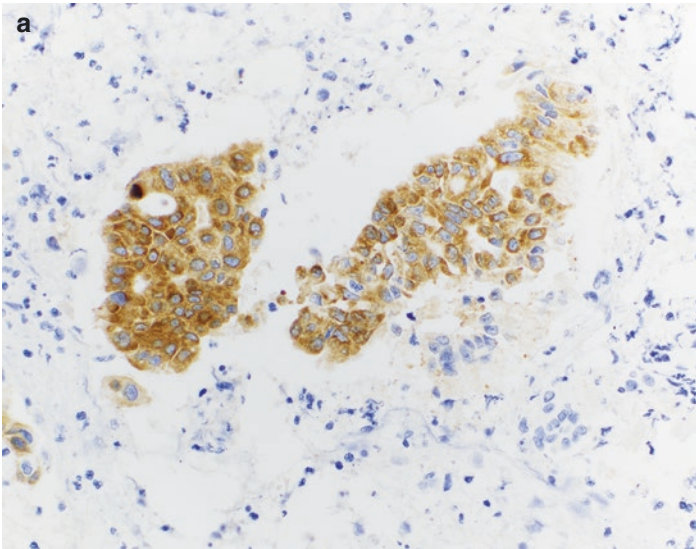


Fig. 12.1 IMP3, S100P, and SMAD4 expression in samples of pancreatic ductal adenocarcinoma procured by endoscopic ultrasound-guided fine needle aspiration biopsy. Immunohistochemical analysis performed on cell block sections demonstrates expression of (a) IMP3 (400 \times magnification) and (b) S100P (400 \times magnification) in malignant glandular epithelial cells but not in incidentally sampled benign glandular epithelial cells. Immunohistochemical analysis also demonstrates (c) loss of SMAD4 expression in malignant glandular epithelial cells but not in incidentally sampled benign glandular epithelial cells

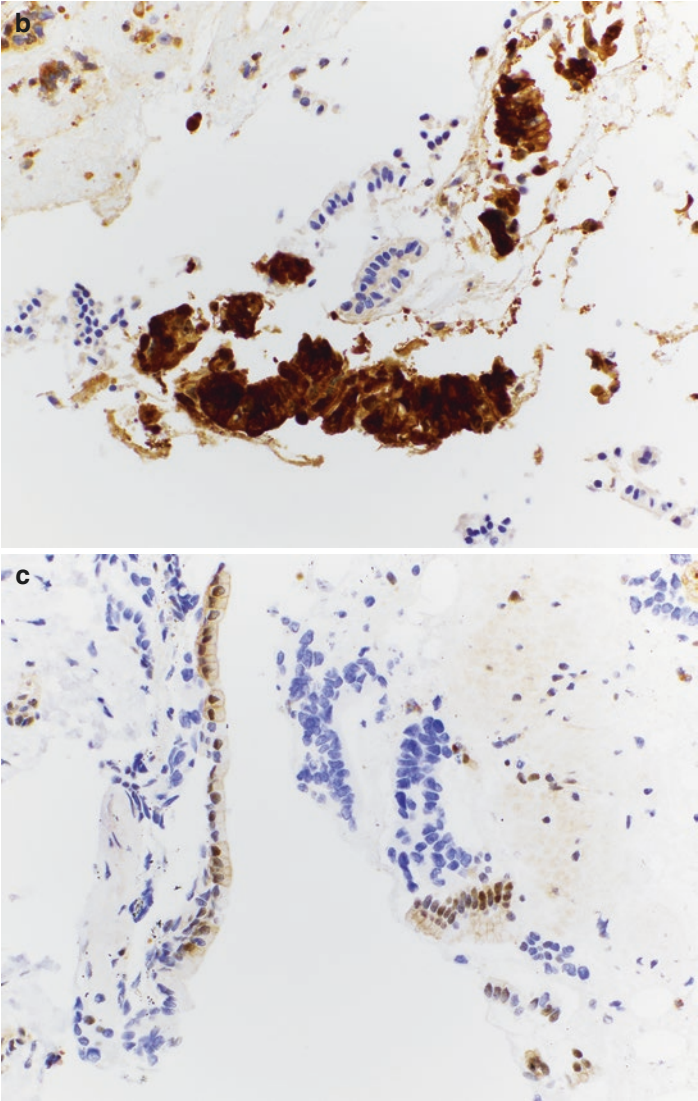


Fig. 12.1 (continued)

Table 12.1 Expected expression profiles of potential immunohistochemical markers in pancreatic ductal adenocarcinoma

	Expression	Loss of expression	Overexpression
SMAD4		X	
pVHL		X	
CD10		X	
IMP3	X		
S100P	X		
Maspin	X		
Mesothelin	X		
Claudin-4	X		
p53		X	X

analysis, multiple immunostains are required to rule out the presence of any *IDH* mutation. Currently detectable mutations include Arg132His, Arg132Ser, Arg132Gly, and Arg132Leu in *IDH1* and Arg172Lys, Arg172Met, and Arg172Trp in *IDH2*. Unfortunately, the vast majority of studies evaluating the efficacy of such antibodies have been performed in specimens of glioma and acute myeloid leukemia. Few studies have evaluated the efficacy of IHC analysis of *IDH* in ChACA, and further investigation will be required to determine the optimal antibody and most suitable method of detection for *IDH* mutations in ChACA.

Fluorescence In Situ Hybridization

Fluorescence in situ hybridization (FISH) analysis has shown promise as an adjunct in improving the sensitivity of cytomorphology for detection of malignancy in EUS-FNA biopsy specimens, although the majority of studies have been performed on bile duct fluid, washing, and brushing samples (see below). The UroVysion probe set (Abbott Molecular Inc., Des Plaines, IL) is commonly employed, even though it was originally designed for use in urine specimens. Levy et al. utilized the probe set to render a diagnosis of malignancy in four cases deemed either indetermi-

nate or benign by cytomorphology [21]. More recently, Ribeiro et al. utilized the probe set to render a diagnosis of malignancy in 20 EUS-FNA biopsy-derived pancreatic samples deemed either indeterminate or benign by cytomorphology [22]. Further investigation is required to optimize the diagnostic criteria for FISH analysis of EUS-FNA biopsy-derived samples of solid pancreatic lesions.

Genetic Sequencing and Other Genetic Testing

The role of next-generation sequencing (NGS) in the cytologic diagnosis of pancreatic lesions has been extensively reviewed [23]. Different methods of genetic testing provide different sets of information that pathologists may use for diagnostic, prognostic, or predictive purposes.

Next-Generation Sequencing of DNA

At present, NGS is primarily used for genetic profiling of pancreatico-biliary tumors after diagnosis. Depending on the extent of profiling required, either a limited or extended gene panel may be employed. Interestingly, results have been similar across studies employing limited and extended gene panels [24–27]. The gene most commonly found to be altered is *KRAS*, followed by *TP53*, *SMAD4*, and *CDKN2A* (Fig. 12.2). It is important to remember that *KRAS* mutation is not specific for the presence of malignancy. However, the ability to detect alterations only in *TP53*, *SMAD4*, and *CDKN2A* may be of clinical significance, as the number of driver mutations has been shown to be of prognostic significance in PDACA [28].

When selecting a sequencing panel, it is important to consider both sequencing depth and breadth. Increased sequencing depth may allow for detection of copy number changes, in addition to mutations. High sequencing depth is also critical in evaluating specimens of low neoplastic cellularity and those that evoke a brisk desmoplastic tissue response, like PDACA. Increased sequencing breadth may allow for detection of mutational signatures such

Fig. 12.2 Massively parallel sequencing of DNA using the AmpliSeq Cancer Hotspot Panel version 2 (Life Technologies, Carlsbad, CA) extracted from endoscopic ultrasound-guided fine needle aspiration biopsy-derived cell block sections. Genetic sequence pileups are visualized with the Integrative Genomics Viewer (Broad Institute, Cambridge, MA). **(a)** A c.35G>T missense mutation in KRAS with variant allelic frequency of 34% results in an activating p.Gly12Val (G12V) substitution. **(b)** A c.742C>T missense mutation in TP53 with variant allelic fraction of 35% results in a loss-of-function p.Arg248Try (R248W) substitution in the DNA-binding domain of the protein. **(c)** A c.1333C>T nonsense mutation in SMAD4 with variant allelic fraction of 22% results in substitution of a stop codon at p.Arg445 (R445Ter) and premature truncation and loss of function of the protein product. The low variant allelic fraction in SMAD4 suggests tumor aneuploidy, the presence of which may be proven by another method, if clinically indicated. Images are courtesy of Dr. Jordan Baum

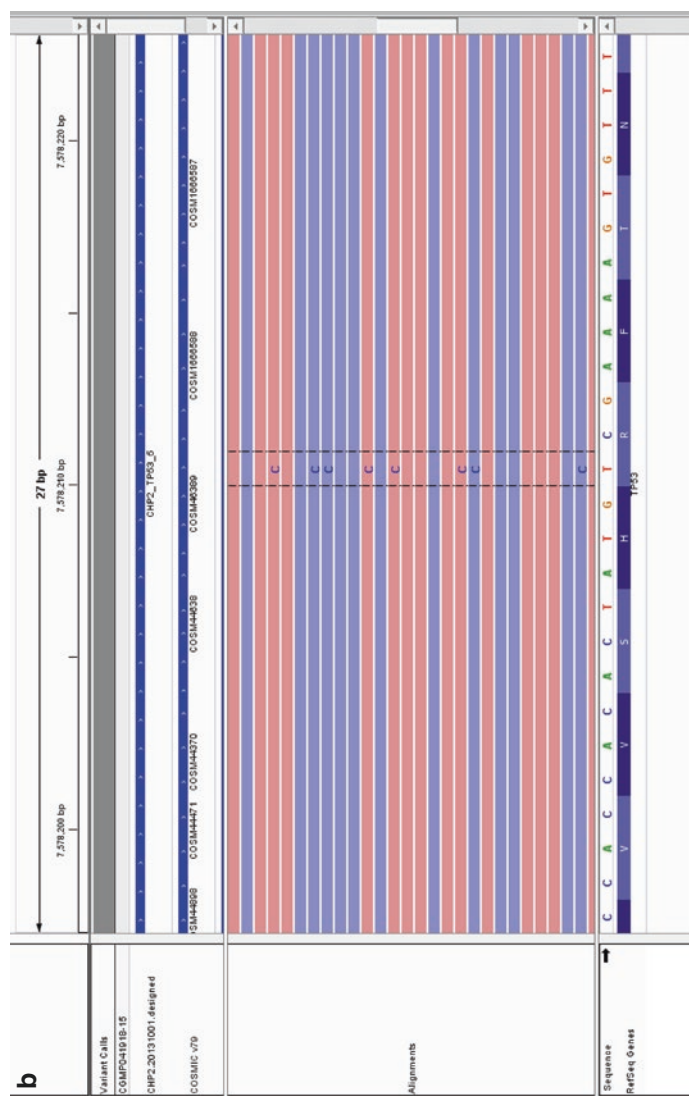


Fig. 12.2 (continued)

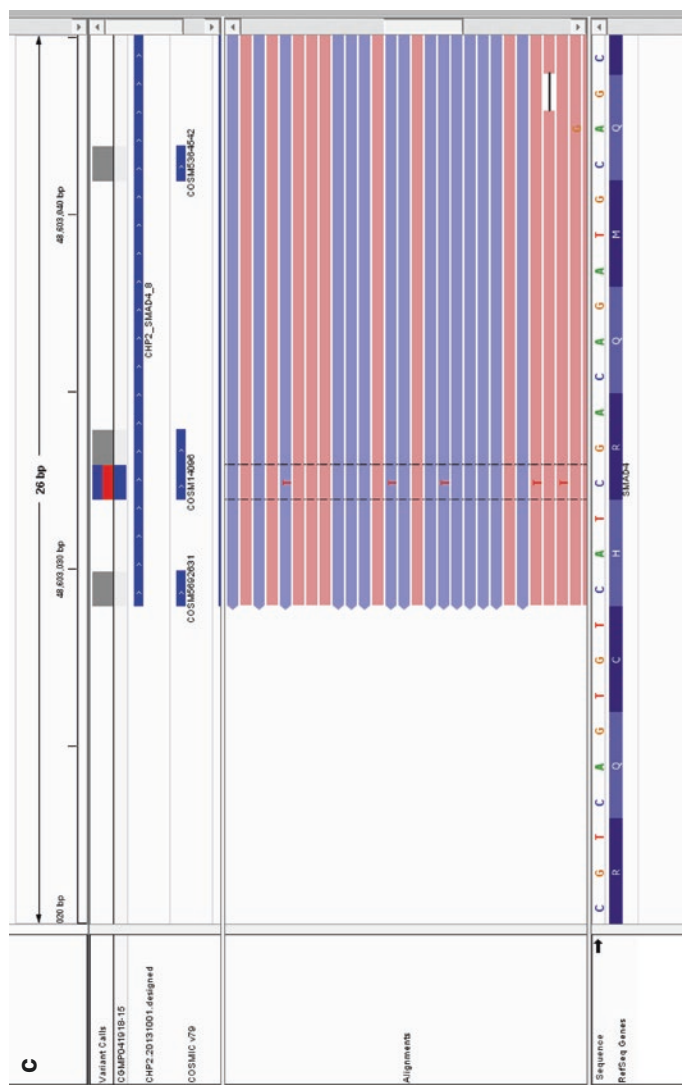


Fig. 12.2 (continued)

as those associated with mismatch repair deficiency. Mismatch repair deficiency is rare in PDACA and ChACA, but it renders tumors potentially susceptible to immune checkpoint blockade. Alternately, tumors harboring alterations in DNA repair pathway genes may respond to PARP inhibitors.

Loss of Heterozygosity

LoH is typically evaluated by capillary electrophoresis after amplification of appropriate microsatellite sequences. Techniques to identify LoH should normalize overall signals and control for neoplastic cellularity to assure validity. A majority of validation studies have been performed on samples of biliary strictures and pancreatic cysts (see below). Evaluation of heterozygosity has demonstrated variable utility in the diagnosis of pancreaticobiliary adenocarcinoma, and studies have focused on the number of loci at which heterozygosity is lost, rather than the specific loci themselves [29, 30]. Ultimately, evaluation of LoH in the diagnosis of PDACA on EUS-FNA requires further validation before integration into clinical practice.

MicroRNA Profiling

MicroRNA profiling is a relatively new technique for determining malignancy in EUS-FNA biopsy specimens. MicroRNA species are short (20–25-nucleotide) RNA molecules containing regions complementary to various mRNA species. Binding in regions of complementarity serves as a regulatory mechanism of protein translation. MicroRNA can be robustly quantified using allele-specific real-time polymerase chain reaction (qPCR), and microRNA profiles in PDACA have been reviewed [31].

MicroRNA species highly expressed in PDACA include miR-21, miR-155, and miR-196a, among others; and studies utilizing EUS-FNA biopsy samples of PDACA have demonstrated that differential expression of microRNA species in benign and malignant tissues can be detected, even in small samples. Notably, Ali et al. observed that expression of let-7c, let-7f,

and miR-200c was significantly reduced in most of a series of cases of PDACA, whereas expression of miR-486-5p and miR-451 was significantly elevated in all PDACA cases [32]. Hong et al. identified five microRNA species significantly upregulated (miR-21, miR-27a, miR-146a, miR-200a, and miR-196a) and three microRNA species significantly downregulated (miR-217, miR-20a, and miR-96) in almost all of a series of malignant tissues [33]. In neither study were the results validated on samples with indeterminate cytomorphology. Such lack of validation stands in contrast to the study by Brand et al., in which a panel of five microRNA species—upregulation of miR-196a, expression of miR-135b normalized to that of miR-24, and downregulation of miR-148a and miR-130b—was validated for the diagnosis of PDACA in EUS-FNA pancreatic biopsy specimens [34]. In that study, the microRNA panel correctly identified 22/39 (56%) cases of PDACA with indeterminate, nondiagnostic, or falsely benign cytomorphology and 7/10 (70%) benign lesions with indeterminate or nondiagnostic cytomorphology. Potential microRNA markers of PDACA are presented in Table 12.2. The clinical utility of microRNA profiling remains to be more firmly established, especially in tumors of low purity and in comparison and in conjunction with other techniques.

Sanger Sequencing

Dideoxy chain termination (Sanger) sequencing can only evaluate a limited number of genetic foci at a time and is, therefore, heavily dependent on high tumor quantity and purity. Sanger sequencing is an appropriate method of evaluation of oncogenes, such as *KRAS* and *GNAS*, in which gain-of-function mutations are present at a limited number of hotspots. The same is true for *IDH1* and *IDH2*, in which change-of-function mutations are present at a limited number of hotspots. Because NGS can detect mutations at a lower allele frequency and may be used to sequence multiple genes at the same time, it is preferred where available and necessary.

Table 12.2 Expected expression profiles of potential microRNA markers in pancreatic ductal adenocarcinoma

miR	Upregulated	Downregulated
miR-20a		X
miR-21	X	
miR-23a	X	
miR-27a	X	
miR-31	X	
miR-96		X
miR-100	X	
miR-130b		X
miR-135b	X	
miR-143	X	
miR-146a	X	
miR-148a		X
miR-155	X	
miR-181b	X	
miR-196a	X	
miR-200a	X	
miR-200c		X
miR-217		X
miR-221	X	
miR-375		X
let-7c		X
let-7f		X

Pancreatic Neuroendocrine Tumors and Other Solid Tumors of the Pancreas

The genetic characteristics of well-differentiated neuroendocrine tumor (NET) along with its high-grade, poorly differentiated counterpart, neuroendocrine carcinoma (NECA), have been compiled from multiple sources and reviewed [35–38]. Characteristic genomic alterations include whole chromosomal arm-level copy number gains and losses. The most frequent genetic alterations in well-differentiated NET are encountered in *MEN1*, *VHL*, *ATRX*,

DAXX, and *PHLDA3*. Alteration is also relatively common in *PIK3CA*, *PTEN*, or *TSC2* in the mammalian target of rapamycin (mTOR) pathway [39]. Loss-of-function mutations in *TP53* and *RBI* are common in and confined to NECAs. Interestingly, inactivating mutations in *ATRX* and *DAXX* have not been reported in NECA [40]. The most frequent germline mutations are encountered in *MEN1*, *VHL*, *NF1*, *TSC1*, and *TSC2*; and the clear cell variant of NET is particularly enriched in patients with germline mutation of the *VHL* gene.

Acinar cell carcinoma (ACCA), pancreatoblastoma, and solid pseudopapillary neoplasm (SPN) may all morphologically resemble NET. Chromosomal instability is a common feature among ACCAs, and up to 10% of tumors demonstrate microsatellite instability [41]. Loss of the maternal alleles on chromosome 11p is characteristic of pancreatoblastoma [42, 43], and pancreatoblastoma may occur in patients with Beckwith-Wiedemann syndrome (BWS), a disorder associated with imprinting dysregulation of chromosome 11p [44]. Loss of chromosome 11p is also common in ACCA [45], as are loss of *APC* gene function and activating fusion of the *BRAF* gene [46, 47]. In contrast, activating mutations in *CTNNB1* occur in a significant proportion of pancreatoblastomas and in virtually all SPNs [48, 49]. Recurrent genetic and genomic alterations in NET and other solid tumors of the pancreas are summarized in Table 12.3. Just as for PDACA and ChACA, ancillary testing for cytologic specimens derived from NET, ACCA, pancreatoblastoma, and SPN may proceed according to Pap Society guidelines [9].

Immunohistochemistry

IHC analysis of cell block material is the standard method to supplement morphologic analysis in differentiation among NET, ACCA, pancreatoblastoma, and SPN. NETs express general markers of endocrine differentiation, including chromogranin (Fig. 12.3a), synaptophysin, CD56 (neural cell adhesion molecule), CD57, insulinoma-associated protein 1 (INSM1), and neuron-specific enolase (NSE). They have also been shown to express

Table 12.3 Recurrent genetic and genomic alterations that have been described in neuroendocrine tumors and other solid tumors of the pancreas

Gene/genetic locus	Well-differentiated neuroendocrine tumor	Neuroendocrine carcinoma	Acinar cell carcinoma	Pancreatoblastoma	Solid pseudopapillary neoplasm
<i>MEN1</i>	LoF ^a				
<i>VHL</i>	LoF ^a				
<i>PHLDA3</i>	LoF				
<i>ATRX</i>	LoF				
<i>DAXX</i>	LoF				
<i>PIK3CA</i>	GoF				
<i>PTEN</i>	LoF				
<i>TSC1</i>	LoF ^a				
<i>TSC2</i>	LoF ^a				
<i>NF1</i>	LoF ^a				
<i>RBI</i>		LoF			
<i>TP53</i>		LoF	LoF		
<i>SMAD4</i>			LoF		

<i>APC</i>			LoF	
<i>BRAF</i>			Fusion	
<i>CTNNB1</i>			GoF	GoF
BWS critical region on chromosome 11p			LoH ^a	LoH ^a
Other			Microsatellite instability	

Abbreviations: *LoF* loss of function, *GoF* gain of function, *LoH* loss of heterozygosity

^aMay be germline

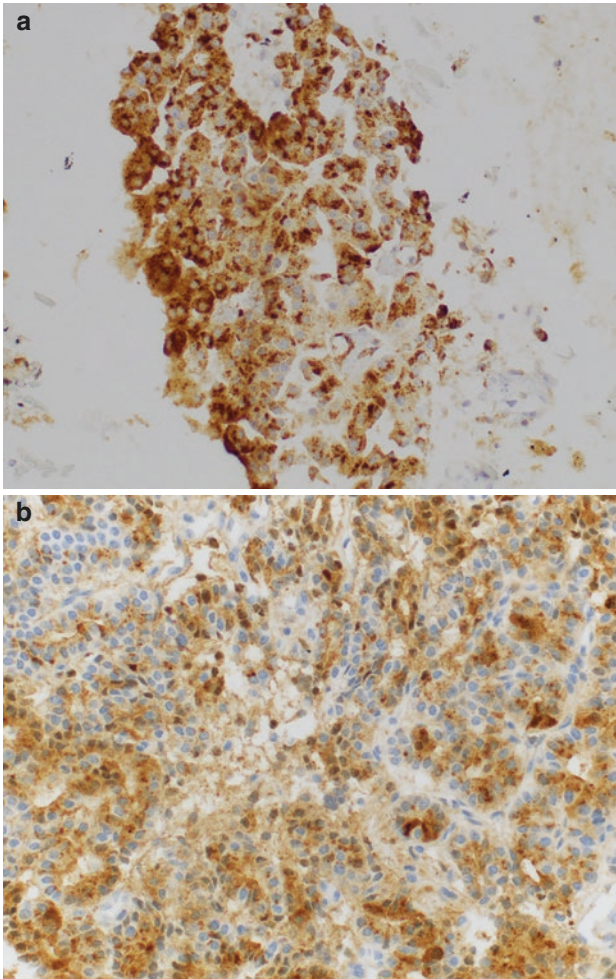


Fig. 12.3 Chromogranin, chymotrypsin, and β -catenin expression in samples of neoplastic pancreatic lesions procured by endoscopic ultrasound-guided fine needle aspiration biopsy. Immunohistochemical analysis performed on cell block sections demonstrates (a) punctate cytoplasmic expression of chromogranin in a pancreatic neuroendocrine tumor (400 \times magnification, photomicrograph courtesy of Dr. Abha Goyal), (b) granular cytoplasmic expression of chymotrypsin in an acinar cell carcinoma (400 \times magnification, photomicrograph courtesy of Dr. Abha Goyal), and (c) nuclear localization of β -catenin expression in a solid pseudopapillary neoplasm (400 \times magnification, photomicrograph courtesy of Dr. Momin Siddiqui)

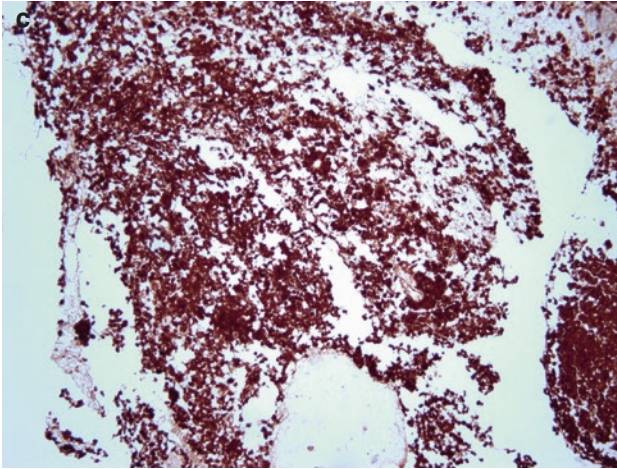


Fig. 12.3 (continued)

cytokeratin 8 (CK8), CK18, and cancer antigen (CA)-19-9; and they demonstrate a membranous pattern of E-cadherin expression [50]. NECAs have a similar IHC profile to NETs, although chromogranin expression tends to be patchy or even absent.

ACCAs and pancreatoblastomas express general markers of pancreatic acinar differentiation, although the IHC profile of pancreatoblastoma has been less well characterized than that of ACCA. Pancreatic acinar cell products demonstrable by IHC analysis include amylase, lipase, trypsin, and chymotrypsin (Fig. 12.3b). ACCAs have also been shown to express B-cell lymphoma/leukemia 10 (BCL-10) [51, 52], claudin-7 [53], and p120 [54]; and occasional cases demonstrate nuclear expression of beta [β]-catenin.

SPNs display a unique IHC profile, characterized chiefly by nuclear localization of β -catenin, the protein product of the *CTNNB1* gene (Fig. 12.3c). They also express vimentin, α -1-antitrypsin (in cells containing hyaline globules), synaptophysin, CD56, NSE, CD10, progesterone receptor, lymphoid enhancer-binding factor 1 (LEF-1) [55], and claudin-5 [53]; and they demonstrate paranuclear, dot-like expression of CD99 [56]. Characteristic IHC profiles of NET and other solid tumors of the pancreas are summarized in Table 12.4.

Table 12.4 Characteristic immunohistochemical profiles of neuroendocrine tumors and other solid tumors of the pancreas

	Neuroendocrine tumor	Acinar cell carcinoma	Pancreatoblastoma	Solid pseudopapillary neoplasm
Chromogranin	+	-	-	-
Synaptophysin	+	-	-	+/-
CD56	+	-	-	+/-
Neuron-specific enolase	+	-	-	+
E-Cadherin	Membranous			Loss of membranous expression
Progesterone receptor	Faint, dot-like (rare)			+
Amylase	-	+	+	-
Trypsin	-	+	+	+/-
Chymotrypsin	-	+	+	+/-
BCL-10	-	+	+	-
Claudin-7	+	+	+	-
p120 (2P-1-2-1)	-	+	Insufficient data	-
CD10	-			+
β -Catenin	Nonnuclear	Rare nuclear expression	Nuclear (in squamous morules)	Nuclear
CD99	Cytoplasmic (rare)	-	Insufficient data	Paranuclear, dot-like
LEF-1	-	-	Insufficient data	Nuclear
Claudin-5	-	-	-	+

Multiple small studies have evaluated the utility of IHC analysis of the proliferation marker Ki-67 (MIB-1) for grading of NETs as well as distinction between NET and NECA, with promising results [57–60]. A constant finding across all studies is that determination of MIB-1 labeling index in preoperative biopsy specimens is more likely to underestimate than to overestimate tumor grade as determined upon resection. As the majority of these studies were retrospective in nature, the clinical consequences of underestimating tumor grade preoperatively are uncertain. Several studies have correlated the MIB-1 labeling index in cytologic biopsy material with clinical tumor behavior [61, 62]. IHC analysis of Ki-67 to stratify NETs to determine biologic behavior and predict disease recurrence requires further study.

Genetic Sequencing and Other Genetic Testing

The role of NGS and other sequencing methods in the cytologic diagnosis of NET, ACCA, and SPN is currently less well established than for PDACA. However, recent FDA approval of two targeted small molecule inhibitors is likely to enhance the importance of genetic profiling for patients with advanced NET. Specifically, everolimus is an mTOR inhibitor [63], and sunitinib is a tyrosine kinase inhibitor with activity against several growth factor receptors that act upstream of mTOR, including vascular endothelial and platelet-derived growth factor receptors [64]. Clinical trials for these agents, as well as early trials for other agents that have demonstrated activity against advanced NET and NECA, have not selected patients based on genetic alterations [65, 66], although genetic profiling may facilitate selection of patients for future clinical trials. Somatic alterations in genes in the mTOR pathway would be of particular interest. Of course, identification of germline alterations that render carriers susceptible to cancer at other sites would also provide great clinical benefit. Germline alterations in *MEN1* (associated with multiple endocrine neoplasia type 1), *VHL* (von Hippel-Lindau syndrome), *NF1* (neurofibromatosis type 1), *TSC1* or *TSC2* (tuberous sclerosis), or the BWS locus on chromosome 11p would be of particular interest.

Loss of Heterozygosity

Investigation of changes in heterozygosity in cytologic samples of NET and NECA is still in its early stages. Nodit et al. evaluated heterozygosity using a panel of 17 microsatellite markers at 10 genetic loci, in EUS-FNA biopsy-derived cell block material from 25 NET patients with significant clinical follow-up [67]. The most frequently affected marker overall was located on chromosome 17q; and microsatellite markers located on chromosomes 3p, 5q, 17q, and 21q were lost only in NETs of high stage. Overall fractional allelic loss (FAL) was significantly higher in NETs of high stage than those of low stage, and FAL was significantly greater in those with disease progression as compared with patients with stable disease. Replication of their results in larger prospective studies will be required to confirm the clinical value of heterozygosity studies in the evaluation of NET and NECA.

Next-Generation and Sanger Sequencing of DNA

Sequencing is an appropriate method of detection of genetic alterations with great enough specificity to differentiate among NET, NECA, ACCA, and SPN, especially when cytomorphologic and IHC analyses are indeterminate. The principle of diagnostic sequencing was illustrated by Kubota et al., who investigated *CTNNB1* using NGS in a series of EUS-FNA biopsy-derived specimens of PDACA, NET, and SPN [68]. Mutations in *CTNNB1* were detected in all SPNs, in 1/11 cases of NET, and in no PDACA specimens. More recently, Sigel et al. performed NGS using an extended gene panel on predominantly histologic samples corresponding to 23 cytology specimens of NET or NECA [69]. They were able to use genetic alteration in *ATRX*, *DAXX*, or *MEN1* to support a diagnosis of NET in 13 patients and genetic alteration in *RBI* or *KRAS* to support a diagnosis of NECA in 2 patients.

Cystic Lesions of the Pancreas

Cystic lesions of the pancreas are a diverse group, including both neoplastic and nonneoplastic entities, such as lymphoepithelial cyst and pseudocyst. Cystic pancreatic neoplasms include serous

and mucinous forms, and mucinous neoplasms themselves may be subclassified further into intraductal papillary mucinous neoplasms (IPMNs) and/or mucinous cystic neoplasms (MCNs). SPN and NET may also undergo cystic degeneration. Among all pancreatic cystic lesions, IPMN and MCN have the potential to progress to PDACA [70]. Therefore, after successful identification of a mucinous neoplasm, it is prudent to attempt to identify the presence of high-grade dysplasia or even invasive adenocarcinoma.

Several studies have identified and characterized recurrent genetic alterations in pancreatic cystic neoplasms. Wu et al. performed whole-exome sequencing on eight resection cases each of serous cystadenoma (SCA), IPMN, MCN, and SPN [71]. Four of the eight cases of SCA contained mutation of *VHL*. In addition to activating mutation in *KRAS* and *GNAS*, inactivating mutation in *RNF43* was identified in six of eight IPMNs and three of eight MCNs. Unsurprisingly, all SPNs contained a *CTNNB1* mutation.

Studies specifically focused on characterizing IPMN have produced similar results. In a second study, Wu et al. detected *GNAS* mutations in 66% of 113 IPMN fluid specimens, while either *KRAS* or *GNAS* mutation could be identified in 96% of specimens [72]. Neither *GNAS* nor *KRAS* mutations were found in non-mucinous cystic lesions. Also, *GNAS* mutations were not found in PDACA specimens not associated with IPMN. Similarly, Amato et al. sequenced 51 genes in 48 resected IPMN specimens [73]. *GNAS* and/or *KRAS* mutations were found in 44/48 cases with *GNAS* mutated in 38, *KRAS* in 24, and both in 18. *RNF43* was the third most commonly mutated gene. Mutations in *TP53* and *BRAF* were only observed in IPMNs with high-grade dysplasia. Dysregulation of specific microRNA species [74, 75] and aberrant methylation of numerous genes [76, 77] have also been described during development and progression of IPMN.

Gross Cyst Fluid Evaluation

Among many ancillary studies available for evaluation of pancreatic cyst fluid, visual examination is a particularly cost-effective method for differentiating mucinous from non-muci-

nous cysts. Thick, viscous fluid that is difficult to pull into and express from the needle indicates the presence of mucin. Leung et al. examined the role of a surrogate marker of cyst fluid viscosity in differentiating various pancreatic cyst etiologies [78]. By placing the fluid between the thumb and index finger and gently pulling the fingers apart, the fluid would form a “string” of median length 3.5 mm if mucinous. The presence of a thick cyst wall or intracystic growth on EUS, elevated cyst fluid carcinoembryonic antigen (CEA) level, and a long “string sign” were associated with mucinous cysts, although the parameters were not independent of one another. Similarly, Oh et al. reported that the “string” sign was accurate in 33/47 examined cases of pancreatic cysts of various types and the combination of cytomorphology, biochemical testing, and string sign assessment was accurate in 45/48 cases [79]. Despite lower accuracy, its low cost makes visual inspection an attractive option for evaluation of pancreatic cyst fluid, especially when used in conjunction with other ancillary techniques.

Histochemical Stains for Mucin and Glycogen

Stains are available to detect the presence of intracellular mucin, including Alcian blue and mucicarmine. Periodic acid-Schiff (PAS) staining will highlight intracellular mucin associated with IPMNs and MCNs, as well as intracellular glycogen associated with serous cysts. However, after treatment with diastase, PAS will not stain glycogen. Staining is technically feasible using direct smears and liquid-based (LB) preparations, as well as cell block sections, although at present staining of LB preparations is not considered diagnostically valid per Pap Society guidelines [9]. Staining cannot separate benign from malignant lesions, and standardization of how much staining constitutes a positive result in EUS-FNA-derived specimens with contamination of luminal gastrointestinal tract epithelium has not been determined.

Biochemical Tests of Cyst Fluid

Biochemical testing is one of the most accurate methods to identify mucinous pancreatic cysts and to distinguish them from non-mucinous cysts. While such testing does not reliably identify the presence or absence of dysplasia and malignancy, its relative cost-effectiveness compared to genetic sequencing makes it an attractive option for determination of cyst etiology.

Cyst Fluid Amylase

Amylase activity is elevated in cysts that communicate with the pancreatic ductal system, such as IPMNs, and activity is also typically markedly elevated in pseudocysts. Amylase activity may be quantified using a colorimetric assay to measure formation of the degradation products of enzyme-catalyzed reactions. Although MCNs do not communicate with the pancreatic ductal system, amylase activity may be elevated in their fluid such that quantification of amylase activity is of little value for distinguishing IPMN from MCN. In a pooled review of 12 studies including data from 450 patients, van der Waaij et al. found that a cyst fluid amylase level of less than 250 IU/L has a very high specificity (98%) for exclusion of pseudocyst [80]. Therefore, quantification of amylase activity may be valuable in cases in which the differential diagnosis includes pseudocyst. Superior markers are available for differentiation among pancreatic cystic neoplasms.

Cyst Fluid CEA

Numerous studies have indicated and confirmed the reliability of carcinoembryonic antigen (CEA) as an indicator of mucinous cyst differentiation and fluid CEA level by immunoassay as the most accurate marker of mucinous pancreatic cysts [81, 82]. The primacy of CEA was firmly established in a multicenter, prospective cooperative study in 2004, which demonstrated that the accuracy—79%, with sensitivity and specificity of 75% and 84%, respectively—of CEA quantification in cyst fluid alone is superior to the combination of EUS, cytomorphology, and quantification

of other tumor markers for identification of mucin-producing cysts [83]. Several studies have since been published in an attempt to optimize detection of mucinous cysts using cyst fluid CEA quantification [78, 84–88], including a pooled review of 12 studies that included the multicenter cooperative study [80]. Notably, Thornton et al. conducted a more recent meta-analysis of 12 studies that included data from 885 patients, again including those from the multicenter cooperative study [89]. The pooled accuracy of CEA quantification in cyst fluid was 79%, with respective pooled sensitivity and specificity of 63% and 88% for identification of mucin-producing cysts, although all parameters were markedly heterogenous across studies. Heterogeneity in sensitivity and specificity is likely due to the fact that the meta-analysis only included studies that utilized the threshold for CEA concentration proposed in the multicenter cooperative study (192 ng/mL). Therefore, it is advisable that each laboratory independently determine the pancreatic cyst fluid CEA concentration at which diagnostic accuracy is optimal for discrimination between mucinous and non-mucinous cysts. At the present time, it is also inappropriate to use quantification of pancreatic cyst fluid CEA to support a diagnosis of dysplasia or malignancy.

Assessment of CEA levels is limited by the requirement that endoscopists obtain sufficient cyst fluid for analysis, which is often not possible, particularly in very small cysts or those with very viscous fluid. Difficulties in obtaining sufficient pancreatic cyst fluid were highlighted in a prospective study in which CEA levels were successfully quantified in only 68/128 cases for which EUS-FNA was performed [90]. Approximately 0.2–1.0 mL of cyst fluid is required to run the test. Other diagnostic methods must be pursued for pancreatic cysts in which insufficient cyst fluid is collected for biochemical testing.

Mucin Expression Patterns in Pancreatic Cyst Fluid

Mucins include soluble, gel-forming, and membrane-associated forms, of which MUC1 is expressed in normal pancreatic ductal epithelium. Alterations in mucin glycosylation have been observed in tumor tissues across multiple organ systems, and aberrant expression has been described in pancreatic neoplasms.

IHC analysis of resected mucinous pancreatic neoplasms has demonstrated that mucin expression patterns can distinguish different histopathologic types of IPMN [91–93]. Mucin expression patterns also demonstrate a correlation with the presence of dysplasia and carcinoma.

Multiple different methods have been employed to determine mucin expression patterns, and only rare, retrospective studies have employed biochemical testing of cyst fluid. The preoperative value of biochemical evaluation of pancreatic cyst fluid for expression of mucins remains undefined. Jabbar et al. were able to demonstrate that proteomic mucin profiling by mass spectrometry is more accurate than cytomorphology and cyst fluid CEA quantification in identifying lesions with high-grade dysplasia or invasive carcinoma in both a discovery ($n = 29$) and a validation ($n = 50$) cohort [94]. Mass spectrometry is not widely available as a clinical test and, therefore, may not be an appropriate methodology for a majority of laboratories.

Among the mucins, MUC16 (CA-125) is one of the most studied and well characterized, and quantification by immunoassay is widely available across many laboratories. Unfortunately, studies that have assessed the usefulness of quantification of MUC16 in determining cyst type and malignant potential have generally included few cases and demonstrated conflicting results [83, 95].

Other Biochemical Markers in Pancreatic Cyst Fluid

Biochemical testing of numerous other markers has been performed to determine if their levels in pancreatic cyst fluid can determine cyst type and malignant potential. Such markers include, but are not limited to, lipase, pancreatitis-associated protein, CA-72-4, CA-19-9, CA-15-3, granulocyte-macrophage colony-stimulating factor, hepatocyte growth factor, vascular endothelial growth factor, interleukin-1 β (IL-1 β), IL-5, IL-8, prostaglandin E2, olfactomedin-4, Brg1, and glucose [83, 84, 96–100]. Among these, the latter is of particular interest, because it may be quantified at low cost and with a rapid turnaround time. Recently, Carr et al. collected fluid of 153 pancreatic cysts (41 by EUS-FNA, preoperatively), 106 of which were mucinous in nature [101]. The efficiency of glucose quantification in cyst fluid

for the diagnosis of a mucinous pancreatic cyst was similar to that of quantification of CEA. These results, as well as results for other markers, will need to be confirmed in future studies before they are considered appropriate for clinical use.

Immunohistochemistry

Although EUS-FNA of pancreatic cysts typically yields scant material with insufficient cellularity for cell block preparation, new methods of EUS-guided tissue procurement allow for sampling of tissue from the cyst wall and/or septations [102–104]. Preparation of high-quality cell blocks on which IHC analysis can be performed is especially valuable in a limited number of clinical and morphologic settings. IHC analysis may be essential to the specific diagnosis of secondarily cystic neoplasms, such as NET and SPN (see Chap. 9 for additional information). While recognition of ovarian-type stroma in the cyst wall may be accomplished by morphology alone for the differentiation of MCN from IPMN, indeterminate cases may require IHC analysis of estrogen and/or progesterone receptor. Multiple IHC studies have demonstrated differences in mucin expression patterns between IPMNs with and without a dysplastic or an invasive component [91, 93, 105], and one study even confirmed mucin expression by in situ hybridization analysis [106]. However, all of these studies have been performed on pancreatic resection specimens. At present, the value of IHC analysis of mucin expression patterns in EUS-FNA-derived cytologic cell block material remains undefined.

Optical Density

Rare studies have examined the utility of quantifying the optical density of pancreatic cyst fluid as a determinant of the presence or absence of malignancy. When quantified at a wavelength of 260 nm, the optical density is proportional to the quantity of nucleic acid that it contains. In their prospective study of fluid

derived from 88 pancreatic cysts, 40 of which were malignant, Khalid et al. demonstrated that malignant cysts contain a significantly greater quantity of nucleic acid than do benign cysts [107]. A significant association between optical density and malignancy was independent of biochemical and genetic testing methods in a multivariate regression model, although genetic sequencing methods were more accurate and specific for the presence of malignancy than was optical density. Quantification of nucleic acid in mucinous cysts may present an attractive option for determination of the presence of malignancy either in combination with genetic sequencing methods or where genetic sequencing methods are unavailable.

Genetic Sequencing and Other Genetic Testing

Identification of mutations and other genetic alterations in pancreatic cyst fluid is limited by the low number of mutant alleles present compared with that of solid lesions, such as PDACA. The advent of NGS has conferred upon pathologists the ability to identify such low levels of mutant alleles. Fortunately, genetic sequencing of pancreatic cyst fluid is typically employed by clinicians only to decide whether or not to resect the cystic lesion; comprehensive genetic profiling, such as that available for PDACA and other solid lesions, is unnecessary. NGS of a limited number of genes, with or without identification of LoH at key genomic loci, has been extensively studied. Such testing will often suffice for determination of the necessity of resection, especially when employed in combination with cytomorphology, optical density, and biochemical testing of cyst fluid. Although not yet approved by the FDA, tests are commercially available that combine mutational profiling in a limited panel of oncogenes, quantification of DNA, and evaluation of its quality, with evaluation of heterozygosity at several genomic loci for characterization of pancreatic cyst lesions. Some centers offer similar analysis as a laboratory-developed test. The role of NGS in the characterization of cystic pancreatic lesions has been extensively reviewed [23, 81, 82, 108–110].

In a prospective study of fluid derived from pancreatic cysts [107], Khalid et al. expanded upon results from a previous study in which the authors sequenced *KRAS* and amplified microsatellite markers to look for LoH at loci on chromosomes 1p, 3p, 5q, 9p, 9q, 10q, and 17p [111]. Among 88 mucinous cysts, the authors identified an activating *KRAS* mutation in 40. Of those, 17 also demonstrated LoH in at least two genomic loci, including 15/40 total cysts with high-grade dysplasia and/or invasive adenocarcinoma. In contrast, *KRAS* mutation was identified in only 1/25 non-mucinous cysts. Both *KRAS* mutation and allelic loss amplitude had associations with mucinous etiology independent of cytomorphology and CEA level, and allelic loss amplitude had an independent association with the presence of high-grade dysplasia with or without invasive malignancy. The authors concluded that genetic testing should be considered when cytomorphologic examination is negative for the presence of high-grade dysplasia.

In their prospective study of 48 pancreatic cystic lesions that were subsequently resected, Al-Haddad et al. utilized criteria for the presence of mucinous cyst first established by Khalid et al., namely, activating mutation in *KRAS* and/or LoH at two or more genomic loci, to identify mucinous pancreatic lesions [112]. Specifically, molecular testing was 50% sensitive (19/38 cases) for the presence of a mucinous cyst, while evaluation of *KRAS* and heterozygosity were 90% (present in 1/10 non-mucinous cysts) and 100% specific, respectively, for the presence of a mucinous cyst. Analysis of *KRAS* and heterozygosity were particularly helpful in cases for which preoperative cytology was nondiagnostic or CEA cyst fluid level was indeterminate. The authors expanded upon their results in a subsequent multicenter, retrospective study utilizing a commercially available genetic testing panel that examined *KRAS*, DNA content, and heterozygosity at several tumor suppressor genomic loci [113]. Among 492 patients with pancreatic cysts that did NOT undergo resection, the combination of a lack of high-risk cytomorphologic features and molecular genetic criteria for risk of progression to malignancy provided a 97% probability of benign follow-up for up to 7 years. In contrast, the presence of multiple molecular genetic criteria was associated with a relative hazard ratio for malignant outcome of 50.2.

Preoperative sequencing of the combination of *GNAS* and *KRAS* in pancreatic cyst fluid is also highly sensitive and specific for the presence of IPMN. Singhi et al. sequenced both *GNAS* and *KRAS* in pancreatic cyst fluid from 91 pancreatic cysts, including 50 cases of IPMN, 9 of which contained adenocarcinoma [114]. Mutations in either gene were present in 42/50 cases of IPMN, including 8/9 cases with an invasive malignant component. In contrast, no mutations were identified in fluid from cases of NET, serous cystadenoma, pseudocyst, or lymphoepithelial cyst.

More recent evidence suggests that addition of several more genes to sequencing panels may facilitate the diagnosis of pancreatic cysts. Rosenbaum et al. performed NGS on EUS-FNA-derived pancreatic cyst fluid using a hybrid capture-based NGS panel of hotspots in 39 genes [115]. As expected, *KRAS* was the gene most frequently mutated (60/113 cases), followed by *GNAS* (27 cases). Among samples that subsequently underwent surgical resection, activating *KRAS* mutation was identified in 19/30 cases of IPMN, including 18/24 cases with a component of invasive adenocarcinoma, compared to only 1/8 non-mucinous cysts. *GNAS* mutation was identified in 9/30 cases of IPMN, including 6/24 cases with an invasive component. Alterations in *TP53*, *SMAD4*, *CDKN2A*, and *NOTCH1* were detected only in fluid from malignant cysts, although, interestingly, cytomorphology was more sensitive than was NGS for detection of malignancy. The combination of NGS with quantification of cyst fluid CEA reached 90% sensitivity and 88% specificity for cystic mucinous lesions. These results expanded on those previously obtained in a similar study from the same group [116].

In a large, retrospective multicenter study, Springer et al. attempted to combine NGS of an expanded genetic panel with evaluation of heterozygosity and aneuploidy to classify cystic pancreatic lesions [117]. In addition to *KRAS* and *GNAS*, the authors' genetic panel included hotspots in nine genes (*BRAF*, *CDKN2A*, *CTNNB1*, *NRAS*, *PIK3CA*, *RNF43*, *SMAD4*, *TP53*, and *VHL*). LoH was determined not by conventional microsatellite analysis, but by single-nucleotide polymorphism analysis of five genes (*CDKN2A* on chromosome 9p, *RNF43* on 17q, *SMAD4* on 18q, *TP53* on 17p, and *VHL* on 3p). Among 130 pancreatic

cyst fluid samples, 24 of which were collected preoperatively by EUS-FNA, *KRAS* was the most frequently mutated gene in cases of IPMN (75/96 cases) and MCN (6/12 cases), as expected followed by *GNAS*, which was mutated in 56/96 cases of IPMN but none of 12 cases of MCN. Overall, 86/96 cases of IPMN harbored a mutation in either *KRAS* or *GNAS*. Each of 10 SPNs harbored a *CTNNB1* mutation, and 5/12 serous cysts harbored a *VHL* mutation. In addition, 7/12 serous cysts demonstrated LoH at the *VHL* locus.

Numerous smaller studies have produced variable estimates of the value of genetic testing of pancreatic cyst fluid [118, 119], and several have directly compared the accuracy of CEA quantification to genetic analysis [120, 121]. With rare exceptions [122], quantification of CEA and genetic sequencing have been shown to complement one another to identify a majority of mucinous cysts. Our own group compared cytomorphologic analysis of fluid from 20 small pancreatic cysts to a commercially available genetic testing panel that examined *KRAS*, DNA content, and heterozygosity at several tumor suppressor genomic loci [123]. Cytomorphologic and laboratory diagnoses were concordant in only 7/20 cases. Among four cases for which resection was performed, two cases proven to be mucinous cysts were misclassified by genetic testing, and one case of a mucinous cyst was misclassified by cytomorphology.

Genetic testing of pancreatic cyst fluid is limited by the requirement that endoscopists obtain sufficient cyst fluid for analysis, which may not be possible, particularly in very small cysts or those with very viscous fluid. However, data suggest that it may be easier to obtain fluid that is sufficient for genetic testing than to obtain fluid that is sufficient for biochemical testing or cytomorphologic analysis. In a prospective study that focused specifically on evaluation of *KRAS* for the presence of an activating mutation, Nikiforova et al. found that of 618 pancreatic cyst fluid specimens obtained by EUS-FNA, 603 were satisfactory for genetic sequencing [124]. Although sufficient for molecular analysis, 320 of those 603 specimens were either less than optimal or unsatisfactory for cytomorphologic diagnosis. Interestingly, among 53 *KRAS*-mutated and 89 *KRAS* wild-type cysts for which

surgical follow-up information was available, the presence of a *KRAS* mutation was 54% sensitive and 100% specific for mucinous differentiation. When stratified by cyst type, the finding of an activating *KRAS* mutation was 67% and 14% sensitive for the presence of IPMN and MCN, respectively.

Meta-analysis provides some of the strongest evidence for sequencing of *KRAS* in pancreatic cyst fluid. In a review that included 12 studies totaling 1115 patients, including multiple studies outlined above, the combination of cytomorphology and *KRAS* sequencing was 71% sensitive and 88% specific for the presence of a mucinous cyst [125].

A limited number of studies have examined changes in the molecular genetics of cysts overtime. In a retrospective study of 40 resected pancreatic cysts with intermediate-risk clinical features and available data from a commercially available genetic testing panel that examined *KRAS*, DNA content, and heterozygosity at several tumor suppressor genomic loci, Winner et al. identified 16 patients who had serial analyses performed on EUS-FNA-derived fluid samples [126]. Ten cysts demonstrated newly detectable activating *KRAS* mutation or LoH, and three cysts accumulated a pattern of both *KRAS* mutation and LoH at more than one locus that was specific for malignancy. Similarly, in a prospective study of pancreatic cysts with low-risk clinical features and available data from the same commercially available genetic testing panel, DeWitt et al. identified patients who had analyses performed on EUS-FNA-derived fluid samples both before and after cyst ablation with paclitaxel and ethanol [127]. Genetic sequencing demonstrated elimination of all five baseline *KRAS* mutations, restoration of heterozygosity at all five loci in three of four patients with focal loss, and new LoH in three patients, one of whom already demonstrated LoH at one locus before ablation. These results will need to be confirmed in larger studies before repeating molecular analysis beyond the initial (index) examination becomes standard practice.

Rare studies have evaluated differences in microRNA expression in cyst fluid samples from patients with pancreatic cysts. Notably, Ryu et al. analyzed expression by qPCR of a limited panel of microRNA species in postoperatively collected cyst fluid

samples, including 16 non-mucinous cysts, 10 MCNs, and 14 IPMNs, 3 of which harbored an invasive malignant component [128]. Significantly greater expression of three microRNA species, including miR-21, was observed in the mucinous vs. non-mucinous cysts. Expression of no microRNA species was able to differentiate MCN from IPMN. More recently, Wang et al. analyzed expression by NGS of a broad panel of microRNA species in EUS-FNA-derived cyst fluid samples from patients with mucinous cysts, 11 of which demonstrated high-grade dysplasia, 3 of which demonstrated a component of invasive carcinoma [129]. Differential expression between cystic neoplasms with low-grade and high-grade dysplasia reached statistical significance for 15 microRNA species. Similarly, Matthaei et al. analyzed expression using an array-based qPCR method of a broad panel of microRNA species in discovery and validation cohorts of resected pancreatic cystic lesions and postoperatively collected cyst fluid samples [130]. A logistic regression model using expression of nine microRNA species separated IPMNs with high-grade dysplasia, NETs, and SPNs from IPMNs with low-grade dysplasia and serous cysts with a sensitivity of 89% and a specificity of 100%. In addition, expression of a subset of 18 microRNA species differentiated cases of IPMN with high-grade dysplasia from those without, and five of those species were the same as those identified by Wang et al. (miR-125b, miR-214, miR-26a, miR-30b, and miR-217). However, the clinical utility of microRNA profiling in pancreatic cyst fluid and the most important microRNA targets remain to be more firmly established.

As elevated telomerase activity has been associated with malignancy across organ systems, a study has evaluated the diagnostic performance of an assay to quantify telomerase activity in pancreatic cyst fluid [131]. Telomerase activity was measured in intraoperatively collected pancreatic cyst fluid samples using a telomerase repeat amplification protocol with digital droplet PCR (ddPCR) in discovery ($n = 184$) and validation ($n = 35$) cohorts of patients who underwent resection for a cystic lesion. Although telomerase activity was reduced in samples that had undergone prior thawing, among those not previously thawed, fluid from cystic neoplasms with high-grade dysplasia had significantly higher

telomerase activity than that from those without high-grade dysplasia. In a multivariate analysis, telomerase activity predicted the presence of high-grade dysplasia independently from clinical and radiographic cyst features. In 36 samples preoperatively obtained by EUS-FNA, the telomerase activity correlated well with that subsequently measured in the resected cyst fluid sample. However, the value of evaluating pancreatic cyst fluid telomerase activity in the preoperative setting requires further validation before integration into clinical workflows.

As increasing prevalence of aberrant DNA methylation has been demonstrated in precancerous and cancerous lesions [132], a study has evaluated the diagnostic utility of gene methylation markers in pancreatic cyst fluid for their ability to predict the presence of high-grade dysplasia in pancreatic cystic neoplasms [133]. Methylation of a limited panel of genes was evaluated using methylation-specific ddPCR in postoperatively collected pancreatic cyst fluid samples in discovery ($n = 29$) and validation ($n = 154$) cohorts of patients who underwent resection for a cystic lesion. Methylation of all genes accurately and independently distinguished neoplasms in the validation cohort with high-grade dysplasia from those without, and methylation of *SOX17* was the most accurate single marker. Importantly, a combination of *SOX17* methylation and cytomorphologic analysis better predicted grade of dysplasia than cytomorphology alone. As with telomerase activity, the value of methylation profiling of pancreatic cyst fluid in the preoperative setting requires further validation before integration into clinical workflows.

With such an abundance of ancillary techniques available for diagnostic and prognostic evaluation of pancreatic cyst fluid, it is difficult to determine which ones are most appropriate for any given clinical situation and in what combination and sequence. Selection of markers will most likely be limited by the quality and quantity of material collected, the availability of cell block material, cost and workflow considerations, and the availability of sequencing and laboratory technologies at the institution. Ideally, each laboratory would work with its respective clinical teams to develop a volume-based pancreatic cyst fluid handling protocol suited to its clinical needs and technical capabilities

[134]. An example of such a protocol is presented in Fig. 12.4. At present, quantification of CEA for determination of the nature of the cyst—mucinous vs. non-mucinous—and cytomorphic analysis for the presence of dysplasia and exclusion of cystic degeneration of solid neoplasms remain important in the evaluation of almost all cysts. It is advisable that each laboratory independently determine the pancreatic cyst fluid CEA concentration at which diagnostic accuracy is optimal for discrimination between mucinous and non-mucinous cysts. Alternately, laboratories may use CEA values established in previous studies outlined above. Optical density and NGS of hotspots in a limited number of genes, especially *KRAS* and *GNAS* to determine malignant potential, but potentially also including *RNF43*, *CDKN2A*, *VHL*, *CTNNB1*, *BRAF*, *NOTCH1*, *TP53*, and *SMAD4*, may be appropriate, as is evaluation of microsatellite sequences for LoH at genomic loci, including 1p, 3p, 5q, 9p, 9q, 10q, 17p, 17q, 18q, 21q, and 22q. An overview of genetic and genomic alterations detectable in pancreatic cystic neoplasms is presented in Table 12.5.

Pancreatico-biliary Duct Fluid, Washing, and Brushing Samples

Analysis of pancreatic and bile duct strictures proceeds on the assumption that the great diversity of genetic and epigenetic alterations in PDACA and ChACA may be represented in duct fluid, washing, and brushing samples. Multiple approaches of various efficacy have been developed to complement cytomorphic analysis of pancreatic and bile duct samples. Just as for solid neoplasms, the Pap Society guidelines include ancillary studies with diagnostic, predictive, and prognostic utility for pancreatic and bile duct strictures [9]. Such ancillary studies are diverse; and, given the paucity of material commonly obtained during cholangiopancreatography, selection of the most appropriate study or studies may be crucial for diagnosis.

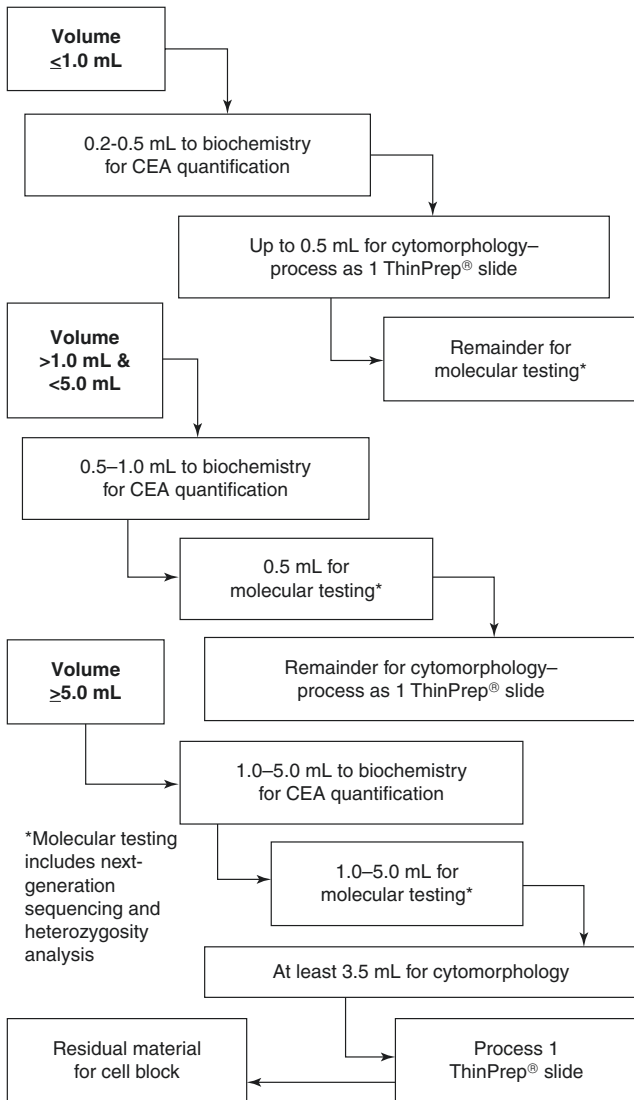


Fig. 12.4 Flowchart for theoretical volume-dependent pancreatic cyst fluid handling protocol. Each laboratory should develop its own protocol to suit its clinical needs and technical capabilities

Table 12.5 Landscape of detectable genomic alterations in pancreatic cystic neoplasms

Genomic locus	Gene	Activating mutation	Loss-of-function mutation	Loss of heterozygosity	Neoplasm	Progression to malignancy	Notes
12p	<i>KRAS</i>	X			Mucinous cyst		
20q	<i>GNAS</i>	X			IPMN		
17q	<i>RNF43</i>		X	X	Mucinous cyst	X	
9p	<i>CDKN2A</i>		X	X	Mucinous cyst	X	
17p	<i>TP53</i>		X	X	Nonspecific	X	
18q	<i>SMAD4</i>		X	X	Mucinous cyst	X	
10q	<i>PTEN</i>		X	X	Nonspecific	X	
9q	<i>NOTCH1</i>		X	X	Nonspecific	X	
1p	<i>ARID1A</i>		X	X	Mucinous cyst		Data limited
7q	<i>BRAF</i>	X			Nonspecific	X	Potentially targetable
3p	<i>VHL</i>		X	X	Serous cyst, clear cell NET		May be germline

11q	<i>MEN1</i>		X	X	NET	May be germline
Xq	<i>ATRX</i>		X	X	NET	Data limited
6p	<i>DAXX</i>		X	X	NET	Data limited
1q	<i>PHLDA3</i>			X	NET	Data limited
3p	<i>CTNNB1</i>	X			SPN	
1q	Aneuploidy				IPMN	
8p	Aneuploidy				IPMN	X
Others	Aneuploidy or loss of heterozygosity				Nonspecific	X

Abbreviations: *IPMN* Intraductal pancreatic mucinous neoplasm, *NET* Neuroendocrine tumor

Digital Image Analysis

Quantification of nuclear DNA content may help identify malignant lesions of the biliary tract. Methods of nuclear quantification include flow cytometric analysis, although such analysis requires a large quantity and proportion of tumor cells [135]. When quantified at an appropriate wavelength after staining with Feulgen dye, optical density is proportional to the quantity of nucleic acid. Such quantification may be performed by any one of a variety of commercially available image analyzers. Because each cell is analyzed individually, such quantification is applicable for specimens with limited cellularity. Results are characterized as diploid, aneuploid, or tetraploid. Aneuploidy in particular, as well as tetraploidy, is supportive of the presence of malignancy.

Digital image analysis (DIA) has demonstrated variable sensitivity and specificity for the presence of malignancy in samples of pancreatic or biliary duct strictures. In a retrospective analysis of 27 specimens, Rumalla et al. reported a sensitivity of 85% for malignancy using DIA [136]. Aneuploid cells were detected in 13 of 16 specimens for which routine cytomorphologic analysis was unrevealing. In a subsequent study by the same group, Baron et al. prospectively compared DIA to routine cytomorphologic analysis in 56 malignant and 44 benign strictures [137]. The sensitivities for malignancy of DIA and cytomorphology were 39% and 18%, respectively; the specificities for malignancy of DIA and cytomorphology were 77% and 98%, respectively. Depending on cost and availability, quantification of nuclear DNA in cytologic samples derived from the pancreatic or bile duct may present an attractive option for determination of the presence of malignancy in combination with traditional cytomorphologic analysis and other ancillary techniques discussed below.

Immunohistochemistry and Immunocytochemistry

Several IHC markers have been evaluated to aid in distinction of malignant from benign lesions of the pancreatic and bile ducts. Evaluation has predominantly been performed on resection or

other histologic material; and evaluated markers include S100P, S100A4, CD24, SMAD4, P-cadherin, claudin-18, mesothelin, survivin, BCL-2, BCL-2-associated X protein (BAX), p16, p34, p53, cyclooxygenase 2 (Cox-2), topoisomerase-II α , fascia, 14-3-3 σ , MUC4, heat shock protein 47 (HSP-47), minichromosome maintenance complex components 2 and 5 (MCM-2 and MCM-5), IDH1, IDH2, and Ki-67 [138–145]. Notably, Levy et al. observed expression of S100P and IMP3 with loss of pVHL in 28/42 (70%) bile duct biopsy specimens of adenocarcinoma; 22/32 (69%) benign samples retained expression of pVHL and demonstrated no expression of S100P or IMP3 [146]. More recently, in a study that predominantly consisted of histologic biopsy specimens as well as several resection and EUS-FNA biopsy specimens, Tretiakova et al. demonstrated loss of CD10 expression in 43/45 (96%) foci of high-grade dysplasia and 29/30 (97%) foci of invasive adenocarcinoma, compared to 3/121 (2%) foci without high-grade dysplasia [147]. No difference in expression pattern was identified between cytologic cell block and histologic specimens. These results corroborated those of several smaller studies of CD10 expression in both intrahepatic [148, 149] and extrahepatic [150] ChACA specimens.

Rare studies have evaluated the efficacy of IHC or immunocytochemical (ICC) analysis performed directly on pancreaticobiliary brush or aspirate material. Notably, Stewart and Burke evaluated ICC expression of p53 in a series of pancreaticobiliary brush cytology specimens [151]. Expression of p53 was identified in 41/45 (91%) cases of pancreaticobiliary adenocarcinoma, compared to 1/54 (2%) benign specimens. However, among cytomorphologically indeterminate specimens, p53 expression was identified in only four of ten (40%) malignant specimens compared to one of nine (11%) benign specimens. The authors concluded that lack of sensitivity compared to conventional morphologic analysis does not support routine use of ICC analysis of p53 expression in pancreaticobiliary brush cytology. More recently, Hart et al. evaluated ICC expression of a different ICC marker—IMP3—in a series of pancreaticobiliary brush cytology specimens [152]. Expression of IMP3 was identified in 25/39 (64%) cases of adenocarcinoma with no false-positive cases.

Among 14 cytomorphologically indeterminate specimens, IMP3 expression was identified in 8 (57%). However, all cytomorphologically indeterminate specimens were later determined to be malignant. More recently, Tokumitsu et al. evaluated ICC expression of maspin in a series of pancreatobiliary brush cytology specimens [153]. Expression of maspin was identified in 28/35 (80%) cases of adenocarcinoma with no false-positive cases. Among 12 cytomorphologically indeterminate specimens, maspin expression was identified in 5 (42%). However, as in the study by Hart et al., all cytomorphologically indeterminate specimens were later determined to be malignant. Ultimately, the value of IHC or ICC analysis of cytologic material derived from pancreatic or bile duct strictures requires additional validation before incorporation into standard clinical practice.

Fluorescence In Situ Hybridization

As both PDACA and ChACA are characterized by a high frequency of numerical and structural chromosomal abnormalities, the utility of FISH for the detection of malignancy in cytologic specimens of pancreatic and bile duct strictures has been reported and reviewed [154, 155]. Initial studies utilized the UroVysion probe set (Abbott Molecular Inc., Des Plaines, IL), which consists of a specific probe for the *CDKN2A* locus on chromosome 9p21, as well as enumeration probes for chromosomes 3, 7, and 17. In the first study to examine the clinical role of FISH in the evaluation of malignancy in pancreatic and bile duct strictures, Kipp et al. examined pancreatobiliary tract brushings with or without bile aspirate specimens from 131 patients, 58 of whom had a primary pancreatobiliary malignancy [156]. The authors observed that the presence of polysomy (defined as the presence of >2 signals in at least two of the three centromeric probes) was a more sensitive indicator of malignancy without significantly decreased specificity than cytomorphologic analysis alone. Several studies from the same group have compared performance characteristics of FISH with DIA and traditional cytomorphologic analysis [157–159]. In the most comprehen-

sive of such studies, the same FISH probe set was used to assess pancreatico-biliary tract brushings from 498 patients—189 with primary sclerosing cholangitis (PSC) and 222 of whom had a primary pancreatico-biliary malignancy [160]. The authors observed that the presence of polysomy was a more sensitive indicator of the presence of malignancy than cytomorphologic analysis such that a specimen with polysomy was approximately 77 times more likely to harbor malignancy than one with disomy and twice as likely to harbor malignancy than one with isolated trisomy 7. Both FISH and cytomorphologic analysis demonstrated excellent specificity, suggesting that the two methods may complement one another.

Subsequent studies at other institutions have largely confirmed and refined the role of FISH in detection of pancreatico-biliary tract malignancy [161]. Notably, Gonda et al. observed that evaluation of polysomy increased the sensitivity of brush cytology for the presence of malignancy (correctly identified in 11/19 cases) without sacrificing specificity (1 false positive among 31 cases) [162]. In addition, when the presence of 9p21 loss was included as a positive result, the sensitivity of brush cytology for the presence of malignancy increased significantly (correctly identified in 16/19 cases) without a concomitant decrease in specificity. Although studies have reported a range of sensitivities and specificities for FISH analysis of pancreatico-biliary strictures, the highest analytic sensitivity was reported in a study by Boldorini et al. who reported polysomy in 23/24 (96%) cases of ChACA and 20/24 (83%) cases of PDACA with only 1 false-positive result [163]. Interestingly, among 12 cases with indeterminate cytomorphology, polysomy was present in 8/9 (89%) cases of malignancy and 1/3 benign cases.

Patients with PSC have a particularly high annual and cumulative lifetime risk of developing ChACA. The role of FISH in analysis of PSC-associated biliary strictures has been studied extensively, as marked reactive and reparative cellular changes that mimic carcinoma render morphologic interpretation of bile duct brushings particularly difficult. Eaton et al. retrospectively studied polysomic specimens derived from 371 PSC patients [164]. The authors reported that polysomy detected in multiple

areas of the biliary tree was the strongest independent predictor of subsequent cancer diagnosis, although suspicious cytomorphology and unifocal polysomy were also independently predictive of development of ChACA. The authors also noted that 71% of patients diagnosed with ChACA had polysomy detected at a region of the biliary tree where malignancy was not detected by routine cytomorphology, suggesting that multiple locations of the biliary tree should be sampled in PSC patients. These results largely confirmed results of previous studies from the same group [165–167]. Meta-analysis of studies including 690 PSC patients has also confirmed performance characteristics of FISH with 51% and 93% sensitivity and specificity, respectively [168]. Overall, the combination of FISH analysis of chromosomes 3, 7, and 17 with routine cytomorphologic analysis of pancreatic and bile duct brushing specimens improves sensitivity for the presence of malignancy over cytomorphologic analysis alone without sacrificing specificity in patients with and without PSC, provided that the definition of a positive FISH result is appropriately stringent.

While chromosomes 3, 7, and 17 are variably lost and gained, optimization of FISH analysis has been attempted using probes for genomic regions more typically altered in malignant pancreaticobiliary tumors. Specifically, Fritcher et al. selected an optimized set of 4 probes for validation in a set of pancreaticobiliary duct brushing samples from 183 patients, including 85 patients with pancreaticobiliary malignancy and 114 patients with PSC: 1q21 (including the *MCL1* locus), 7p12 (including the *EGFR* locus), 8q24 (including the *MYC* locus), and p16 (*CDKN2A*) locus on 9p21 [169]. The optimized FISH probe set identified samples from patients with malignancy with significantly greater sensitivity (65%) than probes for chromosomes 3, 7, and 17 (46%) or routine cytomorphologic analysis (19%), but similar specificity (93%), particularly in the absence of PSC (100%). Utilization of FISH analysis using an optimized set of probes is a promising approach to evaluation of pancreatic and bile duct brushing specimens, particularly as an adjunct to conventional cytomorphologic analysis. An overview of potential genomic targets, methodology, and interpretation of FISH analysis is presented in Table 12.6.

Table 12.6 Genomic targets, methodology, and interpretation of fluorescence in situ hybridization analysis of pancreatic and bile duct brushing specimens

Traditional probe set		Alternate probe set				
Genomic target	CEP 3	CEP 7	CEP 17	9p21	8q24	9p21
Notable genes			CDKN2A	MCL1	EGFR	MYC
Methodology	Count at least 100 epithelial cells with acceptable probe signal quality					
Positive result	Five cells demonstrating polysomy (gains of two or more centromeric probes in an individual cell) <i>or</i> ten cells demonstrating trisomy (single copy gain of one probe <i>other than</i> CEP 7)					
Equivocal result	Five cells demonstrating single probe gain and single copy loss of 9p21 <i>or</i> five cells demonstrating homozygous 9p21 loss <i>or</i> eight cells demonstrating isolated gain of probe <i>other than</i> CEP 7 <i>or</i> ten cells demonstrating tetrasomy (four copies of all four probes) <i>or</i> ten cells demonstrating isolated trisomy 7					
Notes	May be combined with KRAS sequencing and heterozygosity analysis to increase sensitivity and specificity					

Abbreviations: CEP Chromosome enumeration probe

Genetic Sequencing and Other Genetic Testing

Molecular profiling techniques have the potential to improve diagnosis of PDACA and ChACA in patients with pancreatic and bile duct strictures, respectively, and their use is a field of active study. Evaluation of pancreatic and bile duct strictures is complicated by both the wide range of testing and sampling techniques available, and testing of both bile and pancreatic juice has been suggested as a method of early detection of malignancy [170]. Notably, Yu et al. were able to distinguish a small number of patients with PDACA from those with IPMN or normal pancreata by detecting *SMAD4* and *TP53* mutations by digital NGS of pancreatic juice specimens [171]. A meta-analysis of 16 studies including 1060 patients calculated the pooled sensitivity and specificity for malignancy of detection of *KRAS* mutation in pancreatic juice to be 59% and 87%, respectively [172]. A separate meta-analysis of 39 studies calculated the pooled sensitivity and specificity of detection of *KRAS* mutation in pancreatic juice to be 67% and 82%, respectively [173]. In that study, combination of *KRAS* sequencing and telomerase activity analysis demonstrated higher diagnostic sensitivity (94%) than *KRAS* sequencing alone, and combination of telomerase activity and cytomorphologic analysis demonstrated greater diagnostic sensitivity (88%) and specificity (100%) for malignancy than telomerase activity analysis alone. A subsequent study that was not included in either meta-analysis reported activating *KRAS* mutation in 22/30 (73%) secretin-stimulated pancreatic juice samples from 30 patients with pancreatic cancer, compared to 96/194 (49%) samples from patients deemed to be at high risk for development of cancer and 9/48 (19%) samples from low-risk patient controls [174]. A previous study from the same group demonstrated that detection of *TP53* mutation in secretin-stimulated pancreatic juice samples is a highly specific marker of invasive malignancy and high-grade dysplasia [175]. Although these results highlight the potential power of pancreatic juice as a source of nucleic acid for ancillary testing, genetic sequencing is more commonly applied to pancreatic and bile duct brushing specimens.

KRAS Mutational Analysis

Detection of activating point mutation in the *KRAS* gene by any one of multiple methods, including NGS and with or without concomitant FISH analysis, has been studied as an ancillary testing procedure for analysis of both pancreatic juice and pancreatobiliary duct brushing specimens. Notably, Sturm et al. collected pancreatic and bile duct brushing specimens from 312 consecutive patients with extrahepatic biliary stenosis and found that conventional cytomorphology combined with restriction fragment length analysis of *KRAS* codon 12 only is more sensitive for the presence of malignancy than conventional cytomorphology alone [176]. Kipp et al. later analyzed *KRAS* by qPCR in a retrospectively collected cohort of pancreatobiliary stricture brushing cytology samples [177]. The presence of either *KRAS* mutation or polysomy by FISH analysis was detected in 30/35 (86%) cases of PDACA and 22/41 (54%) cases of ChACA, while *KRAS* mutation alone was identified in 2/52 (4%) benign strictures. It is important to note that activating *KRAS* mutations may be present in benign and premalignant lesions. Therefore, per Pap Society guidelines, current data do not support *KRAS* mutational analysis of pancreatic and bile duct strictures as a useful ancillary test in isolation for diagnosis of malignancy [9].

Loss of Heterozygosity

Several studies have evaluated LoH as a marker of malignancy in pancreatic and biliary duct brushing cytology specimens. Ohori et al. studied heterozygosity at nine genomic loci in eight diagnostic bile duct brushings paired with resection specimens of PDACA ($n = 3$) and ChACA ($n = 5$) [178]. The authors identified LoH at each focus in at least one case, although only three of eight cases demonstrated identical foci of LoH in matched specimens. Researchers from the same group later developed a modified panel of 12 microsatellite markers to detect LoH at 6 genomic loci in pancreatobiliary brushing samples [179]. The authors identified abundant LoH in each of 17 malignant cases, 9 of which were indeterminate by cytomorphologic analysis, while no LoH at any locus was identified in brushing specimens from 9 benign cases, only 1 of which was cytomorphologically indeterminate.

Finkelstein et al. also analyzed heterozygosity in centrifugation-derived supernatant fluid from pancreatico-biliary duct samples [180]. Using a panel of 16 microsatellite markers to evaluate 9 genomic loci, LoH for at least 1 locus was identified in 19/26 (73%) cases of PDACA or ChACA, while no LoH at any locus was identified in specimens from 5 benign cases.

In a more recent and prospective study, Gonda et al. combined cytomorphology, FISH, and *KRAS* sequencing with heterozygosity analysis at 10 genomic loci for 100 consecutively collected brushing specimens of pancreatico-biliary strictures, 41 of which were malignant [181]. FISH probes were directed against chromosomes 3, 7, and 17 and the *CDKN2A* locus on chromosome 9p21. Heterozygosity was evaluated at the following loci: 1p, 3p, 5q, 9p (including the *CDKN2A* locus), 10q, 17p, 17q, 18q, 21q, and 22q. Notably, the specificity of each ancillary test for the presence of malignancy was 100%. In addition, FISH alone identified an additional nine malignant specimens not detected by cytomorphology or heterozygosity analysis, while heterozygosity analysis alone identified an additional seven malignant specimens not identified by cytomorphology or FISH. Ultimately, heterozygosity analysis, with or without FISH analysis, may be appropriate for cytomorphologically indeterminate pancreatico-biliary brushing specimens. While FISH has been studied more extensively than heterozygosity analysis, FISH requires significant tumor cellularity. Heterozygosity analysis may be performed on supernatant fluid, even in specimens of low cellularity. Additional studies will help clarify the optimal sequence for testing and specific genomic loci at which to evaluate heterozygosity.

Next-Generation Sequencing of DNA

Scattered studies have addressed the role of NGS in diagnostic evaluation of pancreatico-biliary duct specimens. In the largest of these, Dudley et al. subjected pancreatic and bile duct brushing specimens to cytomorphology; FISH analysis of chromosomes 3, 7, and 17 and 9p21; and NGS of hotspots in 39 genes [182]. Cytomorphologic analysis successfully identified 23/33 malignant specimens and was falsely positive in 1/48 benign cases. FISH and NGS analysis identified an additional two and five malignant

cases, respectively. Both additional cases identified by FISH were also identified by NGS, suggesting that NGS may be appropriate as an alternative or adjunct to FISH testing in cytomorphologically indeterminate pancreatico-biliary brushing specimens.

DNA Methylation Marker Profiling

As increasing prevalence of aberrant DNA methylation has been demonstrated in precancerous and cancerous lesions, several studies have evaluated the diagnostic utility of gene methylation for its ability to detect the presence of high-grade dysplasia and invasive carcinoma in specimens derived from pancreatico-biliary duct strictures. In a study utilizing quantitative methylation-specific PCR, Parsi et al. identified methylation of *TFPI2*, *NPTX2*, and *CCND2* as the three best markers with which to discriminate benign from malignant biliary and pancreatic duct brush samples [183]. In a similar study, Andresen et al. identified methylation of *CDO1*, *CNRIP1*, *SEPT9*, and *VIM* as the four best markers with which to discriminate benign from malignant biliary and pancreatic duct brush samples [184]. In another similar study, Kisiel et al. identified methylation of *CD1D* as being particularly sensitive and specific for the presence of malignancy in pancreatic juice samples [185]. More recently, Prachayakul et al. demonstrated that evaluation of the methylation status by quantitative methylation-specific PCR of two gene promoters (*HOXA1* and *NEUROG1*) successfully identified malignancy in eight of nine (89%) biliary brush samples from ChACA patients [186]. None of the methylation studies specifically evaluated specimens with indeterminate cytomorphology, and further investigation will be required to optimize utilization of methylation marker profiling for diagnosis of pancreatico-biliary malignancy.

MicroRNA Profiling

Extracellular vesicles (EV), which are released by a diversity of cell types and, thus, present in a diversity of biologic fluids, including bile, play an essential role in cell-to-cell communication and contain abundant microRNA and long, noncoding RNA (lncRNA). In particular, microRNA species have emerged as promising diagnostic markers of both PDACA and ChACA [187,

188]. Notably, Li et al. used qPCR to identify a panel of four biliary EV-derived microRNA species (miR-191, miR-486-3p, miR-1274b, and miR-484) that was 67% sensitive and 96% specific for the presence of malignancy in bile aspirate from 46 ChACA patients and 50 control patients, 13 of whom had PSC [189]. Other studies have identified other microRNA species differentially expressed in the bile of ChACA and healthy patients, including miR-145, miR-9 [190], miR-412, miR-640, miR-1537, and miR-3189 [191]. The overall capacity of microRNA analysis to diagnose ChACA has been evaluated in a meta-analysis [192]. Although the meta-analysis was not limited to studies of bile, microRNA in bile and serum demonstrated higher diagnostic value for ChACA than in tissue and urine. More recently, a study has also identified lncRNA species differentially expressed in bile of ChACA and healthy patients, including ENST00000588480.1 and ENST00000517758.1 [193].

A number of other biliary brushing- and bile-derived biomarkers of malignancy have been examined. These include acrylonitrile, 3-methylhexane, benzene, MCM-5, insulin-like growth factor-1, carcinoembryonic cell adhesion molecule-6, and a wide variety of other proteins [194–197]. Such biomarkers may be detected by immunoassay or mass spectrometry, among other methods. Although bile proteomics and microRNA profiling are promising adjuncts to pancreatico-biliary cytomorphology, their efficacy in a clinical setting will require further investigation.

References

1. Cancer Genome Atlas Research Network. Integrated genomic characterization of pancreatic ductal adenocarcinoma. *Cancer Cell*. 2017;32(2):185–203.e13.
2. Murphy KM, Brune KA, Griffin C, Sollenberger JE, Petersen GM, Bansal R, et al. Evaluation of candidate genes MAP2K4, MADH4, ACVR1B, and BRCA2 in familial pancreatic cancer: deleterious BRCA2 mutations in 17%. *Cancer Res*. 2002;62(13):3789–93.
3. Al-Sukhni W, Rothenmund H, Borgida AE, Zogopoulos G, O’Shea AM, Pollett A, et al. Germline BRCA1 mutations predispose to pancreatic adenocarcinoma. *Hum Genet*. 2008;124(3):271–8.

4. Jones S, Hruban RH, Kamiyama M, Borges M, Zhang X, Parsons DW, et al. Exomic sequencing identifies PALB2 as a pancreatic cancer susceptibility gene. *Science*. 2009;324(5924):217.
5. Roberts NJ, Jiao Y, Yu J, Kopelovich L, Petersen GM, Bondy ML, et al. ATM mutations in patients with hereditary pancreatic cancer. *Cancer Discov*. 2012;2(1):41–6.
6. Zhen DB, Rabe KG, Gallinger S, Syngal S, Schwartz AG, Goggins MG, et al. BRCA1, BRCA2, PALB2, and CDKN2A mutations in familial pancreatic cancer: a PACGENE study. *Genet Med*. 2015;17(7):569–77.
7. Waddell N, Pajic M, Patch AM, Chang DK, Kassahn KS, Bailey P, et al. Whole genomes redefine the mutational landscape of pancreatic cancer. *Nature*. 2015;518(7540):495–501.
8. Farshidfar F, Zheng S, Gingras MC, Newton Y, Shih J, Robertson AG, et al. Integrative genomic analysis of cholangiocarcinoma identifies distinct IDH-Mutant molecular profiles. *Cell Rep*. 2017;18(11):2780–94.
9. Layfield LJ, Ehya H, Filie AC, Hruban RH, Jhala N, Joseph L, et al. Utilization of ancillary studies in the cytologic diagnosis of biliary and pancreatic lesions: the Papanicolaou Society of Cytopathology guidelines for pancreatobiliary cytology. *Diagn Cytopathol*. 2014;42(4):351–62.
10. Wilentz RE, Iacobuzio-Donahue CA, Argani P, McCarthy DM, Parsons JL, Yeo CJ, et al. Loss of expression of Dpc4 in pancreatic intraepithelial neoplasia: evidence that DPC4 inactivation occurs late in neoplastic progression. *Cancer Res*. 2000;60(7):2002–6.
11. Liu H, Shi J, Anandan V, Wang HL, Diehl D, Blansfield J, et al. Reevaluation and identification of the best immunohistochemical panel (pVHL, Maspin, S100P, IMP-3) for ductal adenocarcinoma of the pancreas. *Arch Pathol Lab Med*. 2012;136(6):601–9.
12. Argani P, Iacobuzio-Donahue C, Ryu B, Rosty C, Goggins M, Wilentz RE, et al. Mesothelin is overexpressed in the vast majority of ductal adenocarcinomas of the pancreas: identification of a new pancreatic cancer marker by serial analysis of gene expression (SAGE). *Clin Cancer Res*. 2001;7(12):3862–8.
13. Agarwal B, Ludwig OJ, Collins BT, Cortese C. Immunostaining as an adjunct to cytology for diagnosis of pancreatic adenocarcinoma. *Clin Gastroenterol Hepatol*. 2008;6(12):1425–31.
14. Ali A, Brown V, Denley S, Jamieson NB, Morton JP, Nixon C, et al. Expression of KOC, S100P, mesothelin and MUC1 in pancreatico-biliary adenocarcinomas: development and utility of a potential diagnostic immunohistochemistry panel. *BMC Clin Pathol*. 2014;14:35.
15. Dim DC, Jiang F, Qiu Q, Li T, Darwin P, Rodgers WH, et al. The usefulness of S100P, mesothelin, fascin, prostate stem cell antigen, and 14–3-3 sigma in diagnosing pancreatic adenocarcinoma in cytological specimens obtained by endoscopic ultrasound guided fine-needle aspiration. *Diagn Cytopathol*. 2014;42(3):193–9.
16. Zhu L, Liu Y, Chen G. Diagnostic value of mesothelinin pancreatic cancer: a meta-analysis. *Int J Clin Exp Med*. 2014;7(11):4000–7.

17. Furuhashi A, Minamiguchi S, Shirahase H, Kodama Y, Adachi S, Sakurai T, et al. Immunohistochemical antibody panel for the differential diagnosis of pancreatic ductal carcinoma from gastrointestinal contamination and benign pancreatic duct epithelium in endoscopic ultrasound-guided fine-needle aspiration. *Pancreas*. 2017;46(4):531–8.
18. McCarthy DM, Maitra A, Argani P, Rader AE, Faigel DO, Van Heek NT, et al. Novel markers of pancreatic adenocarcinoma in fine-needle aspiration: mesothelin and prostate stem cell antigen labeling increases accuracy in cytologically borderline cases. *Appl Immunohistochem Mol Morphol*. 2003;11(3):238–43.
19. Ezzat NE, Tahoun NS, Ismail YM. The role of S100P and IMP3 in the cytologic diagnosis of pancreatic adenocarcinoma. *J Egypt Natl Canc Inst*. 2016;28(4):229–34.
20. Sweeney J, Rao R, Margolskee E, Goyal A, Heymann JJ, Siddiqui MT. Immunohistochemical staining for S100P, SMAD4, and IMP3 on cell block preparations is sensitive and highly specific for pancreatic ductal adenocarcinoma. *Journal of the American Society of Cytopathology*. 2018;7(6):318–23.
21. Levy MJ, Oberg TN, Campion MB, Clayton AC, Halling KC, Henry MR, et al. Comparison of methods to detect neoplasia in patients undergoing endoscopic ultrasound-guided fine-needle aspiration. *Gastroenterology*. 2012;142(5):1112–21.
22. Ribeiro A, Peng J, Casas C, Fan YS. Endoscopic ultrasound guided fine needle aspiration with fluorescence in situ hybridization analysis in 104 patients with pancreatic mass. *J Gastroenterol Hepatol*. 2014;29(8):1654–8.
23. de Biase D, Visani M, Acquaviva G, Fornelli A, Masetti M, Fabbri C, et al. The role of next-generation sequencing in the cytologic diagnosis of pancreatic lesions. *Arch Pathol Lab Med*. 2018;142(4):458–64.
24. Kameta E, Sugimori K, Kaneko T, Ishii T, Miwa H, Sato T, et al. Diagnosis of pancreatic lesions collected by endoscopic ultrasound-guided fine-needle aspiration using next-generation sequencing. *Oncol Lett*. 2016;12(5):3875–81.
25. Valero V, Saunders TJ, He J, Weiss MJ, Cameron JL, Dholakia A, et al. Reliable detection of somatic mutations in fine needle aspirates of pancreatic cancer with next-generation sequencing: implications for surgical management. *Ann Surg*. 2016;263(1):153–61.
26. Young G, Wang K, He J, Otto G, Hawryluk M, Zwirco Z, et al. Clinical next-generation sequencing successfully applied to fine-needle aspirations of pulmonary and pancreatic neoplasms. *Cancer Cytopathol*. 2013;121(12):688–94.
27. Gleeson FC, Kerr SE, Kipp BR, Voss JS, Minot DM, Tu ZJ, et al. Targeted next generation sequencing of endoscopic ultrasound acquired cytology from ampullary and pancreatic adenocarcinoma has the potential to aid patient stratification for optimal therapy selection. *Oncotarget*. 2016;7(34):54526–36.

28. Hayashi H, Kohno T, Ueno H, Hiraoka N, Kondo S, Saito M, et al. Utility of assessing the number of mutated KRAS, CDKN2A, TP53, and SMAD4 genes using a targeted deep sequencing assay as a prognostic biomarker for pancreatic cancer. *Pancreas*. 2017;46(3):335–40.
29. Deftereos G, Finkelstein SD, Jackson SA, Ellsworth EM, Krishnamurti U, Liu Y, et al. The value of mutational profiling of the cytocentrifugation supernatant fluid from fine-needle aspiration of pancreatic solid mass lesions. *Mod Pathol*. 2014;27(4):594–601.
30. Khalid A, Dewitt J, Ohori NP, Chen JH, Fasanella KE, Sanders M, et al. EUS-FNA mutational analysis in differentiating autoimmune pancreatitis and pancreatic cancer. *Pancreatology*. 2011;11(5):482–6.
31. Steele CW, Oien KA, McKay CJ, Jamieson NB. Clinical potential of microRNAs in pancreatic ductal adenocarcinoma. *Pancreas*. 2011;40(8):1165–71.
32. Ali S, Saleh H, Sethi S, Sarkar FH, Philip PA. MicroRNA profiling of diagnostic needle aspirates from patients with pancreatic cancer. *Br J Cancer*. 2012;107(8):1354–60.
33. Hong TH, Park IY. MicroRNA expression profiling of diagnostic needle aspirates from surgical pancreatic cancer specimens. *Ann Surg Treat Res*. 2014;87(6):290–7.
34. Brand RE, Adai AT, Centeno BA, Lee LS, Rateb G, Vignesh S, et al. A microRNA-based test improves endoscopic ultrasound-guided cytologic diagnosis of pancreatic cancer. *Clin Gastroenterol Hepatol*. 2014;12(10):1717–23.
35. Shi C, Klimstra DS. Pancreatic neuroendocrine tumors: pathologic and molecular characteristics. *Semin Diagn Pathol*. 2014;31(6):498–511.
36. Wood LD, Hruban RH. Genomic landscapes of pancreatic neoplasia. *J Pathol Transl Med*. 2015;49(1):13–22.
37. Pea A, Hruban RH, Wood LD. Genetics of pancreatic neuroendocrine tumors: implications for the clinic. *Expert Rev Gastroenterol Hepatol*. 2015;9(11):1407–19.
38. Hackeng WM, Hruban RH, Offerhaus GJ, Brosens LA. Surgical and molecular pathology of pancreatic neoplasms. *Diagn Pathol*. 2016;11(1):47.
39. Jiao Y, Shi C, Edil BH, de Wilde RF, Klimstra DS, Maitra A, et al. DAXX/ATRX, MEN1, and mTOR pathway genes are frequently altered in pancreatic neuroendocrine tumors. *Science*. 2011;331(6021):1199–203.
40. Yachida S, Vakilani E, White CM, Zhong Y, Saunders T, Morgan R, et al. Small cell and large cell neuroendocrine carcinomas of the pancreas are genetically similar and distinct from well-differentiated pancreatic neuroendocrine tumors. *Am J Surg Pathol*. 2012;36(2):173–84.
41. La Rosa S, Sessa F, Capella C. Acinar Cell carcinoma of the pancreas: overview of clinicopathologic features and insights into the molecular pathology. *Front Med (Lausanne)*. 2015;2:41.
42. Abraham SC, Wu TT, Klimstra DS, Finn LS, Lee JH, Yeo CJ, et al. Distinctive molecular genetic alterations in sporadic and familial adenoma-

- tous polyposis-associated pancreatoblastomas : frequent alterations in the APC/beta-catenin pathway and chromosome 11p. *Am J Pathol.* 2001;159(5):1619–27.
43. Abraham SC, Wu TT, Hruban RH, Lee JH, Yeo CJ, Conlon K, et al. Genetic and immunohistochemical analysis of pancreatic acinar cell carcinoma: frequent allelic loss on chromosome 11p and alterations in the APC/beta-catenin pathway. *Am J Pathol.* 2002;160(3):953–62.
 44. Weksberg R, Shuman C, Beckwith JB. Beckwith-Wiedemann syndrome. *Eur J Hum Genet.* 2010;18(1):8–14.
 45. Jiao Y, Yonescu R, Offerhaus GJ, Klimstra DS, Maitra A, Eshleman JR, et al. Whole-exome sequencing of pancreatic neoplasms with acinar differentiation. *J Pathol.* 2014;232(4):428–35.
 46. Furlan D, Sahnane N, Bernasconi B, Frattini M, Tibiletti MG, Molinari F, et al. APC alterations are frequently involved in the pathogenesis of acinar cell carcinoma of the pancreas, mainly through gene loss and promoter hypermethylation. *Virchows Arch.* 2014;464(5):553–64.
 47. Chmielecki J, Hutchinson KE, Frampton GM, Chalmers ZR, Johnson A, Shi C, et al. Comprehensive genomic profiling of pancreatic acinar cell carcinomas identifies recurrent RAF fusions and frequent inactivation of DNA repair genes. *Cancer Discov.* 2014;4(12):1398–405.
 48. Tanaka Y, Kato K, Notohara K, Hojo H, Ijiri R, Miyake T, et al. Frequent beta-catenin mutation and cytoplasmic/nuclear accumulation in pancreatic solid-pseudopapillary neoplasm. *Cancer Res.* 2001;61(23):8401–4.
 49. Abraham SC, Klimstra DS, Wilentz RE, Yeo CJ, Conlon K, Brennan M, et al. Solid-pseudopapillary tumors of the pancreas are genetically distinct from pancreatic ductal adenocarcinomas and almost always harbor beta-catenin mutations. *Am J Pathol.* 2002;160(4):1361–9.
 50. Burford H, Baloch Z, Liu X, Jhala D, Siegal GP, Jhala N. E-cadherin/beta-catenin and CD10: a limited immunohistochemical panel to distinguish pancreatic endocrine neoplasm from solid pseudopapillary neoplasm of the pancreas on endoscopic ultrasound-guided fine-needle aspirates of the pancreas. *Am J Clin Pathol.* 2009;132(6):831–9.
 51. La Rosa S, Franzi F, Marchet S, Finzi G, Clerici M, Vigetti D, et al. The monoclonal anti-BCL10 antibody (clone 331.1) is a sensitive and specific marker of pancreatic acinar cell carcinoma and pancreatic metaplasia. *Virchows Arch.* 2009;454(2):133–42.
 52. Hosoda W, Sasaki E, Murakami Y, Yamao K, Shimizu Y, Yatabe Y. BCL10 as a useful marker for pancreatic acinar cell carcinoma, especially using endoscopic ultrasound cytology specimens. *Pathol Int.* 2013;63(3):176–82.
 53. Comper F, Antonello D, Beghelli S, Gobbo S, Montagna L, Pederzoli P, et al. Expression pattern of claudins 5 and 7 distinguishes solid-pseudopapillary from pancreatoblastoma, acinar cell and endocrine tumors of the pancreas. *Am J Surg Pathol.* 2009;33(5):768–74.
 54. Yasumoto M, Hamabashiri M, Akiba J, Ogasawara S, Naito Y, Taira T, et al. The utility of a novel antibody in the pathological diagnosis of pancreatic acinar cell carcinoma. *J Clin Pathol.* 2012;65(4):327–32.

55. Singhi AD, Lilo M, Hruban RH, Cressman KL, Fuhrer K, Seethala RR. Overexpression of lymphoid enhancer-binding factor 1 (LEF1) in solid-pseudopapillary neoplasms of the pancreas. *Mod Pathol*. 2014;27(10):1355–63.
56. Guo Y, Yuan F, Deng H, Wang HF, Jin XL, Xiao JC. Paranuclear dot-like immunostaining for CD99: a unique staining pattern for diagnosing solid-pseudopapillary neoplasm of the pancreas. *Am J Surg Pathol*. 2011;35(6):799–806.
57. Larghi A, Capurso G, Carnuccio A, Ricci R, Alfieri S, Galasso D, et al. Ki-67 grading of nonfunctioning pancreatic neuroendocrine tumors on histologic samples obtained by EUS-guided fine-needle tissue acquisition: a prospective study. *Gastrointest Endosc*. 2012;76(3):570–7.
58. Hasegawa T, Yamao K, Hijioka S, Bhatia V, Mizuno N, Hara K, et al. Evaluation of Ki-67 index in EUS-FNA specimens for the assessment of malignancy risk in pancreatic neuroendocrine tumors. *Endoscopy*. 2014;46(1):32–8.
59. Weynand B, Borbath I, Bernard V, Sempoux C, Gigot JF, Hubert C, et al. Pancreatic neuroendocrine tumour grading on endoscopic ultrasound-guided fine needle aspiration: high reproducibility and inter-observer agreement of the Ki-67 labelling index. *Cytopathology*. 2014;25(6):389–95.
60. Diaz Del Arco C, Diaz Perez JA, Ortega Medina L, Sastre Valera J, Fernandez Acenero MJ. Reliability of Ki-67 determination in FNA samples for grading pancreatic neuroendocrine tumors. *Endocr Pathol*. 2016;27(4):276–83.
61. Ozaslan E, Demir S, Karaca H, Guven K. Evaluation of the concordance between the stage of the disease and Ki-67 proliferation index in gastroenteropancreatic neuroendocrine tumors. *Eur J Gastroenterol Hepatol*. 2016;28(7):836–41.
62. Diaz Del Arco C, Esteban Lopez-Jamar JM, Ortega Medina L, Diaz Perez JA, Fernandez Acenero MJ. Fine-needle aspiration biopsy of pancreatic neuroendocrine tumors: correlation between Ki-67 index in cytological samples and clinical behavior. *Diagn Cytopathol*. 2017;45(1):29–35.
63. Yao JC, Shah MH, Ito T, Bohas CL, Wolin EM, Van Cutsem E, et al. Everolimus for advanced pancreatic neuroendocrine tumors. *N Engl J Med*. 2011;364(6):514–23.
64. Raymond E, Dahan L, Raoul JL, Bang YJ, Borbath I, Lombard-Bohas C, et al. Sunitinib malate for the treatment of pancreatic neuroendocrine tumors. *N Engl J Med*. 2011;364(6):501–13.
65. Phan AT, Halperin DM, Chan JA, Fogelman DR, Hess KR, Malinowski P, et al. Pazopanib and depot octreotide in advanced, well-differentiated neuroendocrine tumours: a multicentre, single-group, phase 2 study. *Lancet Oncol*. 2015;16(6):695–703.
66. Hobday TJ, Qin R, Reidy-Lagunes D, Moore MJ, Strosberg J, Kaubisch A, et al. Multicenter Phase II trial of Temsirolimus and Bevacizumab in pancreatic neuroendocrine tumors. *J Clin Oncol*. 2015;33(14):1551–6.

67. Nodit L, McGrath KM, Zahid M, Jani N, Schoedel KE, Otori NP, et al. Endoscopic ultrasound-guided fine needle aspirate microsatellite loss analysis and pancreatic endocrine tumor outcome. *Clin Gastroenterol Hepatol.* 2006;4(12):1474–8.
68. Kubota Y, Kawakami H, Natsuzaka M, Kawakubo K, Marukawa K, Kudo T, et al. CTNNB1 mutational analysis of solid-pseudopapillary neoplasms of the pancreas using endoscopic ultrasound-guided fine-needle aspiration and next-generation deep sequencing. *J Gastroenterol.* 2015;50(2):203–10.
69. Sigel CS, Krauss Silva VW, Reid MD, Chhieng D, Basturk O, Sigel KM, et al. Assessment of cytologic differentiation in high-grade pancreatic neuroendocrine neoplasms: a multi-institutional study. *Cancer Cytopathol.* 2018;126(1):44–53.
70. Basturk O, Coban I, Adsay NV. Pancreatic cysts: pathologic classification, differential diagnosis, and clinical implications. *Arch Pathol Lab Med.* 2009;133(3):423–38.
71. Wu J, Jiao Y, Dal Molin M, Maitra A, de Wilde RF, Wood LD, et al. Whole-exome sequencing of neoplastic cysts of the pancreas reveals recurrent mutations in components of ubiquitin-dependent pathways. *Proc Natl Acad Sci U S A.* 2011;108(52):21188–93.
72. Wu J, Matthaei H, Maitra A, Dal Molin M, Wood LD, Eshleman JR, et al. Recurrent GNAS mutations define an unexpected pathway for pancreatic cyst development. *Sci Transl Med.* 2011;3(92):92ra66.
73. Amato E, Molin MD, Mafficini A, Yu J, Malleo G, Rusev B, et al. Targeted next-generation sequencing of cancer genes dissects the molecular profiles of intraductal papillary neoplasms of the pancreas. *J Pathol.* 2014;233(3):217–27.
74. Habbe N, Koorstra JB, Mendell JT, Offerhaus GJ, Ryu JK, Feldmann G, et al. MicroRNA miR-155 is a biomarker of early pancreatic neoplasia. *Cancer Biol Ther.* 2009;8(4):340–6.
75. Lubezky N, Loewenstein S, Ben-Haim M, Brazowski E, Marmor S, Pashmanik-Chor M, et al. MicroRNA expression signatures in intraductal papillary mucinous neoplasm of the pancreas. *Surgery.* 2013;153(5):663–72.
76. Hong SM, Kelly D, Griffith M, Omura N, Li A, Li CP, et al. Multiple genes are hypermethylated in intraductal papillary mucinous neoplasms of the pancreas. *Mod Pathol.* 2008;21(12):1499–507.
77. Hong SM, Omura N, Vincent A, Li A, Knight S, Yu J, et al. Genome-wide CpG island profiling of intraductal papillary mucinous neoplasms of the pancreas. *Clin Cancer Res.* 2012;18(3):700–12.
78. Leung KK, Ross WA, Evans D, Fleming J, Lin E, Tamm EP, et al. Pancreatic cystic neoplasm: the role of cyst morphology, cyst fluid analysis, and expectant management. *Ann Surg Oncol.* 2009;16(10):2818–24.
79. Oh SH, Lee JK, Lee KT, Lee KH, Woo YS, Noh DH. The combination of cyst fluid carcinoembryonic antigen, cytology and viscosity increases the diagnostic accuracy of mucinous pancreatic cysts. *Gut Liver.* 2017;11(2):283–9.

80. van der Waaij LA, van Dullemen HM, Porte RJ. Cyst fluid analysis in the differential diagnosis of pancreatic cystic lesions: a pooled analysis. *Gastrointest Endosc.* 2005;62(3):383–9.
81. Rockacy M, Khalid A. Update on pancreatic cyst fluid analysis. *Ann Gastroenterol.* 2013;26(2):122–7.
82. Ngamruengphong S, Lennon AM. Analysis of pancreatic cyst fluid. *Surg Pathol Clin.* 2016;9(4):677–84.
83. Brugge WR, Lewandrowski K, Lee-Lewandrowski E, Centeno BA, Szydlowski T, Regan S, et al. Diagnosis of pancreatic cystic neoplasms: a report of the cooperative pancreatic cyst study. *Gastroenterology.* 2004;126(5):1330–6.
84. Linder JD, Geenen JE, Catalano MF. Cyst fluid analysis obtained by EUS-guided FNA in the evaluation of discrete cystic neoplasms of the pancreas: a prospective single-center experience. *Gastrointest Endosc.* 2006;64(5):697–702.
85. Snozek CL, Mascarenhas RC, O’Kane DJ. Use of cyst fluid CEA, CA19–9, and amylase for evaluation of pancreatic lesions. *Clin Biochem.* 2009;42(15):1585–8.
86. Cizginer S, Turner BG, Bilge AR, Karaca C, Pitman MB, Brugge WR. Cyst fluid carcinoembryonic antigen is an accurate diagnostic marker of pancreatic mucinous cysts. *Pancreas.* 2011;40(7):1024–8.
87. Soyer OM, Baran B, Ormeci AC, Sahin D, Gokturk S, Evirgen S, et al. Role of biochemistry and cytological analysis of cyst fluid for the differential diagnosis of pancreatic cysts: a retrospective cohort study. *Medicine (Baltimore).* 2017;96(1):e5513.
88. Ajaj Saieg M, Munson V, Colletti S, Nassar A. Impact of pancreatic cyst fluid CEA levels on the classification of pancreatic cysts using the Papanicolaou Society of Cytology Terminology System for Pancreaticobiliary cytology. *Diagn Cytopathol.* 2017;45(2):101–6.
89. Thornton GD, McPhail MJ, Nayagam S, Hewitt MJ, Vlavianos P, Monahan KJ. Endoscopic ultrasound guided fine needle aspiration for the diagnosis of pancreatic cystic neoplasms: a meta-analysis. *Pancreatol.* 2013;13(1):48–57.
90. de Jong K, Poley JW, van Hooft JE, Visser M, Bruno MJ, Fockens P. Endoscopic ultrasound-guided fine-needle aspiration of pancreatic cystic lesions provides inadequate material for cytology and laboratory analysis: initial results from a prospective study. *Endoscopy.* 2011;43(7):585–90.
91. Luttges J, Zamboni G, Longnecker D, Kloppel G. The immunohistochemical mucin expression pattern distinguishes different types of intra-ductal papillary mucinous neoplasms of the pancreas and determines their relationship to mucinous noncystic carcinoma and ductal adenocarcinoma. *Am J Surg Pathol.* 2001;25(7):942–8.
92. Luttges J, Feyrerabend B, Buchelt T, Pacena M, Kloppel G. The mucin profile of noninvasive and invasive mucinous cystic neoplasms of the pancreas. *Am J Surg Pathol.* 2002;26(4):466–71.

93. Nakamura A, Horinouchi M, Goto M, Nagata K, Sakoda K, Takao S, et al. New classification of pancreatic intraductal papillary-mucinous tumour by mucin expression: its relationship with potential for malignancy. *J Pathol.* 2002;197(2):201–10.
94. Jabbar KS, Verbeke C, Hylander AG, Sjøvall H, Hansson GC, Sadik R. Proteomic mucin profiling for the identification of cystic precursors of pancreatic cancer. *J Natl Cancer Inst.* 2014;106(2):djt439.
95. Lewandrowski KB, Southern JF, Pins MR, Compton CC, Warshaw AL. Cyst fluid analysis in the differential diagnosis of pancreatic cysts. A comparison of pseudocysts, serous cystadenomas, mucinous cystic neoplasms, and mucinous cystadenocarcinoma. *Ann Surg.* 1993;217(1):41–7.
96. Lee LS, Banks PA, Bellizzi AM, Sainani NI, Kadiyala V, Suleiman S, et al. Inflammatory protein profiling of pancreatic cyst fluid using EUS-FNA in tandem with cytokine microarray differentiates between branch duct IPMN and inflammatory cysts. *J Immunol Methods.* 2012;382(1–2):142–9.
97. Yip-Schneider MT, Wu H, Dumas RP, Hancock BA, Agaram N, Radovich M, et al. Vascular endothelial growth factor, a novel and highly accurate pancreatic fluid biomarker for serous pancreatic cysts. *J Am Coll Surg.* 2014;218(4):608–17.
98. Lee LS, Bellizzi AM, Banks PA, Sainani NI, Kadiyala V, Suleiman S, et al. Differentiating branch duct and mixed IPMN in endoscopically collected pancreatic cyst fluid via cytokine analysis. *Gastroenterol Res Pract.* 2012;2012:247309.
99. Maker AV, Katabi N, Qin LX, Klimstra DS, Schattner M, Brennan MF, et al. Cyst fluid interleukin-1beta (IL1beta) levels predict the risk of carcinoma in intraductal papillary mucinous neoplasms of the pancreas. *Clin Cancer Res.* 2011;17(6):1502–8.
100. Schmidt CM, Yip-Schneider MT, Ralstin MC, Wentz S, DeWitt J, Sherman S, et al. PGE(2) in pancreatic cyst fluid helps differentiate IPMN from MCN and predict IPMN dysplasia. *J Gastrointest Surg.* 2008;12(2):243–9.
101. Carr RA, Yip-Schneider MT, Simpson RE, Dolejs S, Schneider JG, Wu H, et al. Pancreatic cyst fluid glucose: rapid, inexpensive, and accurate diagnosis of mucinous pancreatic cysts. *Surgery.* 2018;163(3):600–5.
102. Barresi L, Tarantino I, Traina M, Granata A, Curcio G, Azzopardi N, et al. Endoscopic ultrasound-guided fine needle aspiration and biopsy using a 22-gauge needle with side fenestration in pancreatic cystic lesions. *Dig Liver Dis.* 2014;46(1):45–50.
103. Shakhathreh MH, Naini SR, Brijbassie AA, Grider DJ, Shen P, Yeaton P. Use of a novel through-the-needle biopsy forceps in endoscopic ultrasound. *Endosc Int Open.* 2016;4(4):E439–42.
104. Zhang ML, Arpin RN, Brugge WR, Forcione DG, Basar O, Pitman MB. Moray micro forceps biopsy improves the diagnosis of specific pancreatic cysts. *Cancer Cytopathol.* 2018;126(6):414–20.

105. Nagata K, Horinouchi M, Saitou M, Higashi M, Nomoto M, Goto M, et al. Mucin expression profile in pancreatic cancer and the precursor lesions. *J Hepato-Biliary-Pancreat Surg.* 2007;14(3):243–54.
106. Terris B, Dubois S, Buisine MP, Sauvanet A, Ruzsniwski P, Aubert JP, et al. Mucin gene expression in intraductal papillary-mucinous pancreatic tumours and related lesions. *J Pathol.* 2002;197(5):632–7.
107. Khalid A, Zahid M, Finkelstein SD, LeBlanc JK, Kaushik N, Ahmad N, et al. Pancreatic cyst fluid DNA analysis in evaluating pancreatic cysts: a report of the PANDA study. *Gastrointest Endosc.* 2009;69(6):1095–102.
108. Reid MD, Lewis MM, Willingham FF, Adsay NV. The evolving role of pathology in new developments, classification, terminology, and diagnosis of pancreatobiliary neoplasms. *Arch Pathol Lab Med.* 2017;141(3):366–80.
109. Al-Haddad M. Role of emerging molecular markers in pancreatic cyst fluid. *Endosc Ultrasound.* 2015;4(4):276–83.
110. Maker AV, Carrara S, Jamieson NB, Pelaez-Luna M, Lennon AM, Dal Molin M, et al. Cyst fluid biomarkers for intraductal papillary mucinous neoplasms of the pancreas: a critical review from the international expert meeting on pancreatic branch-duct-intraductal papillary mucinous neoplasms. *J Am Coll Surg.* 2015;220(2):243–53.
111. Khalid A, McGrath KM, Zahid M, Wilson M, Brody D, Swalsky P, et al. The role of pancreatic cyst fluid molecular analysis in predicting cyst pathology. *Clin Gastroenterol Hepatol.* 2005;3(10):967–73.
112. Al-Haddad M, DeWitt J, Sherman S, Schmidt CM, LeBlanc JK, McHenry L, et al. Performance characteristics of molecular (DNA) analysis for the diagnosis of mucinous pancreatic cysts. *Gastrointest Endosc.* 2014;79(1):79–87.
113. Al-Haddad MA, Kowalski T, Siddiqui A, Mertz HR, Mallat D, Haddad N, et al. Integrated molecular pathology accurately determines the malignant potential of pancreatic cysts. *Endoscopy.* 2015;47(2):136–42.
114. Singhi AD, Nikiforova MN, Fasanella KE, McGrath KM, Pai RK, Ohori NP, et al. Preoperative GNAS and KRAS testing in the diagnosis of pancreatic mucinous cysts. *Clin Cancer Res.* 2014;20(16):4381–9.
115. Rosenbaum MW, Jones M, Dudley JC, Le LP, Iafraite AJ, Pitman MB. Next-generation sequencing adds value to the preoperative diagnosis of pancreatic cysts. *Cancer Cytopathol.* 2017;125(1):41–7.
116. Jones M, Zheng Z, Wang J, Dudley J, Albanese E, Kadayifci A, et al. Impact of next-generation sequencing on the clinical diagnosis of pancreatic cysts. *Gastrointest Endosc.* 2016;83(1):140–8.
117. Springer S, Wang Y, Dal Molin M, Masica DL, Jiao Y, Kinde I, et al. A combination of molecular markers and clinical features improve the classification of pancreatic cysts. *Gastroenterology.* 2015;149(6):1501–10.
118. Shen J, Brugge WR, Dimaio CJ, Pitman MB. Molecular analysis of pancreatic cyst fluid: a comparative analysis with current practice of diagnosis. *Cancer.* 2009;117(3):217–27.

119. Toll AD, Kowalski T, Loren D, Bibbo M. The added value of molecular testing in small pancreatic cysts. *JOP*. 2010;11(6):582–6.
120. Sawhney MS, Devarajan S, O'Farrel P, Cury MS, Kundu R, Vollmer CM, et al. Comparison of carcinoembryonic antigen and molecular analysis in pancreatic cyst fluid. *Gastrointest Endosc*. 2009;69(6):1106–10.
121. Talar-Wojnarowska R, Pazurek M, Durko L, Degowska M, Rydzewska G, Smigielski J, et al. A comparative analysis of K-ras mutation and carcinoembryonic antigen in pancreatic cyst fluid. *Pancreatology*. 2012;12(5):417–20.
122. Mertz H. K-ras mutations correlate with atypical cytology and elevated CEA levels in pancreatic cystic neoplasms. *Dig Dis Sci*. 2011;56(7):2197–201.
123. Panarelli NC, Sela R, Schreiner AM, Crapanzano JP, Klimstra DS, Schnoll-Sussman F, et al. Commercial molecular panels are of limited utility in the classification of pancreatic cystic lesions. *Am J Surg Pathol*. 2012;36(10):1434–43.
124. Nikiforova MN, Khalid A, Fasanella KE, McGrath KM, Brand RE, Chennat JS, et al. Integration of KRAS testing in the diagnosis of pancreatic cystic lesions: a clinical experience of 618 pancreatic cysts. *Mod Pathol*. 2013;26(11):1478–87.
125. Gillis A, Cipollone I, Cousins G, Conlon K. Does EUS-FNA molecular analysis carry additional value when compared to cytology in the diagnosis of pancreatic cystic neoplasm? A systematic review. *HPB (Oxford)*. 2015;17(5):377–86.
126. Winner M, Sethi A, Poneris JM, Stavropoulos SN, Francisco P, Lightdale CJ, et al. The role of molecular analysis in the diagnosis and surveillance of pancreatic cystic neoplasms. *JOP*. 2015;16(2):143–9.
127. DeWitt JM, Al-Haddad M, Sherman S, LeBlanc J, Schmidt CM, Sandrasegaran K, et al. Alterations in cyst fluid genetics following endoscopic ultrasound-guided pancreatic cyst ablation with ethanol and paclitaxel. *Endoscopy*. 2014;46(6):457–64.
128. Ryu JK, Matthaei H, Dal Molin M, Hong SM, Canto MI, Schulick RD, et al. Elevated microRNA miR-21 levels in pancreatic cyst fluid are predictive of mucinous precursor lesions of ductal adenocarcinoma. *Pancreatology*. 2011;11(3):343–50.
129. Wang J, Paris PL, Chen J, Ngo V, Yao H, Frazier ML, et al. Next generation sequencing of pancreatic cyst fluid microRNAs from low grade-benign and high grade-invasive lesions. *Cancer Lett*. 2015;356(2 Pt B):404–9.
130. Matthaei H, Wylie D, Lloyd MB, Dal Molin M, Kempainen J, Mayo SC, et al. miRNA biomarkers in cyst fluid augment the diagnosis and management of pancreatic cysts. *Clin Cancer Res*. 2012;18(17):4713–24.
131. Hata T, Dal Molin M, Suenaga M, Yu J, Pittman M, Weiss M, et al. Cyst fluid telomerase activity predicts the histologic grade of cystic neoplasms of the pancreas. *Clin Cancer Res*. 2016;22(20):5141–51.

132. Vincent A, Omura N, Hong SM, Jaffe A, Eshleman J, Goggins M. Genome-wide analysis of promoter methylation associated with gene expression profile in pancreatic adenocarcinoma. *Clin Cancer Res.* 2011;17(13):4341–54.
133. Hata T, Dal Molin M, Hong SM, Tamura K, Suenaga M, Yu J, et al. Predicting the grade of dysplasia of pancreatic cystic neoplasms using cyst fluid DNA methylation markers. *Clin Cancer Res.* 2017;23(14):3935–44.
134. Chai SM, Herba K, Kumarasinghe MP, de Boer WB, Amanuel B, Grieco-Iacopetta F, et al. Optimizing the multimodal approach to pancreatic cyst fluid diagnosis: developing a volume-based triage protocol. *Cancer Cytopathol.* 2013;121(2):86–100.
135. Ryan ME, Baldauf MC. Comparison of flow cytometry for DNA content and brush cytology for detection of malignancy in pancreaticobiliary strictures. *Gastrointest Endosc.* 1994;40(2 Pt 1):133–9.
136. Rumalla A, Baron TH, Leontovich O, Burgart LJ, Yacavone RF, Therneau TM, et al. Improved diagnostic yield of endoscopic biliary brush cytology by digital image analysis. *Mayo Clin Proc.* 2001;76(1):29–33.
137. Baron TH, Harewood GC, Rumalla A, Pochron NL, Stadheim LM, Gores GJ, et al. A prospective comparison of digital image analysis and routine cytology for the identification of malignancy in biliary tract strictures. *Clin Gastroenterol Hepatol.* 2004;2(3):214–9.
138. Hamada S, Satoh K, Hirota M, Kanno A, Ishida K, Umino J, et al. Calcium-binding protein S100P is a novel diagnostic marker of cholangiocarcinoma. *Cancer Sci.* 2011;102(1):150–6.
139. Agrawal S, Kuvshinoff BW, Khoury T, Yu J, Javle MM, LeVea C, et al. CD24 expression is an independent prognostic marker in cholangiocarcinoma. *J Gastrointest Surg.* 2007;11(4):445–51.
140. Javle MM, Tan D, Yu J, LeVea CM, Li F, Kuvshinoff BW, et al. Nuclear survivin expression predicts poor outcome in cholangiocarcinoma. *Hepato-Gastroenterology.* 2004;51(60):1653–7.
141. Swierczynski SL, Maitra A, Abraham SC, Iacobuzio-Donahue CA, Ashfaq R, Cameron JL, et al. Analysis of novel tumor markers in pancreatic and biliary carcinomas using tissue microarrays. *Hum Pathol.* 2004;35(3):357–66.
142. Tascilar M, Offerhaus GJ, Altink R, Argani P, Sohn TA, Yeo CJ, et al. Immunohistochemical labeling for the Dpc4 gene product is a specific marker for adenocarcinoma in biopsy specimens of the pancreas and bile duct. *Am J Clin Pathol.* 2001;116(6):831–7.
143. Zhao H, Davydova L, Mandich D, Cartun RW, Ligato S. S100A4 protein and mesothelin expression in dysplasia and carcinoma of the extrahepatic bile duct. *Am J Clin Pathol.* 2007;127(3):374–9.
144. Karamitopoulou E, Tornillo L, Zlobec I, Cioccarri L, Carafa V, Borner M, et al. Clinical significance of cell cycle- and apoptosis-related markers in

- biliary tract cancer: a tissue microarray-based approach revealing a distinctive immunophenotype for intrahepatic and extrahepatic cholangiocarcinomas. *Am J Clin Pathol.* 2008;130(5):780–6.
145. Ayaru L, Stoeber K, Webster GJ, Hatfield AR, Wollenschlaeger A, Okoturo O, et al. Diagnosis of pancreaticobiliary malignancy by detection of minichromosome maintenance protein 5 in bile aspirates. *Br J Cancer.* 2008;98(9):1548–54.
 146. Levy M, Lin F, Xu H, Dhall D, Spaulding BO, Wang HL. S100P, von Hippel-Lindau gene product, and IMP3 serve as a useful immunohistochemical panel in the diagnosis of adenocarcinoma on endoscopic bile duct biopsy. *Hum Pathol.* 2010;41(9):1210–9.
 147. Tretiakova M, Antic T, Westerhoff M, Mueller J, Himmelfarb EA, Wang HL, et al. Diagnostic utility of CD10 in benign and malignant extrahepatic bile duct lesions. *Am J Surg Pathol.* 2012;36(1):101–8.
 148. Lau SK, Prakash S, Geller SA, Alsabeh R. Comparative immunohistochemical profile of hepatocellular carcinoma, cholangiocarcinoma, and metastatic adenocarcinoma. *Hum Pathol.* 2002;33(12):1175–81.
 149. Komuta M, Spee B, Vander Borgh S, De Vos R, Verslype C, Aerts R, et al. Clinicopathological study on cholangiolocellular carcinoma suggesting hepatic progenitor cell origin. *Hepatology.* 2008;47(5):1544–56.
 150. Nishihara Y, Aishima S, Hayashi A, Iguchi T, Fujita N, Taketomi A, et al. CD10+ fibroblasts are more involved in the progression of hilar/extrahepatic cholangiocarcinoma than of peripheral intrahepatic cholangiocarcinoma. *Histopathology.* 2009;55(4):423–31.
 151. Stewart CJ, Burke GM. Value of p53 immunostaining in pancreatobiliary brush cytology specimens. *Diagn Cytopathol.* 2000;23(5):308–13.
 152. Hart J, Parab M, Mandich D, Cartun RW, Ligato S. IMP3 immunocytochemical staining increases sensitivity in the routine cytologic evaluation of biliary brush specimens. *Diagn Cytopathol.* 2012;40(4):321–6.
 153. Tokumitsu T, Sato Y, Yamashita A, Moriguchi-Goto S, Kondo K, Nanashima A, et al. Immunocytochemistry for Claudin-18 and Masp1 in biliary brushing cytology increases the accuracy of diagnosing pancreatobiliary malignancies. *Cytopathology.* 2017;28(2):116–21.
 154. Kipp BR, Barr Fritcher EG, Pettengill JE, Halling KC, Clayton AC. Improving the accuracy of pancreatobiliary tract cytology with fluorescence in situ hybridization: a molecular test with proven clinical success. *Cancer Cytopathol.* 2013;121(11):610–9.
 155. Rizvi S, Eaton J, Yang JD, Chandrasekhara V, Gores GJ. Emerging technologies for the diagnosis of perihilar cholangiocarcinoma. *Semin Liver Dis.* 2018;38(2):160–9.
 156. Kipp BR, Stadheim LM, Halling SA, Pochron NL, Harmsen S, Nagorney DM, et al. A comparison of routine cytology and fluorescence in situ hybridization for the detection of malignant bile duct strictures. *Am J Gastroenterol.* 2004;99(9):1675–81.

157. Moreno Luna LE, Kipp B, Halling KC, Sebo TJ, Kremers WK, Roberts LR, et al. Advanced cytologic techniques for the detection of malignant pancreatobiliary strictures. *Gastroenterology*. 2006;131(4):1064–72.
158. Barr Fritcher EG, Kipp BR, Slezak JM, Moreno-Luna LE, Gores GJ, Levy MJ, et al. Correlating routine cytology, quantitative nuclear morphometry by digital image analysis, and genetic alterations by fluorescence in situ hybridization to assess the sensitivity of cytology for detecting pancreatobiliary tract malignancy. *Am J Clin Pathol*. 2007;128(2):272–9.
159. Levy MJ, Baron TH, Clayton AC, Enders FB, Gostout CJ, Halling KC, et al. Prospective evaluation of advanced molecular markers and imaging techniques in patients with indeterminate bile duct strictures. *Am J Gastroenterol*. 2008;103(5):1263–73.
160. Fritcher EG, Kipp BR, Halling KC, Oberg TN, Bryant SC, Tarrell RF, et al. A multivariable model using advanced cytologic methods for the evaluation of indeterminate pancreatobiliary strictures. *Gastroenterology*. 2009;136(7):2180–6.
161. Smoczynski M, Jablonska A, Matyskiel A, Lakomy J, Dubowik M, Marek I, et al. Routine brush cytology and fluorescence in situ hybridization for assessment of pancreatobiliary strictures. *Gastrointest Endosc*. 2012;75(1):65–73.
162. Gonda TA, Glick MP, Sethi A, Poneros JM, Palmas W, Iqbal S, et al. Polysomy and p16 deletion by fluorescence in situ hybridization in the diagnosis of indeterminate biliary strictures. *Gastrointest Endosc*. 2012;75(1):74–9.
163. Boldorini R, Paganotti A, Sartori M, Allegrini S, Miglio U, Orsello M, et al. Fluorescence in situ hybridisation in the cytological diagnosis of pancreatobiliary tumours. *Pathology*. 2011;43(4):335–9.
164. Eaton JE, Barr Fritcher EG, Gores GJ, Atkinson EJ, Tabibian JH, Topazian MD, et al. Biliary multifocal chromosomal polysomy and cholangiocarcinoma in primary sclerosing cholangitis. *Am J Gastroenterol*. 2015;110(2):299–309.
165. Bangarulingam SY, Bjornsson E, Enders F, Barr Fritcher EG, Gores G, Halling KC, et al. Long-term outcomes of positive fluorescence in situ hybridization tests in primary sclerosing cholangitis. *Hepatology*. 2010;51(1):174–80.
166. Barr Fritcher EG, Kipp BR, Voss JS, Clayton AC, Lindor KD, Halling KC, et al. Primary sclerosing cholangitis patients with serial polysomy fluorescence in situ hybridization results are at increased risk of cholangiocarcinoma. *Am J Gastroenterol*. 2011;106(11):2023–8.
167. Barr Fritcher EG, Voss JS, Jenkins SM, Lingineni RK, Clayton AC, Roberts LR, et al. Primary sclerosing cholangitis with equivocal cytology: fluorescence in situ hybridization and serum CA 19–9 predict risk of malignancy. *Cancer Cytopathol*. 2013;121(12):708–17.
168. Navaneethan U, Njei B, Venkatesh PG, Vargo JJ, Parsi MA. Fluorescence in situ hybridization for diagnosis of cholangiocarcinoma in primary

- sclerosing cholangitis: a systematic review and meta-analysis. *Gastrointest Endosc.* 2014;79(6):943–50.e3.
169. Barr Fritcher EG, Voss JS, Brankley SM, Campion MB, Jenkins SM, Keeney ME, et al. An optimized set of fluorescence in situ hybridization probes for detection of pancreatobiliary tract cancer in cytology brush samples. *Gastroenterology.* 2015;149(7):1813–24.e1.
 170. Young MR, Wagner PD, Ghosh S, Rinaudo JA, Baker SG, Zaret KS, et al. Validation of biomarkers for early detection of pancreatic cancer: summary of the alliance of pancreatic cancer consortia for biomarkers for early detection workshop. *Pancreas.* 2018;47(2):135–41.
 171. Yu J, Sadakari Y, Shindo K, Suenaga M, Brant A, Almario JAN, et al. Digital next-generation sequencing identifies low-abundance mutations in pancreatic juice samples collected from the duodenum of patients with pancreatic cancer and intraductal papillary mucinous neoplasms. *Gut.* 2017;66(9):1677–87.
 172. Yang J, Li S, Li J, Wang F, Chen K, Zheng Y, et al. A meta-analysis of the diagnostic value of detecting K-ras mutation in pancreatic juice as a molecular marker for pancreatic cancer. *Pancreatol.* 2016;16(4):605–14.
 173. Hata T, Ishida M, Motoi F, Yamaguchi T, Naitoh T, Katayose Y, et al. Telomerase activity in pancreatic juice differentiates pancreatic cancer from chronic pancreatitis: a meta-analysis. *Pancreatol.* 2016;16(3):372–81.
 174. Eshleman JR, Norris AL, Sadakari Y, Debeljak M, Borges M, Harrington C, et al. KRAS and guanine nucleotide-binding protein mutations in pancreatic juice collected from the duodenum of patients at high risk for neoplasia undergoing endoscopic ultrasound. *Clin Gastroenterol Hepatol.* 2015;13(5):963–9.e4.
 175. Kanda M, Sadakari Y, Borges M, Topazian M, Farrell J, Syngal S, et al. Mutant TP53 in duodenal samples of pancreatic juice from patients with pancreatic cancer or high-grade dysplasia. *Clin Gastroenterol Hepatol.* 2013;11(6):719–30.e5.
 176. Sturm PD, Rauws EA, Hruban RH, Caspers E, Ramsoekh TB, Huibregtse K, et al. Clinical value of K-ras codon 12 analysis and endobiliary brush cytology for the diagnosis of malignant extrahepatic bile duct stenosis. *Clin Cancer Res.* 1999;5(3):629–35.
 177. Kipp BR, Fritcher EG, Clayton AC, Gores GJ, Roberts LR, Zhang J, et al. Comparison of KRAS mutation analysis and FISH for detecting pancreatobiliary tract cancer in cytology specimens collected during endoscopic retrograde cholangiopancreatography. *J Mol Diagn.* 2010;12(6):780–6.
 178. Ohori NP, Fowler MH, Swalsky PA, Pal R, Thompson J, Finkelstein SD. Comparative molecular analysis of loss of heterozygosity in adenocarcinoma in bile duct brushings and corresponding surgical pathology specimens. *Cancer.* 2003;99(6):379–84.

179. Khalid A, Pal R, Sasatomi E, Swalsky P, Slivka A, Whitcomb D, et al. Use of microsatellite marker loss of heterozygosity in accurate diagnosis of pancreaticobiliary malignancy from brush cytology samples. *Gut*. 2004;53(12):1860–5.
180. Finkelstein SD, Bibbo M, Loren DE, Siddiqui AA, Solomides C, Kowalski TE, et al. Molecular analysis of centrifugation supernatant fluid from pancreaticobiliary duct samples can improve cancer detection. *Acta Cytol*. 2012;56(4):439–47.
181. Gonda TA, Viterbo D, Gausman V, Kipp C, Sethi A, Poneros JM, et al. Mutation profile and fluorescence in situ hybridization analyses increase detection of malignancies in biliary strictures. *Clin Gastroenterol Hepatol*. 2017;15(6):913–9.e1.
182. Dudley JC, Zheng Z, McDonald T, Le LP, Dias-Santagata D, Borger D, et al. Next-generation sequencing and fluorescence in situ hybridization have comparable performance characteristics in the analysis of pancreaticobiliary brushings for malignancy. *J Mol Diagn*. 2016;18(1):124–30.
183. Parsi MA, Li A, Li CP, Goggins M. DNA methylation alterations in endoscopic retrograde cholangiopancreatography brush samples of patients with suspected pancreaticobiliary disease. *Clin Gastroenterol Hepatol*. 2008;6(11):1270–8.
184. Andresen K, Boberg KM, Vedeld HM, Honne H, Jebesen P, Hektoen M, et al. Four DNA methylation biomarkers in biliary brush samples accurately identify the presence of cholangiocarcinoma. *Hepatology*. 2015;61(5):1651–9.
185. Kisiel JB, Raimondo M, Taylor WR, Yab TC, Mahoney DW, Sun Z, et al. New DNA methylation markers for pancreatic cancer: discovery, tissue validation, and pilot testing in pancreatic juice. *Clin Cancer Res*. 2015;21(19):4473–81.
186. Prachayakul V, Kanchanapermpoon J, Thuwajit C, Boonyaarunnate T, Pongpaibul A, Chobson P, et al. DNA methylation markers improve the sensitivity of endoscopic retrograde cholangiopancreatography-based brushing cytology in extrahepatic cholangiocarcinoma. *Technol Cancer Res Treat*. 2017;16(6):1252–8.
187. Rizvi S, Khan SA, Hallemeier CL, Kelley RK, Gores GJ. Cholangiocarcinoma—evolving concepts and therapeutic strategies. *Nat Rev Clin Oncol*. 2018;15(2):95–111.
188. Olaizola P, Lee-Law PY, Arbelaiz A, Lapitz A, Perugorria MJ, Bujanda L, et al. MicroRNAs and extracellular vesicles in cholangiopathies. *Biochim Biophys Acta*. 2018;1864(4 Pt B):1293–307.
189. Li L, Masica D, Ishida M, Tomuleasa C, Umegaki S, Kalloo AN, et al. Human bile contains microRNA-laden extracellular vesicles that can be used for cholangiocarcinoma diagnosis. *Hepatology*. 2014;60(3):896–907.
190. Shigehara K, Yokomuro S, Ishibashi O, Mizuguchi Y, Arima Y, Kawahigashi Y, et al. Real-time PCR-based analysis of the human bile microRNAome identifies miR-9 as a potential diagnostic biomarker for biliary tract cancer. *PLoS One*. 2011;6(8):e23584.

191. Voigtlander T, Gupta SK, Thum S, Fendrich J, Manns MP, Lankisch TO, et al. MicroRNAs in serum and bile of patients with primary Sclerosing cholangitis and/or cholangiocarcinoma. *PLoS One*. 2015;10(10):e0139305.
192. Liang Z, Liu X, Zhang Q, Wang C, Zhao Y. Diagnostic value of microRNAs as biomarkers for cholangiocarcinoma. *Dig Liver Dis*. 2016;48(10):1227–32.
193. Ge X, Wang Y, Nie J, Li Q, Tang L, Deng X, et al. The diagnostic/prognostic potential and molecular functions of long non-coding RNAs in the exosomes derived from the bile of human cholangiocarcinoma. *Oncotarget*. 2017;8(41):69995–70005.
194. Keane MG, Huggett MT, Chapman MH, Johnson GJ, Webster GJ, Thorburn D, et al. Diagnosis of pancreaticobiliary malignancy by detection of minichromosome maintenance protein 5 in biliary brush cytology. *Br J Cancer*. 2017;116(3):349–55.
195. Navaneethan U, Parsi MA, Lourdasamy V, Bhatt A, Gutierrez NG, Grove D, et al. Volatile organic compounds in bile for early diagnosis of cholangiocarcinoma in patients with primary sclerosing cholangitis: a pilot study. *Gastrointest Endosc*. 2015;81(4):943–9.e1.
196. Alvaro D, Macarri G, Mancino MG, Marzioni M, Bragazzi M, Onori P, et al. Serum and biliary insulin-like growth factor I and vascular endothelial growth factor in determining the cause of obstructive cholestasis. *Ann Intern Med*. 2007;147(7):451–9.
197. Navaneethan U, Lourdasamy V, Gk Venkatesh P, Willard B, Sanaka MR, Parsi MA. Bile proteomics for differentiation of malignant from benign biliary strictures: a pilot study. *Gastroenterol Rep (Oxf)*. 2015;3(2):136–43.

Index

A

- Acinar cell carcinoma (ACC), 289, 293, 295, 296
 - CT imaging, 159, 161
 - cytologic features, 160–162
 - differential diagnosis, 163, 165
 - histologic features, 163
 - immunohistochemical features, 158
 - somatic mutations, 159
 - symptoms, 159
 - treatment, 166
- Acinar cell cystadenoma, 234, 235
- Acquire® Franseen needle, 9
- Adenocarcinoma, 265, 266
- Adenosquamous carcinoma (AdSCa), 207
 - ancillary testing and molecular signature, 131
 - cytologic features, 128, 129
 - diagnosis, 128
 - differential diagnosis, 130, 131
 - histologic features, 129
 - prognosis, 128
- American Gastroenterological Association (AGA), 198
- APC/ β [beta]-catenin pathway, 159–160, 166
- APC gene function, 289
- Autoimmune pancreatitis (AIP)
 - cell block preparation, 79

- cytomorphologic atypia, 77
- cytomorphologic features, 74, 76
- Diff Quik stained FNA smear slide, 74
- differential diagnosis, 77, 79
- duct destruction and obstruction, 73
- fibroinflammatory clusters, 76
- histologic features, 76, 77, 80
- ICDC, 73
- IgG4/IgG ratio, 73
- imaging and gross findings, 73, 74
- prevalence, 72
- steroid therapy, 73
- ThinPrep image, 75
- ThinPrep slide, 78
- type I, 73
- type II, 73

B

- Beckwith-Wiedemann syndrome (BWS), 166, 289
- Benign duodenal epithelium, 54, 56, 57
- Benign gastric epithelium, 55, 56, 58
- Benign hepatocytes, 56, 59
- β -catenin (CTNNB1) gene, 148, 171, 226

- Bile duct brushing cytology
 adenocarcinoma, 265, 266
 diagnostic challenges, 270
 dysplasia, 265
 EUS-FNA, 261
 FISH probes, 271
 IPN-B, 269, 270
 markers, 271
 normal bile duct epithelium,
 262, 265
 reactive bile duct epithelium,
 262, 265
 targeted next generation
 sequencing, 271
 ThinPrep preparation, 261, 262
- Bile duct strictures, 259–261
- Biliary intraepithelial neoplasia
 (BiIN), 265
- BRAF* gene, 289
- Branch duct IPMN (BD-IPMN),
 183
- C**
- Carcinoembryonic antigen (CEA),
 195, 196
- CDX-2 staining, 251
- Charlson comorbidity index, 5
- Cholangiocarcinoma (ChACA),
 271
 detectable mutations, 280
IDH mutations, 276, 278
 immunohistochemistry, 276
- Chronic pancreatitis (CP)
 causes, 66
 cytomorphologic features,
 67–70
 differential diagnosis, 72
 histologic features, 70–72
 imaging and gross findings,
 66, 67
 laboratory findings, 66
 symptoms, 66
- Claudin-18 immunohistochemical
 expression, 271
- Colloid (mucinous noncystic)
 carcinoma, 123–126,
 184, 186
- Confocal laser endomicroscopy
 (CLE), 12
- Courvoisier sign, 96
- Cyst fluid amylase levels, 196
- Cyst fluid analysis, 5
- Cystic lesions of pancreas
 biochemical testing
 biochemical markers,
 301, 302
 cyst fluid amylase, 299
 cyst fluid CEA, 299, 300
 mucins, 300, 301
 CEA concentration, 310
 CEA quantification, 306
 DNA methylation, 309
 genetic testing, 306
GNAS mutation, 305, 306
 gross cyst fluid evaluation,
 297, 298
 immunohistochemistry, 302
KRAS mutation, 304, 306
 LoH, 304
 microRNA, 307
 NGS, 303
 optical density, 302, 303
 periodic acid-Schiff (PAS)
 staining, 298
 periodic liquid-based
 preparations, 298
 telomerase activity, 308
- Cystic pancreatic neuroendocrine
 tumor (PANNET),
 226–228
- Cytologic atypia, 184, 186, 189
- D**
- Dideoxy chain termination (Sanger)
 sequencing, 287
- Digital image analysis (DIA), 314
- Dpc4 protein expression, 210
- Dysplasia, 265

E

- Endoscopic retrograde
 - cholangiopancreatography (ERCP), 4, 37, 66, 260
- Endoscopic ultrasound (EUS)
 - accuracy, 4
 - goal of, 2
 - linear array echoendoscopes, 2
 - of pancreatic adenocarcinoma, 2, 3
 - of pancreatic serous cystadenoma, 2, 3
 - radial array echoendoscopes, 2
- Endoscopic ultrasound with
 - fine-needle aspiration (EUS-FNA)
 - accuracy, 4, 38
 - algorithmic approach, 58, 60
 - Charlson comorbidity index, 5
 - complementary techniques, 11, 12
 - vs. CT-guided biopsies, 4
 - cyst fluid analysis, 5
 - vs. ERCP, 4
 - features, 4
 - microforceps biopsy, 9, 10
 - needle choice, 7
 - onsite cytopathology, 11
 - position and number of passes, 6, 7
 - sensitivity and specificity, 38
 - stylet, 11
 - suction, 10
 - tissue diagnosis, 1
 - tissue sampling, 8
- Endoscopic ultrasound with
 - fine-needle biopsy (EUS-FNB)
 - of chronic pancreatitis, 8
 - needles choice, 9
 - randomized controlled trials, 8
- Epidermoid cyst of accessory spleen, 233

- Estrogen receptor (ER), 204
- Everolimus, 295

F

- Familial adenomatous polyposis, 166
- Familial syndromes, 96
- Foamy cell pattern, 112
- Foamy gland pattern, 111
- Fractional allelic loss (FAL), 296
- Fukuoka guidelines, 182, 183, 197

G

- Gastrinomas, 149
- Gastrointestinal carcinoma, 251
- Gastrointestinal contamination
 - benign duodenal epithelium, 54–57
 - benign gastric epithelium, 56, 58
 - benign hepatocytes, 56, 59
 - differential diagnosis, 57, 61
 - extracellular neoplastic mucin, 54, 55
- 22 G FNA needles, 9
- GNAS* mutations, 210
- GNAS* testing, 196

H

- Hemorrhagic cystic degeneration, 222
- Hepatocellular carcinoma, 251
- Hepatoid carcinoma of the pancreas (HC), 137–139
- Hereditary nonpolyposis colorectal cancer (HNPCC)/Lynch syndrome, 135
- High-grade pancreatic ductal adenocarcinoma, 110
- High-risk stigmata, 197
- Hyalinized stroma, 155, 156

I

- Insulinomas, 149
- International consensus diagnostic criteria (ICDC), 73
- Intraductal papillary mucinous neoplasms (IPMNs)
 - American Gastroenterological Association guidelines, 198
 - BD-IPMN, 183
 - carcinoembryonic antigen, 195, 196
 - clinical features, 182
 - colloid-type mucin, 188
 - endoscopic ultrasound, 183
 - fine needle aspiration, 188, 189
 - gastric type, 184
 - GNAS* testing, 196
 - gross findings, 184
 - high-grade dysplasia, 184, 186, 187, 190, 192
 - high-risk stigmata, 197, 198
 - intermediate-grade dysplasia, 184, 185, 190, 194
 - intestinal type, 186
 - intranuclear cytoplasmic inclusions, 190, 191
 - KRAS* testing, 196
 - low-grade dysplasia, 184, 185, 190, 191
 - MD-IPMN, 183
 - microforceps pancreatic cyst biopsy, 193–195
 - miRNAs, 197
 - MRI/MRCP, 183
 - oncocytic type, 187
 - pancreatobiliary type, 186
 - Worrisome features, 197
- Intraductal papillary neoplasm of the bile ducts (IPN-B), 269, 270
- Intranuclear cytoplasmic inclusions, 190, 191
- Intranuclear cytoplasmic pseudoinclusions, 254

- Intrapancreatic accessory spleen (IPAS)
 - cytomorphologic features, 84, 85
 - differential diagnosis, 86, 87
 - histologic features, 86
 - imaging and gross findings, 83
 - prevalence, 83
- Intrapancreatic reactive lymph nodes, 87, 88

K

- KRAS* gene, 196

L

- Linear array echoendoscopes, 2
- Loss of heterozygosity (LoH), 275, 286
- Low-grade pancreatic ductal adenocarcinoma, 110
- Lymphoepithelial cysts
 - CEA levels, 231
 - clinical features, 231
 - cytology, 231
 - treatment, 233
- Lymphoid enhancer binding factor 1 (LEF1), 224

M

- Macrocytic SCAs, 219
- Magnetic resonance
 - cholangiopancreatography (MRCP), 260
- Main duct IPMN (MD-IPMN), 183
- Malignant melanoma, 254
- Maspin, 271
- Medullary carcinoma, 134–137
- Mesothelin, 277
- Metastases to pancreas
 - EUS-FNA, 240
 - gastrointestinal carcinoma, 251
 - hepatocellular carcinoma, 251
 - incidence, 239

- malignant melanoma, 254
 - neuroendocrine carcinoma, 248, 251
 - pulmonary non-small cell carcinoma, 240, 243, 248
 - renal cell carcinoma, 240–243
 - Metastatic clear cell carcinoma, 113
 - Metastatic lung adenocarcinoma, 244, 245
 - Metastatic renal cell carcinoma, 240
 - Metastatic small cell carcinoma, 249
 - Metastatic squamous cell carcinoma, 131
 - MIB-1 labeling index, 295
 - Microcystic serous cystadenoma, 219
 - MicroRNA profiling, 286, 287
 - Mixed ductal-endocrine carcinomas (MDECs)
 - ancillary testing and molecular signature, 134
 - cytologic features, 132
 - differential diagnosis, 133
 - histologic features, 133
 - Molecular testing, 276, 304
 - MUC16 (CA-125), 277, 301
 - MUC2 expression, 209
 - Mucinous cystic neoplasms (MCNs), 182
 - clinical features, 203
 - CT scan, 205
 - cyst fluid biochemistry, 210
 - cytologic diagnosis, 207–209
 - endoscopic ultrasound, 205
 - GNAS* mutation, 210
 - gross findings, 206
 - high-grade dysplasia, 207
 - immunohistochemistry, 209, 210
 - intermediate-grade dysplasia, 207
 - invasive carcinomas, 207
 - KRAS* mutation, 210
 - low-grade dysplasia, 207
 - mucinous epithelium, 206
 - pathogenesis, 204
 - prognosis, 211, 212
 - subepithelial ovarian-type stroma, 207
 - treatment, 210, 211
 - Mucosal atypia, 260
 - Multiple endocrine neoplasia type 1 (MEN1), 149
- N**
- Neoplastic cysts of pancreas
 - acinar cell cystadenoma, 234, 235
 - non-neoplastic cysts (*see* Non-neoplastic cysts)
 - SCAs (*see* Serous cystadenomas (SCAs))
 - SPN (*see* Solid pseudopapillary neoplasm (SPN))
 - Neoplastic mucinous cysts, 182, 188, 192, 207, 208
 - Neuroendocrine carcinoma (NECA), 248, 251
 - IHC, 293
 - MIB-1 labeling index, 295
 - mutation, 289
 - Neuroendocrine tumor (NET)
 - genetic alterations, 288
 - loss of heterozygosity, 296
 - next generation sequencing, 296
 - recurrent genetic and genomic alterations, 289–291
 - Sanger sequencing of DNA, 296
 - Neurofibromatosis type 1 (NF1), 149
 - Non-neoplastic cysts
 - epidermoid cyst of accessory spleen, 233
 - lymphoepithelial cysts
 - CEA levels, 231
 - clinical features, 231
 - cytology, 231, 232
 - imaging, 231
 - treatment, 233

- Non-neoplastic cysts (*cont.*)
- pseudocyst
 - amylase level, 229
 - clinical features, 228
 - cytology, 228, 229
 - imaging, 228
 - treatment, 229
 - retention cyst, 233
 - SCOP, 234
- Normal biliary epithelium, 262
- O**
- Osteoclast-like giant cells (UOC), 118
- ancillary testing and molecular signature, 121, 122
 - cytologic features, 119, 120
 - differential diagnosis, 121, 122
 - histologic features, 120, 121
- P**
- Pancreas
- anatomy and embryology, 38–40
 - benign acinar cells
 - cytologic features, 45, 48
 - differential diagnosis, 48–50
 - histologic features, 45, 48
 - benign ductal cells
 - cytologic features, 40–42
 - differential diagnosis, 43, 44
 - exocrine ductal and acinar cells, 40
 - histologic features, 41, 43
 - islet cells
 - cytologic features, 50, 51
 - differential diagnosis, 52, 54
 - histologic features, 50
 - salt and pepper granularity, 50
- Pancreatic cancer
- EUS (*see* Endoscopic ultrasound (EUS))
 - EUS-FNA (*see* Endoscopic ultrasound with fine-needle aspiration (EUS-FNA))
 - prognosis of, 1
 - survival rates, 1
 - Pancreatic cyst lesions
 - classification, 217, 218
 - prevalence, 181
 - Pancreatic ductal adenocarcinoma (PDCA)
 - adenosquamous carcinoma
 - ancillary testing and molecular signature, 131
 - cytologic features, 128, 129
 - diagnosis, 128
 - differential diagnosis, 130, 131
 - histologic features, 129
 - prognosis, 128
 - colloid (mucinous noncystic) carcinoma, 123–126
 - conventional type
 - ancillary testing and molecular signature, 113, 115
 - cytologic features, 109
 - differential diagnosis, 113, 114
 - high grade PDCA, 109, 110
 - histologic features, 111–113
 - low grade PDCA, 110
 - well-differentiated PDCA, 106, 109
 - cytologic and histologic features, 97–100
 - environmental risk factors, 95
 - fine needle aspiration, 101, 104
 - FISH, 280, 281
 - hepatoid carcinoma of the pancreas, 137–139
 - IHC markers, 277, 278, 280
 - immunohistochemistry, 276
 - laboratory testing, 97

- medullary carcinoma, 134–137
- mesothelin, 277
- microRNA markers, 288
- mixed ductal-endocrine carcinomas
 - ancillary testing and molecular signature, 134
 - cytologic features, 132
 - differential diagnosis, 133
 - histologic features, 133
- mutations, 275
- next-generation sequencing
 - DNA, 281, 286
 - loss of heterozygosity, 286
 - microRNA profiling, 286, 287
- pancreatic intraepithelial neoplasia
 - ancillary testing and molecular signature, 107–108
 - cytologic features, 106
 - differential diagnosis, 107, 108
 - histologic spectrum, 104, 105
 - PanIN-3 cytology and histology, 104, 105
 - well-differentiated, 106
- physical examination, 96
- prevalence, 95
- prognosis, 97
- radiologic imaging, 101–104
- Sanger sequencing, 287
- signet ring cell carcinoma of the pancreas, 126–128
- SMAD4 gene, 277
- symptoms, 96
- TP53 gene, 277
- undifferentiated carcinoma, 115
 - ancillary testing and molecular signature, 117
 - cytologic and histologic features, 115, 116
 - differential diagnosis, 117, 118
 - with osteoclast-like giant cells, 118–122
- Pancreatic intraepithelial neoplasia (PanIN)
 - ancillary testing and molecular signature, 107–108
 - cytologic features, 106
 - differential diagnosis, 107, 108
 - histologic spectrum, 104, 105
 - histologic features, 107
 - PanIN-3 cytology and histology, 104, 105
 - well-differentiated, 106
- Pancreatic neuroendocrine neoplasia (PNET)
 - grading, 149
 - PNET vs. PNEC, 148
- Pancreatic neuroendocrine tumor (PNET), 220
 - cystic degeneration, 149, 150
 - cytoplasm, 151, 153, 154
 - differential diagnosis, 155
 - eccentric plasmacytoid nuclei, 151
 - grading, 148
 - histologic features, 155, 156
 - immunohistochemical features, 158
 - inherited syndromes, 149
 - monotonous polygonal and plasmacytoid cells, 151, 152
 - MRI, 149, 151
 - pseudorosette formation, 151, 152
 - scattered binucleate cells, 154
 - small cell carcinoma/large cell neuroendocrine, 154, 155
 - smooth nuclear contours and ‘salt and pepper’ chromatin, 151, 153
 - treatment, 159
- Pancreatic tissue procurement, 37

- Pancreatico-biliary cytology,
see Pap Society reporting scheme
- Pancreatico-biliary duct fluid
 digital image analysis, 314
 DNA methylation marker profiling, 323
 fluorescence in situ hybridization, 316–319
 immunocytochemical analysis, 315, 316
 immunohistochemistry markers, 314, 315
 KRAS mutational analysis, 321
 loss of Heterozygosity, 321, 322
 microRNA profiling, 323, 324
 next-generation sequencing of DNA, 322, 323
- Pancreatico-biliary lesions,
see Cholangiocarcinoma (ChACA); Pancreatic ductal adenocarcinoma (PDADCA)
- Pancreatico-biliary tract malignancy, 260
- Pancreatoblastoma (PB), 289
 cytologic features, 167, 168
 differential diagnosis, 170
 histologic features, 168, 170
 imaging, 166
 symptoms, 166
 treatment, 170
- Pap Society reporting scheme
 atypical category, 25–27
 impact of, 32, 33
 negative category, 23, 24
 neoplastic
 benign, 28
 high-grade dysplasia, 29
 high-grade epithelial atypia, 29
 intermediate-grade dysplasia, 29
 IPMNs, 28
 low-grade dysplasia, 29
 MCNs, 28
 neoplastic mucinous cyst, 29
 pancreatic neuroendocrine tumor, 30
 non-diagnostic, 22, 23
 positive for malignant cells, 31, 32
 risk stratification, 32
 suspicious for malignancy, 30, 31
- Papanicolaou Society of Cytopathology (Pap Society), 21, 190, 208
- Paraduodenal groove pancreatitis (GP)
 cytomorphologic features, 82
 histologic features, 83
 imaging and gross findings, 81–82
 surgical resection, 81
- Periodic acid–Schiff (PAS) staining, 221, 298
- p16 expression, 196
- p53 gene, 277
- Pleomorphic carcinoma, *see* Undifferentiated carcinoma (UC)
- Pleomorphic giant cell carcinoma, *see* Undifferentiated carcinoma (UC)
- Pleomorphic large cell carcinoma, *see* Undifferentiated carcinoma (UC)
- Poly-(adenosine diphosphate-ribose) polymerase-1 (PARP) inhibitors, 275
- Polysomy, 271, 316
- Poorly differentiated neuroendocrine tumors, 134
- Primary sclerosing cholangitis, 270
- Procore™ 22 G FNB needle, 9
- Progesterone receptor (PR), 204
- Pseudocysts
 amylase level, 229

- clinical features, 228
 - cytology, 228, 229
 - imaging, 228
 - treatment, 229
- Pulmonary non-small cell carcinoma, 240, 243, 248
- R**
- Radial array echoendoscopes, 2
- Rapid on site evaluation (ROSE), 30
- Reactive bile duct epithelium, 262
- Reactive ductal atypia, 230
- Renal cell carcinoma, 241–243
- Retention cyst, 233
- RNF43 gene, 196
- S**
- S100 protein family, 271
- Sanger sequencing, 287
- Sarcoidosis
 - cytologic features, 89, 90
 - differential diagnosis, 90
 - histologic features, 90
- Sarcomatoid carcinoma, *see* Undifferentiated carcinoma (UC)
- Serous cystadenomas (SCAs), 181, 297
 - clinical features, 218, 219
 - cyst fluid biochemistry, 222
 - fine needle aspiration, 221
 - gross findings, 219
 - histology, 220
 - imaging, 219
 - molecular genetics, 222
 - PanNET cells, 221
 - periodic acid–Schiff, 221
 - treatment, 222
- SharkCore™ 22 G and 25 G needles, 9
- Signet ring cell carcinoma of the pancreas (SRCC), 126–128
- SMAD4 expression, 196
- SMAD4 gene, 277
- Solid pancreatic tumors, 147, 159
- Solid-pseudopapillary neoplasm (SPN), 289, 293, 295–297, 302, 306, 308
 - beta-catenin
 - immunohistochemistry, 224, 225
 - CD10 immunohistochemistry, 224, 226
 - clinical features, 222
 - cystic degeneration, 171
 - cytologic features, 171, 172, 223
 - differential diagnosis, 176, 177
 - gross findings, 223
 - histologic features, 173, 176, 223
 - imaging, 222
 - immunohistochemical features, 158
 - LEF-1 immunohistochemistry, 224, 225
 - molecular genetics, 226
 - PanNET, 226–228
 - symptoms, 171
 - treatment, 177, 226
- Solid serous adenomas, 220
- Somatostatin analogue
 - chemotherapy, 159
- Sporadic PNET, 149
- Squamoid cyst of the pancreatic ducts (SCOP), 234
- Steroidogenic enzymes, 204
- Stromal hyalinization, 176
- Subepithelial ovarian-type stroma, 207
- Sunitinib, 295
- T**
- TP53 gene, 277
- TP53 mutations, 196, 197
- Trosseau sign, 96
- TTF-1 staining, 245
- Tuberous sclerosis complex type 1 and 2 (TSC 1&2), 149

U

- Undifferentiated carcinoma (UC),
 - 115, 207
 - ancillary testing and molecular signature, 117
 - cytologic and histologic features, 115, 116
 - differential diagnosis, 117, 118
 - with osteoclast-like giant cells, 118–122
- UroVysion probe set, 270–271, 280

V

- Virchow sign, 96
- von Hippel-Lindau (VHL) syndrome, 149, 218

W

- Well-differentiated PDCA, 106, 109
- Whipple procedure, 97
- Worrisome features, 197